Reversible chemistry to control the synthesis and folding of polymeric materials

Jorge Gómez Magenti

Downing College

University of Cambridge

Supervisor: Prof. Christopher A. Hunter FRS

This dissertation is submitted for the degree of Doctor of Philosophy

October 2019

"Listen, Morty, I hate to break it to you but what people call "love" is just a chemical reaction that compels animals to breed. It hits hard, Morty, then it slowly fades, leaving you stranded in a failing marriage. I did it. Your parents are gonna do it. Break the cycle, Morty. Rise above. Focus on science."

Rick Sanchez

Declaration

This dissertation is the result of my own work carried out at the University of Cambridge and Eindhoven University of Technology from April 2015 to January 2019 and includes nothing which is the outcome of work done in collaboration except as declared in the Preface and specified in the text.

It is not substantially the same as any that I have submitted, or, is being concurrently submitted for a degree or diploma or other qualification at the University of Cambridge or any other University or similar institution except as declared in the Preface and specified in the text. I further state that no substantial part of my dissertation has already been submitted, or, is being concurrently submitted for any such degree, diploma or other qualification at the University of Cambridge or any other University or similar institution except as declared in the Preface and specified in the text

It does not exceed the prescribed word limit for the relevant Degree Committee.

Jorge Gomez Magenti

ABSTRACT

Reversible chemistry to control the synthesis and folding of polymeric materials

Jorge Gomez Magenti

Mimicking Nature's ability to create well-defined functional materials is a major goal in the field of polymer chemistry. Two distinct approaches are explored in this work.

Part I of the thesis deals with the templated synthesis of sequence-defined oligomers. The ultimate strategy to synthesize macromolecules that have a specific functionality is the selection and evolution cycle, in which template reactions amplify the most promising sequences. All the work done in the field involve biomolecules or bio-inspired systems but there are not, to the best of our knowledge, examples of purely synthetic oligomers than can undergo efficient supramolecular replication. Covalent duplex formation has risen as a promising alternative in order to ensure template saturation during the templating process. This thesis expands on this strategy. A new molecular system was designed, which comprised phenol and carboxylic acid monomers that could selectively and quantitatively couple to each other, thus ensuring duplex formation. The monomers were linked by Glaser-Hay chemistry. A homodimer and a heterodimer were used as templates to synthesize the complementary partners through a replication cycle. The conditions for the base-pair chemistry and the zip-up reactions were optimized. In an expansion of this strategy, spacer units with symmetrical chemical handles were introduced between the template and daughter strand. This helped achieve the replication of two homodimers in a single cycle.

Part II of the thesis explores the synthesis of materials making use of living polymerizations and subsequent post-functionalizations in order to obtain systems that fold on themselves, forming polymer nanoparticles. This process is reminiscent of the folding of proteins to form three-dimensional tertiary structures. Since protein functionality is derived from this precise folding of the backbone into a well-defined structure, it would be of great interest to achieve control over the folding of a synthetic polymer. Benzene-1,3,5-tricarboxamide (BTA) and solubilizing units were grafted onto a polycarbonate backbone and the folding behavior of this system was investigated by circular dichroism (CD). In another part of this work, a polyacrylate chain was functionalized with a proportion of permanently anchored BTAs, and with some which were dynamically attached via thermally reversible Diels-Alder adducts. We varied the environmental parameters of the reversible reaction. We propose that this led to the anchoring position of the dynamically-attached BTA adapting to reach a more thermodynamically stable structure. CD measurements of the system were performed to investigate polymer folding as a result of environmental molecular adaptation.

Acknowledgements

Thanks to Chris for giving me the means to do groundbreaking science and the freedom to develop as an adult, independent worker, in what was my first paid job “out of university”. I am genuinely grateful for this.

Thanks to Petr for being the best flat mate and an okay friend. Or maybe it was the other way around? Wish more people were as direct and conscientious as he is, and at the same time had his incredibly good heart. I wish we appreciated and sought that more often.

Thanks to Giulia for being an excellent lab manager. The working conditions in the lab have been by far the best I have seen in a university lab so far. One could always tell how much she cared for her job and how much she wanted us to have the best possible conditions to do work.

Thanks to Elena for caring (more than she should have) and for being a really good friend all this time. Thanks to Stefan for Castle Hill. To Judith for the positivity. To Pavle for the “Jorgitos” with a mischievous smile on his face. To Yudi for being sweet. To Ennio for being amusing. To Nicola and Mark W., for being and behaving how I wish I were and behaved more often. To Filip for being a walking reminder that I can’t let my privileges go unchecked. Thanks to Maria for filling the silences. To Diego for always being ready to help when I asked. To Istvan because he came so little to the gym that made me feel good with my routine. To Mike for showing me that if you talk with confidence and look mature people will buy anything. To Geneva because she was the first one who cared when my first year was going down the toilet. And because she was great, and I missed her a lot. Thanks to Cristina & Rafel, and Pavle & Anđela for helping me when I was in need. Thanks to Ana for her incredibly encouraging words right before my first-year examination. She inspired me so much that I still occasionally think of that, three and a half years later.

Thanks to everyone who put up with me when I was more dogmatic than principled. But above all, thanks to everyone who doesn’t do contract work for murderous, autocratic regimes.

In general, thanks to everyone who has made my experience in the group more enjoyable. Or at the very least, more memorable. I know 95% of you will only open this thesis to read my acknowledgments. Shame on you (though I kinda get it).

Gracias a mi familia, porque si estoy donde estoy es por su trabajo y por su énfasis en la importancia de estudiar. Sin ellos jamás hubiese llegado al momento de escribir los agradecimientos en una tesis por la Universidad de Cambridge.

Contents

"Sucking at something is the first step to being sorta good at something"

Jake the Dog

1

Introduction: Synthetic Strategies to Control Monomer Sequence

1.1 Sequence. Shape. Function.

For years scientists have tried to emulate nature's unique ability to create well-defined polymeric materials with specific properties and three-dimensional structures that depend on the monomer sequence.[1] Monomer sequence has a fundamental role in biology and is the cornerstone of some features that determined the origin and evolution of life on this planet: heredity, self-replication, self-assembly and molecular recognition all rely on sequence-defined architectures.[2] A defined primary structure leads to specific secondary, tertiary and even quaternary structures that confer on biomacromolecules their highly advanced functionality. The degree of functionality that any macromolecule may have is much related to the degree of sequence complexity that its chains can achieve (Figure 1.1).[3]

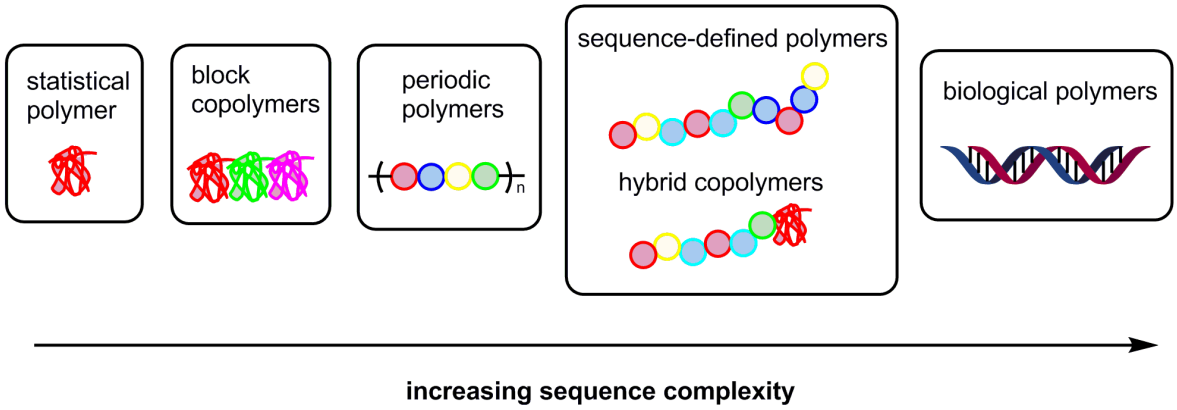

Figure 1.1. Increasing complexity of polymeric materials depending on the monomer sequence and system polydispersity.

Therefore, it is not surprising that perfecting the synthesis of polymeric molecules is so interesting for the scientific community. In the last several decades, polymer research has advanced from the creation of block copolymers to tune determined properties of a given material,[4,5] to the synthesis of sequence-specific chains to improve the binding to a certain protein,[6] up to the creation of systems capable of undergoing biological functions.[7] The interest in sequenced material has risen notably over the past 6 years, where over 75% of the publications that contained the terms "sequence-controlled" or "sequence-defined" have been released.

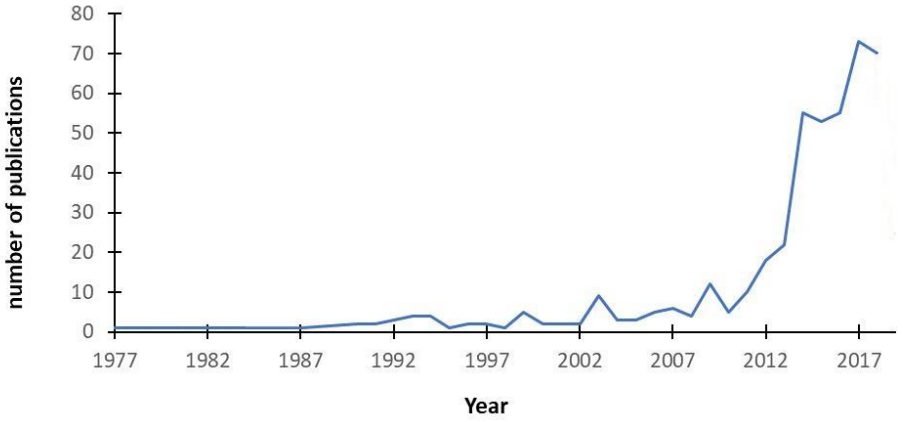

Figure 1.2. Number of papers published per year containing the following search terms: (sequence PRE/1 (defined OR controlled)) AND (polymer* OR oligomer*)). Search performed on Scopus.

Nucleic acids (e.g. DNA, RNA) and proteins are nature's defined polymeric materials based on the coupling of certain monomers, nucleotides and amino acids, respectively. During the last

few decades researchers have done extensive work in the use of these biological molecules for non-biological applications, such as data storage, nanoelectronics or catalysis.[8-10]

A well-known strategy for the development of bio-inspired materials with specific sequences that confer on them defined functionalities is the selection and evolution cycle (Figure 1.3).[11-13] In the cycle, a polymeric mixture of nucleic acids with different primary structures undergoes a selection process (e.g. binding to a target) and only the chains that have a sequence that binds with enough strength are retained. These chains are then replicated by polymerase chain reaction (PCR), a technique that makes use of template reactions to amplify functional materials. The cycle is repeated until the chain with the best specific sequence to bind the target is obtained.

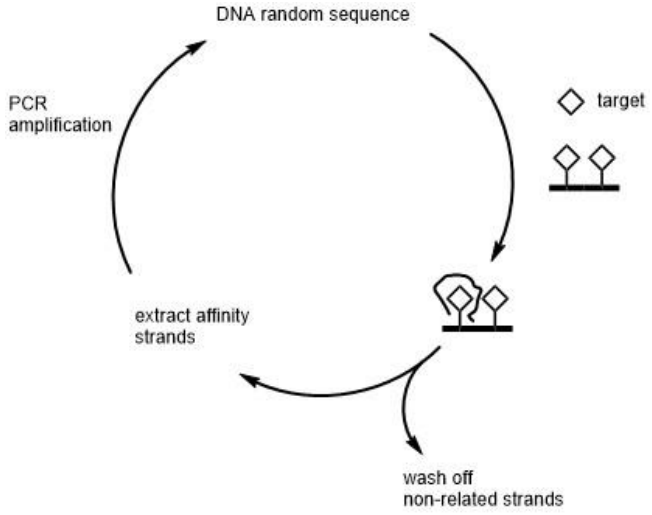

Figure 1.3. Selection and evolution cycle to make functional materials from DNA aptamers. Random DNA sequences are exposed to a target (square shape). Only the sequences that bind strongly enough are retained in the cycle. They are then amplified by PCR and the process is repeated several times until the target optimal binding sequence is selected.

Most of the studies of the key relation between sequence and function have been done in the field of biological-related molecules. Great effort is being put in the development of purely synthetic alternatives to DNA, RNA, proteins, or polypeptides, as functional materials that present efficient synthetic methods, easier handleability, improved storage possibilities, and the ability to be amplified. The next sections provide a brief review and discussion of such recent research efforts.

1.2 Synthesis of polymeric materials: sequence-controlled approaches

The development of living polymerization techniques has been of big importance for the field of functional materials.[14] Living polymerization allows for rapid and homogenous growth of polymeric chains in the reaction. Chains continue growing until there are no free monomeric units available in solution. This offers the interesting possibility of performing sequential additions of various monomers that produce materials with different monomer blocks. The result is chains with a well-defined length and low polydispersity. Research has been conducted over the past 20 years on how to bias the monomer positioning along the polymer chain in living polymerization techniques.

In 2000, Hawker and co-workers reported for the first time an efficient controlled copolymerization of styrene and N-substituted maleimides, exploiting the tendency to cross polymerize when an excess of styrene was present.[15] The maleimides were sequentially inserted into a growing polystyrene chain that was reacted by atom transfer radical polymerization (ATRP). The ability of styrene and maleimides to cross-propagate led to materials with well-defined microstructures. Following a similar principle, Lutz et al. presented a series of papers in which they showed that electron poor monomers (N-substituted maleimides) could be precisely inserted in the reaction of electron rich monomers (styrene). Insertions of single monomer units were achieved under very precise kinetic conditions that could be adjusted by multiple injections of acceptor or donor monomer (Figure 1.4). A method was automated to achieve the synthesis in controlled conditions without having to do successive manual injections.[16-19]

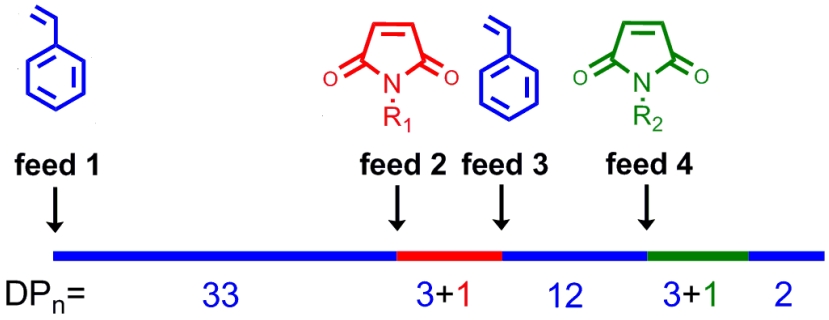

Figure 1.4. Injections of different monomers on a growing polystyrene chain (blue monomer) help form multi-block chains. DP indicates the degree of polymerization of each block. When the injections are precisely controlled and timed, maleimide insertion can be as small as a single monomer unit, with just three styrene monomers reacting on average in that same block. After the maleimide is consumed, the polystyrene chain continues growing until it is interrupted by the next injection.

Another example of what different reactivity ratios and careful study of experimental conditions can achieve was shown by Kamigaito and co-workers.[20] When limonene (L) and N-phenyl maleimides (M) were reacted in DMF and cumyl alcohol, they produced random uncontrolled polymerizations. But when the monomers were reacted in a strongly hydrogen-bonding fluoro-cumyl alcohol they produced materials with a perfect sequence of [C-(M-M-L)$_n$-M-S] (C and S are the RAFT polymerization chain transfer agent). This "MML" distribution was independent of the initial monomer ratio feed.

O'Reilly and her group achieved perfect alternation in a styrene-derivative copolymerization by functionalizing the styrene monomers with complementary nucleic acid bases.[21] If the solvent was changed from chloroform to DMF, the alternation between complementary monomers worsened, which affected the primary structure of the polymer and in turn produced different self-assembled structures after the polymerization (Figure 1.5).

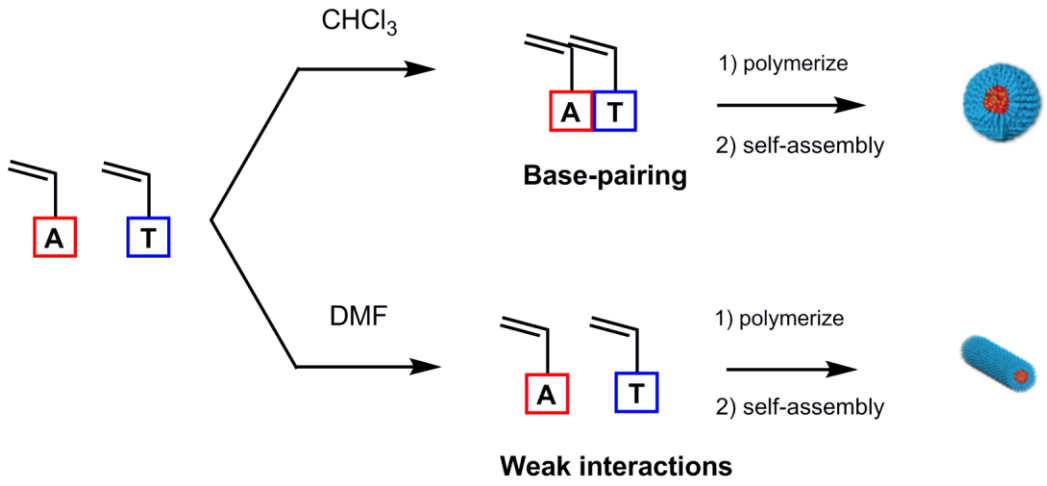

Figure 1.5. Adenine-functionalized styrene (red square) and thymine-functionalized styrene (blue square) were copolymerized in two solvents of different polarity. In chloroform, the alternation between the monomers prior the reaction initiation led the formation of globular micellar structures after the polymerization. In DMF, weakened interactions between the monomers changed the primary structure of the polymeric material, producing elongated micellar structures.

An interesting possibility for controlling multi-block polymer architecture is the use of external stimuli to affect the final chain sequence. For example, Haddleton and coworkers demonstrated the efficient synthesis of multiblock copolymers using UV light activation.[22] Up to eleven blocks made from four different acrylate monomeric units were synthesized with high conversions and low polydispersity (PDI < 1.2). More recently, You et al. were able to take this strategy a step further by combining two orthogonal polymerization techniques (anionic ring-opening polymerization (AROP) and photoinduced electron transfer-reversible addition-fragmentation chain transfer (PET-RAFT)) that could be interconverted and switched ON and OFF by applying two different stimuli: heat and light.[23] When AROP was in the ON state, only the cyclic monomers present in solution could react. After lowering the temperature and exposing the solution to light, the vinyl monomers were incorporated along the polymer chain. By sequentially exposing the solution to both stimuli the researchers were able to make multiblock copolymers with relatively low dispersity.

There are also several examples of precise polymer synthesis using ring opening metathesis.[24-26] Cyclic monomers with multiple functionalization produce polymer chains with defined repeating patterns (Figure 1.6).

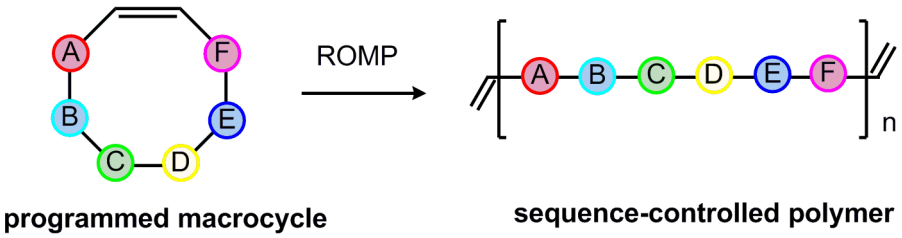

Figure 1.6. General concept of ring opening metathesis polymerization (ROMP) to give sequence-controlled polymers.

Even though great advances have been made during the past 15 years in the improvement of these chain-growth strategies, the best examples to date are all polydisperse materials, and they rely on extremely specific experimental conditions or monomer characteristics. If perfect sequence control is desired, then other approaches must be considered.

1.3 Synthesis of polymeric materials: sequence-defined approaches

One of the best techniques to date to synthesize long chains of sequence-defined materials is solid phase synthesis. Since Merrifield presented the concept in 1963 with the synthesis of a tetrapeptide,[27] great advances have been made in the field. Monomers with two functional groups that can react with each other (one of them being momentarily protected) are attached one by one to a solid support (e.g. a polystyrene resin) (Figure 1.7). Once the first monomer is attached, its protecting group is cleaved, and the second monomer can react with the first. This process is repeated several times until the desired length and sequence is obtained and the chain is cleaved from the resin. Unreacted monomers, catalyst and protecting groups are easily washed off after each step.

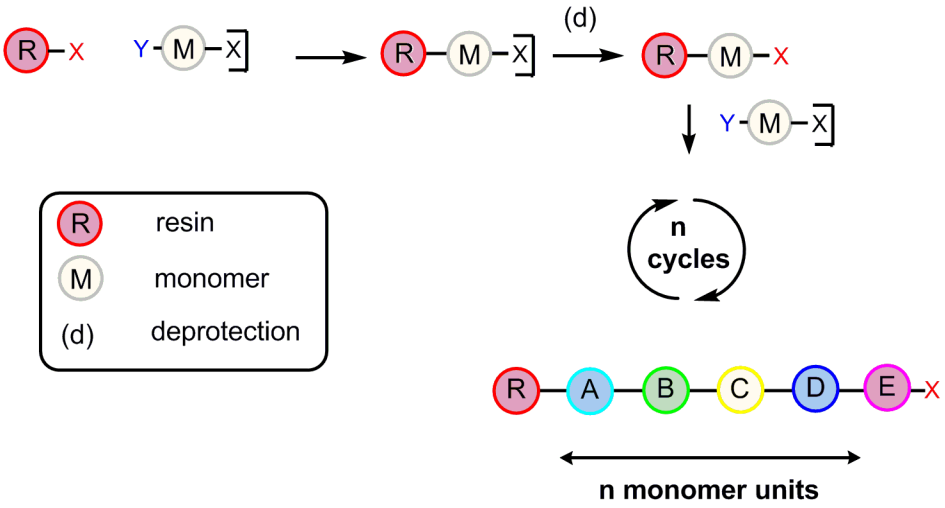

Figure 1.7. General scheme for the solid-phase synthesis of protected oligomers.

This technique has been used in the synthesis of sequence-defined natural (polypeptides, polynucleic acids, polysaccharides)[28-29] and non-natural (polyamidoamines, polyacetylenes, polypeptoids)[30-34] oligomers, and with a great variety of coupling chemistries. Just in the last few years, Lutz and co-workers have presented several examples: polyphosphates by phosphoramidite chemistry,[35] oligo(triazole amide)s via successive copper-catalyzed azide-alkyne Huisgen cycloaddition (CuAAC) and carboxylic acid-amine coupling steps,[36] and oligo(alkoxyamine amide)s via successive anhydride-amine and nitroxide radical coupling steps (Figure 1.8).[37]

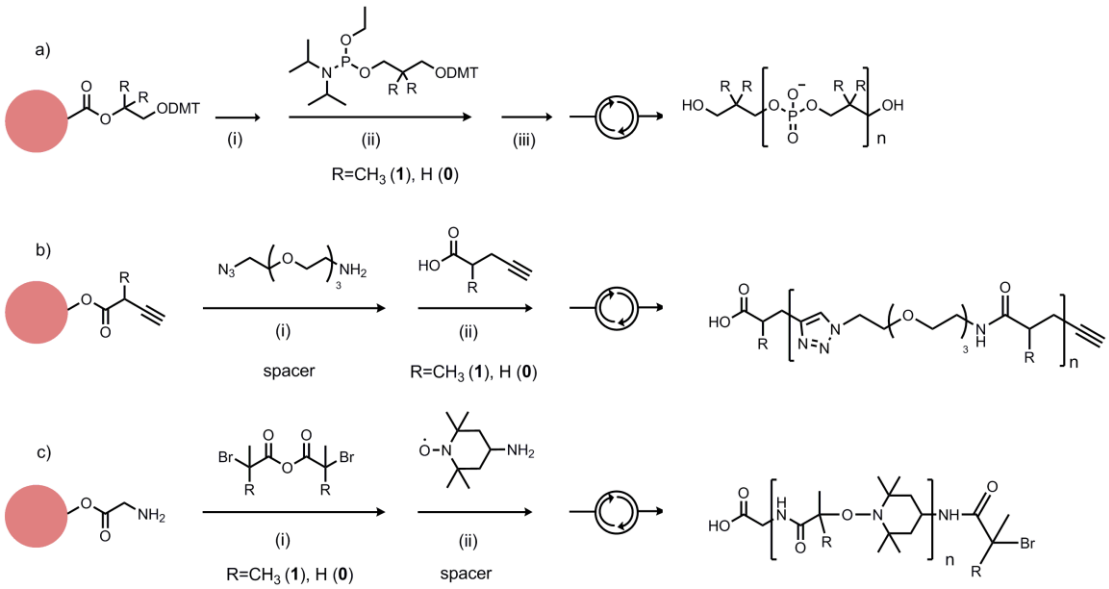

Figure 1.8: Three solid-phase synthesis approaches for the synthesis of sequence-defined oligomers. The sequence is provided by different monomer substitutions (R = methyl or hydrogen) (a) Phosphoramidite chemistry, with three steps (deprotection (i), coupling (ii) and oxidation (iii)) repeated in sequence; (b) click chemistry for the addition of a spacer (i) and amidation for the coupling of the information monomers (ii); (c) nucleophilic substitution for the addition of the information monomer (i) and nitroxide-radical chemistry for the spacer (ii).

In all examples the methodology is the same: there are two monomers with different substituents (hydrogen or methyl groups) that can be differentiated by mass spectrometry. The monomers are bonded together using quantitative reactions that happen within minutes. In Figure 1.8a, each addition involved a coupling, an oxidation and a deprotection step, whereas in 1.9b and 1.9c that was reduced to a coupling and addition of a spacer. Libraries of short sequences have been built that can be put together to generate longer oligomers in few steps,[38] and sequence-defined polyphosphates with DP of over 100 and perfect polydispersity were synthesized making use of DNA synthesizers.[39]

Another very promising approach was presented by Johnson et al.[40] They created long oligomers with control over the sequence and the stereochemistry thanks to an iterative

exponential growth technique (Figure 1.9). Their initial monomer had an epoxide and a protected alkyne. They divided the monomer in two different batches: in one of them they opened the epoxide to form an azide, and proceeded to protect the alcohol. In the other monomer batch, they deprotected the alkyne. They coupled both batches by CuAAC, which produced a dimer that presented an epoxide on one side and a protected alkyne on the other. The repetition of this process allowed the exponential chain growth of the oligomer. They synthesized up to 30-mers with this methodology. Moreover, introduction of different protecting groups on the alcohol allows for selective polymer post-functionalization.

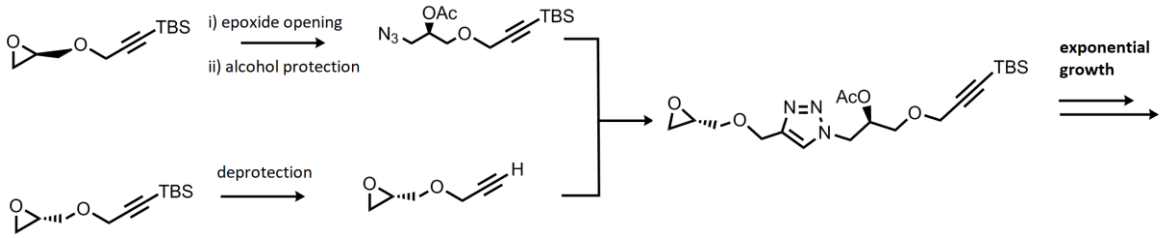

Figure 1.9: Oligomer growth via epoxide opening-alkyne deprotection and click chemistry. Half of the material synthesized in each step will be reacted on the epoxide end of the molecule to produce an azide. The other half of the material will have its alkyne deprotected. Coupling between them allows for the exponential growth of the oligomer in each step of the synthesis.

Meier and co-workers used iterative multicomponent reactions to synthesize sequence defined oligomers with variable side-chains. In one example, they used Passerini three-component reactions to synthesize a decamer in gram scale (Figure 1.10).[41] Variation in the aldehyde component in each step allowed for the introduction of ten different side chains. A final introduction of an olefin in the macromolecule allowed for the self-metathesis to form the corresponding 20-mer. In another example, they used the Ugi four-component reaction to synthesize a tetramer with four different side chains (the amine component was modified in each cycle), and a pentamer with ten distinctive side chains (both the amine and the isocyanide were varied).[42]

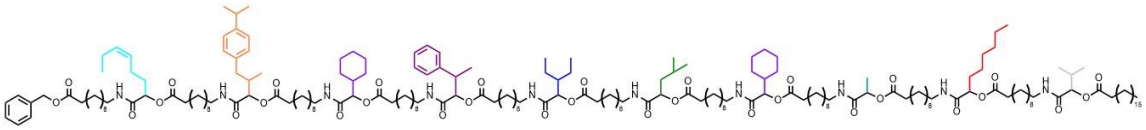

Figure 1.10: Sequence-defined decamer synthesized by Meier and co-workers. The sequence is given by the different alkyl and aryl side chains added in each step of the oligomer growth.

Another solution-phase example for the synthesis of sequence-defined oligomers was provided by Livingston and co-workers.[43] They synthesized polyethers on a three-armed macromolecule. This strategy permitted the efficient sieving of unreacted components and "reaction debris" from the tri-branched growing oligomeric chain. The different ethers carried distinct side chains that permitted the site-selective introduction of functionality once the oligomerization process was over.

Perhaps one of the most sophisticated examples to date to synthesize sequence-defined oligomers was presented by Leigh et al.[44] They developed a molecular machine capable of synthesizing monodisperse oligopeptides (Figure 1.11). It consisted of a thread (orange axle) with several amino acids appended on it by weak phenol ester bonds (colored spheres); and a macrocycle (blue ring) with a reaction "initiation site" in it (yellow-gray-gray spheres). Once the macrocycle and the thread had been assembled into a rotaxane, the ring could only move in one direction due to thread being stoppered on one side (big, orange sphere). The ring was not able to advance along the axle until the amino acid was removed from it and added onto the growing oligopeptide sequence. A free thiol at the beginning of the initiation site (yellow sphere) cleaved the weak phenol esters, and then the recently "picked up" amino acid was transferred at the end of the growing chain (gray sphere) by an intramolecular reaction between the terminal amine of the sequence and the newly formed thioester. This process was repeated four times. The molecular machine produced a single tetrapeptide that was later cleaved from the ring and isolated pure.

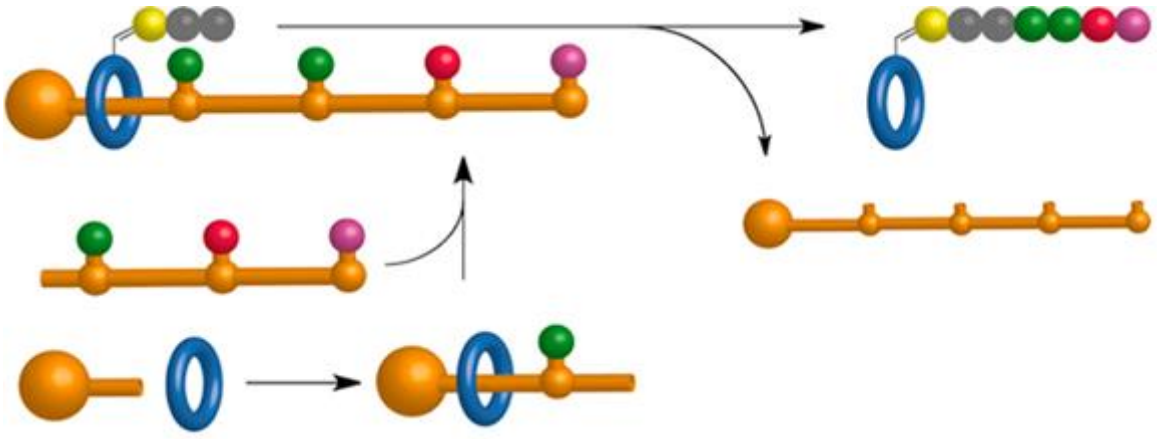

Figure 1.11. Schematic representation of a synthetic molecular machine capable of synthesizing monodisperse sequence-defined oligopeptides. The orange thread represents a rigid elongated molecule along which the rotaxane will move. The thread is functionalized at different locations with amino acids (colored circles) and capped by a bulky triaryl group (big orange ball) that prevents the rotaxane ring from dethreading. The ring is represented by the

blue ring, which is functionalized with three amino acids that act as an initiator sequence (yellow-gray-gray spheres) on which the peptide growth progresses as the ring moves along the thread. Reprinted with permission from the American Chemical Society, from reference 44.

It is envisioned that a potential use of these families of sequence-defined molecules would be data storage.[46-46] Having oligomers with different monomeric units, acting as 1's and 0's in a binary code fashion (Figure 1.12), could lead to the creation of molecules in which information would be written by synthetic methods and read by spectrometric techniques.

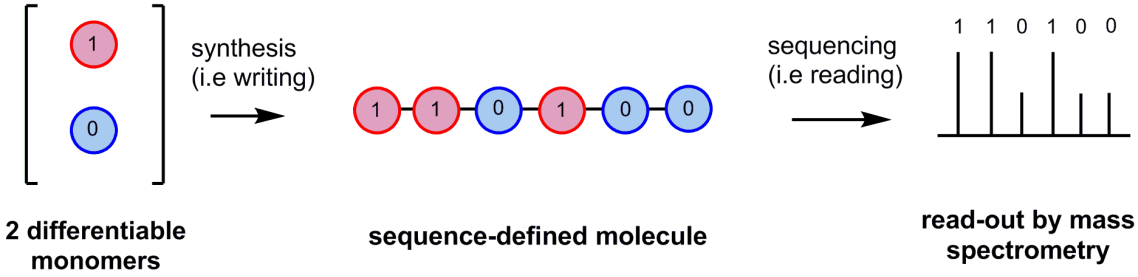

Figure 1.12. Two main conditions necessary to store information in synthetic polymers: having a writing method (i.e. synthesis of the molecules) and a reading method (i.e. sequencing of the polymers).

All the examples introduced in the previous sections to produce sequence-controlled materials would lack the ability to be amplified and evolved, because they cannot act as templates for the synthesis of the complementary strand. The best strategy to make functional materials capable of selection and evolution, then, would piece together a synthetic approach capable of yielding long sequence-defined oligomers and a monomer design bearing functionalities that would allow the templating of complementary molecules.

1.4 Template reactions for polymer synthesis

1.4.1 Mechanistic aspects

Complete kinetic descriptions of template reactions are available.[47,48] For the purposes of this dissertation, only cursory description is provided below. Consider two molecules of a substrate of initial concentration $[S]_0$ that can be coupled together with a bimolecular rate constant k_2, in an intermolecular reaction to give a product P.

$$S + S \xrightarrow{k2} P$$

This reaction will have an initial rate, in the absence of a template:

$$Rate\ untemplated = k_2 [S]_0^2$$

When the substrate is in the presence of a template T with, for example, two binding sites that bind with identical binding constant (K_M), two different complexes can be formed.

$$S + T \overset{K_M}{\rightleftarrows} ST \qquad K_M = \frac{[ST]}{[S][T]}$$

$$S + S + T \overset{K_M^2}{\rightleftarrows} STS \qquad K_M^2 = \frac{[STS]}{[S]^2[T]}$$

Now the two substrates can react unimolecularly to form the T·P complex with a rate constant k_1.

$$STS \xrightarrow{k1} TP$$

The rate of this intramolecular reaction will be:

$$Rate\ intra = k_1[STS] = k_1 K_M^2 [S]^2[T]$$

Therefore, the rate of the reaction in the presence of the template will be the sum of the rates of untemplated reaction and intramolecular reaction.

$$Rate\ templated = Rate\ untemplated + Rate\ intra$$

How much faster the intramolecular reaction proceeds compared with the intermolecular is defined as effective molarity (EM), and describes the effectiveness of the template.

$$EM = \frac{k1}{k2}$$

The rate enhancement due to the presence of the template will be the ratio between the rate of the untemplated reaction and the rate of the templated one:

$$Rate\ enhancement = \frac{Rate\ templated}{Rate\ untemplated}$$

$$= 1 + \frac{EM\ K_M^2\ [S]^4}{2\ [S]_0^3}$$

There are then three key parameters that will determine the effect of said template in the coupling of two molecules:

1. K_M: is a measure of how well the molecules bind to the template
2. EM: is a measure of how much faster the product formation goes when the substrate is bound to the template when compared with the free substrate
3. $[S]_0$: the initial concentration of reacting molecules. Low concentrations diminish the concentration of the substrate-template complex and therefore afford insignificant template directed reaction. On the other hand, at high concentrations the intermolecular reactions compete. It has been calculated that the ideal concentration for a maximum rate enhancement is $[S]_0 = 3/(4K_M)$. [47]

Notably, in purely polymeric techniques such as radical polymerization, there is another factor to be considered. When the system does not have a sufficiently high K_M, monomers start reacting in an untemplated fashion. But this growing chain may reach a critical length *l*, after

which the chain binds to the template. These two cases permit classifying template reactions in two different types:[48]

1. Type I, or zip mechanism, when the K_M is high enough for all the monomers to bind to the template and then react between themselves.
2. Type II, or pick-up mechanism, when the K_M is not very high and the binding to the template occurs once the reaction has already been initiated in the solution (Figure 1.13).

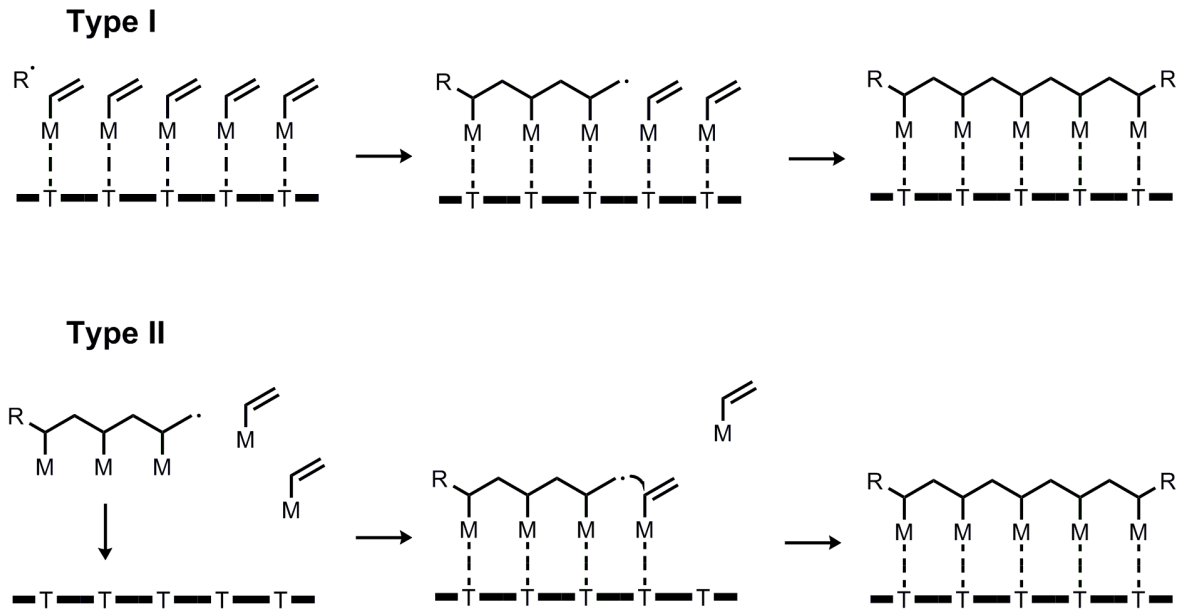

Figure 1.13: Schematic representation of Type I and Type II templated reactions mechanisms.

It is common to find systems that present behaviors that are in between both ideal types. Now that the factors that affect template reactions and the different mechanisms involved have been introduced, a few examples will be given of the different possible definitions of template.

1.4.2 Types of template

The word "template" has been extensively used in scientific literature over the past few decades, and what constitutes a "template reaction" can be the cause of debate.[49] It is therefore of great importance to categorize the basic concepts of the field. The existing literature can be classified in different categories, depending on how the word template has been used:

a) A template can be a factor that affects the length and dispersity of polymers when compared to the same reaction in absence of the template. *It changes the characteristics of the final product or product distribution.*

b) A template can be something that organizes an assembly of atoms in a specific way, allowing the formation of a single product when other possible products could be formed. *It favors a specific reaction pathway over competing reactions.*

c) A template can be something that promotes the synthesis of the same macromolecule or of a molecule complementary in length and sequence. *It can create its own replica or complementary partner.*

Scientific literature has used the word template as an "umbrella term" during the past few decades, so processes with vastly different levels of sophistication have been similarly labelled. In the next few sections we will provide examples of template reactions that fit the three different categories here presented.

1.4.3 Templates that change the characteristics of the final polymer product distribution.

The idea of having a polymer affecting the reaction of monomers was introduced by Szwarc[50] after reading some early work by Melville and Watson.[51] He stated that a chain inducing any kind of change in the synthesis of a polymer (in its molecular weight, dispersity, tacticity, etc.) is acting as template.[52] In the earliest examples, the template effect relied on the presence of homopolymers that interacted specifically with one of the monomers. For example, high molecular weight poly(2-vinylpyridine) was shown to act as template by yielding small blocks of poly(L-alanine) when L-alanine and sarcosine were copolymerized.[53] The copolymerization of styrene and methacrylic acid in the presence of poly(2-vinylpyridine) gave blocks double the size compared to those afforded by the same polymerization in the absence of template.[54] Both examples show that in this case the template induces ordering of the monomers that affects their distribution in the final chain.

One nice example of a template effect was presented by Hattori and co-workers.[55] A study was done on how the incorporation of adenine-functionalized styrene monomers in polystyrene chains affected the polycondensation of thymine-functionalized di-*p*-nitrophenyl methylsuccinate monomers and theophylline-functionalized monomers (a homolog of nucleic acid bases unable to interact with adenine). The presence of adenine-functionalized polystyrene greatly increased the rate of reaction and the final yield of the thymine-containing polyamide but induced no change in the theophylline one (Figure 1.15).

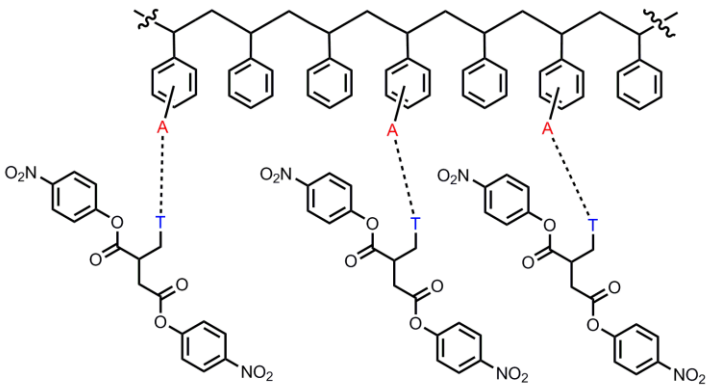

Figure 1.15. Styrene chains functionalized with adenine units (A) template the polycondensation of monomers bearing thymine functionality (T), by inducing organising the monomers to facilitate the reaction.

O'Reilly et al. prepared low molecular weight block copolymers of styrene and thymine-functionalized styrene (PSt-b-PVBT) which in chloroform self-assembled to form micelles.[56] The adenine-functionalized styrene monomer (VBA) was insoluble in chloroform, but dissolved in the presence of the micelles by entering inside their core thanks to the interactions between the complementary nucleobases. Upon addition of initiator and heating, the VBA polymerized to give high molecular weight chains (up to 400,000 g/mol) with very low polydispersity (PDI < 1.1). This low polydispersity was possible thanks to the segregation of the propagating radicals inside the discrete micelle cores and the template effect of the complementary nucleobases (Figure 1.16). Polymerization of the VBA in the absence of the micelles gave uncontrolled polymerizations with low molecular weight products. On the other hand, attempted polymerization of VBT in the presence of the PSt-b-PVBT (non-complementary interactions) produced low molecular weight chains that had grown outside the micellar environment.

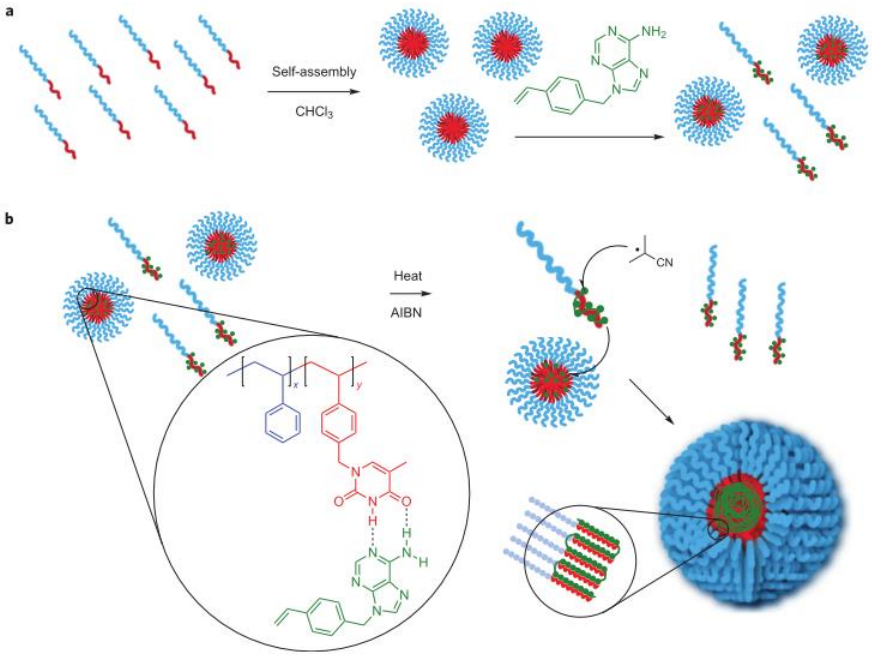

Figure 1.16: A block copolymer of styrene (blue wavy lines) and thymine-functionalised styrene (red wavy lines) self-assembles into micelles in chloroform. Strong complementary interactions between the core of the micelle and an adenine-functionalised styrene monomer promotes radical polymerization of the monomers inside the micelles. Reprinted from reference 56 with permission from Springer Nature.

In general, the type of reactions that fit in this first category are still very far from the final goal of creating artificial polymers capable of self-replicating. Almost all the examples in literature deal with homopolymers, or block copolymers in which the second block does not bear a H-bond interacting unit, and is only there for structural purposes. The template does not create a replica or complementary strand of similar length and dispersity, but merely affects some properties of the final polymer. Nonetheless, the first examples in literature broke ground in the field of studying interactions between a template polymer strand and monomeric units, and were the inspiration for subsequent, more sophisticated studies.

1.4.4 Templates that promote one reaction

It is possible to create a sub classification within this definition of templated reactions:

a) A template can be something that acts as a mould
b) Or it can be something that promotes a reaction due to the specific order in which different parts of the product are assembled.

Regarding the first case, there is multitude of examples in literature making use of different supramolecular interactions. To name one, Sanders and co-workers synthesized cyclic porphyrins of different sizes using Glaser-Hay coupling and polypyridine-metalloporphyrin recognition (Figures 1.17).[57]

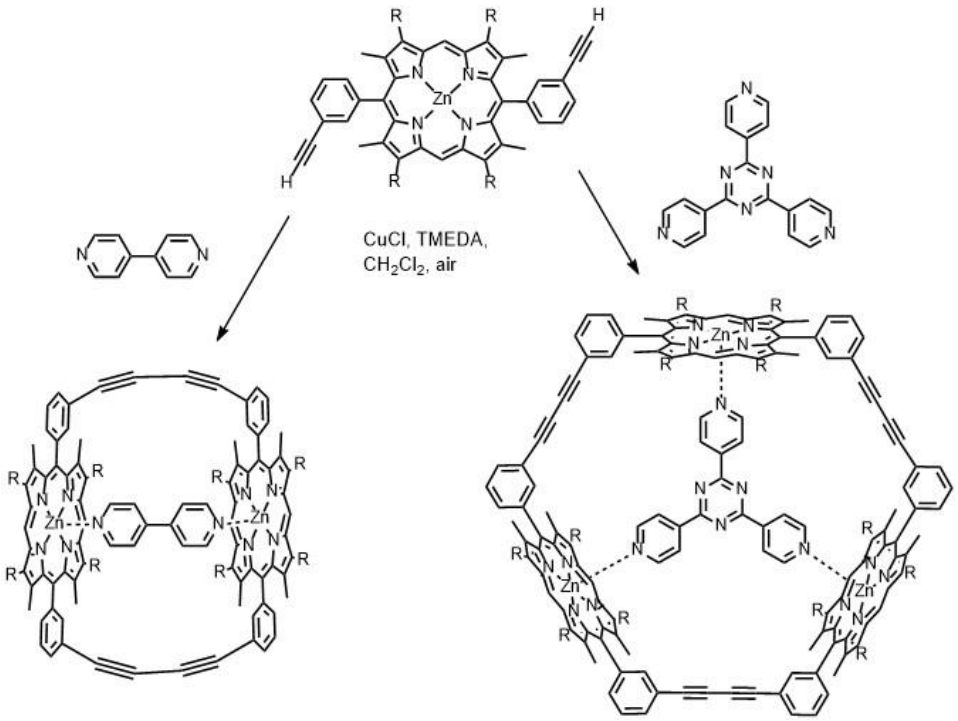

Figure 1.17: Dimeric and trimeric porphyrin macrocycles templated using bidentate and tridentate ligands, respectively.

The first step for template reactions using either 4,4'-bipyridine or tripyridyltriazine is the combination of two porphyrins to form a linear dimer. In the presence of the bidentate template the dimer adopts a conformation in which cyclization is favored. Conversely, linear dimer in the presence of tridentate template reacts intramolecularly with a monomer unit to form a linear trimer. This molecule now has the right conformation to form the trimer cycle. Moreover, when

the linear dimer is in the presence of a tetradentate template, reaction to form the linear tetramer occurs, which can later cyclize into the ring with four porphyrins.

The most studied technique that makes use of a template to promote a reaction is DNA-templated synthesis (DTS).[58] Reactive building blocks (BBs) are placed at the end of a DNA strand that will recognize its complementary partner forming a sequence-selective duplex that brings the two BBs close to each other (Figure 1.18). The strength of this technique is the capacity of synthesizing many templates with BBs that will only bind to their complementary strands even in a very complex mixture (i.e. there is a reaction selectivity between BBs encoded in the DNA template sequence). Moreover, this strategy is compatible with different coupling chemistries between BBs.

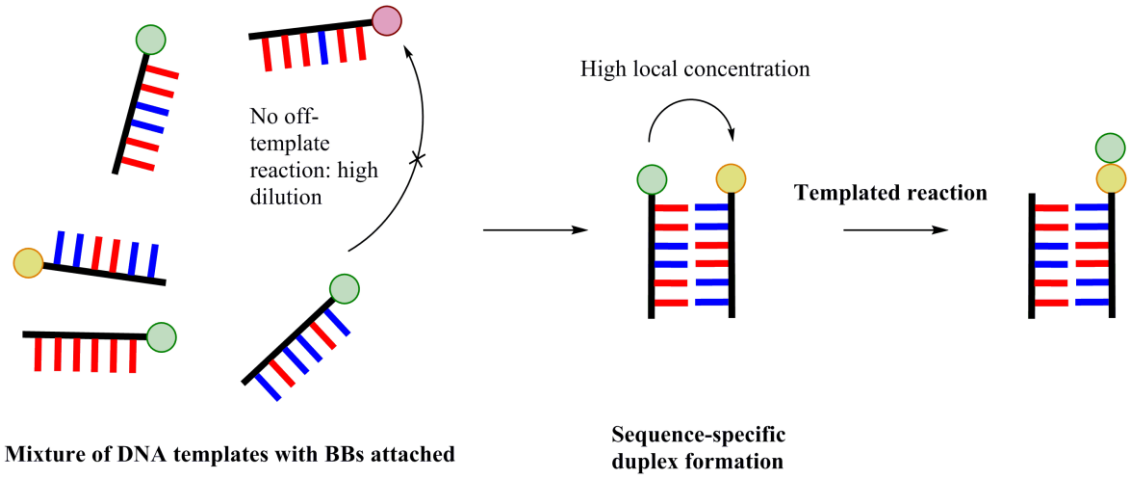

Figure 1.18. Schematic representation of reaction between building blocks (colored circles) at highly dilute concentrations due to their attachment to DNA strands. Sequence-specific DNA duplex formation permits the reaction between BBs in close proximity, leaving the rest of BBs unreacted.

The same underlying concept can be found in nature in Ribosomal Peptide Synthesis, in which base pairing between aminoacyl transfer RNAs carrying an amino acid and a ribosome-bound mRNA template induces peptide bond formation. Since this process can direct multiple reactions sequentially, sequence-defined peptides are obtained. An equivalent synthetic process can be engineered so libraries of macromolecules can be prepared without the need of ribosomes. Different DNA architectures and strategies have been studied for the preparation of these libraries. One of the simplest possible designs consists of a long template that hybridizes in parallel several different codons, each one of them carrying a BB (Figure 1.19). Once the template is fully hybridized, the BBs can be oligomerized, and the codons removed from the template.

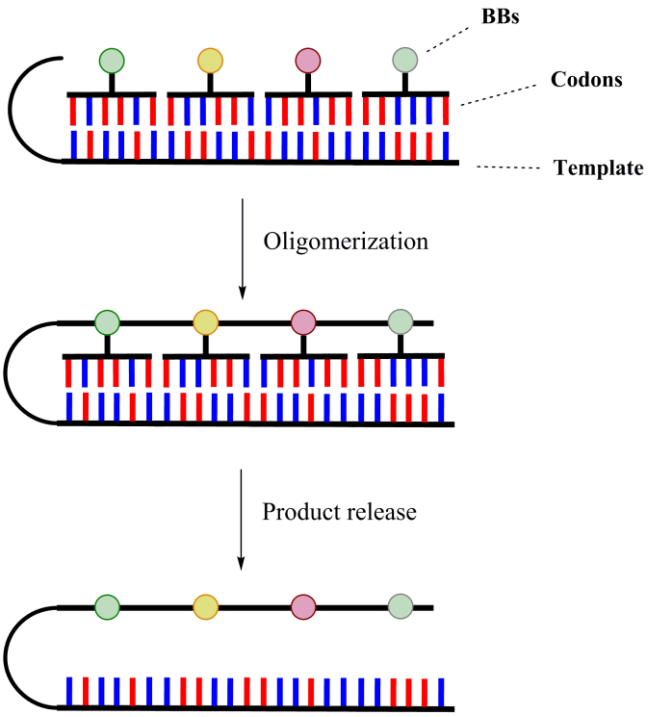

Figure 1.19. Schematic representation of a templated oligomerization. Building blocks are attached to DNA codons, which form a sequence-specific duplex with a DNA template. Reaction between adjacent BBs permits the formation of a sequence-defined oligomer encoded in the DNA sequence.

The final product is an oligomer attached to a DNA template that codes specifically the sequence of the oligomer it carries. A library of macromolecules can be created and run against a target to determine which sequence binds with a better affinity. Those templates attached to molecules with positive results can be amplified through PCR, mutated, and refined until finding the optimal sequence for binding the target.

In an example of what a powerful tool DNA templated synthesis is, Liu and coworkers translated a DNA template into fully synthetic, structurally unrelated macromolecules of up to 26 kDa (Figure 1.20).[59] For that, they created peptide nucleic acids (PNA) aptamers functionalized via cleavable linkers with polymer "building blocks" with reactive ends. They proceeded to hybridize the PNA aptamers with the DNA templates, and the polymer building

blocks were linked together. The newly formed macromolecule was cleaved from the DNA-PNA double strand.

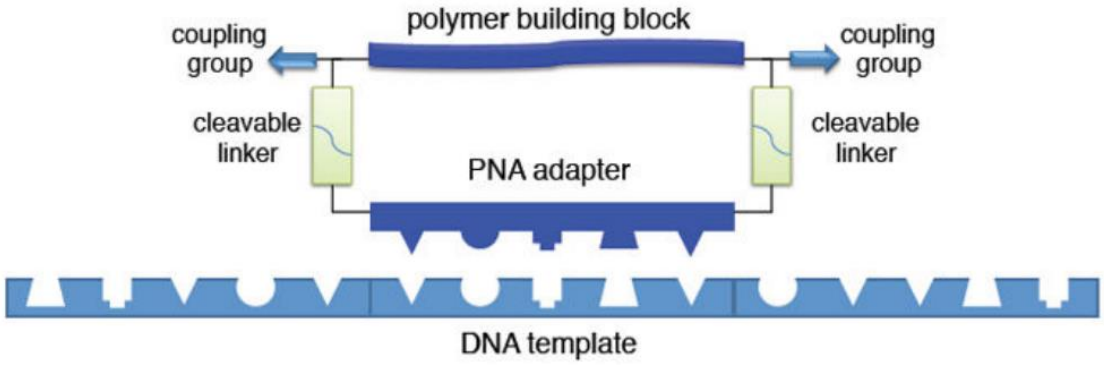

Figure 1.20. Schematic representation of the strategy to translate DNA into an artificial polymer sequence. The macrocycles are formed by a PNA aptamer that hybridises selectively with the DNA template; a polymer backbone with coupling groups at both ends to bind together adjacent macrocycles; and a cleavable linker to separate the DNA-PNA double helix and the newly-formed polymer once the translation process is completed. Reprinted from reference 59 with permission from Springer Nature.

The polymer building blocks were based on polyethylene glycol (PEG) chains of different lengths, β-peptides and α-(D)-peptides with a variety of proteinogenic and non-proteinogenic aryl, alkyl, amino and carboxyl side chains. To couple the building blocks they tested two strategies: linking together "AB" building blocks, and "AA" with "BB" macrocycles (A and B being the reacting groups). Five different chemistries were tested: amine acylation, reductive amination, oxime and hydrazine formation and CuAAC. They reported that the use of AA/BB macrocycles to prevent intramolecular cyclization, and the use of CuAAC chemistry were fundamental for achieving sequence-specific translation of the DNA template. This strategy afforded full-length products coming from 16 consecutive, sequence-specific codon-anticodon interactions. These polymeric chains were successfully submitted to full cycles of translation, purification, PCR amplification and re-translation. When the coupling reactions of the building blocks were done in the absence of template, several high molecular weight products with non-specific sequences were obtained.

Although this work lays the foundation for the development and evolution of fully-synthetic polymers unrelated to DNA, it still relies completely on the use of DNA templates, and the sequence specificity comes from PNA building blocks.

1.4.5 Templates that create a replica/complementary macromolecule

Most of the literature that fits in this category of templated reactions is related in one way or another with DNA. There are examples of templating the synthesis of complementary strands using many strategies: making use of different coupling chemistries; linking together mononucleotides, codons of different lengths or ligating longer oligomers; making use of enzymes; modifying some of the DNA components (nucleobase, sugar, backbone), etc. In general, strategies for templating DNA or DNA-related macromolecules are well understood. Some examples of this research are given below.

Bohler, Nielsen and Orgel presented in 1995 the first report of a DNA-templated synthesis of an oligomer with a non-natural backbone.[60] They oligomerized five PNA guanidine dimers using a cytosine 10-mer template via amine acylation. The reported yield was only 25%, and the sequence specificity could not be determined as the oligomerization proceeded in the absence of some complementary PNA dimers, or even template. In 2000 Saito and co-workers reported the DNA-templated photochemical [2+2] cycloaddition of five DNA 6-mers that contained a 5'-exocyclic vinyl group and a 3'-pyrimidine, using a complementary 30-mer guanine template (Figure 1.21).[61]

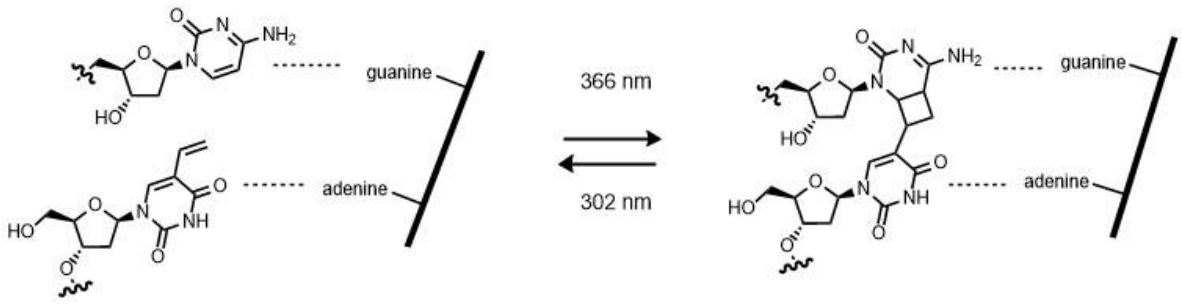

Figure 1.21: Photoreversible templated ligation of pyrimidine units via photochemical [2+2] cycloaddition and complementary interactions with a guanine template. Exposure to a 302 nm wavelength reverses the ligation process restoring individual oligonucleotides.

Two years later Lynn and co-workers used an adenosine 8-mer template to oligomerize a 5'-amino-3'-formyl thymine mononucleotide via reductive amination (Figure 1.22).[62] The full 8-mer was synthesized with over 80% yield, and no molecules larger than octamers were seen.

The reaction did not proceed without the template and the use of mixed adenosine and thymine templates showed that non-complementary interactions did not allow the reactions to continue.

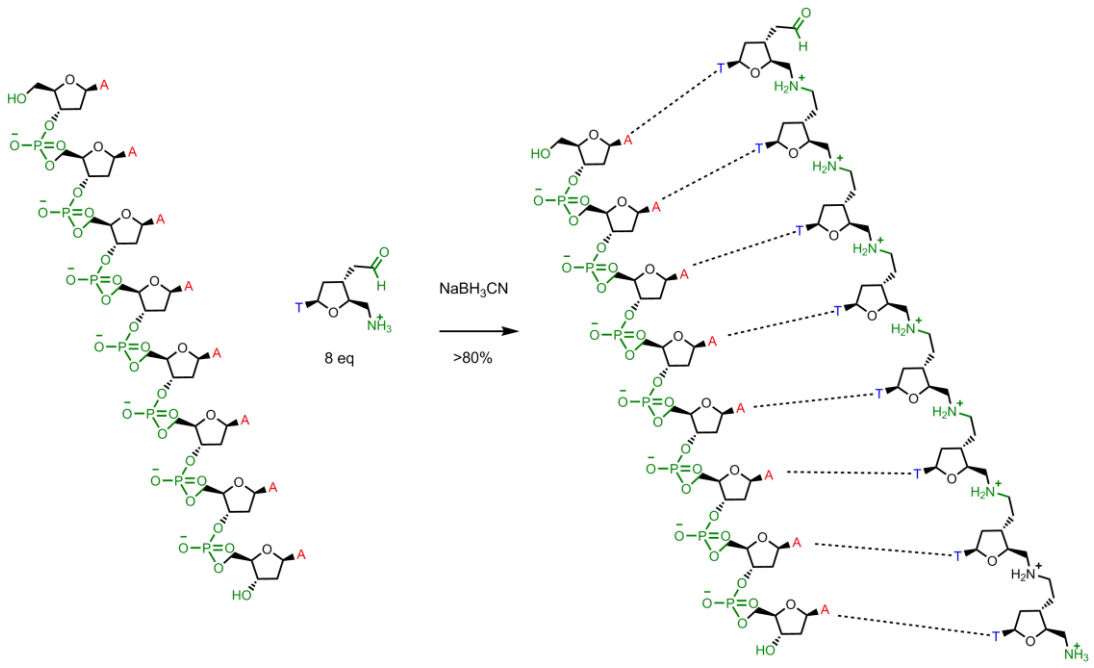

Figure 1.22. Oligomerization of 5'-amino-3'-formyl thymine mononucleotide using an adenine 8-mer template via reductive amination.

Sleiman et al. used efficient adenine-thymine recognition to template the formation of low-polydispersity polymers via Sonogashira coupling (Figure 1.23).[64] The thymine-bearing template was first prepared via ring-opening metathesis. The template effect was demonstrated by comparing the results of the polymerization in the presence of the template, without the template, and in the presence of a template bearing a non-complementary nucleobase. In the templated polymerization with complementary nucleic acid bases, the degree of polymerization was comparable to that of the template (around 25 monomeric units) with similarly low polydispersity (PDI ca. 1.2). On the other hand, non-templated Sonogashira polymerization gave chains no longer than 11 units and PDI of around 2.77. When the incorrect template was used, 7 unit-long chains were obtained with a polydispersity of 2.2.

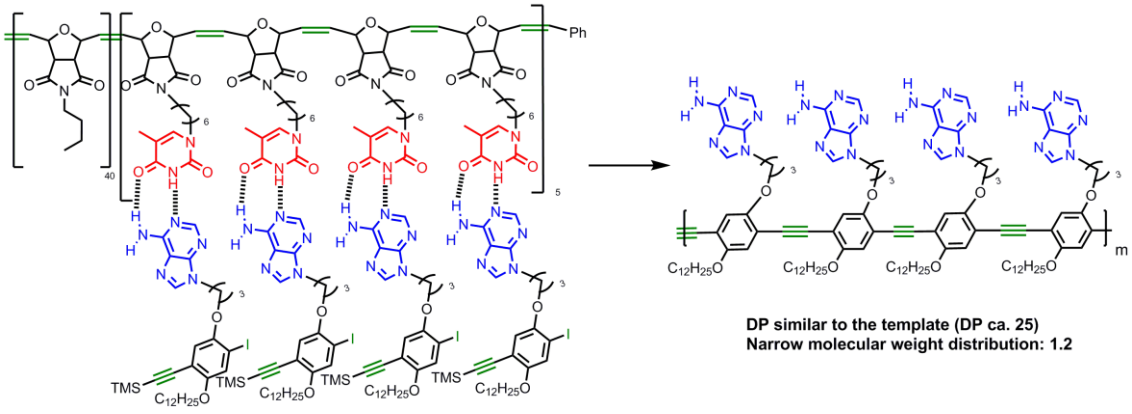

Figure 1.23. Templated synthesis of oligomers via Sonogashira cross-coupling.

In another example, Sawamoto et al. presented a series of papers based on bifunctional template initiators capable of undergoing cationic polymerization and ruthenium-catalized radical addition.[65-67] Both reacting sites were placed in *ortho* position to each other, ensuring their proximity. In the first study, they demonstrated the template effect in selective radical additions of methacrylic acid (MAA) over methyl methacrylate (MMA) with an amino-functionalized template initiator. The ammonium ions recognized the acid monomer via ionic/H-bonding interactions and improved the radical reactivity more than ten times relative to non-templated systems (Figure 1.24). In a continuation of this study, longer template chains were synthesized. The effectiveness of the template was again evaluated by comparison with template initiators bearing the functionalities in *meta* position and with initiator without template functionality. MAA reacted at faster rates than MMA in all cases. But when the template initiator had the reactive sites in *ortho* position to each other the rate increased 40-fold. These results prove how specific interactions between ammonium groups and MAA and a fixed-point initiation of the templated reaction were fundamental in the polymerization reaction.

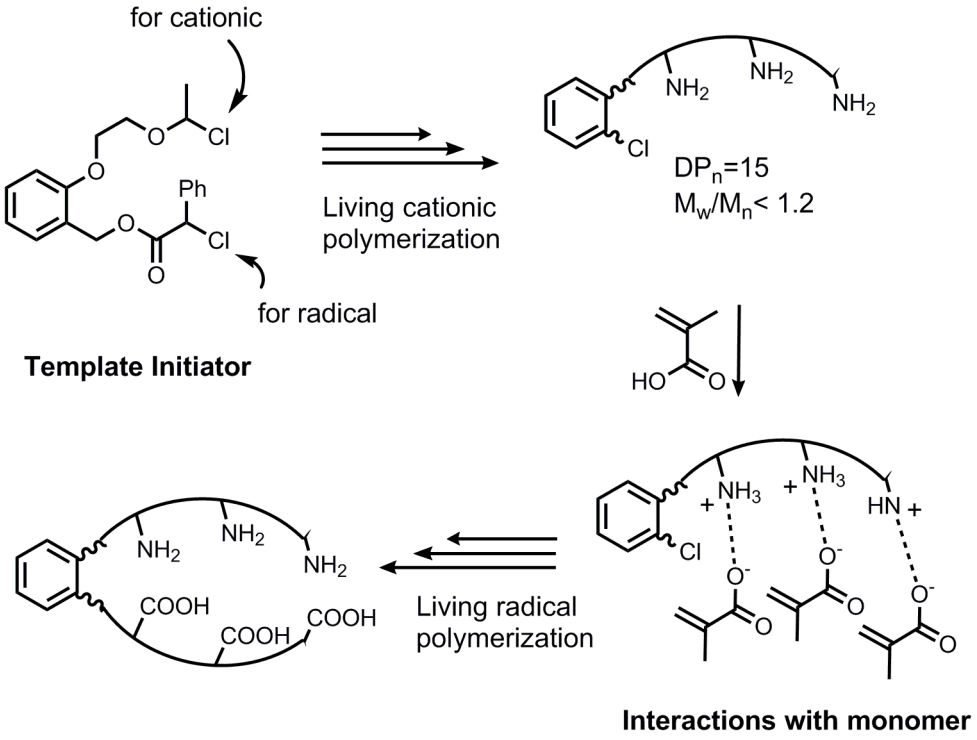

Figure 1.24: General scheme for templated polymer synthesis using an *ortho*-functionalized template initiator. An initial cationic polymerization on one reacting site of the initiator produced a polyamine chain. That chain acted as a template on the radical synthesis of methacrylic acid oligomers thanks to ionic/H-bonding interactions between the polyamine template and the reacting monomers.

During the past 10 years Liu and co-workers have presented a series of related papers that reveal the great extent to which DTS strategies can be effective. The efficiency and sequence specificity of the polymerization of PNAs using codon templates containing the four nucleic bases (5'-AGTC-3') was studied. Formyl-PNA anticodon sequences (NH_2-gvvt-CHO) were synthesized. The first and fourth nucleic acid bases of each anticodon (g and t) were complementary to the bases from the codon templates (A and C). The two units in the middle of the sequence (v) were changed between anticodons with different combinations of g, a and c. When all possible combinations of PNA tetramer anticodons were in the presence of a template with 10 codon units, only the fully complementary PNA NH_2-gact-CHO reacted to form a chain with 40 nucleobases, with yields higher than 90%.[63]

Moreover, when one mismatch was purposely introduced in the PNA template in one of the codons (in some cases the mismatch being changing just one of the four nucleobases), the oligomerization reaction did not proceed any further than the codon preceding the mismatch (Figure 1.25).

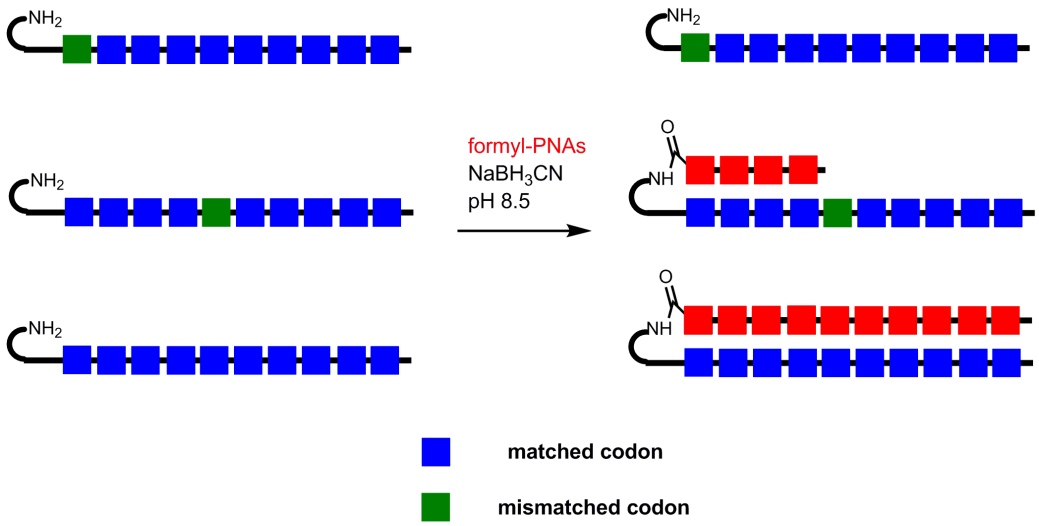

Figure 1.25. Schematic representation of the efficient recognition of mismatches in the template by the PNA anticodons. Each codon and anticodon comprised four different nucleic acid bases, and they were ligated by reductive amination. Mismatches were introduced on the codon sequences. When the mismatch was placed in the first codon (green square), no templated reaction took place. When the mismatch was placed in the fifth codon, the templated reaction produced a PNA tetramer of anticodons (red squares). If no mismatched codon was introduced, full length duplex formation allowed the creation of a PNA decamer.

1.4.6. Covalent template reactions

There are also a few examples of covalent interactions being the driving force of the templated reactions between the mother chain and the free monomers. Covalent bonds present the advantage of allowing templating under a wider range of conditions that are not compatible with non-covalent interactions.

Luh et al. employed this approach over the past decade on several occasions. In all their examples they used ROMP to polymerize norbornene- or cyclobutene-containing monomers to form the template.

Their initial work with these systems cannot be classified as templating, but it is fundamental to understand the strategies they developed in later years. In their earliest examples, they coupled two monomers that can be polymerized via a linker unit, and then used a Grubbs catalyst to generate both polymer strands simultaneously, producing a ladderphane (Figure 1.26).[68] These types of structures were characterized by, among other techniques, STM, which suggested that the systems were highly ordered, and that both strands reacted at the same time forming double-helix architectures.

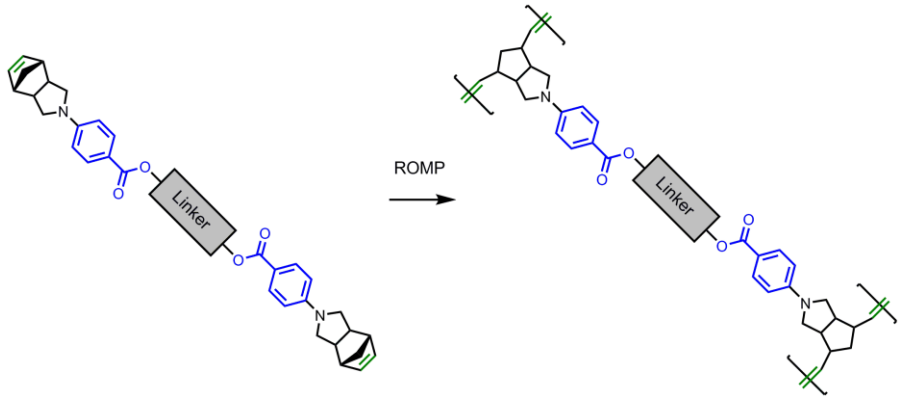

Figure 1.26. Synthesis of ladderphanes by simultaneous ROMP of two polymerizable groups coupled together by a linker unit.

In a continuation of this research, Luh and coworkers created the template and the templated macromolecule step-wise (Figure 1.27).[69-71] Linkers as diverse as porphyrins, crown ethers or ferrocene were used. In any given system, the process comprises: i) a coupling between a norbornene monomer and the linker unit; ii) the polymerization via ROMP of this first compound using a Grubbs I catalyst; iii) the condensation of another monomer unit onto the template; iv) the zip-up of this grafted structure via ROMP, forming a ladderphane; and v) the hydrolysis of this ladderphane to separate the template from the replica. This "replication protocol" relies on the fact that this type of polymerization reaction creates templates that are relatively rigid and well ordered. Once the monomers are attached to the template, all the grafted units are pointing in the same direction, which allows for an efficient zip-up process. In several of their examples both the intermediate ladderphane and the daughter strand had degrees of polymerization and polydispersity similar to those of the template. Moreover, the modification of the linker unit in this step-wise strategy permits the synthesis of a daughter strand that is identical (i.e. replication) or complementary to the template.

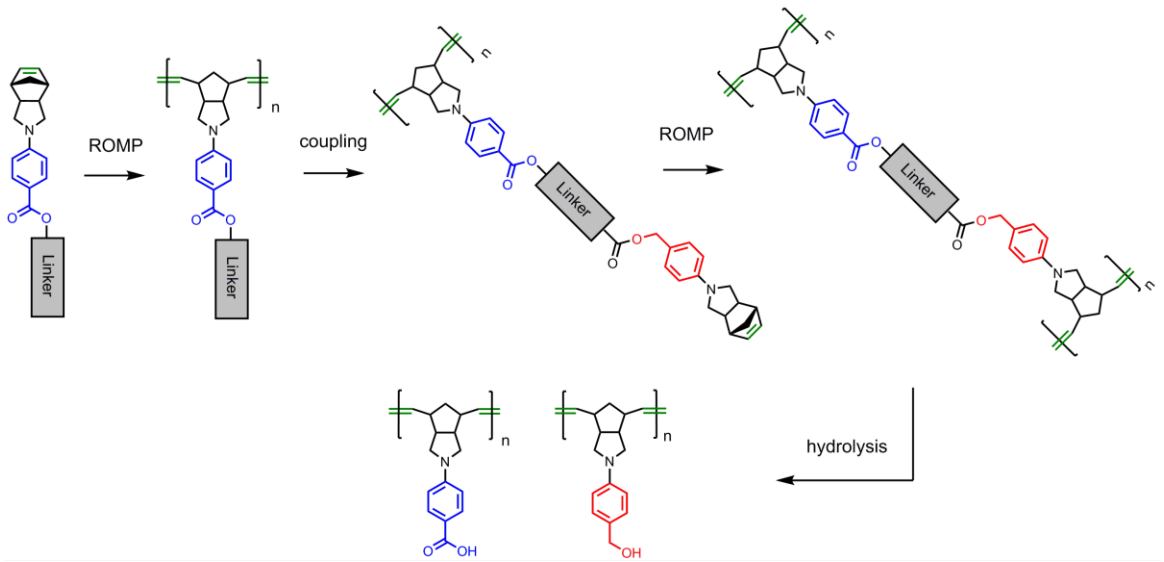

Figure 1.27. Representation of Luh's replication protocol. An initial ROMP to create the template is followed by grafting of monomer units onto that template. A second ROMP creates a ladderphane that can be hydrolyzed to produce the initial template and the daughter strand. The monomers are separated by a linker unit.

In a conceptually similar strategy, they created molecules with two independently polymerizable groups (Figure 1.28).[72] This permitted the step-wise polymerization by changing the reaction conditions. In one of their examples (Figure 1.28 a), reacting the molecule at 0 ºC induced the polymerization of the cyclobutadiene unit only. In a subsequent step, they reacted the molecule at room temperature which prompted the ROMP of the norbornene unit. The second polymerizable group, however, does not need to be constrained to ROMP. They presented a series of papers in which different reactions were used. Figure 1.28 b depicts the use of Glaser coupling to polymerize adjacent alkyne groups, but the strategy has been used with cross-metathesis and Claisen condensation as well. In all the cases Luh's group reports good agreements between the length and polydispersity of the daughter polymer chain and the template after hydrolysis.

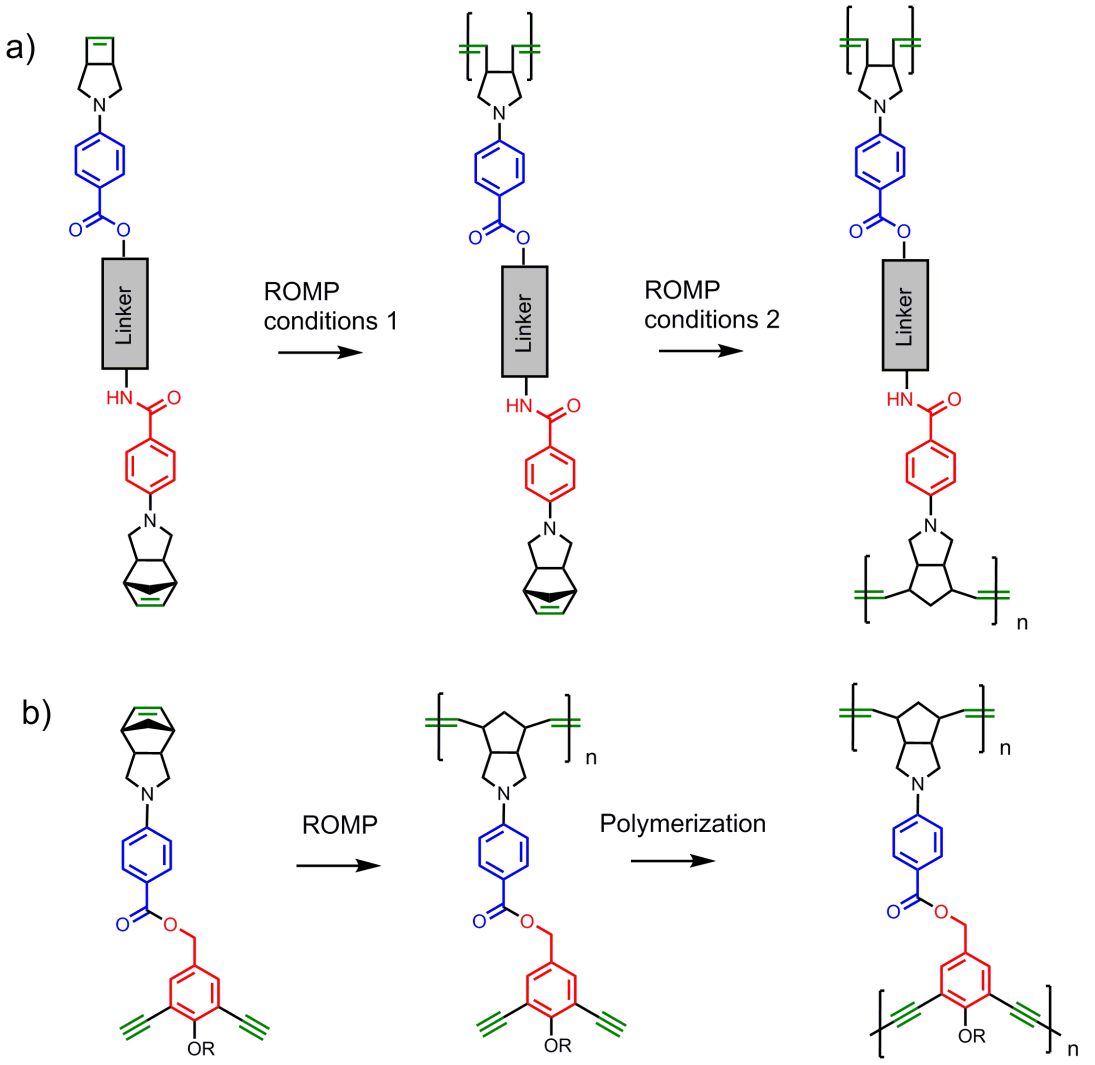

Figure 1.28. Representation of Luh's sequential polymerizations, making use of (a) two reacting groups that react under ROMP conditions at different temperatures; and (b) an initial ROMP reaction followed by Glaser coupling

Part of this work served as inspiration for some of the latest work conducted in the Hunter group. But in order to understand how the group reached the point of using covalent-templated strategies for the replication of oligomers, first a brief summary of the group's previous work in the field is necessary.

1.5 InfoMols

The next section provides an overview on where the work done in the Hunter group falls within the field of sequence-defined materials.

The Information Molecules project (InfoMols, for short) was inspired by the idea that DNA could be dissected into its different constituent parts to form what we called the DNA blueprint (Figure 1.29). Each minimum DNA unit would be formed by:

a) a recognition unit that binds to complementary recognition units, leading to base-pairing and duplex formation - the nucleobases in DNA;
b) a backbone that confers characteristics such as solubility and flexibility - the sugars in DNA;
c) chemical handles that connect monomeric units into longer chains - the phosphodiesters in DNA.

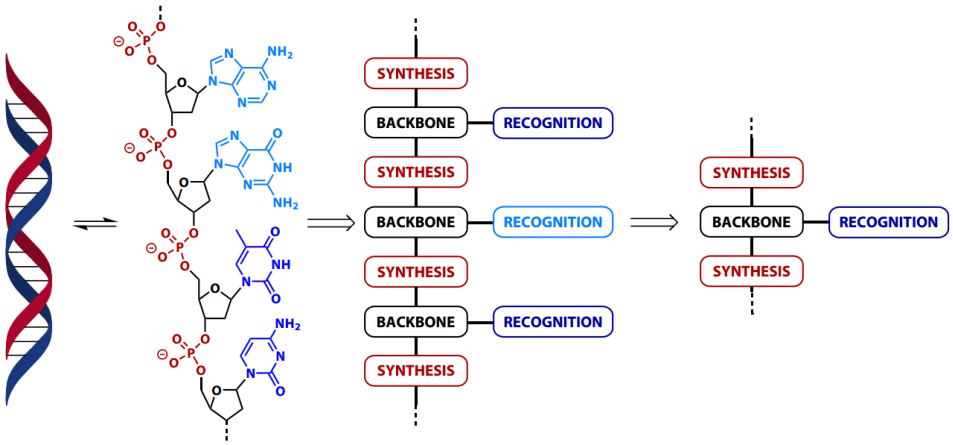

Figure 1.29: "DNA blueprint" used in the design of artificial sequence-defined oligomers in the Hunter group.

The premise of InfoMols is that this blueprint did not necessarily have to be restricted to the chemical space observed in nucleic acids. While the scientific literature is filled with examples of various changes to nucleic acid systems,[73-75] InfoMols wanted to go one step further and develop a system entirely removed from this bio-related chemical toolbox.

To accomplish that it was important to find the optimal recognition units i.e. the chemical groups that would interact with each other as strongly and selectively as possible to drive duplex formation. These recognitions units were chemical groups qualified as strong H-bond donors and acceptors.[76] Moreover, they were groups that were easy to introduce into the monomeric scaffolds that later would be grown into longer oligomers. The modular approach permitted the

study of the interactions between these strong recognition units in different chemical systems. At the time of writing, oligomers synthesized by reductive amination,[77] thiol-ene coupling,[78] Sonogashira,[79] esterification[80] and triazine chemistries had been studied.

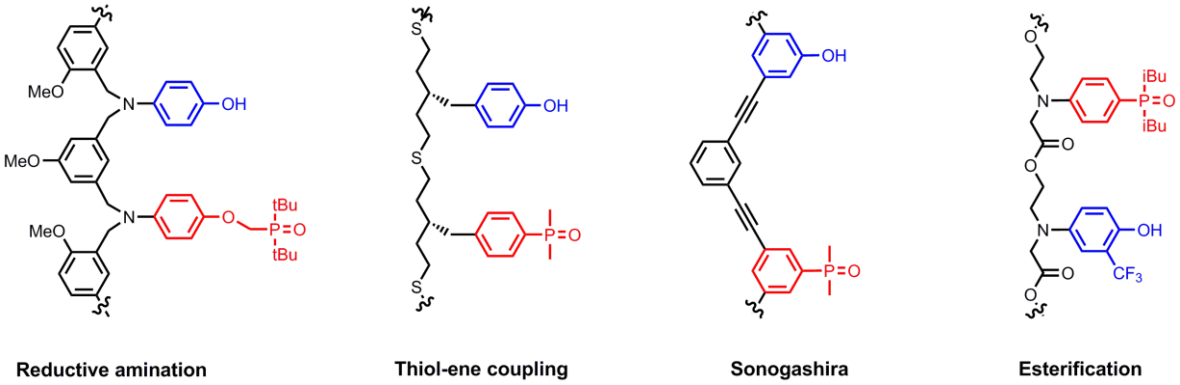

Figure 1.30: Examples of four different chemistries used to bind together monomer scaffolds into longer oligomers.

These systems fell in two categories: ones where intramolecular interactions led to backbone folding,[81] and ones where duplex formation was the preferred outcome when oligomers with complementary sequences were mixed in solution.[82] However, duplex formation required specific conditions (e.g. low solvent polarity, low temperatures, limited range of concentrations). Figure 1.31 summarizes the different supramolecular equilibria that can occur when a template and monomers are mixed in solution to perform a template reaction. At high concentrations the template can undergo duplex formation with other template molecules, in which perfect sequence complementarity might not be a requirement. Moreover, as the length of the template increases so does the probability of the oligomer folding due to intramolecular interactions. Both product inhibition and backbone folding prevent monomers from interacting with the template. Even if these inhibitory processes do not happen in significant quantity, it is still difficult to reach complete template saturation (high values of $K_{M)}$ to form a pre-zip structure in which the monomers are in close proximity for the template reaction to occur. Finally, to perform templated reactions, these systems will need to react in the conditions in which the interactions between recognition units are strong (i.e. low temperature, low solvent polarity). All these limitations with supramolecular template reactions convinced us to look for alternative template strategies.

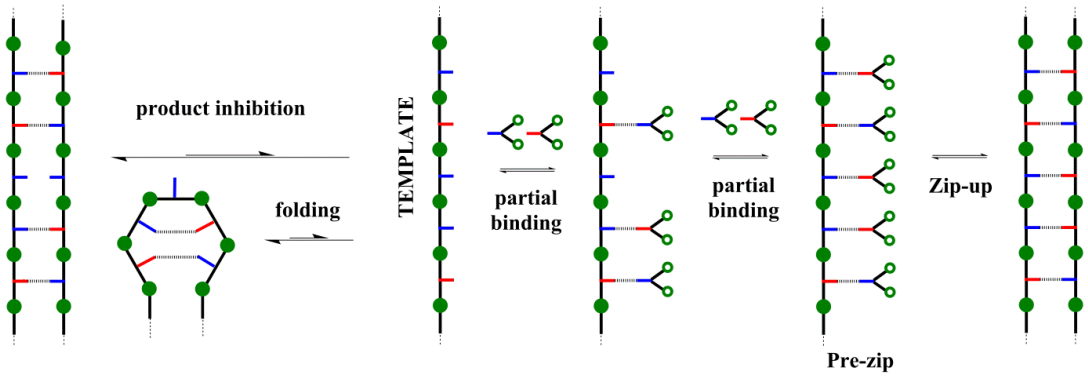

Figure 1.31: Supramolecular templating. Red and blue bars represent the two different recognition units that interact with each other via H-bonds. Several competing equilibria prevent the efficient formation of the pre-zip complex required to perform templated reactions. Blue bars represent hydrogen bond donors; red bars represent hydrogen bond acceptors; wavy lines represent the hydrogen bond interactions between red and blue bars; empty green circles represent reacting groups that can be coupled together; filled green circles represent the union of empty green circles after their coupling.

1.5.1 Covalent InfoMols

The solution we proposed in the group was to develop molecular systems in which the recognition units carry chemical handles that can react in a covalent fashion. Having robust covalent chemistry as the driver of the recognition process, instead of the weaker H-bond interactions, ensures that the template can reach saturation (effectively, $K_M = \infty$). Once again inspired by the DNA blueprint, we called this recognition process between complementary units as "base-pairing". In this case the pairs that were to react covalently and reversibly were carboxylic acid and phenol monomers.

Moreover, the examples shown so far from Luh and coworkers were making use of homo-oligomers as templates. In order to template the replication of oligomers containing both phenol and carboxylic acid monomers, an orthogonal protection and deprotection strategy must de designed to prevent intramolecular reactions from taking place on the template (Figure 1.32).

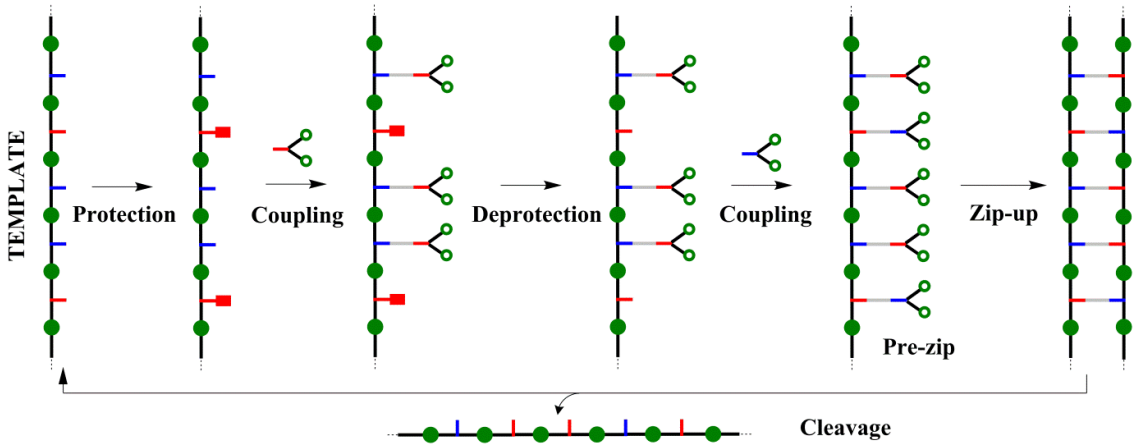

Figure 1.32. Covalent-templating. Red and blue bars represent the two different recognition units that react between each other via covalent bonds. Quantitative steps guarantee the formation of the pre-zip complex necessary to perform templated reactions. Blue bars represent carboxylic acid groups; red bars represent phenol groups; empty green circles represent reacting groups that can be coupled together; filled green circles represent the union of empty green circles after their coupling.

Therefore, a complete base-pair replication cycle of oligomers containing phenol and carboxylic acid monomers will consist of:

i) A TBDMS-protection of the alcohol units of the template;
ii) a coupling between the acid recognition units of the template and phenol monomers, to form a semi-grafted structure;
iii) a deprotection of the phenols of the template using TBAF;
iv) a second coupling between said phenols and acid monomers to form a fully grafted architecture (pre-zip);
v) a zip-up reaction of the pre-zip structure;
vi) and a hydrolysis to separate the initial template (mother strand) from the replicated product (daughter strand).

Following this strategy we ensured that all the recognition units on the template had a complementary monomer grafted to them. If the template can reach saturation, then it was all a matter of finding the conditions under which that pre-zip structure would react to finalize the templating process.

The next step in the project was to find the type of chemistry that would zip-up the grafted monomers ensuring a faithful copy of the mother strand. The reaction of choice was CuACC[83]: i) it is known to be a reliable chemistry that worked in very different reaction conditions, even

at low concentrations (we anticipated that the zip-up reaction would have to be done under high dilution to prevent intermolecular coupling); and ii) the two necessary reacting groups (i.e. alkynes and azides) can be easily introduced into a range of chemical scaffolds.

A heterotrimer composed of two carboxylic acids and a phenol (**AAP** template) was synthesized. The backbone comprised the triazoles created during the click reaction and aromatic rings that introduced a spacer between the recognition units without increasing the number of rotors. The template was subjected to a complete replication cycle which, after capping, yielded the complementary trimer (phenol-phenol-acid **PPA**) in 70% overall yield (Figure 1.33).[84] In the replication cycle a significant amount of information was lost in the undesired synthesis of two side-products. One of them was a strand with the opposite sequence (**APP** 15%) due to directionality in the backbone. The zip-up process can start with an alkyne from the first monomer reacting with the azide of the second monomer, or the other way around. The final duplex could be, then, "parallel" or "antiparallel". The other undesired product had a "scrambled" sequence (**PAP** 15%), originating from coupling between monomers in positions 1 and 3.

Moreover, zipping-up step presented two undesired features: the use of 30 equivalents of copper salt and ligand, defeating thus the catalytic purposes of said compounds, and the use of a 150-fold excess of the capping agent, to prevent intermolecular reactions once the macrocycle had been formed.

These challenges can potentially be overcome by modifying the synthetic design of the system. Early work into this modified strategy is presented in Chapter 2, 3 and 4 of this thesis.

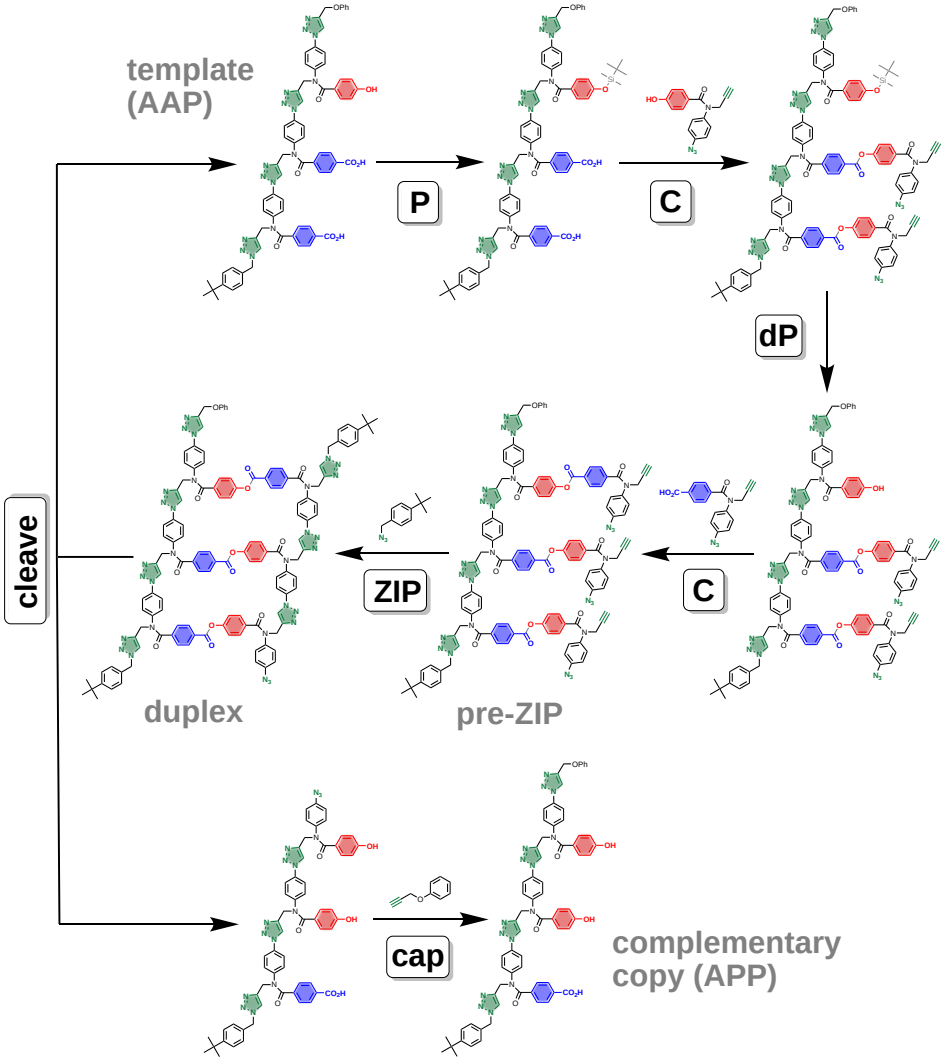

Figure 1.33. Templated-synthesis of a complementary trimer using click chemistry as the ZIP reaction. P stands for protection; C for coupling; dP for deprotection; ZIP refers to the zip-up reaction to create the trimer macrocycle.

1.6 Conclusions

It has been shown above that a lot of effort has been dedicated over the past two decades towards developing synthetic strategies that produce polymeric material with well-defined architectures. A distinction can be made between purely polymeric strategies, that produce polydisperse mixtures with limited sequence control, and solid-phase or step-wise synthetic procedures. In the latter, a perfectly defined primary sequence is achieved.

The ultimate strategy to synthesize macromolecules that have a specific functionality is the selection and evolution cycle. In it, only the polymer chains with the optimal sequence are selected and amplified through template reactions. Most of the examples in the literature in which there is replication of oligomeric chains involve biomolecules or bio-inspired systems, such as DNA, PNA or different oligomers functionalized with nucleobases. There are not, to the best of our knowledge, examples of purely synthetic oligomers than can undergo efficient supramolecular replication.

Covalent duplex formation has risen as a promising alternative in order to ensure template saturation during the templating process. Luh and coworkers showed replication processes of homo-oligomers using base-pairing between carboxylic acids and alcohol groups. In the Hunter group we developed a replication cycle to be able to synthesize the complementary partner of hetero-oligomers, but information was lost in the process due to problems derived from the monomer coupling strategy that was used. The current thesis expands on this templating strategy while exploring an alternative coupling chemistry to prevent information loss in the replication process.

1.7 Bibliography

[1] K. Matyjaszewski, *Science*, 2011, 333, 1104–1105.

[2] W. Saenger, Principles of Nucleic Acid Structure, 1984, Springer Advanced Texts in Chemistry.

[3] A. M. Rosales, R. A. Segalman and R. N. Zuckermann, *Soft Matter*, 2013, 9, 8400.

[4] B. N. Norris, S. Zhang, C. M. Campbell, J. T. Auletta, P. Calvo-Marzal, G. R. Hutchison and T. Y. Meyer, *Macromolecules*, 2013, 46, 1384–1392.

[5] J. Li, R. M. Stayshich and T. Y. Meyer, *Journal of the American Chemical Society*, 2011, 133, 6910–6913.

[6] T. S. Burkoth, E. Beausoleil, S. Kaur, D. Tang, F. E. Cohen and R. N. Zuckermann, *Chemistry & Biology*, 2002, 9, 647–654.

[7] P. E. Nielsen, M. Egholm and O. Buchardt, *Bioconjugate Chemistry*, 1994, 5, 3–7.

[8] J. Davis, *Art Journal*., 1996, 55, 70-74.

[9] G. M. Church, Y. Gao and S. Kosuri, *Science*, 2012, 337, 1628–1628

[10] N. Goldman, P. Bertone, S. Chen, C. Dessimoz, E. M. LeProust, B. Sipos and E. Birney, *Nature*, 2013, 494, 77–80.

[11] A. D. Ellington and J. W. Szostak, *Nature*, 1990, 346, 818–822.

[12] C. M. Yuen and D. R. Liu, *Nature Methods*, 2007, 4, 995–997.

[13] V. B. Pinheiro, A. I. Taylor, C. Cozens, M. Abramov, M. Renders, S. Zhang, J. C. Chaput, J. Wengel, S.-Y. Peak-Chew, S. H. McLaughlin, P. Herdewijn and P. Holliger, *Science*, 2012, 336, 341–344.

[14] O. W. Webster, *Science*, 1991, 251, 887–893.

[15] D. Benoit, C. J. Hawker, E. E. Huang, Z. Lin and T. P. Russell, *Macromolecules*, 2000, 33, 1505–1507.

[16] S. Pfeifer and J.-F. Lutz, *Journal of the American Chemical Society*, 2007, 129, 9542–9543.

[17] M. Zamfir and J.-F. Lutz, Nature *Communications*, 2012, 3, 1138.

[18] S. Srichan, H. Mutlu, N. Badi and J.-F. Lutz, *Angewandte Chemie International* Edition, 2014, 53, 9231–9235.

[19] S. Srichan, H. Mutlu and J.-F. Lutz, *European Polymer Journal*, 2015, 62, 338–346.

[20] K. Satoh, M. Matsuda, K. Nagai and M. Kamigaito, *Journal of the American Chemical Society*, 2010, 132, 10003–10005.

[21] Y. Kang, A. Lu, A. Ellington, M. C. Jewett and R. K. O'Reilly, *ACS Macro Letters*, 2013, 2, 581–586.

[22] A. Anastasaki, V. Nikolaou, N. W. McCaul, A. Simula, J. Godfrey, C. Waldron, P. Wilson, K. Kempe and D. M. Haddleton, *Macromolecules*, 2015, 48, 1404–1411.

[23] Z. Zhang, T.-Y. Zeng, L. Xia, C.-Y. Hong, D.-C. Wu and Y.-Z. You, *Nature Communications*, 2018, 9, 2577.

[24] J. Zhang, M. E. Matta and M. A. Hillmyer, *ACS Macro Letters*, 2012, 1, 1383–1387.

[25] W. R. Gutekunst and C. J. Hawker, *Journal of the American Chemical Society*, 2015, 137, 8038–8041.

[26] B. R. Elling and Y. Xia, *Journal of the American Chemical Society*, 2015, 137, 9922–9926.

[27] R. B. Merrifield, *Journal of the American Chemical Society*, 1963, 85, 2149–2154.

[28] 1F. Albericio, *Current Opinion in Chemical Biology*, 2004, 8, 211–221.

[29] O. J. Plante, E. R. Palmacci and P. H. Seeberger, *Science*, 2001, 291, 1523-1527

[30] H.-A. Klok, N. Franz and G. Kreutzer, *Synlett*, 2006, 12, 1793–1815.

[31] C. A. Briehn and P. Bäuerle, *Chemical Communications*, 2002, 1015–1023.

[32] S. Wendeborn, A. De Mesmaeker, W. K.-D. Brill and S. Berteina, *Accounts of Chemical Research*, 2000, 33, 215–224.

[33] L. Hartmann, E. Krause, M. Antonietti and H. G. Börner, *Biomacromolecules*, 2006, 7, 1239–1244.

[34] J. K. Young, J. C. Nelson and J. S. Moore, *Journal of the American Chemical Society*, 1994, 116, 10841–10842.

[35] A. Al Ouahabi, L. Charles and J.-F. Lutz, *Journal of the American Chemical Society*, 2015, 137, 5629–5635.

[36] S. Pfeifer, Z. Zarafshani, N. Badi and J.-F. Lutz, *Journal of the American Chemical Society*, 2009, 131, 9195–9197.

[37] R. K. Roy, A. Meszynska, C. Laure, L. Charles, C. Verchin and J.-F. Lutz, *Nature Communications*, 2015, 6, 7237.

[38] T. T. Trinh, L. Oswald, D. Chan-Seng, L. Charles and J.-F. Lutz, *Chemistry - A European Journal*, 2015, 21, 11961–11965.

[39] A. Al Ouahabi, M. Kotera, L. Charles and J.-F. Lutz, *ACS Macro Letters*, 2015, 4, 1077–1080.

[40] J. C. Barnes, D. J. C. Ehrlich, A. X. Gao, F. A. Leibfarth, Y. Jiang, E. Zhou, T. F. Jamison and J. A. Johnson, *Nature Chemistry*, 2015, 7, 810–815.

[41] S. C. Solleder, D. Zengel, K. S. Wetzel and M. A. R. Meier, *Angewandte Chemie International Edition*, 2015, 55, 1204–1207.

[42] S. C. Solleder, K. S. Wetzel and M. A. R. Meier, *Polymer Chemistry*, 2015, 6, 3201–3204.

[43] R. Dong, R. Liu, P. R. J. Gaffney, M. Schaepertoens, P. Marchetti, C. M. Williams, R. Chen and A. G. Livingston, *Nature Chemistry*, 2018, 11, 136–145.

[44] B. Lewandowski, G. De Bo, J. W. Ward, M. Papmeyer, S. Kuschel, M. J. Aldegunde, P. M. E. Gramlich, D. Heckmann, S. M. Goldup, D. M. D'Souza, A. E. Fernandes and D. A. Leigh, *Science*, 2013, 339, 189–193.

[45] J.-F. Lutz, *Macromolecules*, 2015, 48, 4759–4767.

[46] H. Colquhoun, and J.-F. Lutz, *Nature Chemistry*, 2014, 6, 455-456.

[47] S. Anderson, H. L. Anderson, *Templates in Organic Synthesis: Definitions and Roles*, chapter 1 from *Templated Organic Synthesis* by F. Diederich and P. J. Stang, Wiley-VCH Verlag GmnH, 2000.

[48] S. Połowiński, *Progress in Polymer Science*, 2002, 27, 537–577.

[49] Hunter Group 2017 Christmas Retreat: "What is a template"

[50] M. Szwarc, *Journal of Polymer Science*, 1954, 12, 317.

[51] H. W. Melville and W. F. Watson, *Journal of Polymer Science*, 1953, 11, 299–305.

[52] S. Połowiński, *Progress in Polymer Science*, 2002, 27, 537–577.

[53] R. A. Volpe and H. L. Frisch, *Macromolecules*, 1987, 20, 1747–1752

[54] H. L. Frisch and Q. Xu, *Macromolecules*, 1992, 25, 5145–5149.

[55] M. Hattori, H. Nagagawa, M. Kinoshita, *Makromol Chem.* 1980, 181, 2325.

[56] R. McHale, J. P. Patterson, P. B. Zetterlund and R. K. O'Reilly, *Nature Chemistry*, 2012, 4, 491–497.

[57] H. L. Anderson and J. K. M. Sanders, *Angewandte Chemie International Edition*, 1990, 29, 1400–1403.

[58] X. Li and D. R. Liu, *Angewandte Chemie International Edition*, 2004, 43, 4848–4870.

[59] J. Niu, R. Hili and D. R. Liu, *Nature Chemistry*, 2013, 5, 282–292.

[60] C. Böhler, P. E. Nielsen and L. E. Orgel, *Nature*, 1995, 376, 578–581.

[61] K. Fujimoto, S. Matsuda, N. Takahashi and I. Saito, *Journal of the American Chemical Society*, 2000, 122, 5646–5647.

[62] X. Li, Z.-Y. J. Zhan, R. Knipe and D. G. Lynn, *Journal of the American Chemical Society*, 2002, 124, 746–747.

[63] D. M. Rosenbaum and D. R. Liu, *Journal of the American Chemical Society*, 2003, 125, 13924–13925.

[64] P. K. Lo and H. F. Sleiman, *Journal of the American Chemical Society*, 2009, 131, 4182–4183.

[65] S. Ida, T. Terashima, M. Ouchi and M. Sawamoto, *Journal of the American Chemical Society*, 2009, 131, 10808–10809.

[66] S. Ida, M. Ouchi and M. Sawamoto, *Journal of the American Chemical Society*, 2010, 132, 14748–14750.

[67] S. Ida, M. Ouchi and M. Sawamoto, *Macromolecular Rapid Communications*, 2011, 32, 209– 214.

[68] T.-Y. Luh and L. Ding, *Tetrahedron*, 2017, 73, 6487–6513.

[69] N.-T. Lin, S.-Y. Lin, S.-L. Lee, C. Chen, C.-H. Hsu, L. P. Hwang, Z.-Y. Xie, C.-H. Chen, S.-L. Huang and T.-Y. Luh, *Angewandte Chemie International Edition*, 2007, 46, 4481–4485.

[70] L. Zhu, N.-T. Lin, Z.-Y. Xie, S.-L. Lee, S.-L. Huang, J.-H. Yang, Y.-D. Lee, C. Chen, C.-H. Chen, and T.-Y. Luh, *Macromolecules*, 2013, 46, 656-663.

[71] H.-W. Wang, C.-H. Chen, T.-S. Lim, S.-L. Huang and T.-Y. Luh, Chemistry - *An Asian Journal*, 2010, 6, 524–533.

[72] Y.-Z. Ke, R.-J. Ji, T.-C. Wei, S.-L. Lee, S.-L. Huang, M.-J. Huang, C. Chen, and T.-Y. Luh, *Macromolecules*, 2013, 46, 6712-6722.

[73] V. Tereshko, S. Portmann, E. C. Tay, P. Martin, F. Natt, K.-H. Altmann and M. Egli, *Biochemistry*, 1998, 37, 10626–10634.

[74] P. Nielsen, M. Egholm, R. Berg and O. Buchardt, *Science*, 1991, 254, 1497–1500.

[75] C. Switzer, S. E. Moroney and S. A. Benner, *Journal of the American Chemical Society*, 1989, 111, 8322–8323.

[76] C. A. Hunter, *Angewandte Chemie International Edition*, 2004, 43, 5310 – 5324

[77] A. E. Stross, G. Iadevaia and C. A. Hunter, *Chemical Science*, 2016, 7, 94–101.

[78] D. Nunez-Villanueva and C. A. Hunter, *Chemical Science*, 2017, 8, 206–213.

[79] J. A. Swain, G. Iadevaia and C. A. Hunter, *Journal of the American Chemical Society*, 2018, 140, 11526–11536

[80] F. T. Szczypinski, C. A. Hunter, *Chemical Science*, 2019, 10, 2444

[81] G. Iadevaia, D. Nunez-Villanueva, A. E. Stross, C. A. Hunter, *Org. Biomol. Chem*., 2018, 16, 4183

[82] Szczypiński, Filip; Gabrielli, Luca; Hunter, Christopher (2019): Emergent Supramolecular Assembly Properties of Recognition-Encoded Oligoesters. *ChemRxiv. Preprint.*

[83] H. Kolb, M. G. Finn, K. B. Sharpless, *Angewandte Chemie International Edition*, 2001, 40, 2004-2021

[84] D. Nunez-Villanueva, M. Ciaccia, G. Iadevaia, E. Sanna, C. A. Hunter, unpublished results

"You should know when you hold hands with me you are holding hands with everything I've ever eaten"

Gene Belcher

2

Aims

The aim of the first part of this thesis is to develop and optimize the conditions in which sequence-encoded oligomers can be replicated and amplified. We will build on some of the research done in the Hunter group in this area, and address the issues encountered during the replication process associated with previous molecular designs.

In Chapter 1 we introduced the problems derived from the use of CuAAC chemistry during the replication process of oligomers. The work in this thesis was designed to overcome the challenges associated with the use of a backbone that shows directionality (Figure 2.1).

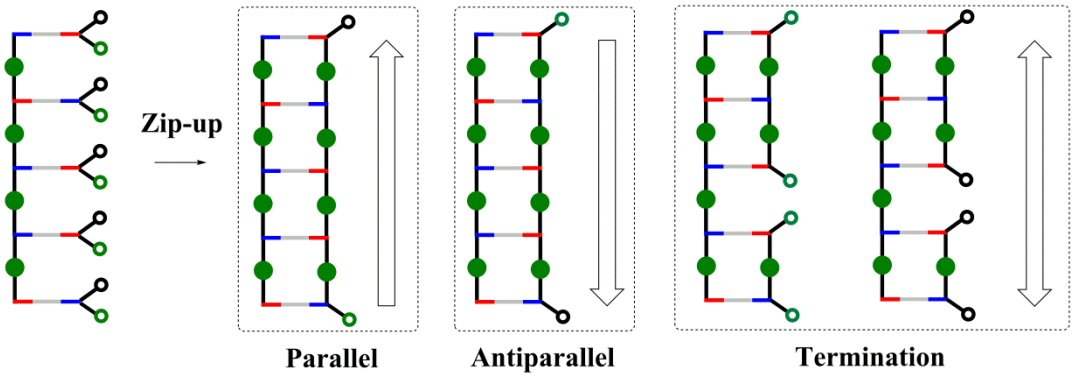

Figure 2.1. Possible products obtained during the zip-up reaction in the replication process of an oligomer composed of "AB" monomers.

"AB" monomers (monomers that present two different reacting groups that couple to each other) can react in two different directions when grafted onto a template. If the zip-up process goes to completion they will produce two different molecules with parallel or antiparallel directionality; but if the reaction starts from both directions in the same template that will lead to termination and incomplete zip-up.

To prevent this we use in this work Glaser-Hay alkyne-alkyne coupling. "AA" monomers with two free alkynes can be grafted on a template and zipped-up, producing a single ladder-like structure that upon hydrolysis will produce the replication product and the starting template.

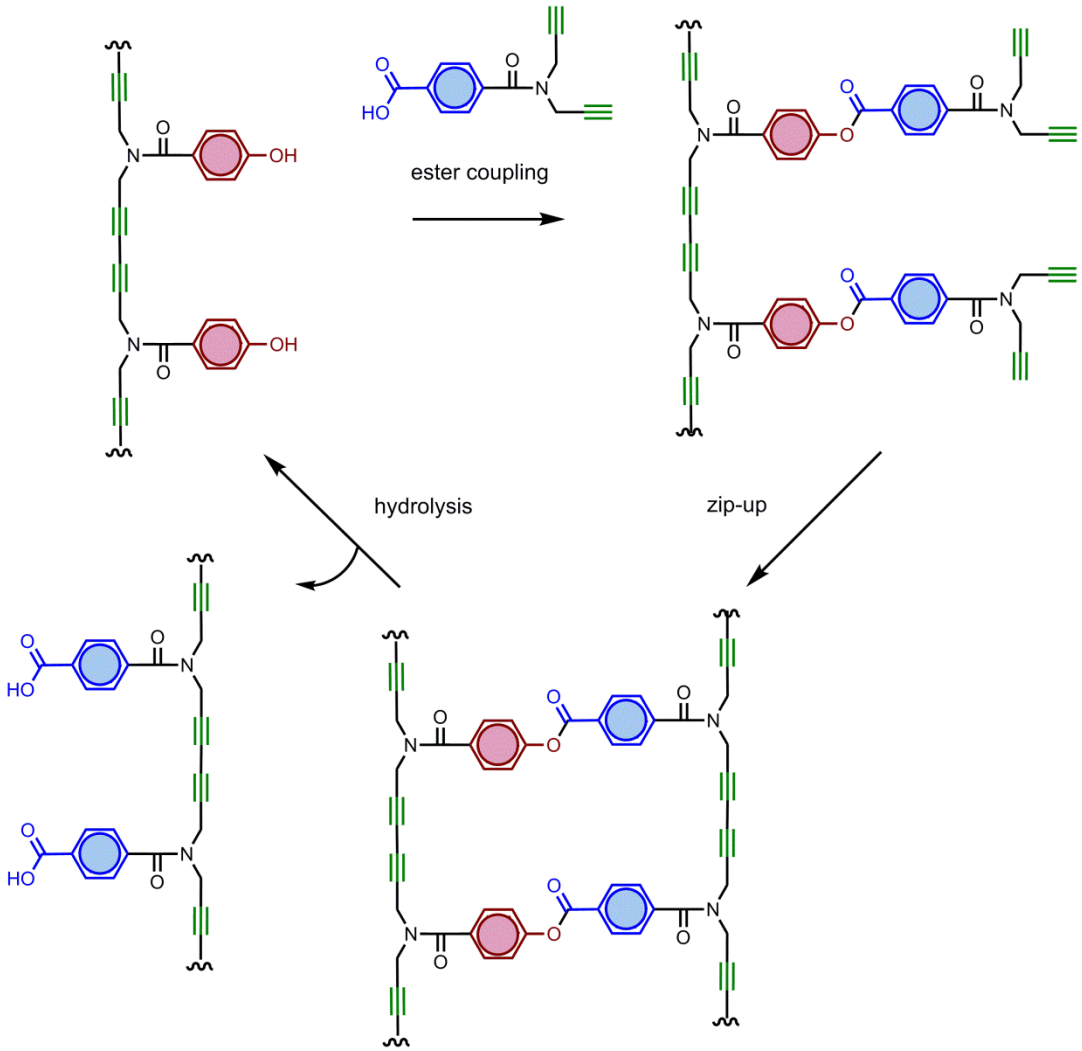

Figure 2.2. Schematic representation of the synthesis of a complementary carboxylic acid oligomer starting from a phenol template. The design of the system comprises the covalent recognition units and two alkynes on the backbone to prevent the coupling errors derived from a AB monomer.

"Fool me once, shame on you. But teach a man to fool me and I'll be fooled for the rest of my life"

BoJack Horseman

3

Templated Synthesis of Complementary Dimers

3.1 Introduction

This chapter discusses the synthesis of a homodimer and a heterodimer and their use as templates following the strategies described in Chapters 1 and Chapter 2. Figure 3.1 shows the general approach followed in this work.

A phenol dimer (Figure 3.1a, red bars) was grafted with its complementary carboxylic acid monomer (blue bar) and the resulting molecule was zipped-up into a macrocycle. Upon hydrolysis, the macrocycle yielded its two conforming dimers, i.e. the starting template and the newly-synthesized carboxylic acid dimer.

Conversely, the mixed phenol-carboxylic acid dimer (Figure 3.1b) was subjected to a complete replication cycle, as it was described in Chapter 1. Figure 3.1b shows the schematic representation of the cycle, which involved several protection-deprotection steps, and grafting of monomers onto the template. The final macrocycle, upon hydrolysis, yielded a single product, i.e. the starting template.

The following sections of Chapter 3 discuss the optimization of the base-pair cycle for this molecular system, as well as the study of the zipping-up conditions to form the dimer macrocycles. Moreover, experiments are presented to characterise the homodimer and the heterodimer as templates.

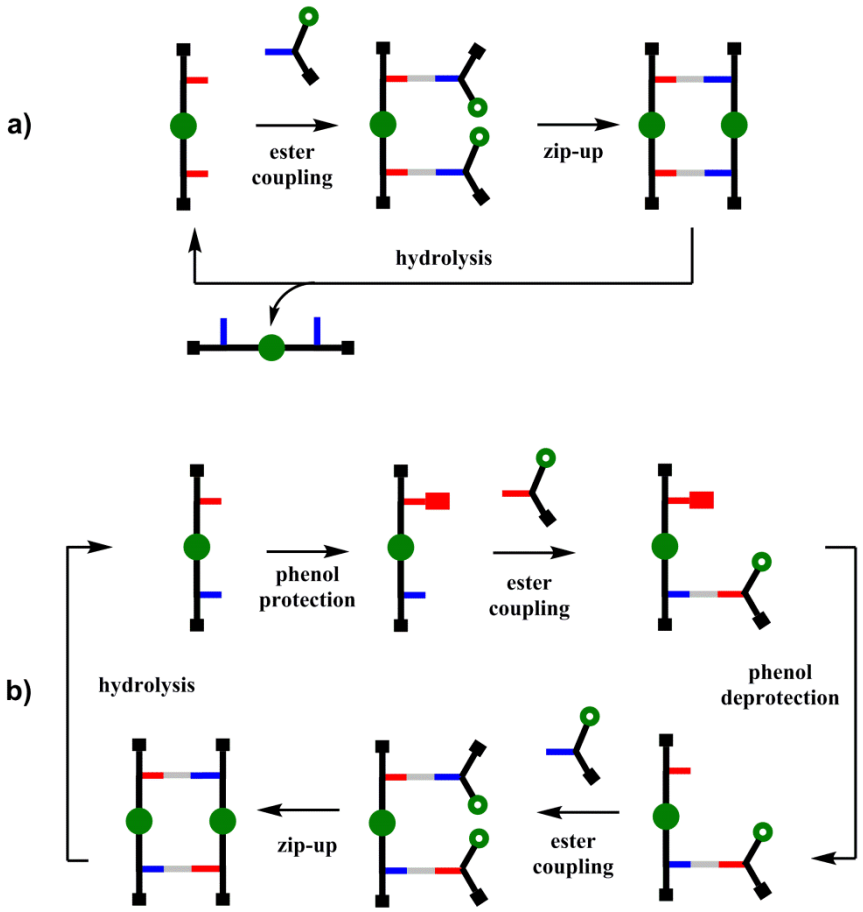

Figure 3.1. Schematic representation of covalent template strategies to synthesise capped dimers. (a) Coupling of two acid monomers on a homodimer template. (b) Coupling of an acid monomer with a phenol monomer on a heterodimer template. Blue bars represent carboxylic acid bases; red bars represent phenol bases; green empty circles represent terminal alkynes; full green circles represent butadiyne links; black squares represent capping groups.

3.2 Monomer and capped-monomer synthesis

The synthesis of the uncapped monomeric units employed in this work is shown in Scheme 3.1 and Scheme 3.2. The first step of the synthesis was the coupling between TBDMS-protected 4-hydroxy benzoic and dipropargylamine. Compound **3.2** was then deprotected using TBAF in THF in a quantitative reaction to produce the phenol monomer, compound **3.3** (Scheme 3.1).

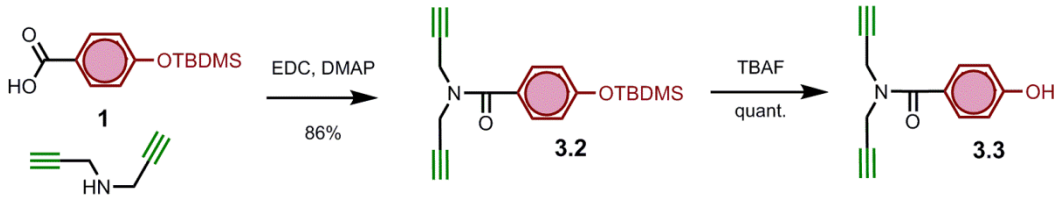

Scheme 3.1. Synthesis of the phenol monomer **3.3**.

The synthesis of the acid monomer (Scheme 3.2) involved the coupling of mono-methyl terephthalate and dipropargylamine to produce **3.4**, which was subsequently hydrolysed in quantitative yield with an aqueous solution of LiOH to produce compound **3.5**.

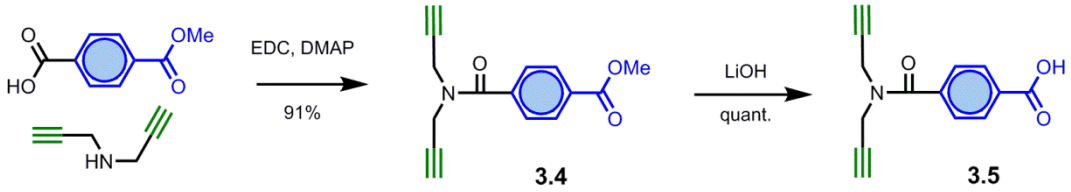

Scheme 3.2. Synthesis of the carboxylic acid monomer **3.5**.

To investigate the zip-up conditions, we wanted to build the knowledge gradually, starting with a simple system first. This entailed ensuring that there were no competing processes that would complicate the analysis of the zip-up reaction (Figure 3.1). For this reason, one of the alkynes, belonging to the monomers **3.3** and **3.5**, was "capped" by clicking a 3,5-tertbutylbenzyl azide. Besides capping the molecule to prevent intermolecular reactions, this increased considerably the solubility due to the presence of tert-butyl side groups in the cap.

Two strategies were studied for the capping of the monomers: one that involved the synthesis of a mono protected dipropargylamine (Scheme 3.3); and other one involving a statistical reaction with the azide (Scheme 3.4). For the former strategy, propargylamine was TIPS-protected with n-BuLi and TIPS-Cl. Compound **3.6** was obtained with a reasonably good yield. After this, the secondary amine on **3.6** was reacted with $(Boc)_2O$ in a quantitative fashion. The following propargylation reaction proved to lack reproducibility. The best yield obtained was poor (28%), which left large quantities of unreacted propargyl bromide. This complicated

greatly the handling of the reaction crude due to the material toxicity and acute smell. After isolation of **3.8**, the Boc group was removed overnight to yield final compound **3.9.**

Compound **3.9** was then coupled to the commercially available monomethyl-terephthalate to produce **3.10**, which was subsequently capped with the solubilising azide, hydrolysed with an aqueous solution of LiOH in THF, and deprotected with TBAF to remove the TIPS group, yielding the capped-acid monomer **3.13** in an 80% yield over three steps (Scheme 3.3).

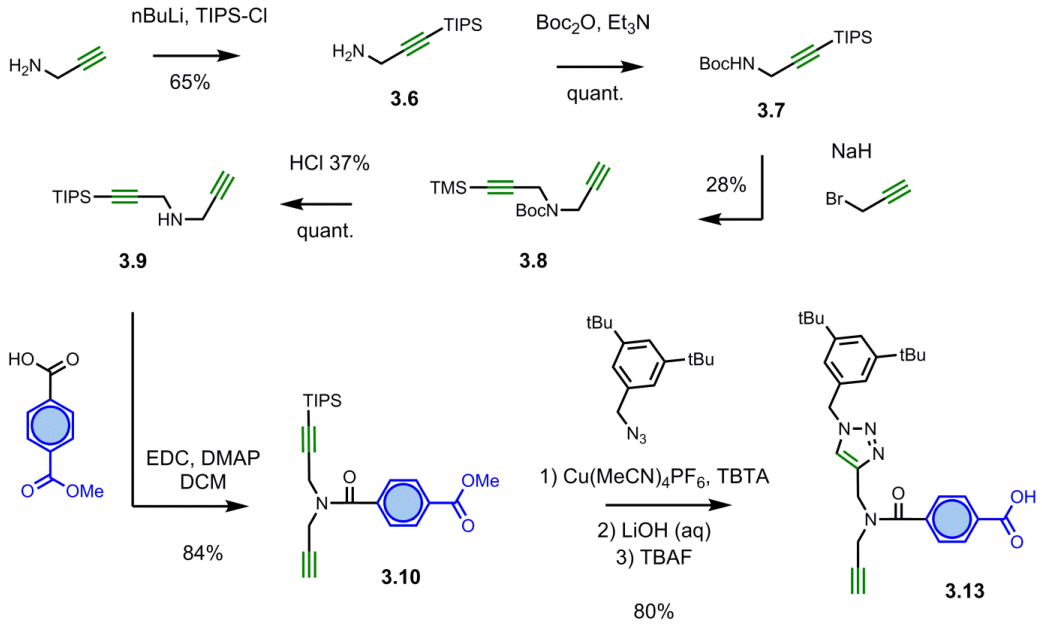

Scheme 3.3. Synthesis of the mono-capped carboxylic acid monomer **3.13.**

When it came to the statistical approach shown in Scheme 3.4, the phenol monomer **3.3** was reacted in a 5-fold excess with the solubilising azide in dilute conditions (10^{-4}-10^{-3} M). The reaction produced the desired capped-phenol monomer **3.14** in a single step in moderate yields, and all the unreacted phenol monomer was recovered. Whilst some material was lost in this process, due to double capping, the difficulty of the synthesis of the TIPS-protected amine led us to select this statistical pathway.

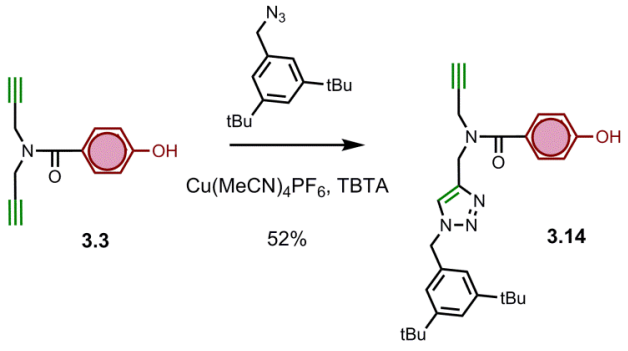

Scheme 3.4. Synthesis of the capped phenol monomer **3.14**.

3.3 Base-Pair Chemistry

Monomer **3.3** and **3.5** were then subjected to the base-pair cycle described in Chapter 1 to confirm that the core was stable under the conditions in which the templating process occurs. All the crude reaction mixtures were subjected to an aqueous work-up and carried on without further purification. As is shown in Figure 3.2, the TBDMS protection of **3.3** led to a big change in retention time in the UPLC trace (0.75 min to 1.7 min, crude A). Subsequent ester coupling of **3.5** with butanol changed the retention time from 0.8 min to 1 min (crude B), and TBDMS deprotection with TBAF returned the peak from the alcohol component in the UPLC to its starting point (crude C). Ester coupling of **3.3** with butanoic acid led to a change in the UPLC retention time from 0.75 to 1.2 min (crude D), before basic hydrolysis of the whole mixture returned the UPLC trace to its starting point (crude E). An unidentified minor impurity appears after the first esterification (crude B) and seems to grow after the second one (crude D), before disappearing during the final hydrolysis step (crude E).

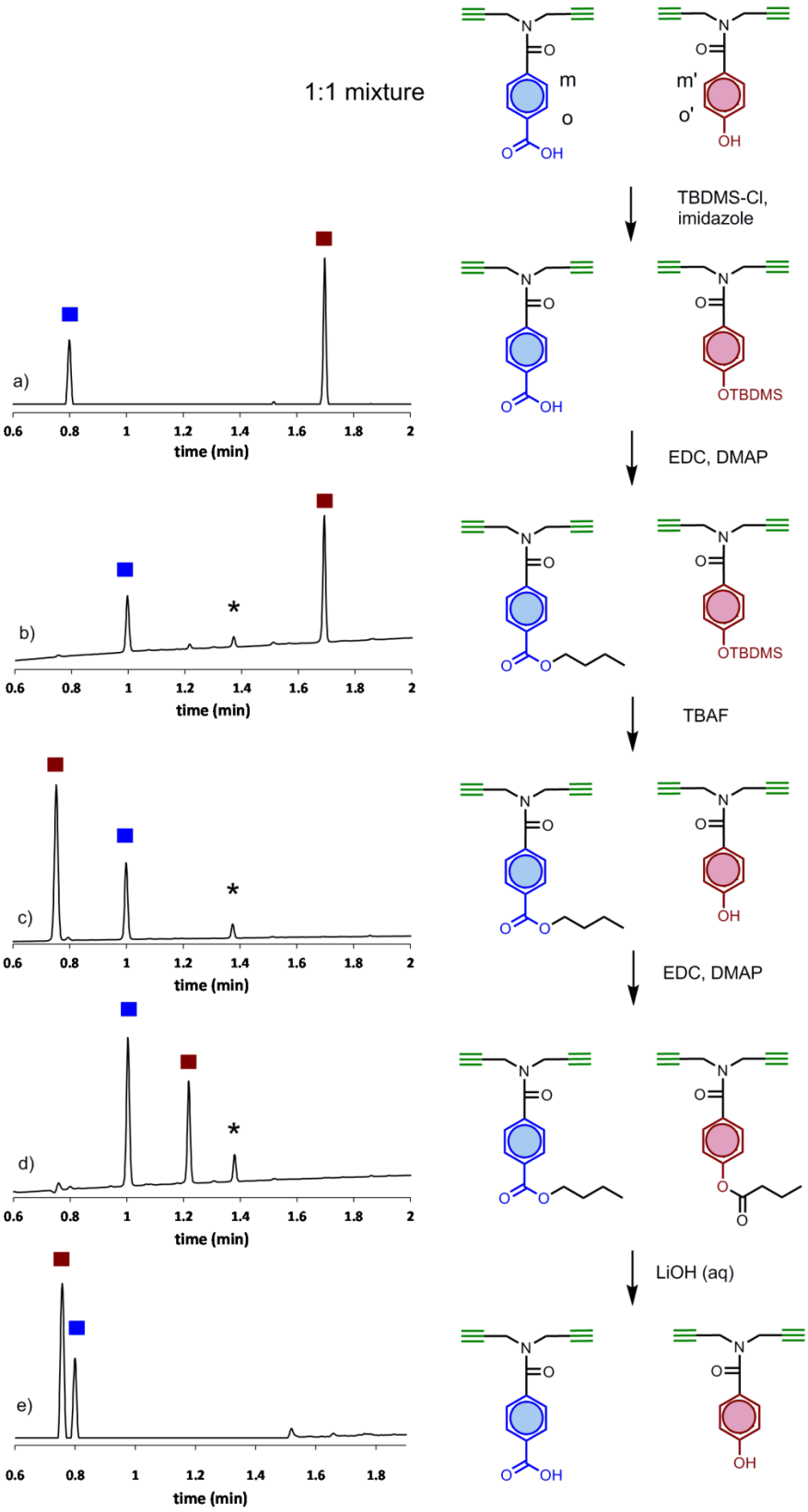

Figure 3.2. UPLC traces of crude reaction mixtures of the base-pair attachment and cleavage cycle. The peaks are labelled red and blue for the phenol and carboxylic acid bases respectively. The asterisks indicate an unidentified impurity. The proton labelling scheme used in Figure 3.3 is shown. The conditions of the UPLC method are as follows: Solvent A: Water +0.1% Formic

acid; Solvent B: Acetonitrile +0.1% Formic acid; Gradient of 0-2 minutes 5% - 100%B + 1 minute 100% B with re-equilibration time of 2 minutes. Flow rate: 0.6 ml/min; Column temperature of 40°C; Injection volume of 2 µL. The signal was monitored at 254 nm.

Figure 3.3 shows the changes in the aromatic region of the ^{1}H NMR spectra of the crudes of reaction shown in Figure 3.2. The signals of the starting carboxylic acid **3.5** at 7.65 ppm and 8.15 ppm do not shift considerably during the process. The signals of the phenol monomer **3.3**, on the other hand, suffer several noticeable changes during the base-pair cycle: i) they shift slightly after TBDMS protection and deprotection (spectra A and C); ii) they move downfield 0.5 ppm after the transformation of the phenol into an ester (spectrum D); iii) this shift is reversed after the hydrolysis step (spectrum E) where the signals return to the shifts of the starting materials.

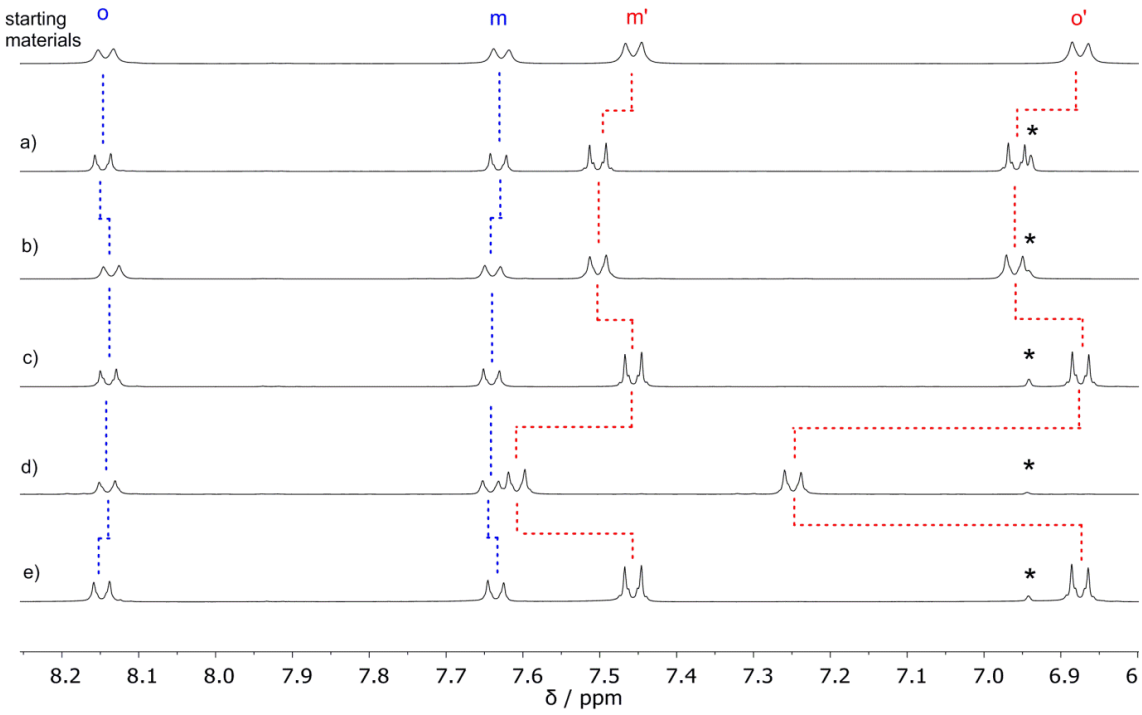

Figure 3.3. Aromatic region of the ^{1}H NMR (400 MHz, d_4-methanol, 298 K, ca. 100 mM) spectra of the crude product mixtures obtained after aqueous work-up for each step of the base-pair attachment and cleavage cycle shown in Figure 3.2. The asterisk depicts an unidentified impurity that appears after the first protection step. See Figure 3.2 for the proton labelling scheme.

In conclusion, it was seen that every step was quantitative or near quantitative, and no purification was required in between steps. This will be important for the overall yield of the base-pair cycle in later experiments. Moreover, while some of these reactions are traditionally left running overnight, if they are performed under moderate concentration (10^{-2}-10^{0}M) they

can be finished in a few hours. This fact, together with no need for purification, potentially reduces the total time needed to perform the cycle to little more than a day of work.

3.4 Synthesis of dimer templates.

The synthesis of the homodimer phenol template is shown in Scheme 3.5. The capped-phenol monomer **3.14** was dimerised in good yield making use of Pd and Cu as catalysts and PPh_3 as a ligand to produce the capped-phenol dimer **3.15.**

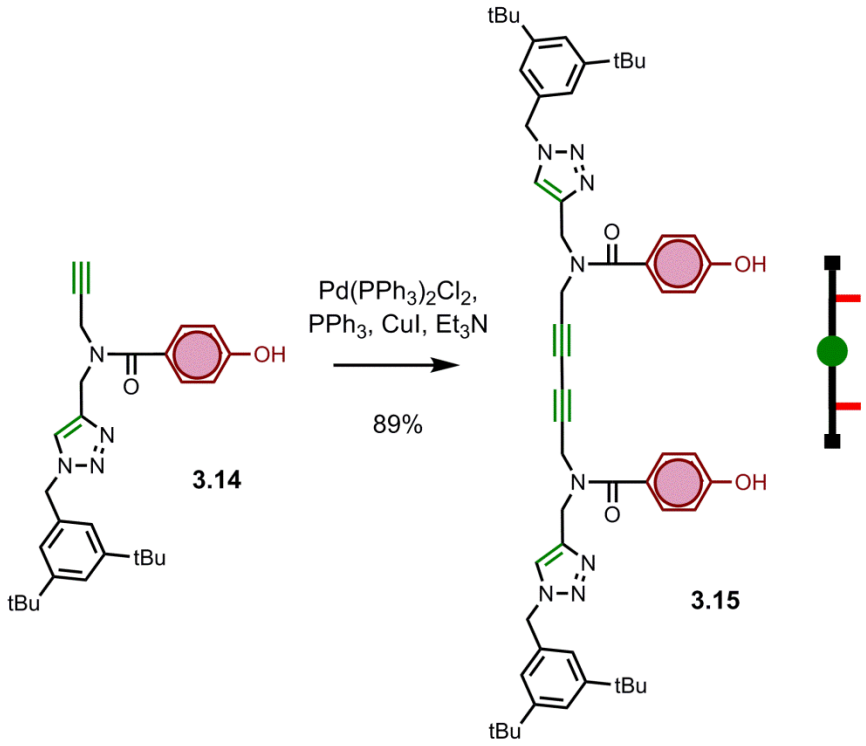

Scheme 3.5. Synthesis of the phenol dimer template **3.15**.

Synthesising the heterodimer was more complicated, especially in terms of purification. To produce a mixed dimer, two different monomers need to be reacted together. Alkyne-alkyne coupling via Glaser-Hay mechanism does not allow for selective coupling, i.e. two monomers in solution will produce a statistical mixture of dimers. Assuming similar reactivity of both monomers, the crude reaction mixture will contain 50% of heterodimer and 25% of each of the homodimers.

To obtain the phenol-acid heterodimer, it was not as simple as reacting capped monomers **3.13** and **3.14**; the carboxylic acid does not react in good yields under Glaser-Hay conditions. We hypothesise that in the basic reaction mixture the carboxylate complexes the Cu(I) ions preventing them from participating in the catalytic cycle. If the amount of catalyst is increased to counteract this fact, depropargylation is observed, as has been described in the literature. [1]

To circumvent these issues, an ester monomer, compound **3.16**, was synthesised (Scheme 3.6). The idea behind this was that ester could be reacted with compound **3.14** and it would be easy to hydrolyse after the Glaser-Hay reaction had taken place, rendering the desired heterodimer.

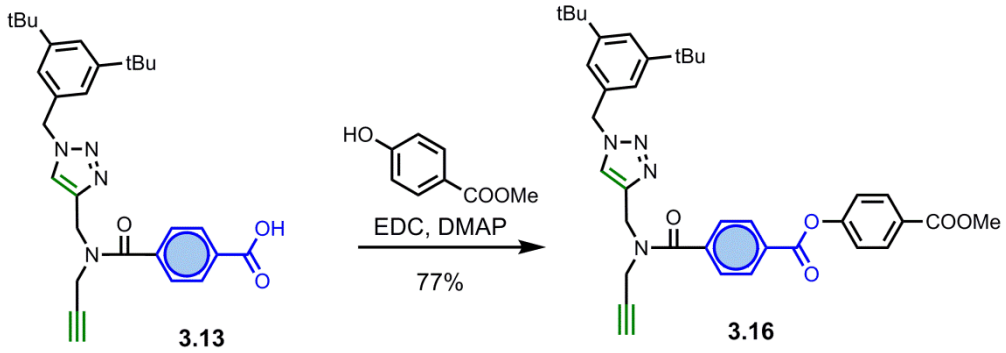

Scheme 3.6. Synthesis of activated-ester monomer **3.16**.

To that effect, compounds **3.14** and **3.16** were coupled together (Scheme 3.7). The expectation was that the two starting monomers would react to produce three different products, but the ester in **3.16** proved to be labile enough that the basic conditions used in the reaction were enough to remove it partially. This led to a mixture of six different dimers that complicated the purification (Figure 3.4). The major compound produced in the reaction was the mixed phenol-ester dimer, which upon isolation was hydrolysed and combined with the isolated compound **3.17** from the statistical dimerization. Dimer **3.15**, and the three carboxylic acid dimer derivatives were utilised in other experiments in the present and the following chapter. Yields are given for products that were isolated, but complete characterization in this chapter is only provided for **3.15** and **3.17**.

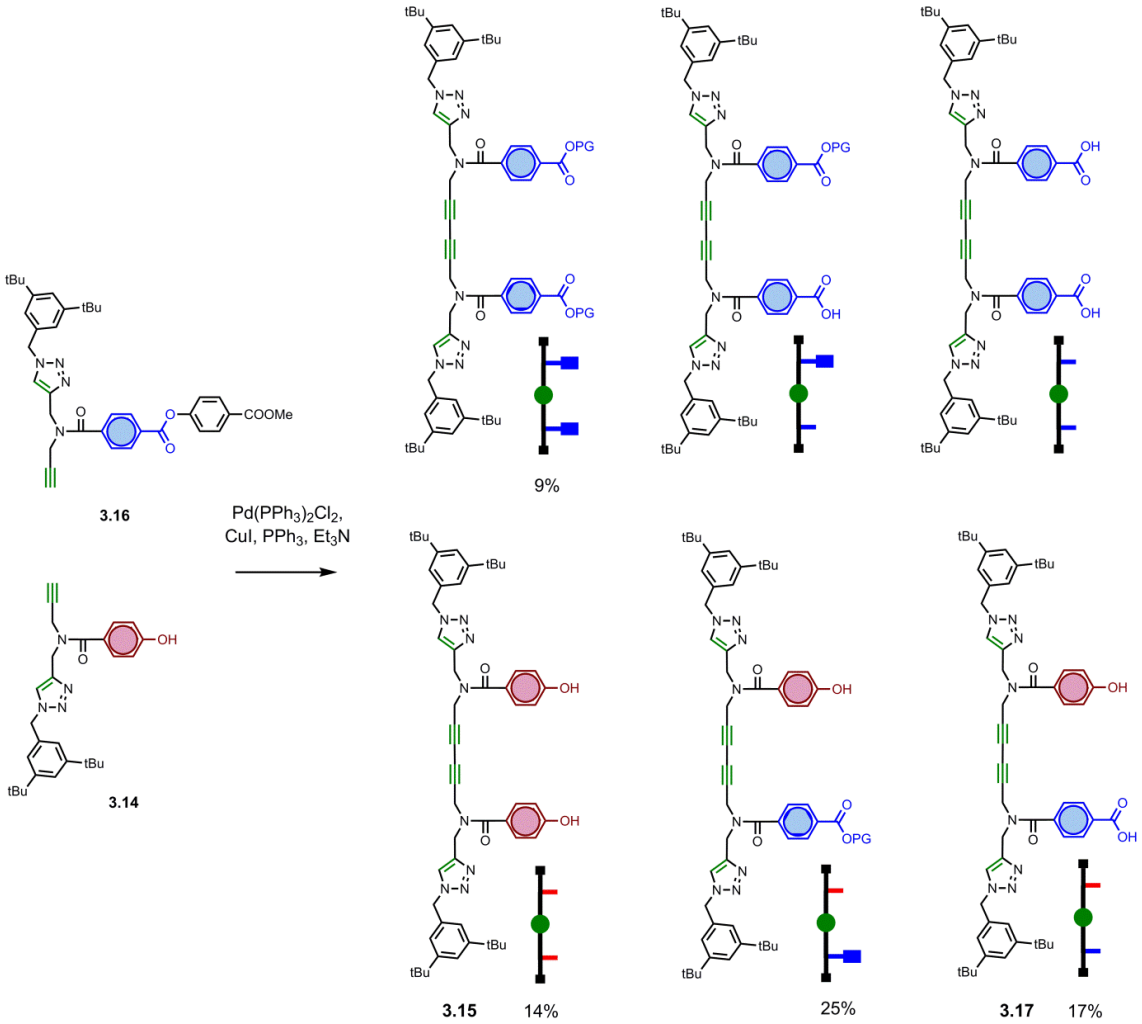

Scheme 3.7. Statistical synthesis of the heterodimer template **3.17**.

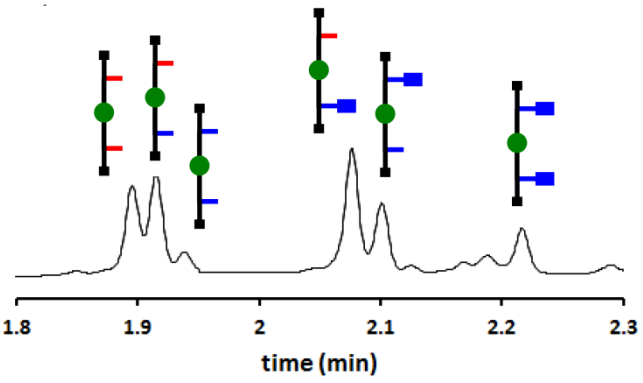

Figure 3.4. UPLC trace of the crude reaction mixture obtained from the coupling reaction shown in Scheme 7. The identity of each peak was determined from the mass spectrum. The conditions of the UPLC method are as follows: Solvent A: Water +0.1% Formic acid; Solvent B: Acetonitrile +0.1% Formic acid; Gradient of 0-2 minutes 5% - 100%B + 1 minute 100% B with re-equilibration time of 2 minutes. Flow rate: 0.6 ml/min; Column temperature of 40°C; Injection volume of 2 µL. The signal was monitored at 254 nm.

3.5 Template-directed synthesis on a homodimer template

The templated synthesis of the acid dimer **3.20** was started by coupling **3.15** and **3.13** to produce the pre-zip compound **3.18** (Scheme 3.8). The zip-up reaction was optimized at this point. Since the intermolecular reaction would be competing with the intramolecular reaction, the way to minimize the undesired cross-linking of **3.18** was to work at high dilution.

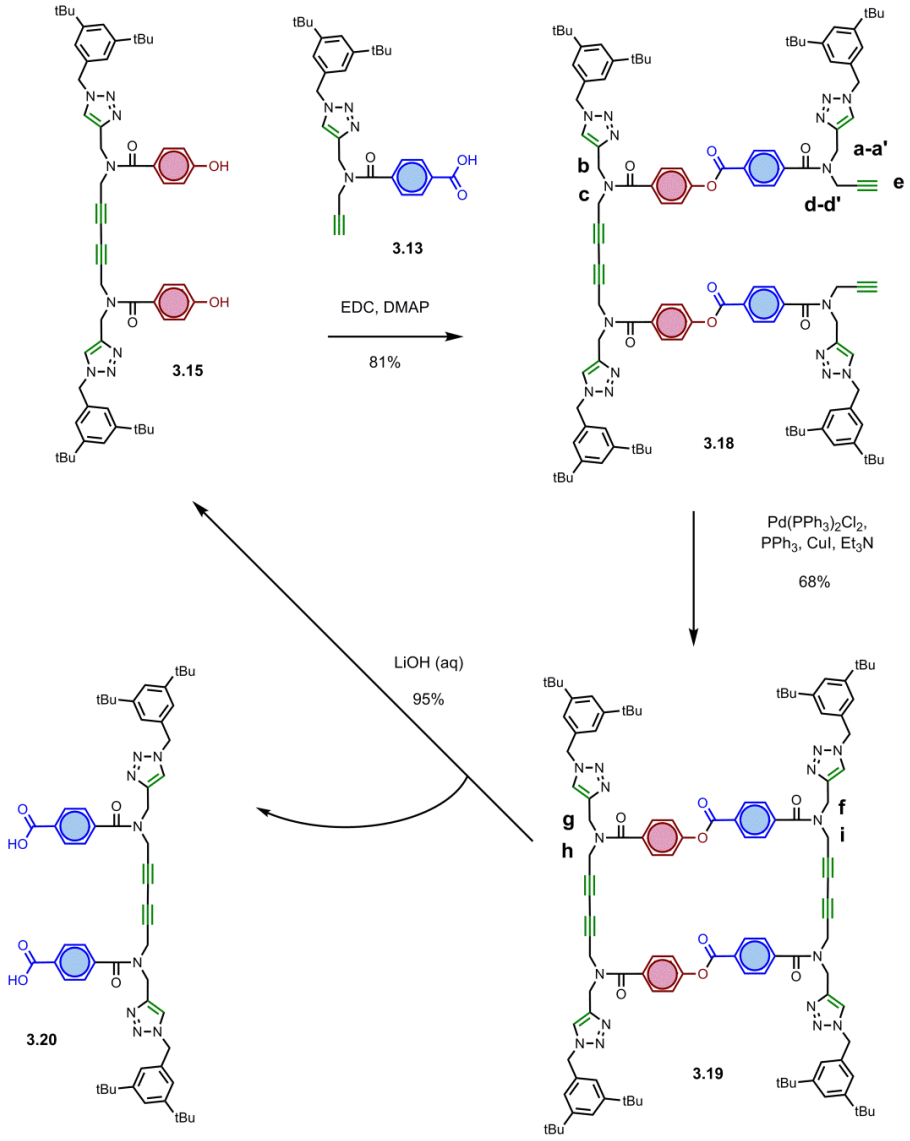

Scheme 3.8. Covalent template-directed synthesis of the carboxylic acid dimer **3.20** on the phenol dimer template **3.15**. The proton labelling scheme used in Figures 3.7-3.9 is shown.

A combination of past experience in the group and some preliminary concentration studies with the monomers led us to set the reaction concentration at 50 µM. Compound **3.18** was set to react at 50 µM using the catalyst loading previously used for the alkyne-alkyne couplings (i.e. 0.1 eq. of $Pd(PPh_3)_2Cl_2$, 0.1 eq. of CuI and 0.3 eq. of PPh_3, Figure 5, orange data series). This reaction was followed by UPLC and it showed slow but steady progress for four days until it

stopped going forward at around six days (ca. 10000 min), probably due to catalyst degeneration over that period. More catalyst could have been added to the reaction once this happened, if it were not for the impracticality of needing over six days for a reaction to go to completion. Instead, the catalyst loading was increased 10-fold and the reaction proceeded to completion in under one hour (Figure 5, blue data series).

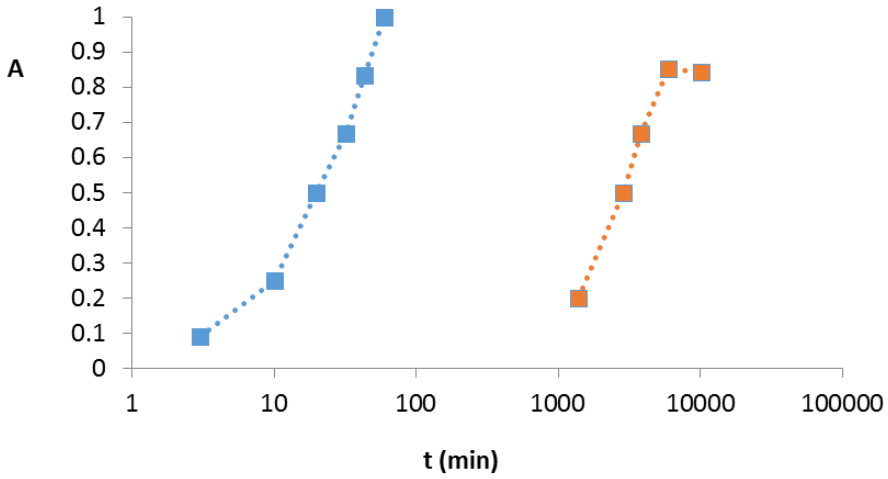

Figure 3.5. Time dependence of the templated Glaser coupling reaction of **3.18** (50 μM) in MeCN at room temperature plotted as UPLC peak area (A). Conditions 1 (orange data series): $Pd(PPh_3)_2Cl_2$ (0.1 eq.), PPh_3 (0.3 eq.), CuI (0.1 eq.), Et_3N (10 eq.). Conditions 2 (blue data series): $Pd(PPh_3)_2Cl_2$ (1 eq.), PPh_3 (3 eq.), CuI (1 eq.), Et_3N (100 eq.). "A" is calculated as the integral of the product UPLC peak area relative to the integral recorded at the latest time point using the absorbance at 254 nm.

As described in Chapter 1, there are many definitions of what constitutes a template. To prove that the closing of **3.18** was a templated reaction an ester version of the monomer (Scheme 3.9, compound **3.21**) was synthesized and reacted under the same zip-up conditions. It was seen that after an initial time in which the reaction was very slow, Glaser coupling of **3.21** reached completion in a little less than six hours (orange data in Figure 3.6). In contrast, consumption of **3.18** is completed in one hour and no intermolecular side-products can be observed (blue data in Figure 3.6). The conclusion of this experiment is that, though the low concentrations do not entirely prevent intermolecular reaction (i.e. dimerization of **3.21** into **3.22)**, the alkyne-alkyne coupling to close **3.18** presents a high effective molarity which leads to reaction acceleration when compared to intermolecular processes. Therefore, phenol dimer **3.15** is acting as a kinetic template that increases the rate of the Glaser-Hay coupling 6-fold.

3.5. Template-directed synthesis on a homodimer template

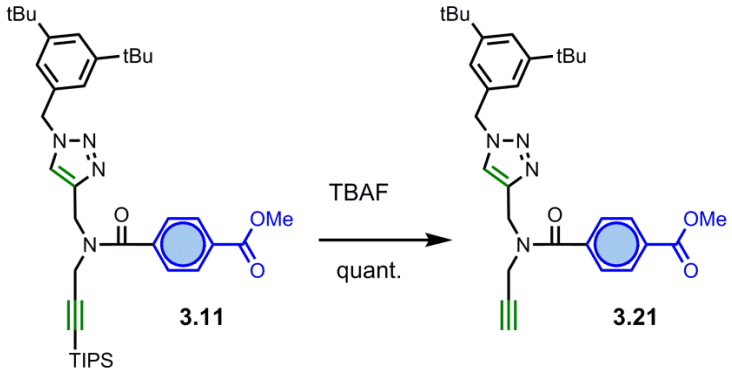

Scheme 3.9. Synthesis of methyl-ester monomer **3.21**.

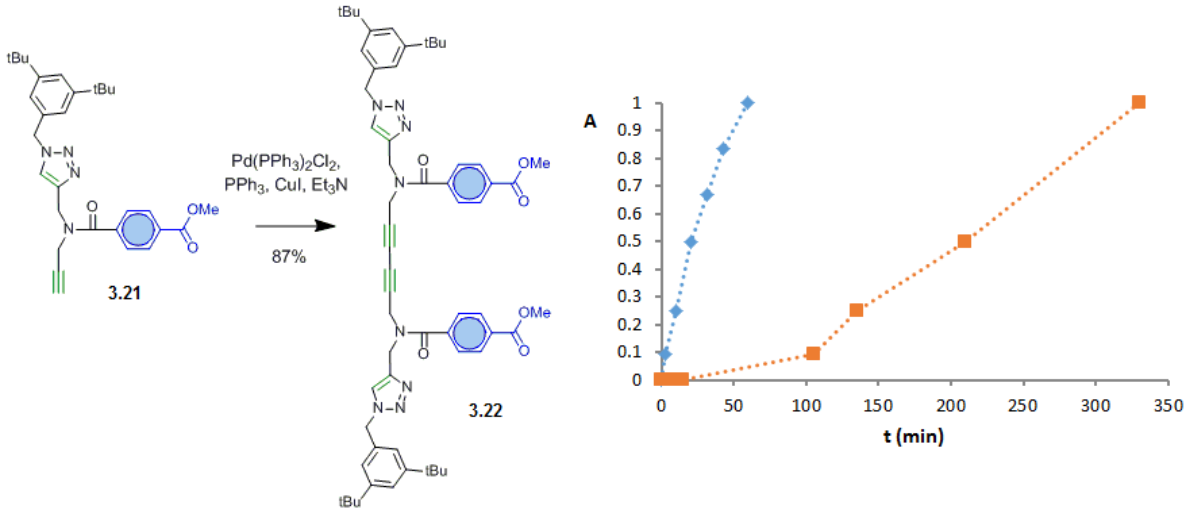

Figure 3.6. Time dependence of product formation plotted as UPLC peak area (A) for reaction of **17** (50 µM, blue data) and a model ester (50 µM, red data). Reaction conditions: $Pd(PPh_3)_2Cl_2$ (1 eq.), PPh_3 (3 eq.), CuI (1 eq.), Et_3N (100 eq.) in MeCN at room temperature. "A" is calculated as the integral of the product UPLC peak area relative to the integral recorded at the latest time point using the absorbance at 254 nm.

Figure 3.7 depicts the UPLC traces of the zip-up reaction of **3.18** into macrocycle **3.19**. The peak at 2.41 min in the UPLC trace completely disappears and is replaced by a peak of similar intensity at 2.52 min. The mass chromatogram of said peaks confirmed the reaction had taken place, i.e. a reduction of 2 units of mass in the $[M+H]^+$ and of 1 unit of mass in the $[M+2H]^{2+}$ could be observed.

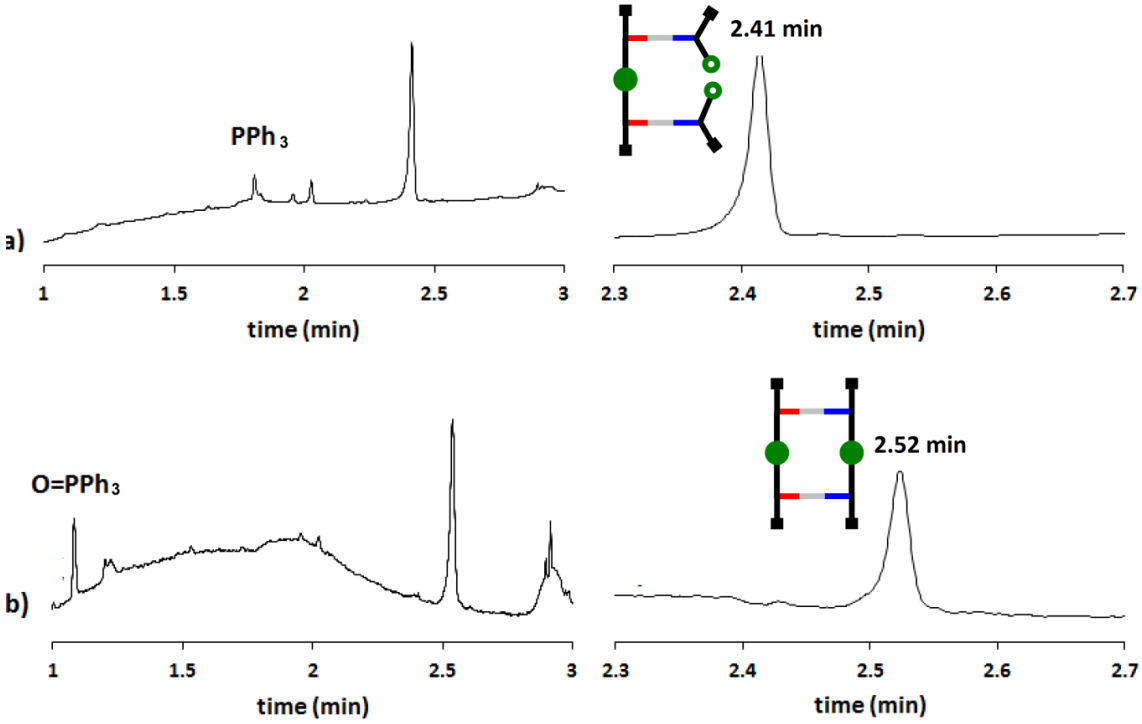

Figure 3.7. UPLC traces for the reaction of **3.18** (50 µM) with $Pd(PPh_3)_2Cl_2$ (1 eq.), PPh_3 (3 eq.), CuI (1 eq.), Et_3N (100 eq.) in MeCN at room temperature after (a) 0 min, with zoom of are of interest; and (b) 60 min, with zoom of area of interest. The conditions of the UPLC method are as follows: Solvent A: Water +0.1% Formic acid; Solvent B: Acetonitrile +0.1% Formic acid; Gradient of 0-2 minutes 5% - 100%B + 1 minute 100% B with re-equilibration time of 2 minutes. Flow rate: 0.6 ml/min; Column temperature of 40°C; Injection volume of 2 µL. The signal was monitored at 254 nm.

Alongside the UV signals for **3.18** and **3.19**, the traces also showed signals belonging to the catalysts. PPh_3 was partially oxidized and the phosphine oxide eluted considerably faster after the reaction. The unoxidized phosphine was eluted over a long period of time giving a broad peak. This happened both in the UPLC and during column chromatography purification. The increased catalyst loading (several equivalent of aromatic ligand per each pre-zip molecule), though necessary to shorten the reaction times, proved to be a difficulty to overcome in the purification process. Column chromatography was insufficient to obtain a pure macrocycle **3.19** so the sample needed to be subjected to HPLC purification which greatly reduced the final isolated yield.

Besides the shift in the UPLC retention time and the observed change in the mass of the molecules, ^1H NMR spectroscopy proved to be a perfect technique to complete the analysis of

the zipping-up reaction. Changes in two distinct areas in the spectra could be observed in the transformation of **3.18** into **3.19** (Figure 3.8):

- Between 4 and 5 ppm, in the range where protons belonging to the CH_2 of the propargyl groups appear: signals **a** and **d** which belonged to the acid monomers were split into two in compound **3.18** due to the existence of rotameric species. Upon macrocyclisation these signals coalesce into a single peak, **f** and **i**, respectively.
- At 2.4 ppm the alkyne proton **e** disappears.

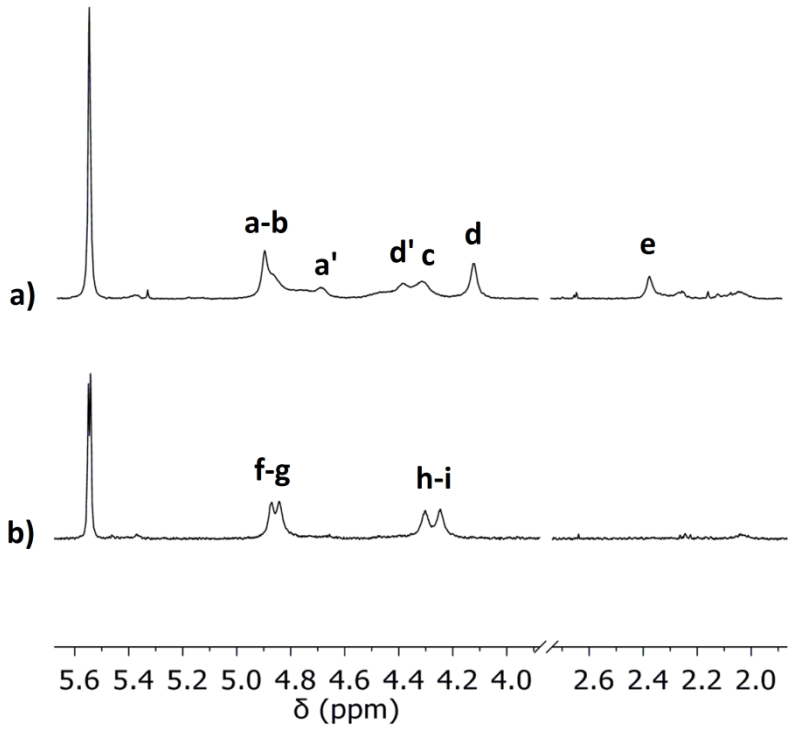

Figure 3.8. Partial ^{1}H NMR (500 MHz, Chloroform-*d*, 298K, ca. 5 mM) spectra of (a) **3.18** and (b) **3.19**. The proton labelling scheme is shown in Scheme 3.8.

Further analysis of the 2D spectra helps us to understand better the conformational isomerism presented by the amides in this family of molecules. Every molecule derived from an ester or an acid monomer showed signs of restricted rotation. This can be seen in the appearance of small extra singlets in the propargyl CH_2 area. To illustrate this, Figure 3.9 shows a stack of ^{1}H NMR spectra going from phenol monomer **3.3** (single propargyl CH_2 environment), to the capped-phenol monomer **3.14** (two CH_2 environments) finishing in the capped-acid monomer **3.13** (two CH_2 environments, each presenting an extra rotameric signal due to a slower exchange between the two possible amide conformations). The electron-donating capabilities of the phenol group, together with the conjugation of the system with the carbonyl from the amide through the aromatic ring, makes the N-carbonyl conjugation within the amide to be less

prominent. Therefore, the N-carbonyl bond has more of a single-bond character in the phenol derivatives. That same bond will in turn have more of double-bond character in the carboxylic acid derivatives, which will restrict the amide rotation and lead to differentiated signals of the possible amide rotamer conformations.

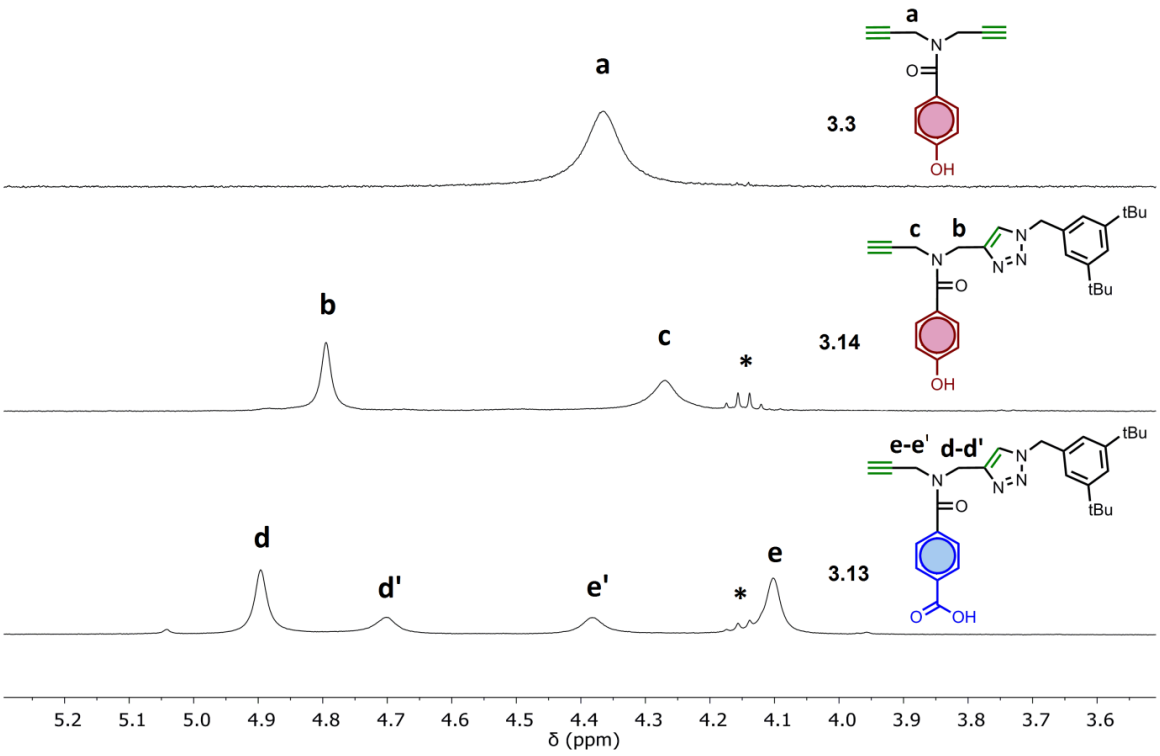

Figure 3.9. Partial ^{1}H NMR (400 MHz, d_4-methanol, 298 K, ca. 50 mM) spectra of monomers **3.3**, **3.14** and **3.13**. The asterisk is ethyl acetate impurity.

Of course, in a more complex molecule like pre-zip **3.18** that region of the spectrum is less straightforward to analyse. For one, the phenol and the acid monomer present slightly different shifts for the CH_2 environments. The acid, as explained, will present extra signals due to rotamer structures. In addition, having two acid monomers grafted onto the template could multiply by two the possible conformational states in which the molecule might be at any given time. All this can be seen in action in the 2D NOESY experiment in Figure 3.10. In the 4 to 5 ppm range of the ^{1}H NMR spectrum of **3.18** there are at least eight different signals, some of which present exchange cross-peaks strong enough to appear in the NOESY spectrum. They are the four signals coming from the acid monomer which have exchange cross-peaks between themselves (**a** with **a'** and **d** with **d'**). On the other hand, once the molecule is zipped-up it becomes conformationally locked and those eight signals become just four: two for the CH_2 next to the triazoles and two more for the CH_2 next to the alkynes.

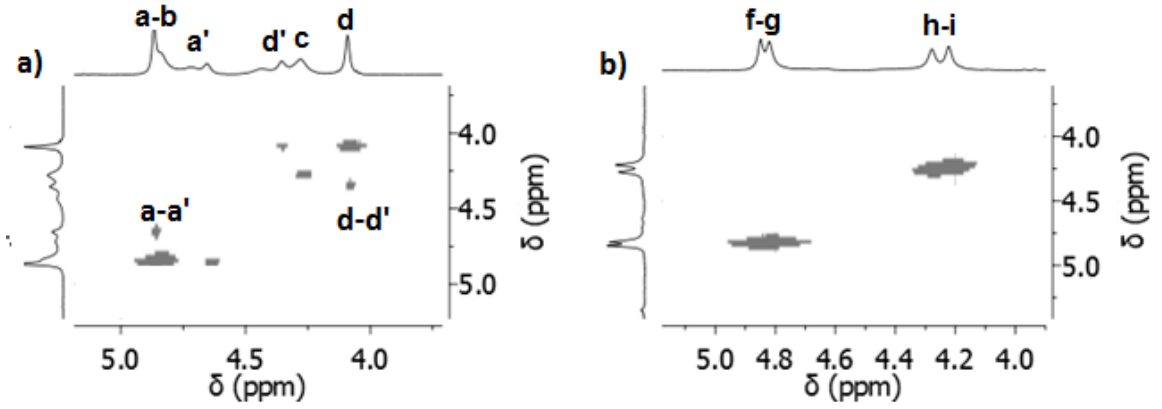

Figure 3.10. 2D NOESY (500 MHz, Chloroform-*d*, 298K, ca. 5 mM) spectra of (a) **3.18** and (b) **3.19**. The proton labelling scheme is shown in Scheme 3.5.

This can be easily visualised if we look at the molecular mechanics simulations of compounds **3.18** and **3.19** (Figure 3.11). While the pre-zip molecule may present many different possible conformations that arise from its different rotors, the constriction caused by the cyclisation severely limits the range of movement of the molecule.

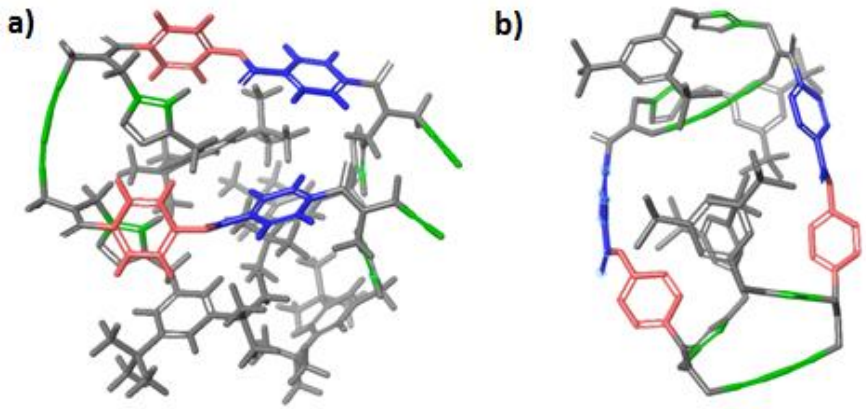

Figure 3.11. Lowest energy structures from molecular mechanics conformational searches (Schrödinger Maestro 11, OPLS3, $CHCl_3$) of (a) **3.18** and (b) **3.19**. Two steps were performed in the conformational search: "Large-Scale Low-Mode sampling" and "Mixed torsional/Low-mode sampling". $CHCl_3$ used as an implicit solvent.

To complete the base-pair cycle and to show that the synthesis of the acid dimer is indeed possible going through a phenol template, it was necessary to hydrolyse macrocycle **3.19** into

the two dimers **3.15** and **3.20**. This hydrolysis of an aromatic ester proved to be quick and efficient, going to completion in around 30 min. Figure 3.12 shows the UPLC traces of compound **3.19** before and after the addition of aqueous LiOH. The reaction afforded the phenol and the acid dimer and no trace of starting material or side products could be identified. Upon purification, the acid dimer **3.20** was isolated in a nearly quantitative yield.

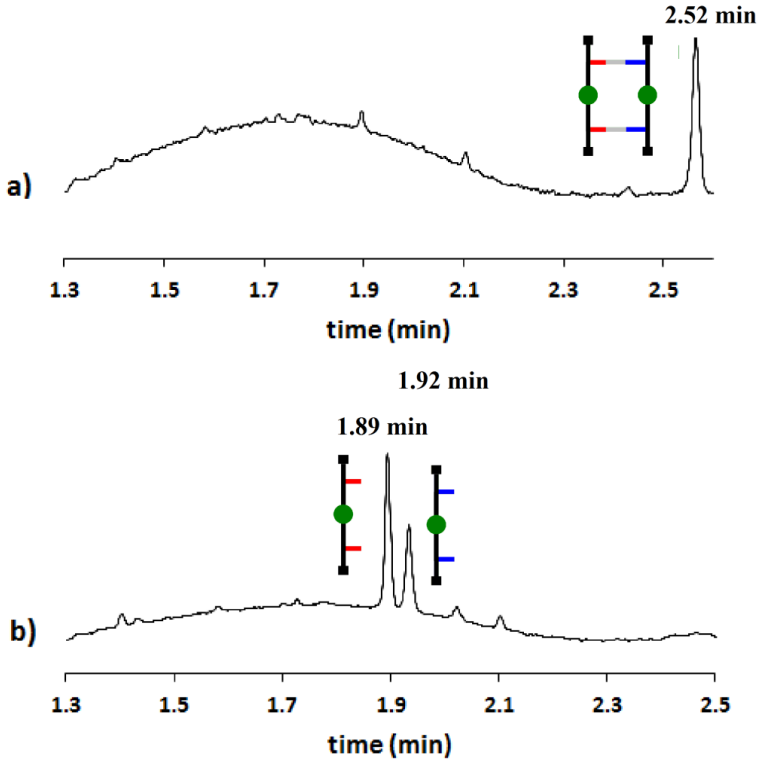

Figure 3.12. UPLC trace for the reaction of **3.18** with aqueous 2M LiOH (10 eq.) in THF at room temperature after (a) 0 min and (b) 30 min. The conditions of the UPLC method are as follows: Solvent A: Water +0.1% Formic acid; Solvent B: Acetonitrile +0.1% Formic acid; Gradient of 0-2 minutes 5% - 100%B + 1 minute 100% B with re-equilibration time of 2 minutes. Flow rate: 0.6 ml/min; Column temperature of 40°C; Injection volume of 2 µL.The signal was monitored at 254 nm.

3.6 Template-directed synthesis on a heterodimer template

To perform the templated synthesis of a heterodimer a full base-pair replication cycle needs to be conducted (Scheme 3.10).

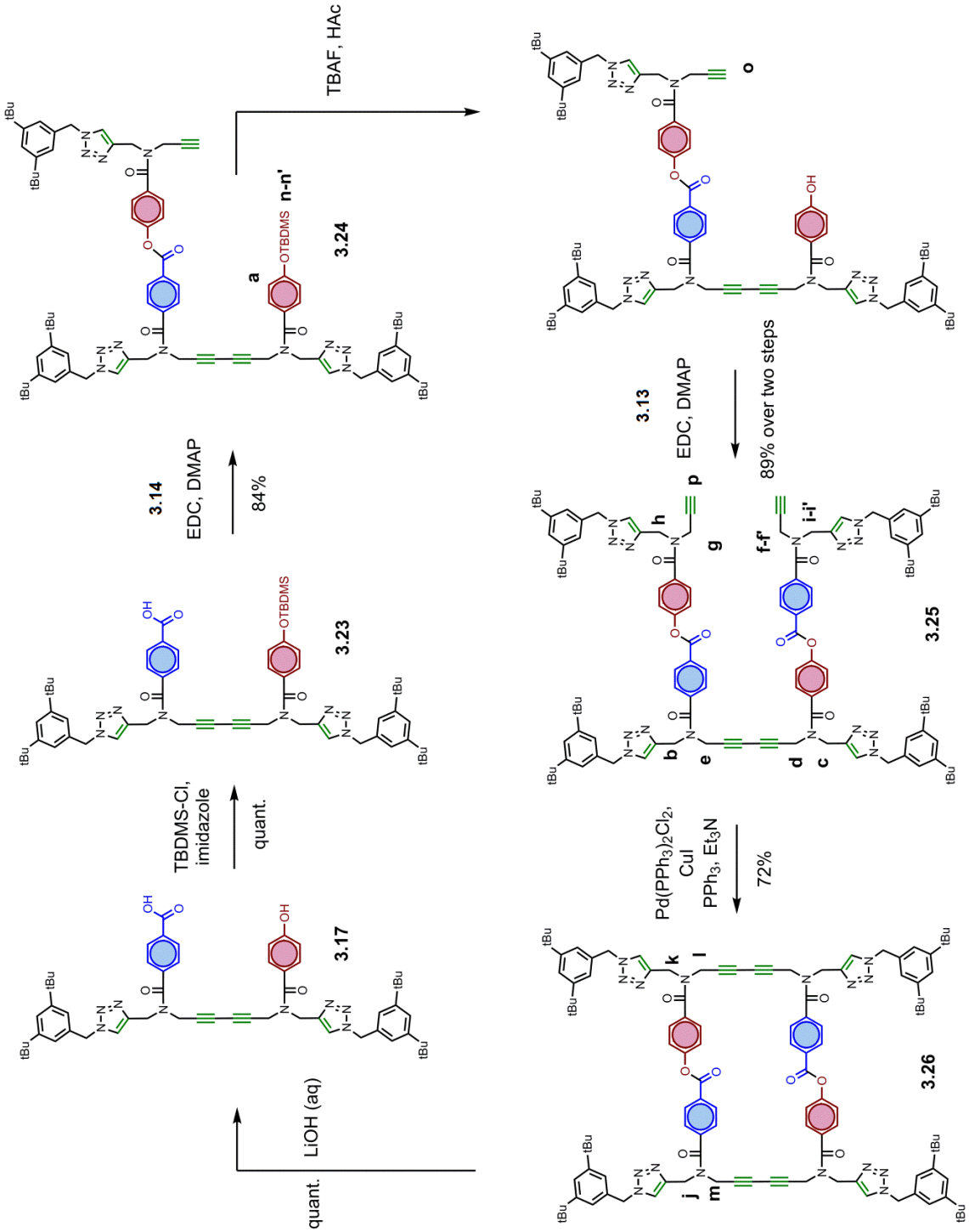

Scheme 3.10. Covalent template-directed replication of the heterodimer **3.17**. The proton labelling scheme used in Figure 3.14 is shown.

To do that, the phenol of the mixed dimer **3.17** was protected with TBDMS-Cl to afford compound **3.23**. Since carboxylic acids also react with silyl chlorides, twice as much of TBDMS-Cl had to be added to the reaction. When no starting material could be seen by UPLC, the crude solution was acidified and stirred for half an hour to restore the carboxylic acid. The UPLC trace showed a change in the peak positioning going from 1.90 min to 2.38 min (Figure 3.13, trace B). The crude reaction was carried over to the next step, in which the acid part of the dimer was esterified with the phenol monomer **3.14** to form compound **3.24**. The UPLC trace shows a decrease in polarity when going from **3.23** to **3.24**, which elutes at 2.62 min (Figure 3.13, trace C). Compound **3.24** was then deprotected using TBAF and acetic acid. Earlier studies showed that the use of only TBAF would hydrolyze the highly labile aromatic ester formed in the previous step. Using one equivalent of acid reduces the basicity of the TBAF and leads it to act only as nucleophile. This reaction crude, which was carried forward, presented a significant decrease in retention time compared to **3.24** (elution at 2.18 min, Figure 3.13, trace D). The pre-zip structure **3.25** was formed in the subsequent esterification (Figure 3.13, trace E) in which a big change in the retention times in the UPLC trace was observed (2.18 min to 2.42 min). **3.25** was purified before performing the zip-up reaction to yield the final macrocycle **3.26**, which presented a similar change in the UPLC retention time as previously observed in the transformation of **3.18** into **3.19** (2.42 min to 2.51 min, Figure 3.13, trace F). To finalize the cycle, the macrocycle was hydrolyzed to restore the starting mixed dimer **3.17** (Figure 3.13, trace G).

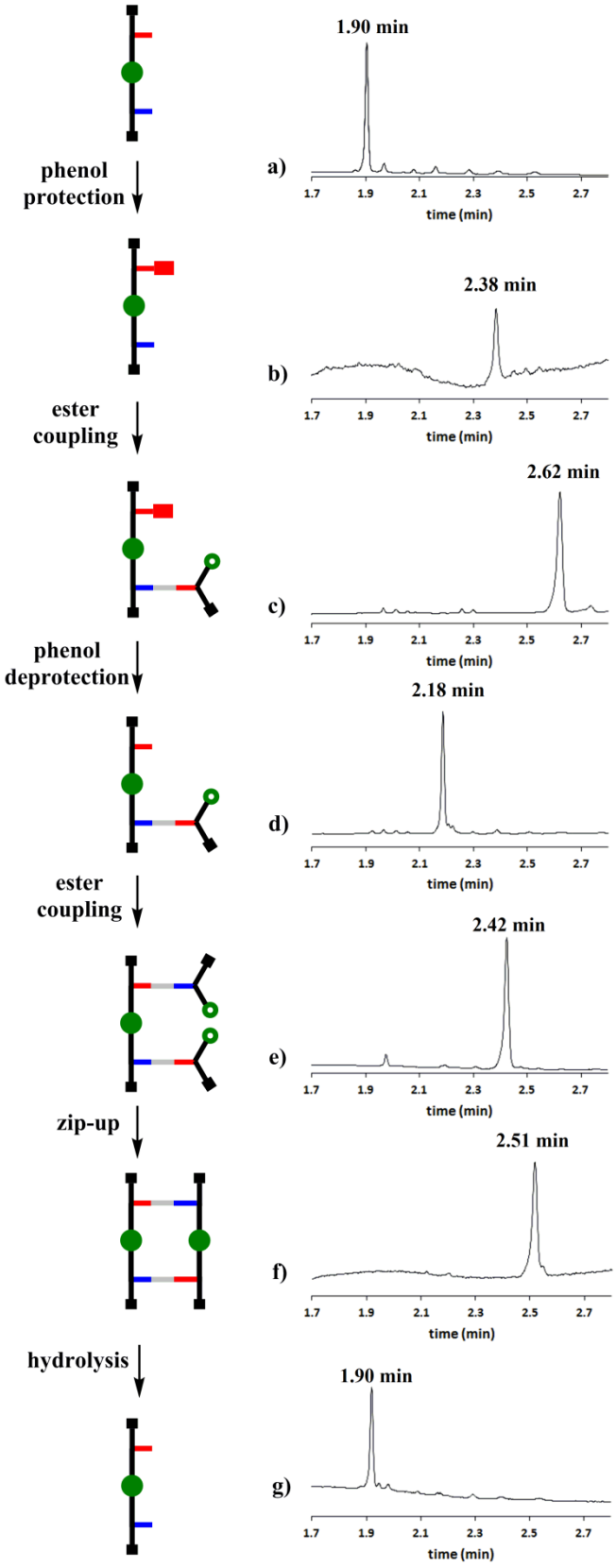

Figure 3.13. UPLC traces of the heterodimer replication cycle. (a), (c), (e) and (f) measured after compound purification by column chromatography. (b), (d) and (g) measured crude reaction mixtures. The conditions of the UPLC method are as follows: Solvent A: Water +0.1% Formic acid; Solvent B: Acetonitrile +0.1% Formic acid; Gradient of 0-2 minutes 5% - 100%B

+ 1 minute 100% B with re-equilibration time of 2 minutes. Flow rate: 0.6 ml/min; Column temperature of 40°C; Injection volume of 2 µL. The signal was monitored at 254 nm.

The base-pair replication cycle of the heterodimer could be followed not only by the UPLC traces, but in addition, via various key changes in the ^{1}H NMR spectra of each compound. Those changes are highlighted in Figure 3.14 in different boxes. Figure 14a shows the most upfield aromatic protons from the phenol monomer moving downfield after the reaction with the acid monomer **3.13** to form compound **3.25**. Figure 14b shows the increase in symmetry caused by the zip-up reaction of **3.25** to form **3.26**. The propargyl CH_2 protons see their rotation completely restricted which leads to the disappearance of the rotameric signals. It is particularly evident in this macrocycle since upon closing the number of different environments goes from ten to only four. A complete labelling of all the environments can be found in Scheme 3.7. In Figure 3.14c we can see the appearance, first, of an alkyne signal after the first esterification of the phenol monomer **3.14** onto the template going from **3.23** to **3.24**. Then we see the alkyne signal increasing in intensity after the second grafting, this time of the acid monomer **3.13**, to form **3.25**. Furthermore, we can see the disappearance of the alkyne protons during the zip-up reaction to form macrocycle **3.26**. Finally, Figure 3.14d shows the appearance and disappearance of the two TBDMS signals after the phenol protection and deprotection going from **3.17**, to **3.24** and then to **3.25**.

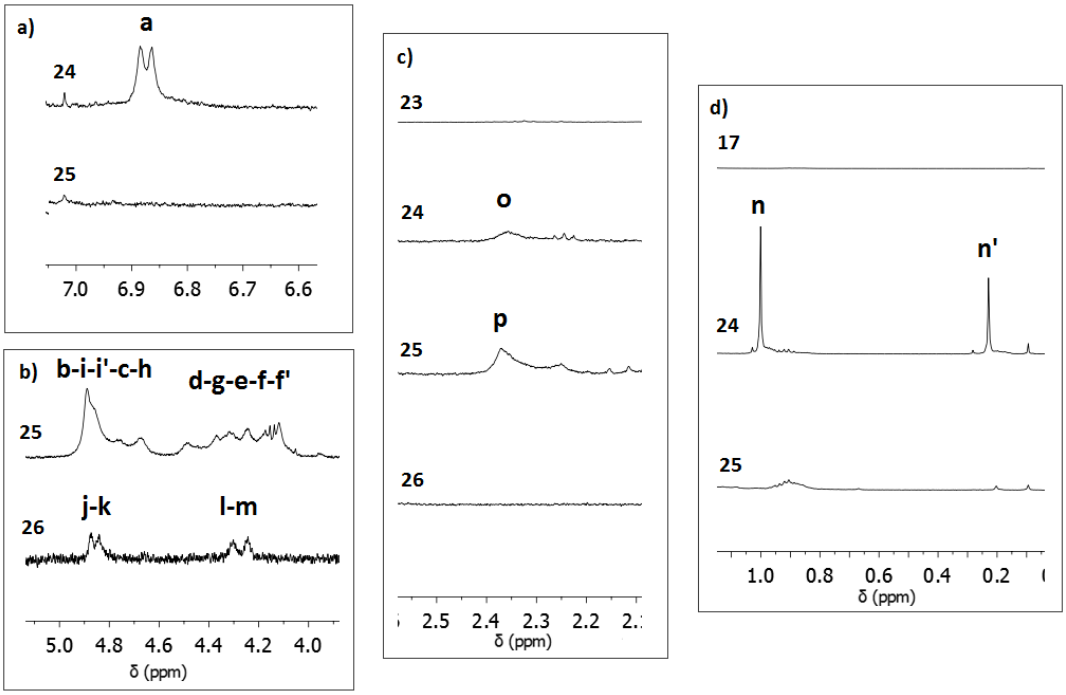

Figure 3.14. Partial ^{1}H NMR (400 MHz, Chloroform-*d*, 298K, ca. 5 mM) spectra of intermediates isolated in the replication cycle for heterodimer **3.16.** (a) 7-6.5 ppm, aromatic

signals; (b) 5-4 ppm, CH_2-N signals; (c) 2.5-2 ppm, alkyne signals; (d) 1-0 ppm, alkyl signals. The proton labelling scheme is shown in Scheme 3.10.

It was mentioned earlier in the chapter that the homophenol dimer was acting as a kinetic template since it increased the reaction rate. The use of heterodimer **3.17** as a template is significant because it affects the final product distribution, i.e. the templated synthesis of the heterodimer gives a single product, while its synthesis through the statistical reaction of the monomers produces a poorly defined product mixture (Figure 3.4).

3.7 Conclusions

In this chapter we synthesized the complementary-sequence strands of two different dimers, and in doing so we developed the chemistry necessary for carrying out an efficient zip-up process. We were able to identify the signs that point towards macrocycle closing (e.g. changes in UPLC, 1D and 2D ^{1}H NMR) which will facilitate following the progress of these closing reactions when we move towards longer oligomers. Furthermore, we demonstrated the templating properties of the two dimers used to develop the chemistry in this chapter: the homodimer increased 6-fold the alkyne-alkyne reaction rate, thus acting as a kinetic template; and the heterodimer changed the product distribution from a mixture containing several products as the outcome of a statistical reaction to a single, pure compound, which is a replica of the initial template.

3. 8 Experimental Section

General methods

All the reagents were obtained from commercial sources (Sigma-Aldrich, Alfa Aesar, Fisher Scientific and Fluorochem) and were used without further purification. Thin layer chromatography was carried out using with silica gel 60F (Merck) on aluminium. Flash chromatography was carried out on an automated system (Combiflash Rf+ or Combiflash Rf Lumen) using prepacked cartridges of silica (25µ or 50µ PuriFlash® Columns). ^{1}H and ^{13}C NMR spectra were recorded on either a Bruker AV3400 or AV3500 spectrometer at 298 K unless specifically stated otherwise. Residual solvent peak was used as an internal standard. All chemical shifts are quoted in ppm on the δ scale and the coupling constants expressed in Hz. Signal splitting patterns are described as follows: s (singlet), d (doublet), t (triplet), m (multiplet). FTIR spectra were recorded on a PerkinElmer Spectrum One FT-IR spectrometer. ES+ was carried out on a Waters LCT-TOF spectrometer or a Waters Xevo G2-S bench top QTOF machine. The LCMS analysis of samples was performed using Waters Acquity H-class UPLC coupled with a single quadrupole Waters SQD2. ACQUITY UPLC CSH C18 Column, 130Å, 1.7 µm, 2.1 mm X 50 mm was used as the UPLC column. The conditions of the UPLC method are as follows: Solvent A: Water +0.1% Formic acid; Solvent B: Acetonitrile +0.1% Formic acid; Gradient of 0-2 minutes 5% - 100%B + 1 minute 100% B with re-equilibration time of 2 minutes. Flow rate: 0.6 ml/min; Column temperature of 40 °C; Injection volume of 2 µL. The signal was monitored at 254 nm.

Synthesis of compound 3.1

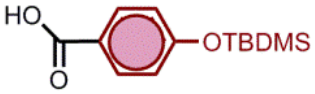

4-Hydroxybenzoic acid (1.9 g, 14.0 mmol) was dissolved in THF (250 mL) and tert-butyldimethylsilyl chloride (4.8 g, 32.2 mmol) and imidazole (3.8 g, 68.0 mmol) were added, and the solution was stirred overnight. HCl 1M (30 mL) was added, and the solution was re-extracted with EtOAc. The organic phase was washed with brine (2 x 20 mL), dried over $MgSO_4$, evaporated and dried under high vacuum to yield compound **3.1** as a white solid (3.5 g, quantitative yield). The product was carried forward without further purification.

^{1}H NMR (400 MHz, Chloroform-*d*) δ 8.03 (d, *J* = 8.8 Hz, 2H), 6.91 (d, *J* = 8.8 Hz, 2H), 1.02 (s, 9H), 0.26 (s, 6H).

^{13}C NMR (101 MHz, Chloroform-*d*) δ 172.21, 160.87, 132.32, 122.30, 119.94, 25.59, 18.26, -4.37.

HRMS (ES+): calcd for $C_{13}H_{21}O_3Si$ 253.1259 $[M+H]^+$, found 253.1263 $[M+H]^+$.

FT-IR (ATR): 2927, 2858, 1677, 1602, 15510, 1475 cm^{-1}

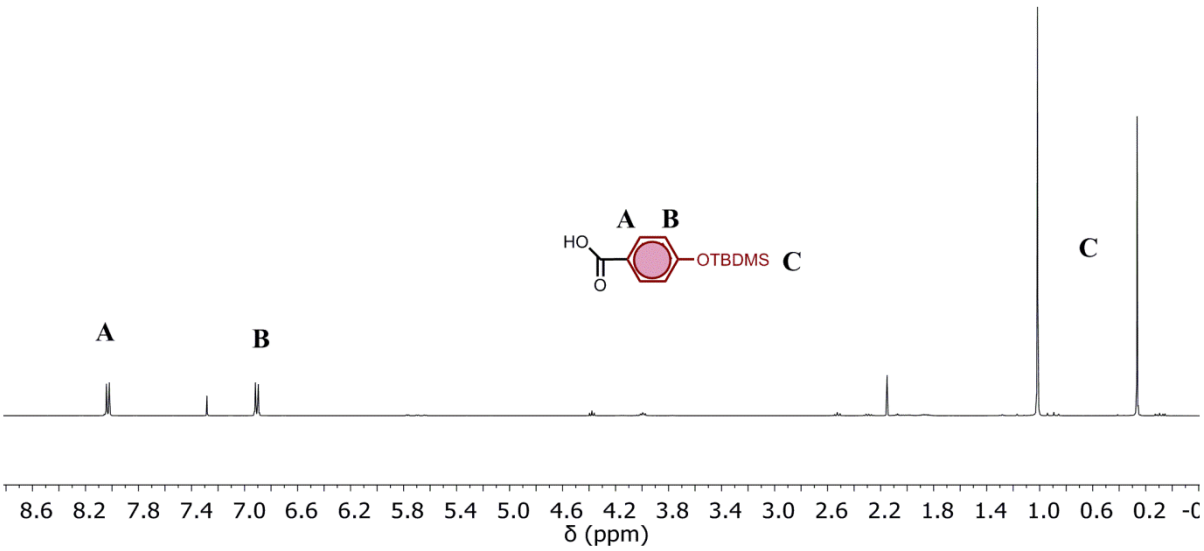
A
B
C
HO
O
OTBDMS
8.6 8.2 7.8 7.4 7.0 6.6 6.2 5.8 5.4 5.0 4.6 4.2 3.8 3.4 3.0 2.6 2.2 1.8 1.4 1.0 0.6 0.2
δ (ppm)

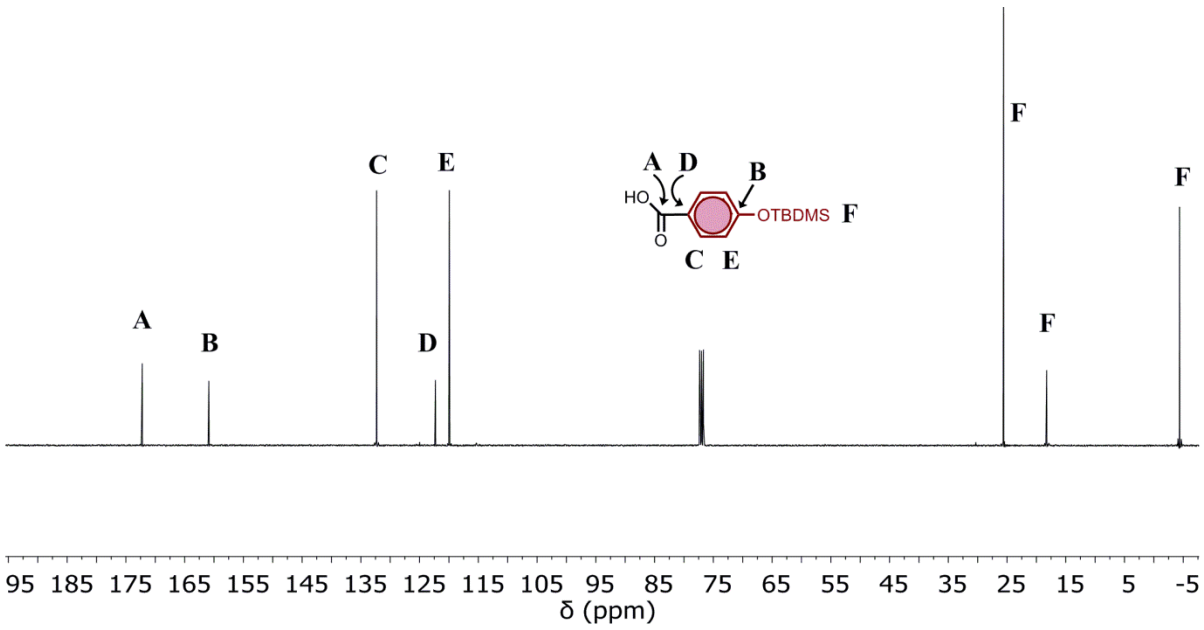
A
B
C
D
E
F
HO
O
OTBDMS
95 185 175 165 155 145 135 125 115 105 95 85 75 65 55 45 35 25 15 5 -5
δ (ppm)

Synthesis of compound 3.2

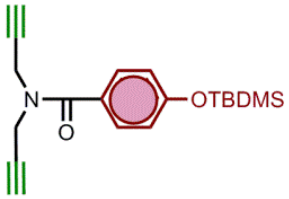

3.1 (550 mg, 2.18 mmol), EDC (544 mg, 2.84 mmol) and DMAP (27 mg, 0.22 mmol) were dissolved in dry DCM (50mL) and stirred under N_2. Dipropargylamine (240 µL, 2.18 mmol) was added and the solution was left stirring overnight. The crude was washed with HCl 1M (2 x 10 mL), and brine (2 x 20 mL). The organic phase was dried with $MgSO_4$, concentrated in vacuo and purified by column chromatography (PET 40-60/EtOAc, gradient of increasing polarity) to yield pure compound as a yellow-orange oil (580 mg, 81%).

^{1}H NMR (400 MHz, Chloroform-*d*) δ 7.44 (d, *J* = 8.6 Hz, 2H), 6.82 (d, *J* = 8.6 Hz, 2H), 4.26 (br s, 4H), 2.30 (s, 2H), 0.93 (s, 9H), 0.16 (s, 6H).

^{13}C NMR (100 MHz, Chloroform-*d*) δ 170.68, 157.81, 129.30, 127.21, 120.01, 78.33, 72.84, 25.61, 18.19, -4.40.

HRMS (ES+): calcd for $C_{19}H_{25}NO_2Si$ 328.1732 $[M+H]^+$, found 328.1731 $[M+H]^+$.

FT-IR (ATR): 3291, 3243, 2954, 2930,2857, 1642, 1603, 1509 cm^{-1}

Retention time: 1.69 min

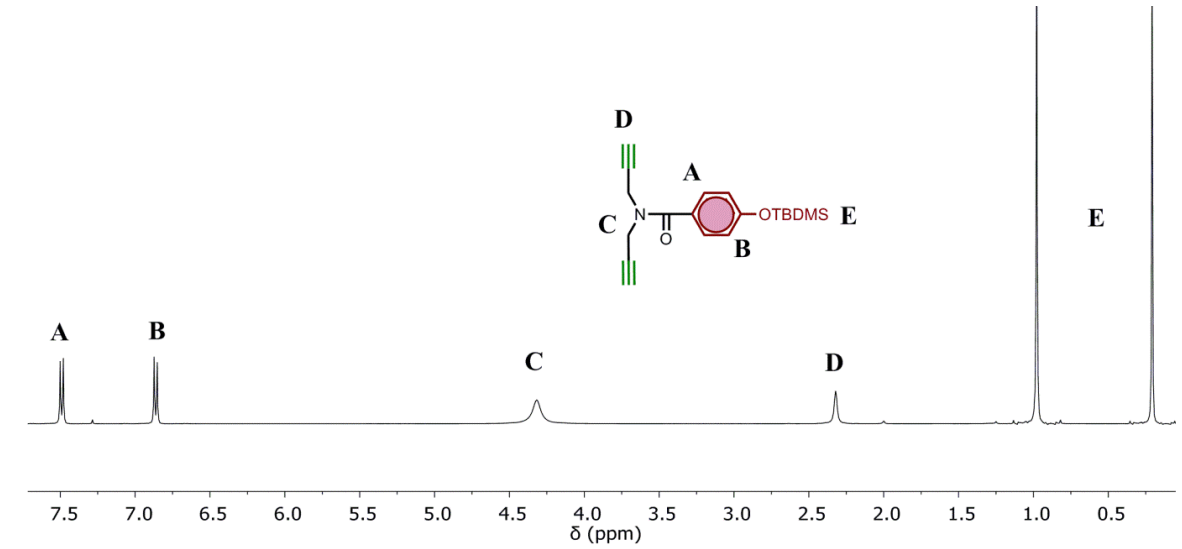
D
A
C
N
O
OTBDMS
E
B
E
A
B
C
D
7.5
7.0
6.5
6.0
5.5
5.0
4.5
4.0
3.5
3.0
2.5
2.0
1.5
1.0
0.5
δ (ppm)

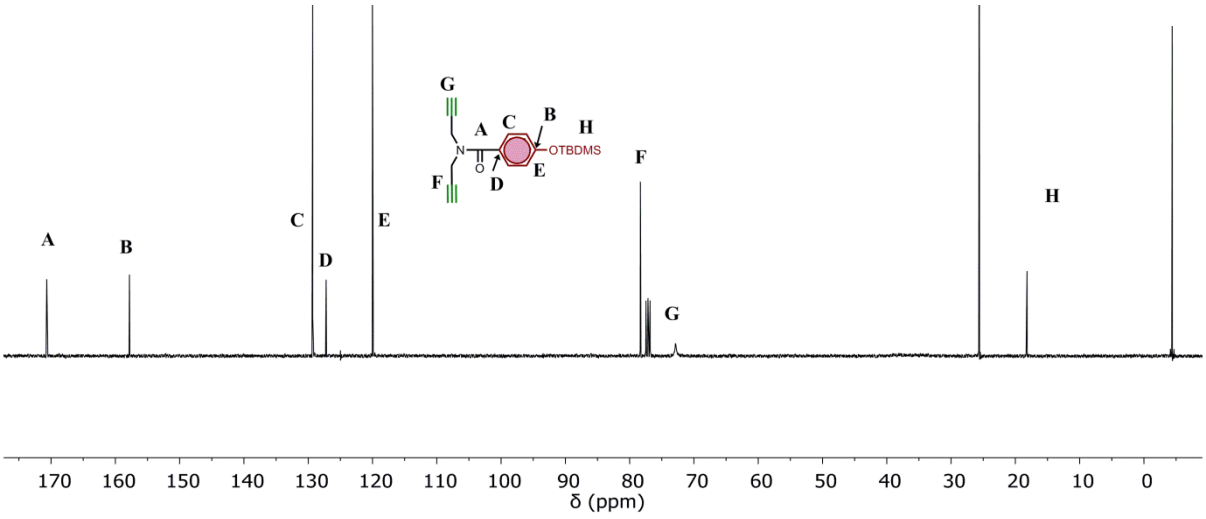
G
A
C
B
H
N
O
OTBDMS
F
D
E
A
B
C
D
E
F
G
H
170
160
150
140
130
120
110
100
90
80
70
60
50
40
30
20
10
0
δ (ppm)

Synthesis of compound 3.3

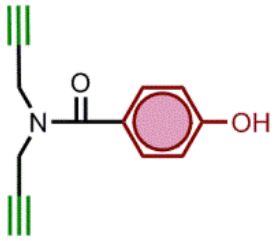

3.2 (78 mg, 0.24 mmol) was dissolved in THF (10 mL) and the solution cooled in ice. TBAF (1M in THF, 0.30 mL) was added dropwise and the reaction was left stirring at room temperature for 20 min before adding HCl 1M until the pH reached 3-4. Water was added (20 mL), the organic compound was reextracted with EtOAc (2 x 20 mL) and this organic phase was washed with brine (2 x 20 mL), dried with $MgSO_4$, filtered and evaporated in vacuo before purification by column chromatography (PET 40-60/EtOAc, gradient of increasing polarity) to yield a white solid (50 mg, 94%)

^{1}H NMR (400 MHz, Chloroform-*d*) δ 7.50 (d, *J* = 8.6 Hz, 2H), 6.85 (d, *J* = 8.6 Hz, 2H), 6.16 (s, 1H), 4.37 (br s, 4H), 2.35 (s, 2H).

^{13}C NMR (100 MHz, Chloroform-*d*) δ 171.43, 160.06, 129.33, 124.62, 115.74, 78.35, 58.84.

HRMS (ES+): calcd for $C_{13}H_{11}NO_2$ 214.0868 $[M+H]^+$, found 214.0860 $[M+H]^+$.

FT-IR (ATR): 3289, 1609, 1515, 1453 cm^{-1}

Retention time: 0.78 min

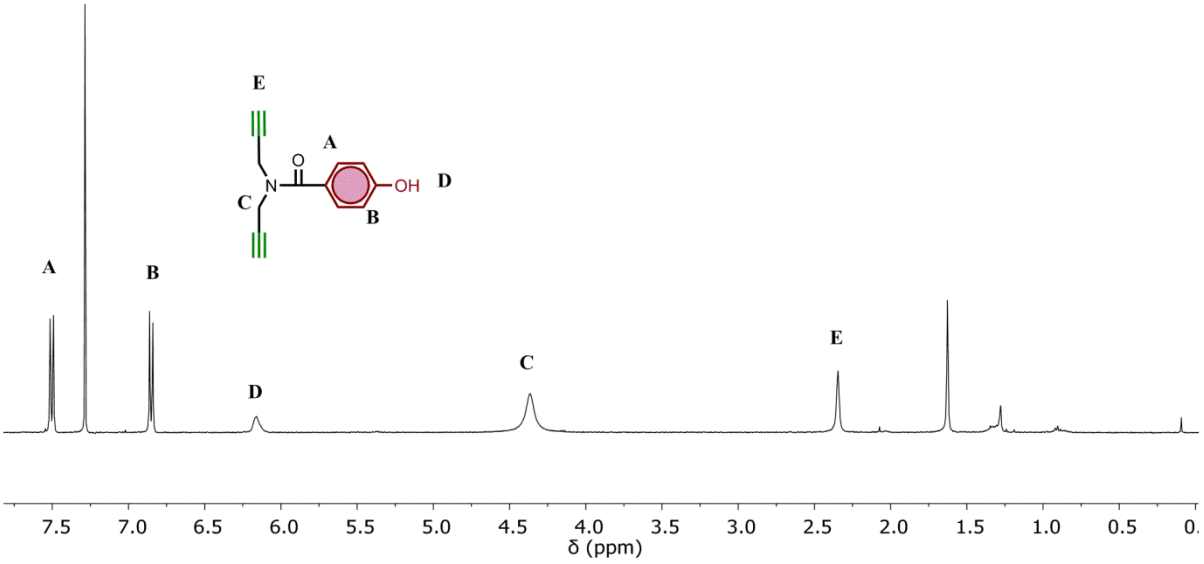
E
A
O
N
OH
D
C
B
A
B
D
C
E
7.5 7.0 6.5 6.0 5.5 5.0 4.5 4.0 3.5 3.0 2.5 2.0 1.5 1.0 0.5
δ (ppm)

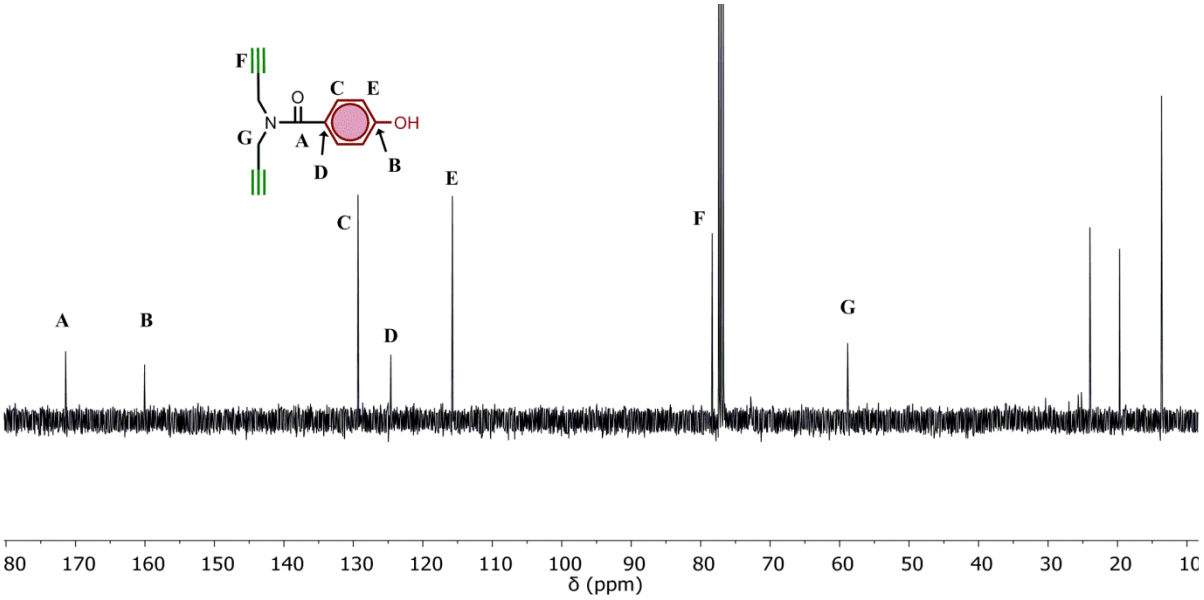
F
C
E
O
N
OH
G
A
D
B
E
C
F
A
B
D
G
80 170 160 150 140 130 120 110 100 90 80 70 60 50 40 30 20
δ (ppm)

Synthesis of compound 3.4

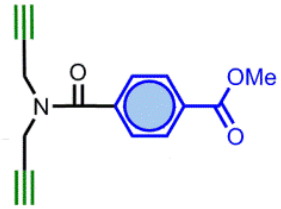

Monomethyl terephthalate (300 mg, 1.67 mmol), EDC (410 mg, 2.16 mmol) and DMAP (61 mg, 0.50 mmol) were dissolved in dry DCM (10 mL) and stirred under N_2. Dipropargylamine (183µL, 1.67 mmol) was added and the solution was left stirring overnight. The crude was washed with HCl 1M (2 x 10 mL), and brine (2 x 20 mL). The organic phase was dried with $MgSO_4$ and concentrated in vacuo to yield pure compound as a yellow-orange oil (387 mg, 91%).

^{1}H NMR (400 MHz, Chloroform-*d*) δ 8.11 (d, *J* = 8.3 Hz, 2H), 7.62 (d, *J* = 8.3 Hz, 2H), 4.49 (br s, 2H), 4.13 (br s, 2H), 3.93 (s, 3H), 2.35 (br s, 2H).

^{13}C NMR (100 MHz, Chloroform-*d*) δ 169.81, 166.18, 138.76, 131.82, 129.86, 127.11, 73.65, 52.38, 38.18, 33.70.

HRMS (ES+): calcd for $C_{15}H_{13}NO_3$ 256.0973 $[M+H]^+$, found 256.0967 $[M+H]^+$.

FT-IR (ATR): 3234, 2936, 1718, 1640, 1442 cm^{-1}

Retention time: 1.00 min

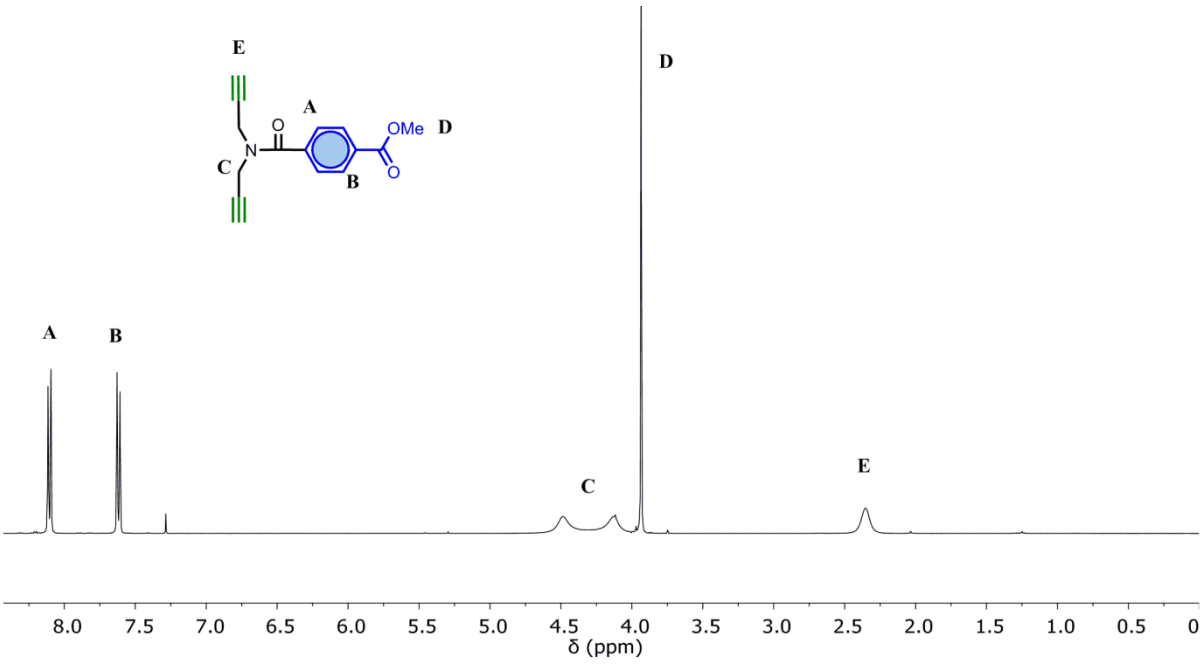
E
A
O
N
C
OMe
D
B
O
D
A
B
C
E
8.0
7.5
7.0
6.5
6.0
5.5
5.0
4.5
4.0
3.5
3.0
2.5
2.0
1.5
1.0
0.5
0
δ (ppm)

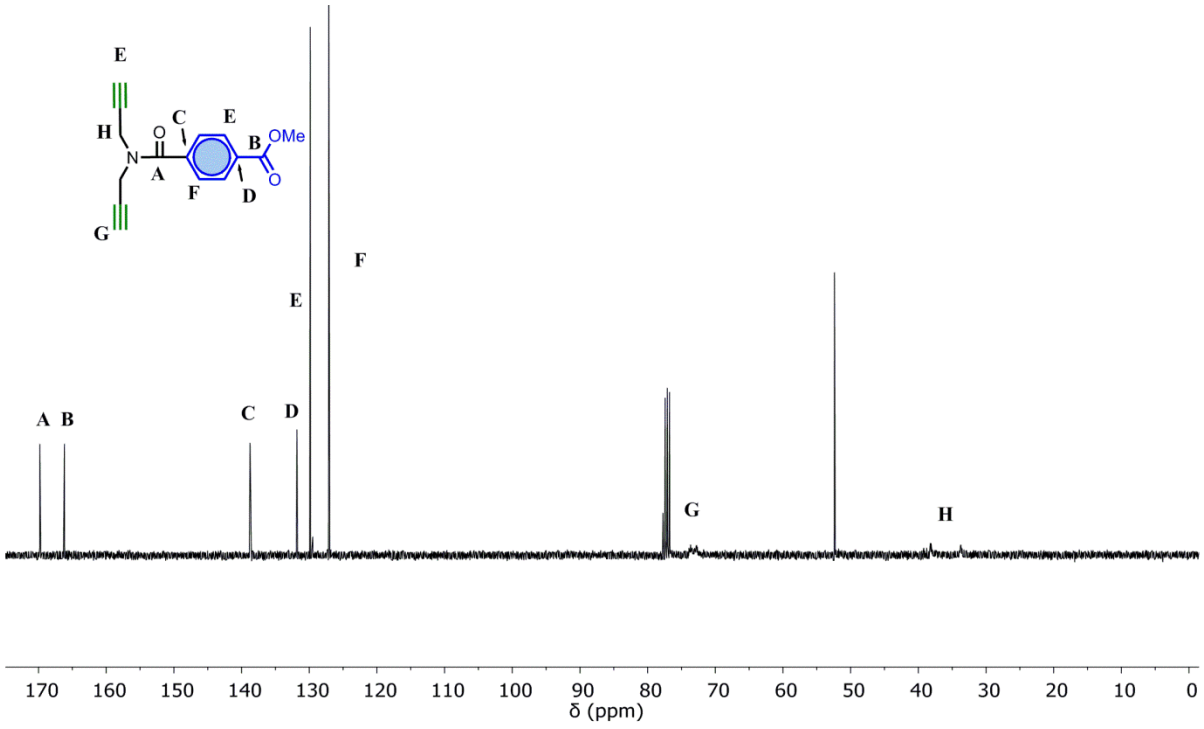
E
H
O
C
E
N
A
B
OMe
O
F
D
G
F
E
A B
C
D
G
H
170
160
150
140
130
120
110
100
90
80
70
60
50
40
30
20
10
0
δ (ppm)

Synthesis of compound 3.5

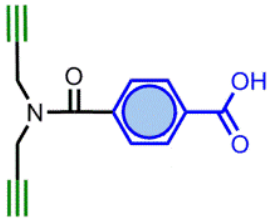

3.4 (70 mg, 0.27 mmol) was dissolved in THF (10 mL) and a solution of LiOH (34 mg, 0.82 mmol) in water (4 mL) was added dropwise. The reaction was left stirring overnight, acidified with HCl 1M to pH 1, diluted with water and reextracted with EtOAc (2 x 20 mL). The organic phase was washed with brine (2 x 20 mL), dried with $MgSO_4$, filtered and dried in vacuo to yield the pure compound as a yellow solid (65 mg, quantitative yield)

^{1}H NMR (400 MHz, Chloroform-*d*) δ 10.69 (s, 1H), 8.15 (d, *J* = 7.9 Hz, 2H), 7.64 (d, *J* = 7.9 Hz, 2H), 4.49 (br s, 1H), 4.12 (br s, 1H), 2.40 (br, 2H).

^{13}C NMR (100 MHz, Chloroform-*d*) δ 170.20, 170.08, 139.10, 131.36, 130.44, 127.18, 73.99, 73.04, 38.31, 33.90.

HRMS (ES+): calcd for $C_{14}H_{11}NO_3$ 242.0817 $[M+H]^+$, found 242.0809 $[M+H]^+$.

FT-IR (ATR): 3280, 1920, 1702, 1632, 1446 cm^{-1}

Retention time: 0.81 min

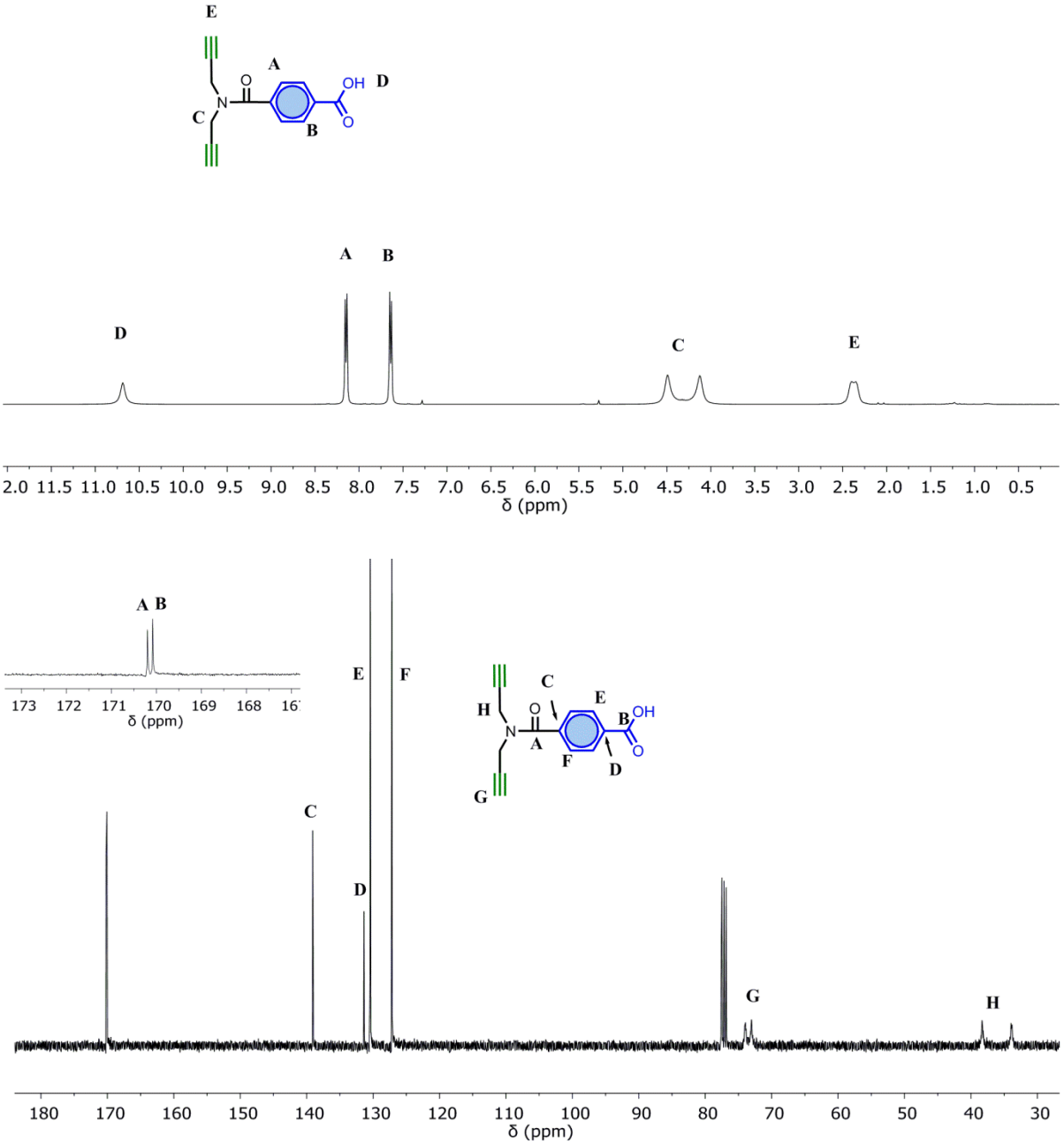
E
A
O
OH
D
C
N
B
O
A B
D
C
E
2.0 11.5 11.0 10.5 10.0 9.5 9.0 8.5 8.0 7.5 7.0 6.5 6.0 5.5 5.0 4.5 4.0 3.5 3.0 2.5 2.0 1.5 1.0 0.5
δ (ppm)
A B
173 172 171 170 169 168
δ (ppm)
E
F
C
H
N
O
A
C
E
B
OH
O
F
D
G
D
C
G
H
180 170 160 150 140 130 120 110 100 90 80 70 60 50 40 30
δ (ppm)

Synthesis of compound 3.6

A solution of propargylamine (0.20 mL, 3.21 mmol) in THF (10 mL) was cooled to –78 °C while stirring in an argon atmosphere. *n*-Butyllithium (1.6 M in hexanes, 2.15 mL, 3.44 mmol) was added slowly, and the reaction was allowed to proceed for 15 min. The mixture was then warmed to 0 °C, and triisopropylsilyl chloride (0.80 mL, 3.75 mmol) was added. After stirring for 1 h at 0 °C, the reaction mixture was diluted with satd. aq. $NaHCO_3$ (5 mL) and stirred for 5 min. The solution was diluted with water (5 mL), and the product was extracted with diethyl ether (3 x 10 mL). The combined organic phase was washed with brine (2 x 20 mL), dried with anhydrous $MgSO_4$, filtered, and the solvents evaporated. The obtained residue was purified by flash chromatography (PET 40-60/EtOAc, gradient of increasing polarity) to afford compound **6** (0.621 g, 94%).

^{1}H NMR (400 MHz, Chloroform-*d*): δ_H = 3.46 (s, 2H, CH_2), 1.44 (bs, 2H, NH_2), 1.06 (m, 21 H, 3x^{i}Pr).

^{13}C NMR (100 MHz, Chloroform-*d*) δ 104.2, 80.2, 32.45, 18.59, 11.21.

HRMS (ES+): calcd for $C_{12}H_{25}NSi$ 212.1834 $[M+H]^+$, found 212.1832 $[M+H]^+$.

Synthesis of compound 3.7

Boc_2O (0.769 g, 3.53 mmol) was added to a solution of **3.6** (0.621 g, 2.94 mmol) in dry DCM (10 mL). Et_3N (0.61 mL, 4.41 mmol) was added and the reaction was allowed to proceed for 1 h. After completion, the reaction was quenched with satd. aq. NH_4Cl and extracted with DCM (3 x 10 mL). The combined organic phase was washed with satd. aq. $NaHCO_3$ (2 x 5 mL), water (20 ml) and brine (2 x 20 mL) and dried with anhydrous $MgSO_4$. The obtained white solid (0.972 g, quantitative) was used in the following step without further purification.

^{1}H NMR (400 MHz, Chloroform-*d*): δ_H = 4.63 (bs, 1H, NH), 3.95 (d, *J*= 5.5 Hz, 2H, CH_2), 1.45 (s, 9H, Boc), 1.05 (m, 21 H, ^{i}Pr).

^{13}C NMR (100 MHz, Chloroform-*d*): δ_C = 155.4 (CO, Boc), 103.7 and 80.1 (C, alkyne), 77.4 (C, Boc), 31.8 (CH_2), 28.5 (CH_3, Boc), 18.7 (CH_3, ^{i}Pr), 11.3 (CH, ^{i}Pr).

HRMS (ES+): calcd for $C_{17}H_{34}NO_2Si$ 312.2359$[M+H]^+$, found 312.2353 $[M+H]^+$.

FT-IR (ATR): 3340, 2942, 2893, 2866, 1700, 1462, 1247, 1170, 1016, 1001, 677 and 664 cm^{-1}

Synthesis of compound 3.8

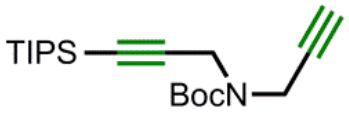

Compound **3.7** (11.67 g, 37.46 mmol) was dissolved in dry THF (50 mL) and added to a suspension of NaH (60% dispersion in mineral oil, 2.25 g, 56.19 mmol) in THF (100 mL) under inert atmosphere. The reaction was allowed to proceed for 45 min. Propargyl bromide (80% in toluene, 6.05 mL, 56.19 mmol) was added dropwise and the reaction was vigorously stirred overnight. Satd. aq. NH_4Cl (20 mL) was carefully added at 0 ºC and the reaction was extracted with EtOAc (3 x 100 mL). The combined organic phase was washed with brine (3 x 20 mL), dried with anhydrous $MgSO_4$, filtered, and the solvents evaporated. The obtained residue was purified by flash chromatography (PET 40-60/EtOAc, gradient of increasing polarity) to afford compound **3.8** (11.2 g, 86%) as a yellow oil.

^{1}H NMR (400 MHz, Chloroform-*d*): δ_H = 4.18 (bs, 4H, CH_2), 2.20 (t, *J*= 2.5 Hz, CH), 1.48 (s, 9H, Boc), 1.06 (m, 21 H, ^{i}Pr).

^{13}C NMR (100 MHz, Chloroform-*d*): δ_C = 154.5 (CO, Boc), 102.5 and 81.1 (C, TIPS-alkyne), 79.2 (CH, terminal alkyne), 77.4 (C, Boc), 72.0 (C, terminal alkyne), 36.6 and 35.2 (CH_2), 28.4 (CH_3, Boc), 18.7 (CH_3, ^{i}Pr), 11.3 (CH, ^{i}Pr).

HRMS (ES+): calcd for $C_{20}H_{36}NO_2Si$ 350.2515 $[M+H]^+$, 350.2513 found $[M+H]^+$.

FT-IR (ATR): 2943, 2866, 1703, 1367, 1243, 1162, 1007, 883, 677 and 663 cm^{-1}

Synthesis of compound 3.9

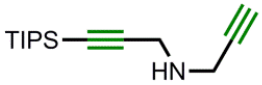

Compound **3.8** (11.2 g, 32.04 mmol) was dissolved in MeOH (100 mL) and aq. HCl (37%, 40 mL) was added dropwise. The reaction was stirred overnight at room temperature. The solvents were evaporated, and co-evaporated with toluene to remove residual water. The crude was dried at high vacuum. Compound **3.9** (9.05 g, 99%) was obtained as a brown solid and used in the following reaction without further purification.

^{1}H NMR (400 MHz, Chloroform-*d*): δ_H = 4.18 (bs, 4H, CH_2), 2.20 (t, *J*= 2.5 Hz, CH), 1.06 (m, 21 H, 3x^{i}Pr).

^{13}C NMR (100 MHz, Chloroform-*d*): δ_C = 93.4 and 94.6 (2xC, alkyne), 78.3 (C-Si), 72.5 (CH; alkyne), 34.3 and 35.5 (2xCH_2), 18.7 (CH_3, TIPS), 11.2 (CH, TIPS).

HRMS (ES+): calcd for $C_{15}H_{28}NSi$ 250.1991 $[M\text{-}HCl+H]^+$, found 250.1992 $[M\text{-}HCl+H]^+$.

FT-IR (ATR): 2942, 2893, 2865, 1462, 1440, 1050, 882, 676, 662 and 633 cm^{-1}

Synthesis of compound 3.10

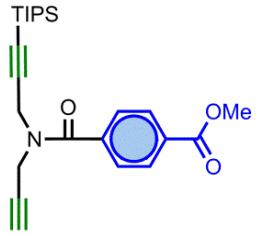

4-(Methoxycarbonyl) benzoic acid (2700 mg, 14 mmol), EDC (2.7 g, 14 mmol) and DMAP (110 mg, 0.9 mmol) were dissolved in dry DCM (50 mL) and stirred under N_2. A solution of **3.9** (2.6 g, 9 mmol) in dry DCM and Et_3N (1010 mg, 10 mmol) was added and the mixture was left stirring overnight. The solution was washed with HCl 1M (2 x 20 mL), and brine (2 x 20 mL). The organic phase was dried with $MgSO_4$ and concentrated in vacuo to yield the product as a dense orange oil (3390 mg, 91%)

^{1}H NMR (400 MHz, Chloroform-*d*) δ 8.11 (d, *J* = 7.9 Hz, 2H), 7.60 (br s, 2H), 4.50 (br s, 2H), 4.15 (br s, 2H), 3.95 (s, 3H), 2.25 (s, 1H), 1.10 (s, 21H).

^{13}C NMR (100 MHz, Chloroform-*d*) δ 169.7, 166.24, 138.99, 131.73, 129.80, 127.09, 101.03, 52.36, 18.56, 11.10.

HRMS (ES+): calcd for $C_{24}H_{34}NO_3Si$ 412.2308 $[M+H]^+$, found 412.2311 $[M+H]^+$.

FT-IR (ATR): 2943, 2865, 1727, 1650, 1434, 1410 cm^{-1}

Retention time: 2.05 min

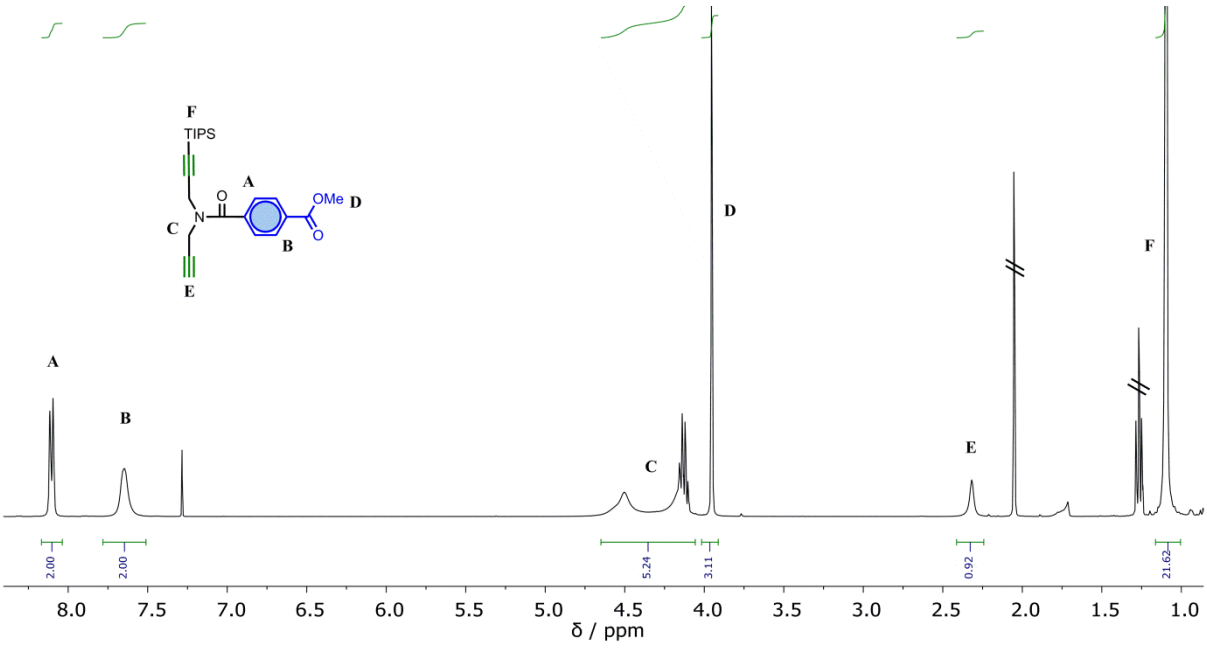
F
TIPS
A
O
N
OMe
D
C
B
O
E
A
B
C
D
E
F
2.00
2.00
5.24
3.11
0.92
21.62
8.0
7.5
7.0
6.5
6.0
5.5
5.0
4.5
4.0
3.5
3.0
2.5
2.0
1.5
1.0
δ / ppm

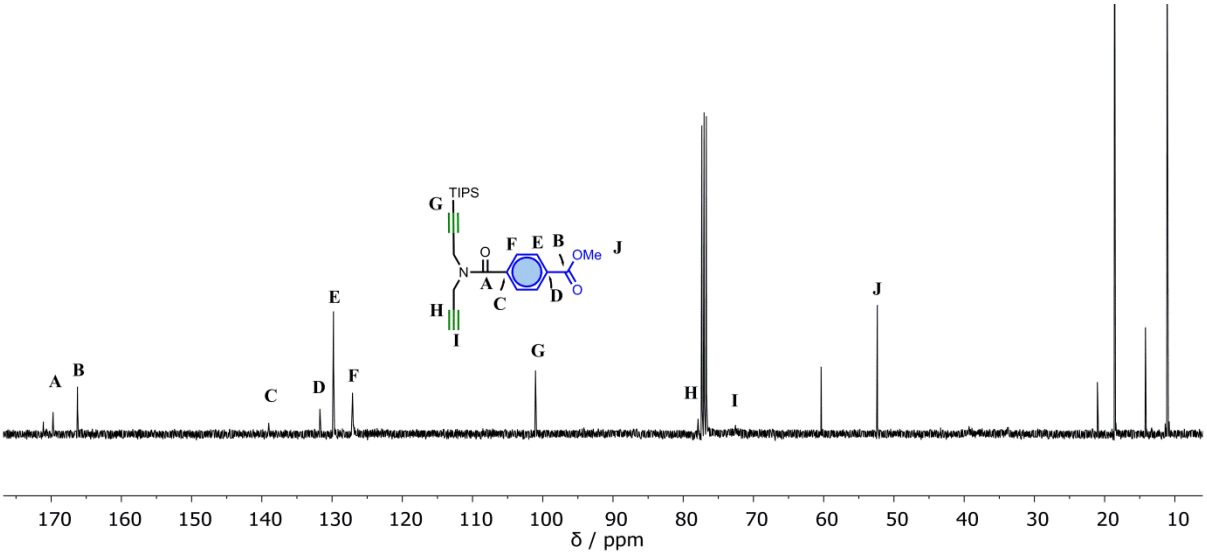
G
TIPS
F
E
B
OMe
J
O
N
A
C
D
H
I
A
B
C
D
E
F
G
H
I
J
170
160
150
140
130
120
110
100
90
80
70
60
50
40
30
20
10
δ / ppm

Synthesis of compound 3.11

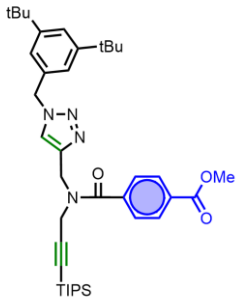

Compound **3.10** (479 mg, 1.16 mmol), $Cu(MeCN)_4PF_6$ (45 mg, 0.12 mmol) and TBTA (64 mg, 0.12 mmol) were dissolved in dry THF (15 mL) under a N_2 atmosphere. A solution of 1-(azidomethyl)-3,5-di-tert-butylbenzene (314 mg, 1.28 mmol) in dry THF (15 mL) was added dropwise and the solution was stirred for 3h. The solution was concentrated in vacuo, redissolved in EtOAc and washed with brine (3 x 20 mL), dried with $MgSO_4$, filtered and evaporated. The crude oil was purified by column chromatography (PET 40-60/EtOAc, gradient of increasing polarity) to yield the pure compound as a yellow oil (692 mg, 91%).

^{1}H NMR (400 MHz, Chloroform-*d*) δ 8.03 (d, *J* = 8.1 Hz, 2H), 7.62 (d, *J* = 8.1 Hz, 2H), 7.40 (t, *J* = 1.8 Hz, 1H), 7.10 (s, 2H), 5.49 (s, 2H), 4.93 – 3.99(4 singlets due to two rotamers, 4H), 3.88 (s, 3H), 1.28 (s, 18H), 1.08 (s, 21H).

^{13}C NMR (101 MHz, Chloroform-*d*) δ 169.7, 166.12, 151.68, 143.63, 139.24, 133.75, 131.65, 129.64, 127.16, 123.43, 122.71, 122.31, 101.96, 86.51, 54.74, 52.24, 34.82, 31.36, 20.93, 18.58, 14.17, 11.09.

HRMS (ES+): calcd for $C_{39}H_{56}N_4O_3Si$ 657.4199 $[M+H]^+$, found 657.4204 $[M+H]^+$.

FT-IR (ATR): 2935, 2875, 1720, 1650, 1427, 1413 cm^{-1}

Retention time: 2.40 min

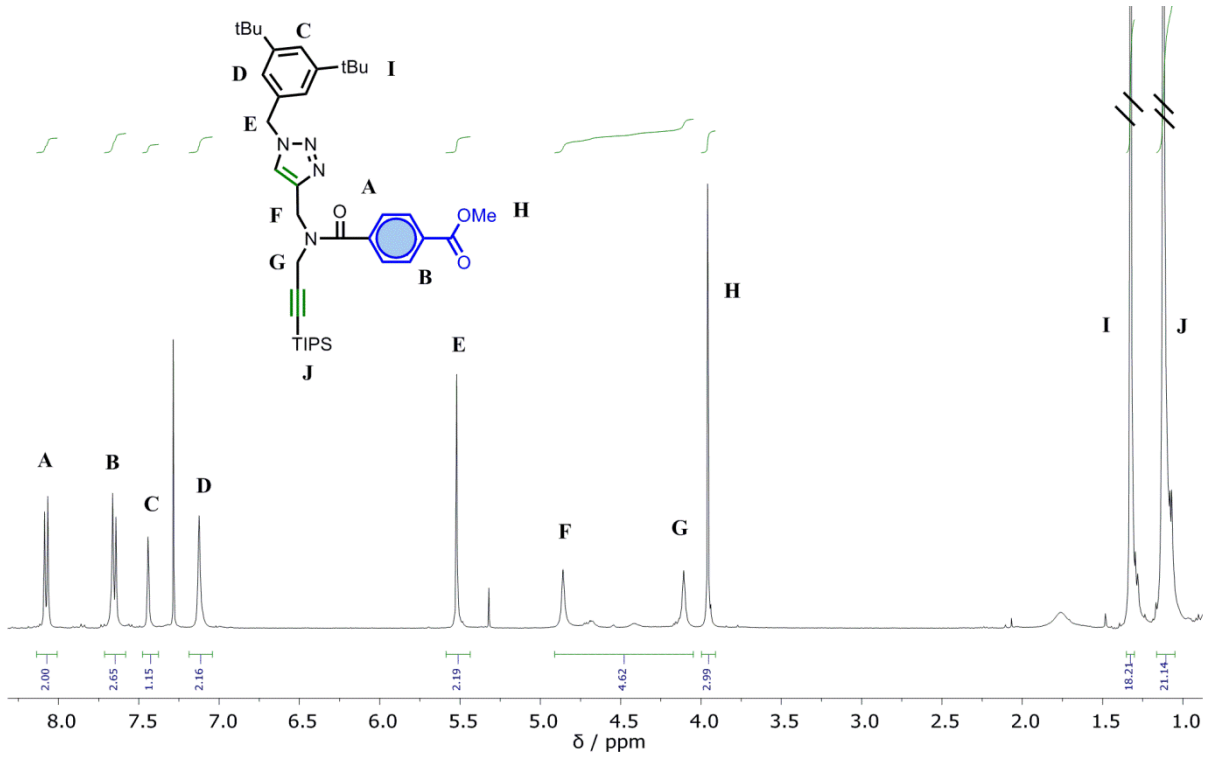
tBu
C
D
tBu
I
E
N-N
N
A
F
O
OMe
H
N
G
B
O
TIPS
J
E
H
I
J
A
B
C
D
F
G
2.00
2.65
1.15
2.16
2.19
4.62
2.99
18.21
21.14
8.0
7.5
7.0
6.5
6.0
5.5
5.0
4.5
4.0
3.5
3.0
2.5
2.0
1.5
1.0
δ / ppm

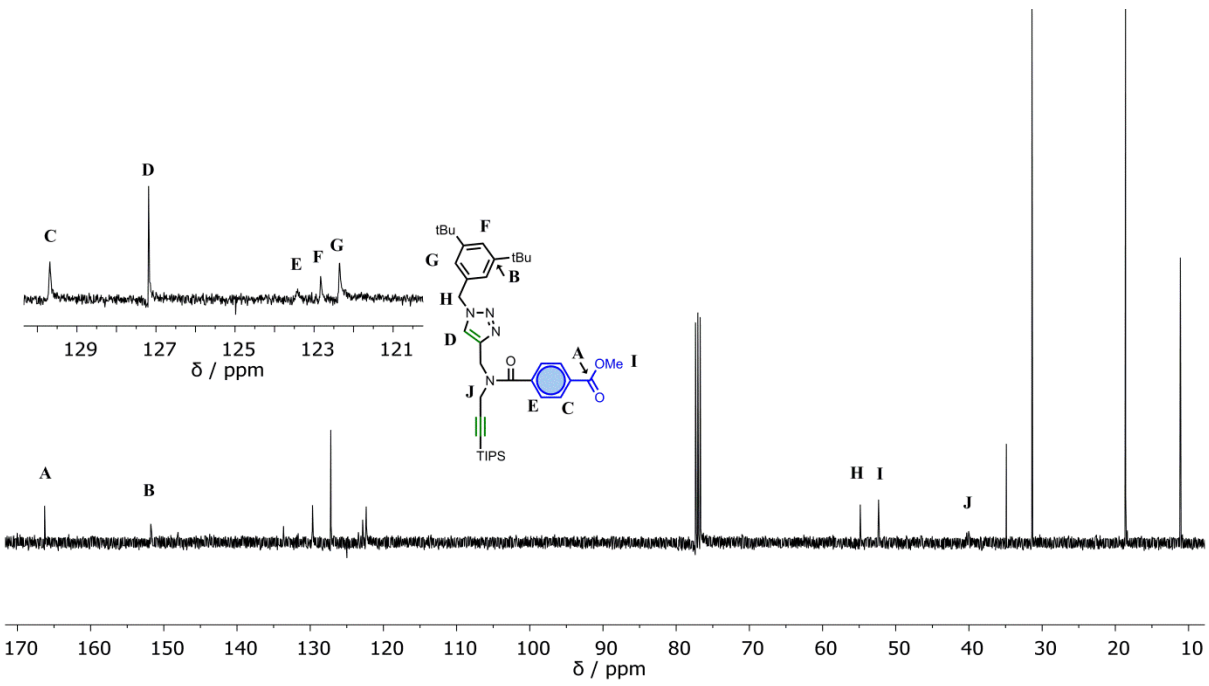
D
C
E
F
G
129
127
125
123
121
δ / ppm
tBu
F
G
tBu
B
H
N-N
N
D
A
OMe
I
O
J
N
O
E
C
TIPS
A
B
H
I
J
170
160
150
140
130
120
110
100
90
80
70
60
50
40
30
20
10
δ / ppm

Synthesis of compound 3.12

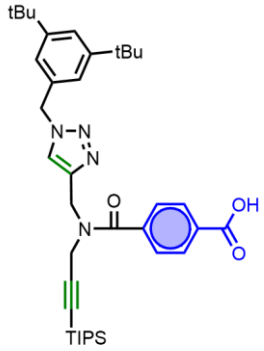

3.11 (400 mg, 0.61 mmol) was dissolved in THF (20 mL) and a solution of LiOH (75 mg, 1.8 mmol) in water (1 mL) was added dropwise. The reaction was left stirring overnight, acidified with HCl 1M to pH 1, diluted with water and reextracted with EtOAc (2 x 20 mL). The organic phase was washed with brine (2 x 20mL), dried with $MgSO_4$, filtered and dried in vacuo to yield the pure compound as a yellow solid (390 mg, quantitative yield).

^{1}H NMR (500 MHz, *d*$_4$-methanol) δ 8.06 (d, *J* = 7.9 Hz, 2H), 7.97 (s, 1H), 7.62 (broad s, 2H), 7.43 (t, *J* = 1.7 Hz, 1H), 7.18 (s, 2H), 5.57 (s, 2H), 4.80 – 4.07 (4 singlets due to two rotamers, 4H), 1.30 (s, 18H), 1.09 (s, 21H).

^{13}C NMR (126 MHz, *d*$_4$-methanol) δ 170.66, 167.35, 152.06, 137.48, 134.40, 132.41, 129.46, 126.48, 124.71, 123.72, 122.16, 121.95, 54.54, 39.62, 34.14, 30.86, 18.01, 11.25.

HRMS (ES+): calcd for $C_{38}H_{54}N_4O_3Si$ 643.4043 $[M+H]^+$, found 643.4052 $[M+H]^+$.

FT-IR (ATR): 2971, 1867, 1715, 1646, 1605, 1510, 1460 cm^{-1}

Retention time: 2.28 min

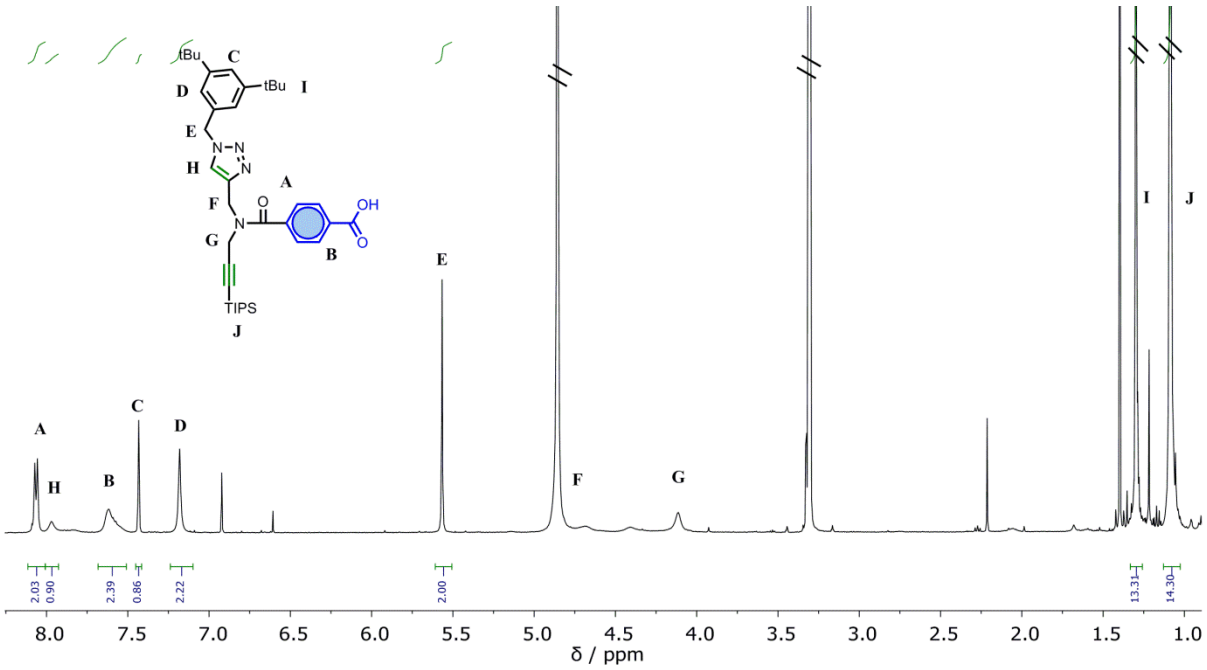
tBu
C
D
tBu
I
E
H
A
F
O
OH
G
B
TIPS
J
A
H
B
C
D
E
F
G
I
J
2.03
0.90
2.39
0.86
2.22
2.00
13.31
14.30
8.0
7.5
7.0
6.5
6.0
5.5
5.0
4.5
4.0
3.5
3.0
2.5
2.0
1.5
1.0
δ / ppm

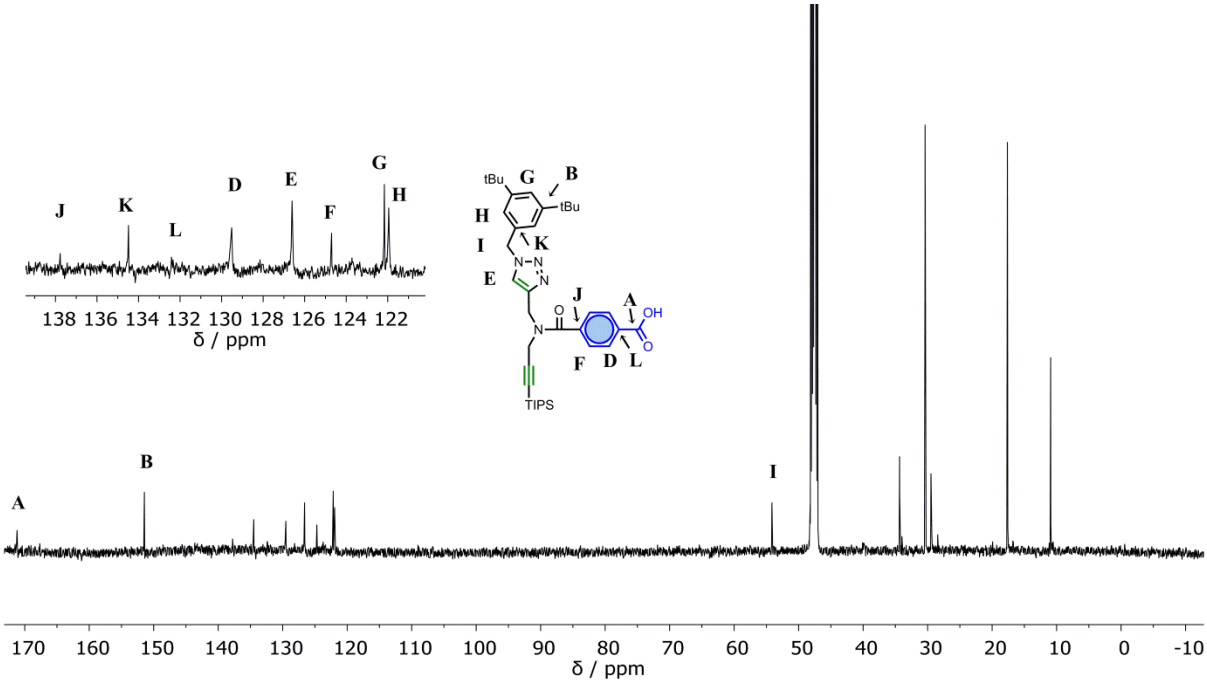
J
K
L
D
E
F
G
H
138 136 134 132 130 128 126 124 122
δ / ppm
tBu
G
B
tBu
H
I
K
E
J
A
OH
O
F
D
L
TIPS
A
B
I
170
160
150
140
130
120
110
100
90
80
70
60
50
40
30
20
10
0
-10
δ / ppm

Synthesis of compound 3.13

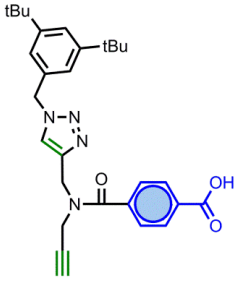

Compound **3.12** (200mg, 0.31 mmol) was dissolved in THF (10 mL) and the solution cooled in ice. TBAF (1M in THF, 0.35 mL) was added dropwise and the reaction was left stirring at room temperature for 20 min before adding HCl 1M until pH reached 1. Water was added (20 mL), the organic compound was reextracted with EtOAc (2 x 20 mL) and this organic phase was washed with brine (2 x 20 mL), dried with $MgSO_4$, filtered and evaporated in vacuo before drying it under high vacuum to yield a white solid (150 mg, quantitative yield)

^{1}H NMR (400 MHz, Chloroform-*d*) δ 8.17 (d, *J* = 8.2 Hz, 2H), 7.74 – 7.59 (m, 3H), 7.45 (s, 1H), 7.14 (s, 2H), 4.90 (two singlets due to rotamers, 2H), 4.10 (two singlets due to rotamers, 2H), 2.36 (s, 1H), 1.33 (s, 18H).

^{13}C NMR (100 MHz, Chloroform-*d*) δ 170.10, 169.48, 151.85, 139.71, 133.61, l130.41, 127.19, 123.57122.91, 122.41, 78.23, 73.48, 54.95, 40.00, 39.23, 34.92, 31.40.

HRMS (ES+): calcd for $C_{29}H_{34}N_4O_3$ 487.2709 $[M+H]^+$, found 487.2717 $[M+H]^+$.

FT-IR (ATR): 3280, 2936, 2906, 1843, 1734, 1640, 1602 cm^{-1}

Retention time: 1.57 min

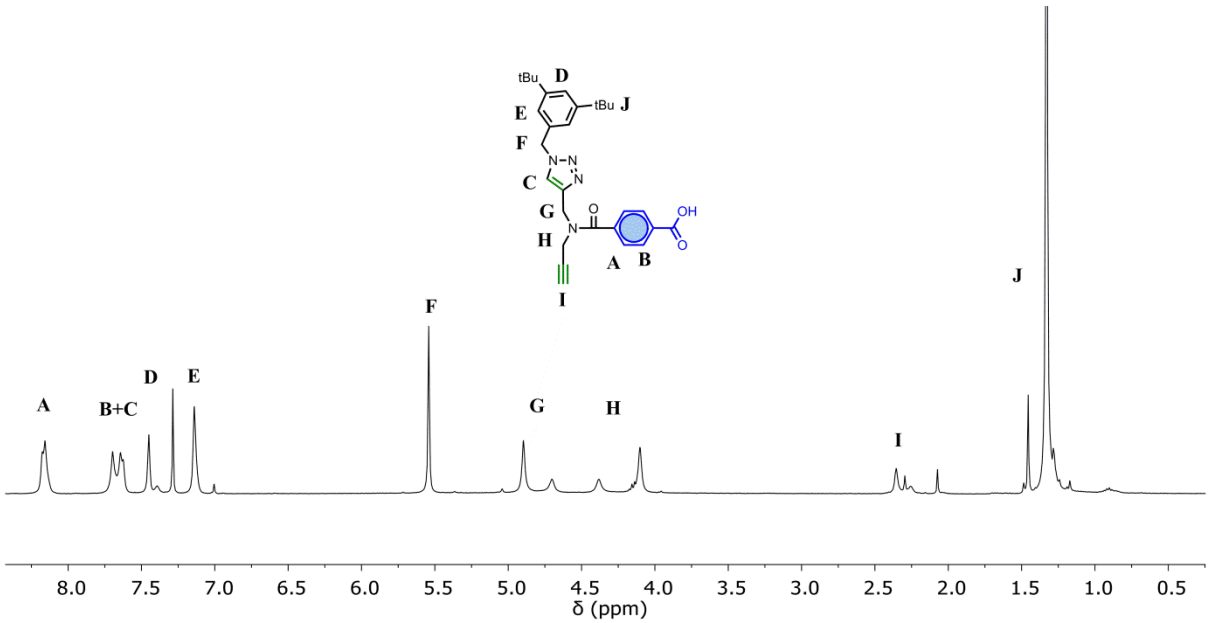
tBu
D
E
tBu
J
F
C
G
H
I
A
B
OH
A
B+C
D
E
F
G
H
I
J
8.0
7.5
7.0
6.5
6.0
5.5
5.0
4.5
4.0
3.5
3.0
2.5
2.0
1.5
1.0
0.5
δ (ppm)

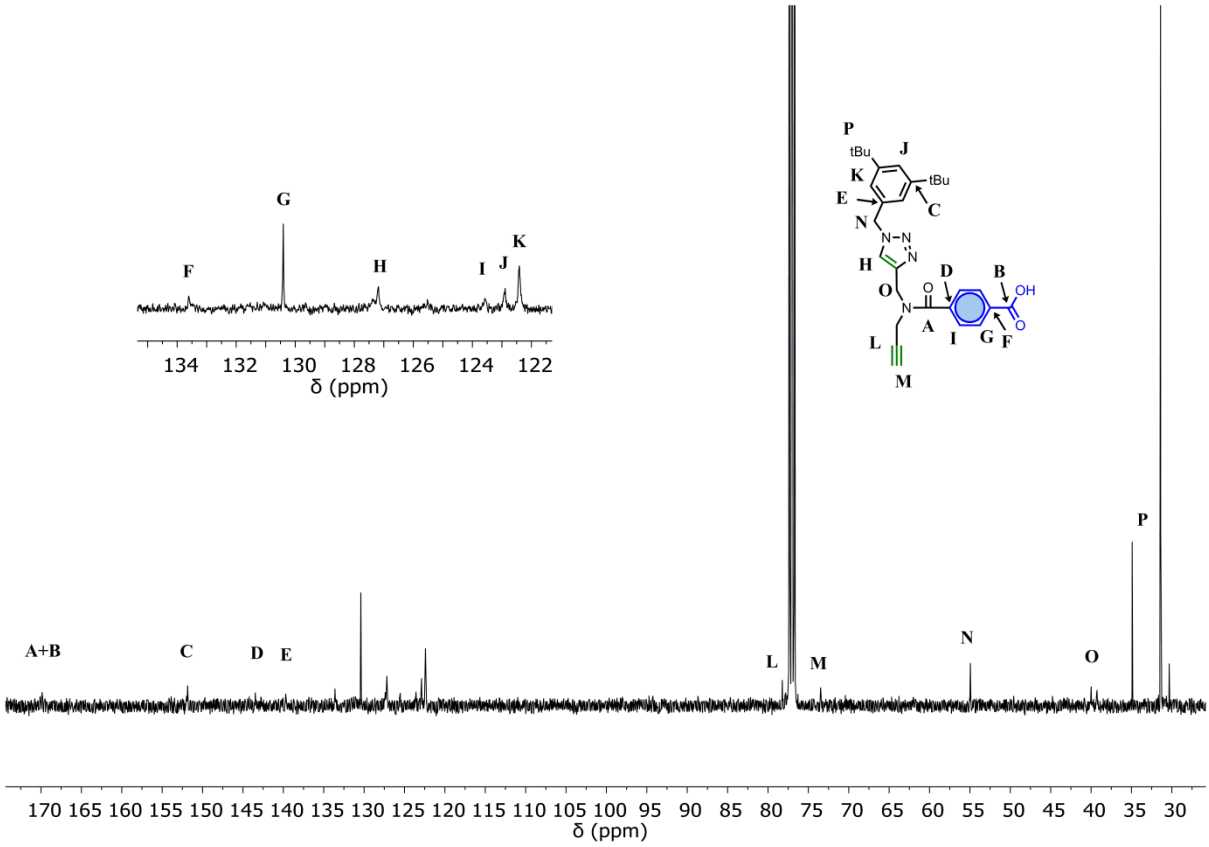
P
tBu
J
K
tBu
E
C
N
H
O
D
B
OH
A
I
G
F
L
M
F
G
H
I
J
K
134
132
130
128
126
124
122
δ (ppm)
A+B
C
D
E
L
M
N
O
P
170
165
160
155
150
145
140
135
130
125
120
115
110
105
100
95
90
85
80
75
70
65
60
55
50
45
40
35
30
δ (ppm)

Synthesis of compound 3.14

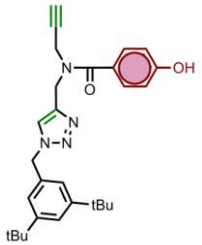

Compound **3.3** (630 mg, 3 mmol), $Cu(MeCN)_4PF_6$ (22.4 mg, 0.06 mmol) and TBTA (32mg, 0.06 mmol) were dissolved in dry THF (400 mL) under a N_2 atmosphere. A solution of 1-(azidomethyl)-3,5-di-tert-butylbenzene (147 mg, 0.6 mmol) in dry THF (150 mL) was added dropwise and the solution was stirred overnight. The crude was concentrated in vacuo, redissolved in EtOAc and washed with brine (3 x 20 mL), dried with $MgSO_4$, filtered and evaporated. The crude oil was purified by column chromatography (PET 40-60/EtOAc, gradient of increasing polarity) to yield the pure compound as a yellow oil (165mg, 60%).

^{1}H NMR (400 MHz, d_4-methanol) δ 7.96 (s, 1H), 7.48 – 7.40 (m, 3H), 7.20 (d, *J* = 1.7 Hz, 2H), 6.83 (t, *J* = 8.1 Hz, 2H), 5.59 (s, 2H), 4.80 (s, 2H), 4.17 (br s, 2H), 1.31 (s, 18H).

^{13}C NMR (100 MHz, d_4-methanol) δ 173.16, 160.76, 151.69, 143.59, 135.49, 128.95, 125.14, 123.66, 122.06, 121.92, 114.72, 78.18, 54.40, 53.04, 40.99, 34.80, 30.34.

HRMS (ES+): calcd for $C_{28}H_{35}N_4O_2$ 459.2760 $[M+H]^+$, found 459.2728 $[M+H]^+$.

FT-IR (ATR): 3610, 3265, 2936, 1624 cm^{-1}

Retention time: 1.56 min

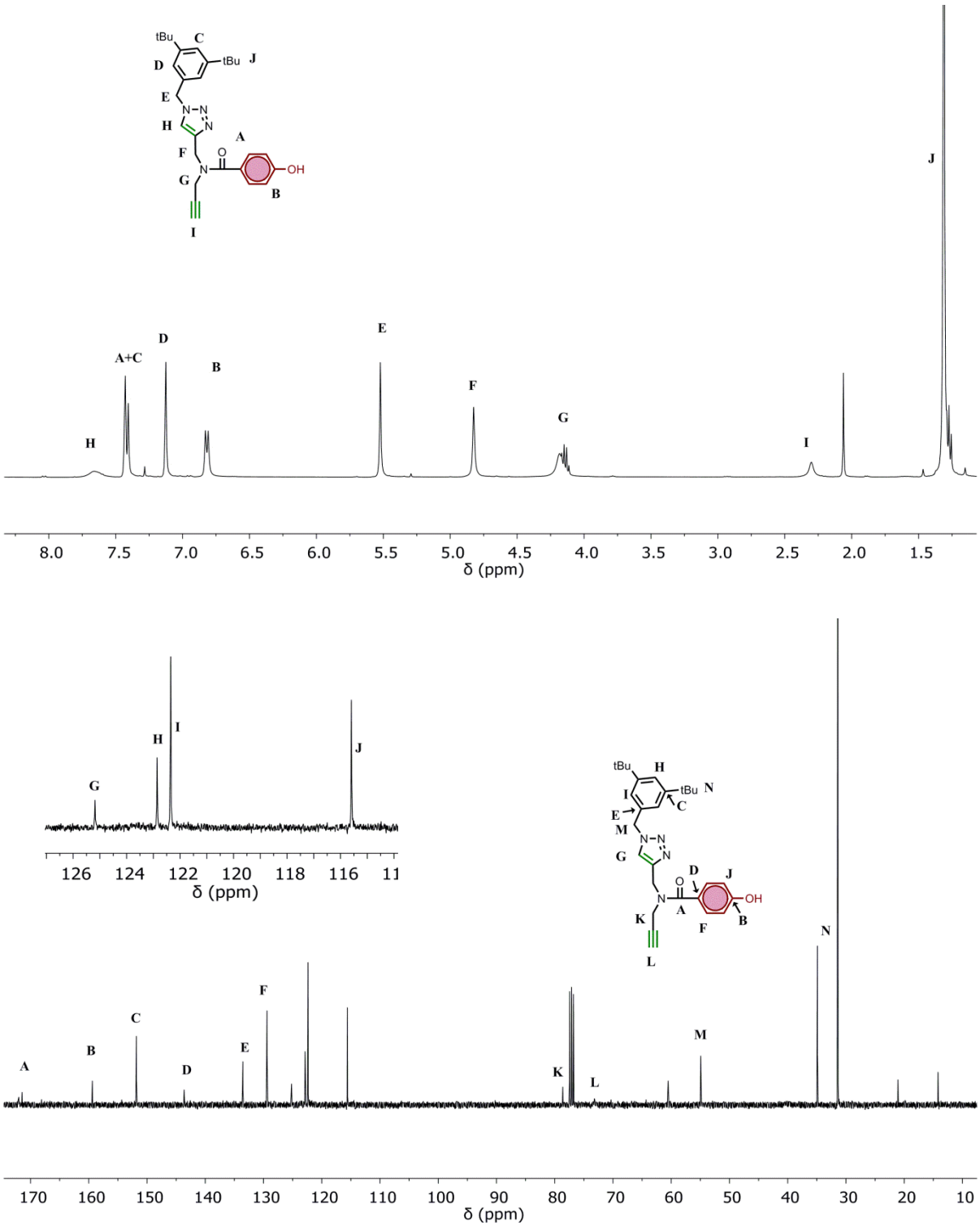
tBu
C
D
tBu
J
E
N
N
N
H
A
F
O
N
OH
G
B
I
H
A+C
D
B
E
F
G
I
J
8.0
7.5
7.0
6.5
6.0
5.5
5.0
4.5
4.0
3.5
3.0
2.5
2.0
1.5
δ (ppm)
G
H
I
J
126
124
122
120
118
116
11
δ (ppm)
tBu
H
I
tBu
N
C
E
M
N
N
N
G
D
J
O
N
OH
K
A
F
B
L
A
B
C
D
E
F
K
L
M
N
170
160
150
140
130
120
110
100
90
80
70
60
50
40
30
20
10
δ (ppm)

Synthesis of compound 3.15

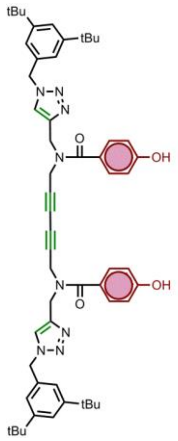

Compound **3.14** (75 mg, 0.16 mmol), $Pd(PPh_3)_2Cl_2$ (12 mg, 0.016 mmol), PPh_3 (13 mg, 0.048 mmol), and CuI (3 mg, 0.016 mmol) were dissolved in acetonitrile (10 mL). Et_3N (220 µL, 1.6 mmol) was added and the reaction was stirred under air overnight. After this time the reaction was neutralized with HCl 1M, diluted with water, and the product reextracted with EtOAc. The organic solution was then washed with brine (2 x 20 mL), dried with $MgSO_4$, filtered and dried in vacuo. The crude was purified via column chromatography (PET 40-60/EtOAc, gradient of increasing polarity) to yield the pure compound as a yellow oil (72mg, 96%).

^{1}H NMR (400 MHz, *d*$_4$-methanol) δ 7.96 (s, 2H), 7.42 (m, 6H), 7.18 (s, 4H), 6.84 (d, *J* = 8.4 Hz, 4H), 5.58 (s, 4H), 4.80 (s, 2H), 4.26 (s, 4H)), 1.29 (s, 36H).

^{13}C NMR (100 MHz, *d*$_4$-methanol) δ 159.50, 151.83, 133.47, 129.46, 124.91, 122.89, 122.38, 115.67, 54.96, 34.38, 31.39.

HRMS (ES+): calcd for $C_{56}H_{66}N_8O_4$ 915.5285 $[M+H]^+$, found 915.5287 $[M+H]^+$.

FT-IR (ATR): 3202 (b), 2962, 2870, 1734, 1605, 1514, 1452 cm^{-1}

Retention time: 1.89 min

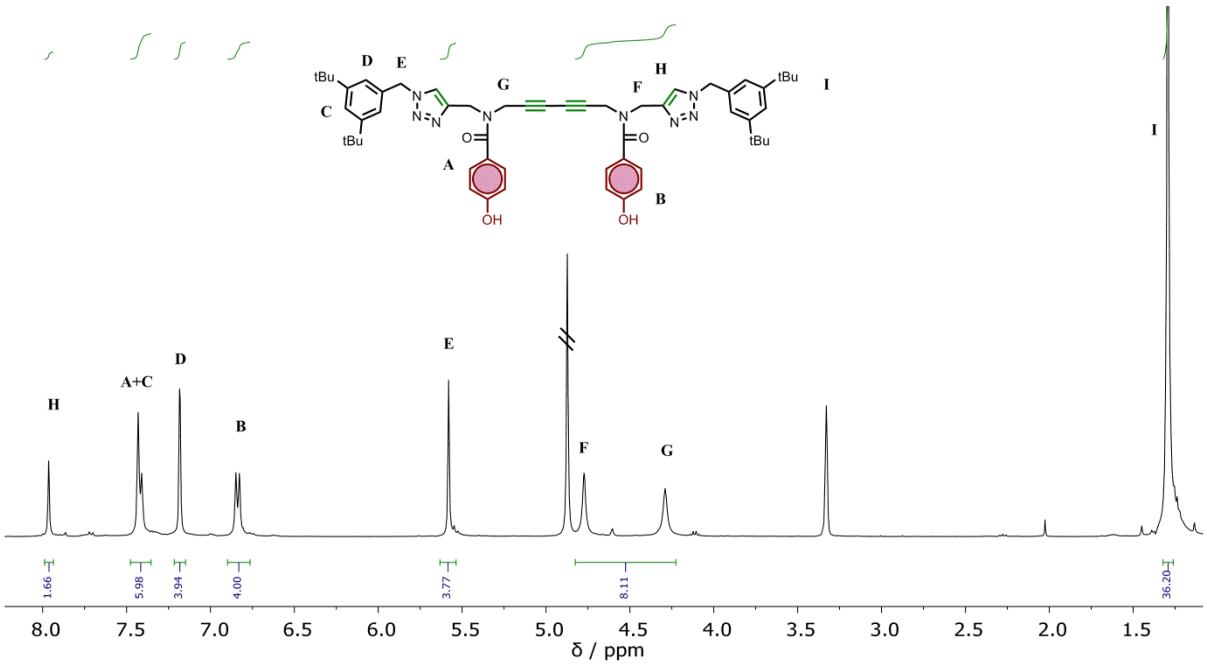
H
A+C
D
B
E
F
G
I
1.66
5.98
3.94
4.00
3.77
8.11
36.20
δ / ppm

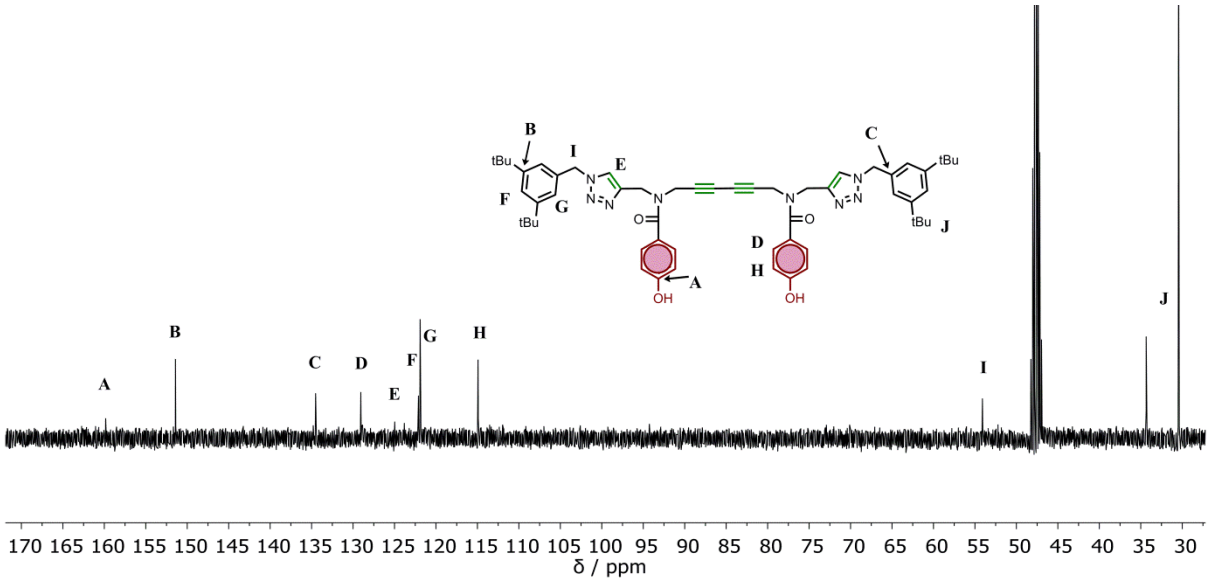
A
B
C
D
E
F
G
H
I
J
δ / ppm

Synthesis of compound 3.16

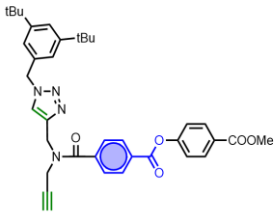

Compound **3.13** (83 mg, 0.17 mmol), methyl 4-hydroxybenzoate (27 mg, 0.18 mmol), EDC (40 mg, 0.21 mmol) and DMAP (6.4 mg, 0.05 mmol) were dissolved in dry DCM (15 mL) and stirred under N_2 overnight. The crude was washed with HCl 1M (2 x 20 mL), and brine (2 x 20 mL). The organic phase was dried with $MgSO_4$, concentrated in vacuo and purified by column chromatography (PET 40-60/EtOAc, gradient of increasing polarity) to yield pure compound as a yellow sticky solid (76 mg, 77%)

^{1}H NMR (500 MHz, Chloroform-*d*) δ 8.24 (d, *J* = 8.0 Hz, 2H), 8.14 (d, *J* = 8.7 Hz, 2H), 7.76 (s, 1H), 7.66 (d, *J* = 9.0 Hz, 2H), 7.43 (t, *J* = 1.8 Hz, 1H), 7.31 (d, *J* = 8.8 Hz, 2H), 7.11 (s, 2H), 5.52 (s, 2H), 4.87 (two singlets due to rotamers, 2H), 4.09 (two singlets dure to rotamers, 2H), 3.94 (s, 3H), 2.35 (s, 1H), 1.31 (s, 18H).

^{13}C NMR (126 MHz, Chloroform-*d*) δ 169.85, 166.27, 163.83, 154.36, 151.84, 143.46, 140.07, 133.64, 131.29, 130.47, 127.99, 127.37, 123.44, 122.88, 122.40, 121.66, 78.26, 73.48, 54.90, 52.26, 39.97, 39.21, 34.91, 31.39.

HRMS (ES+): calcd for $C_{37}H_{41}N_4O_5$ 621.3077 $[M+H]^+$, found 621.3075 $[M+H]^+$.

FT-IR (ATR): 3303, 2959, 2967, 1744, 1721, 1641, 1602, 1504 cm^{-1}

Retention time: 1.80 min

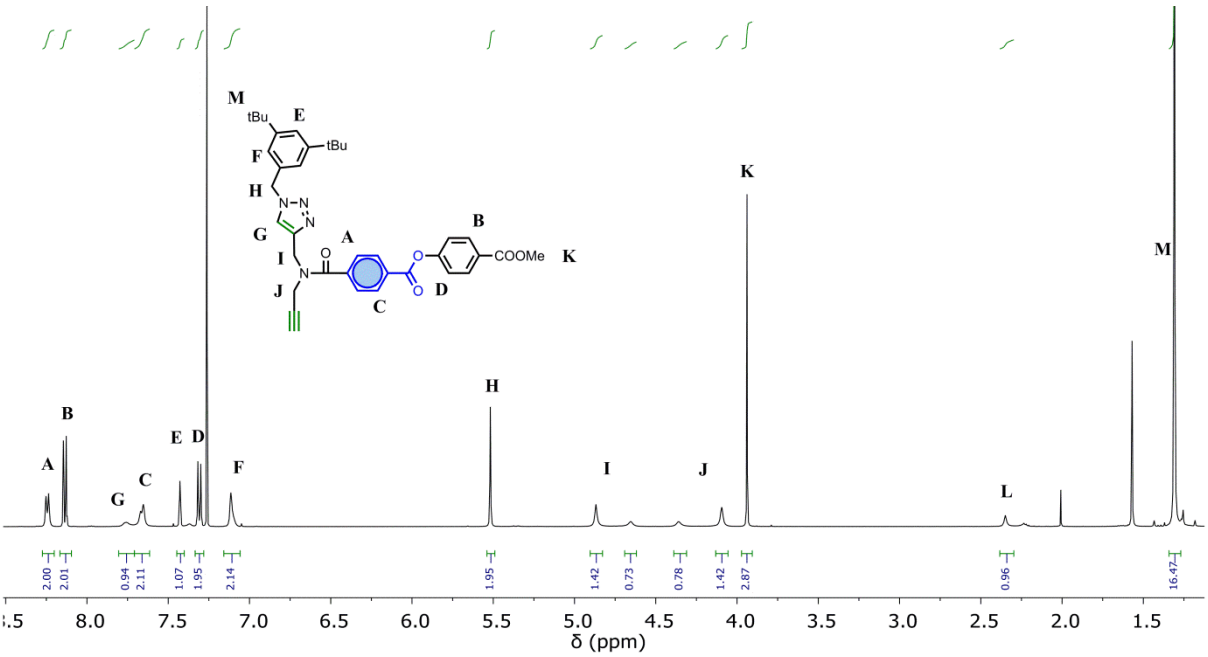
δ (ppm)

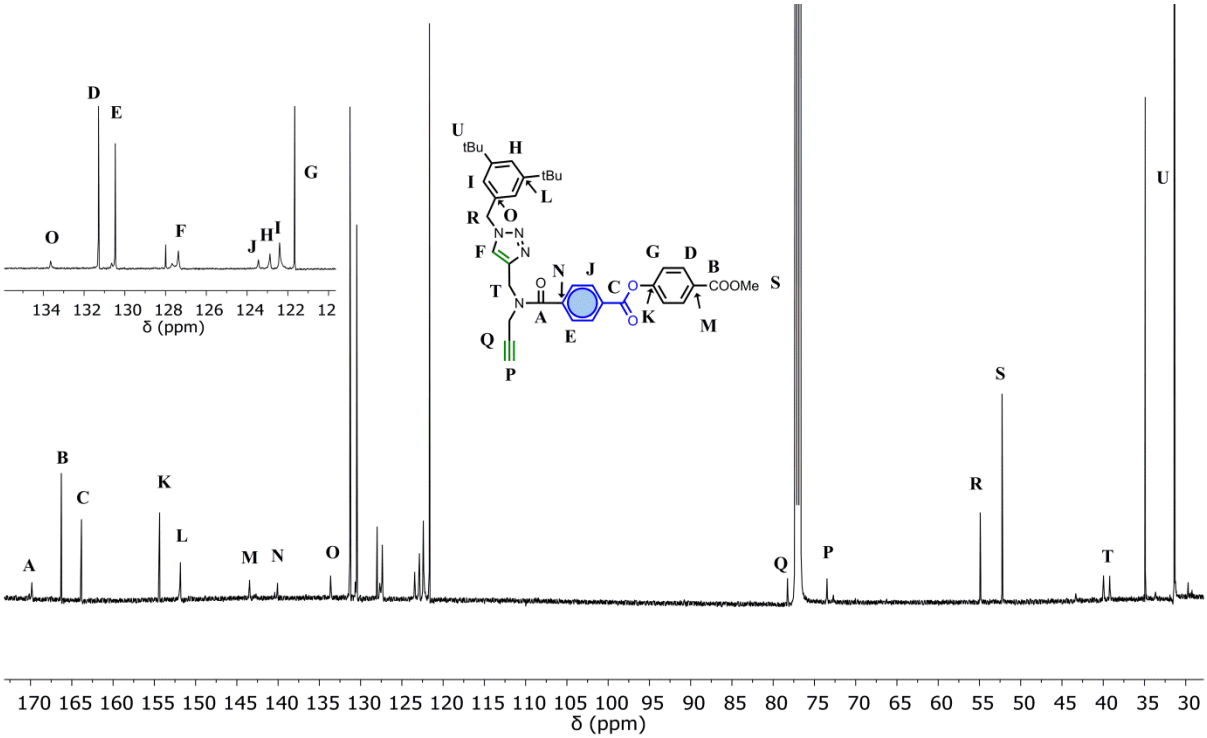
δ (ppm)
δ (ppm)

Synthesis of compound 3.17

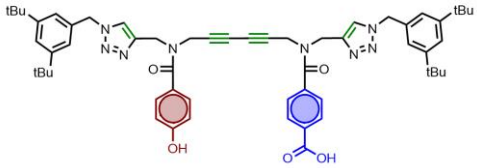

Compound **3.14** (85 mg, 0.19 mmol), compound **3.16** (115 mg, 0.19 mmol), $Pd(PPh_3)_2Cl_2$ (13 mg, 0.019 mmol), PPh_3 (15 mg, 0.056 mmol), and CuI (3.5 mg, 0.019 mmol) were dissolved in acetonitrile (20 mL). Et_3N (2.6 mL, 19 mmol) was added and the reaction was stirred under air overnight. After this time the reaction was neutralized with HCl 1M, diluted with water, and product reextracted with EtOAc. The organic solution was washed with brine (2 x 20 mL), dried with $MgSO_4$, filtered and dried in vacuo. The crude was purified via column chromatography (PET 40-60/EtOAc, gradient of increasing polarity) to yield the pure compound as an orange oil (30mg, 17%).

^{1}H NMR (400 MHz, Chloroform-*d*) δ 8.13 (s, 2H), 7.58 (s, 4H), 7.52 – 7.38 (m, 2H), 7.20 – 7.06 (m, 4H), 6.83 (d, *J* = 8.1 Hz, 2H), 5.53 (d, *J* = 5.8 Hz, 4H), 4.84 (m, overlapping br s due to rotamers, 4H), 4.24 (m, overlapping br s due to rotamers, 4H), 1.32 (d, *J* = 3.6 Hz, 36H).

HRMS (ES+): calcd for $C_{57}H_{67}N_8O_5$ 943.5234 $[M+H]^+$, found 965.5039 $[M+Na]^+$.

FT-IR (ATR): 2965, 2867, 1725, 1636, 1608, 1457, 1417 cm^{-1}

Retention time: 1.90 min

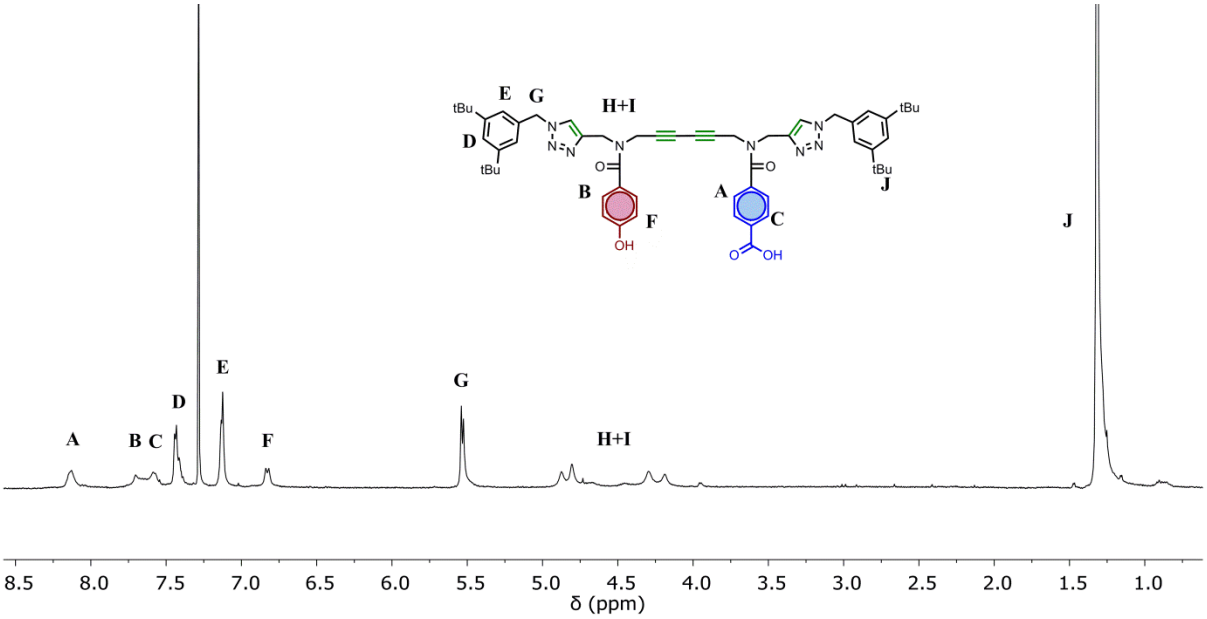
E
G
H+I
tBu
D
tBu
tBu
J
B
F
OH
A
C
O
OH
J
E
G
D
A
B C
F
H+I
8.5
8.0
7.5
7.0
6.5
6.0
5.5
5.0
4.5
4.0
3.5
3.0
2.5
2.0
1.5
1.0
δ (ppm)

Synthesis of compound 3.18

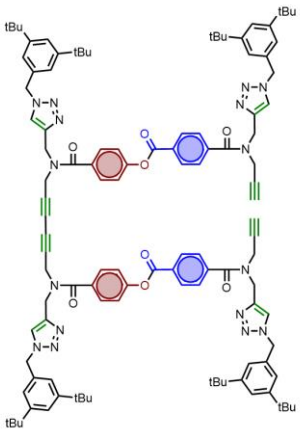

Compound **3.15** (20 mg, 0.022 mmol), compound **3.13** (27 mg, 0.055 mmol), EDC (11 mg, 0.057 mmol) and DMAP (7 mg, 0.057 mmol) were dissolved in dry DCM (5 mL) and stirred under N_2 until no starting dimer could be seen by LCMS. The crude was washed with HCl 1M (2 x 20 mL), and brine (2 x 20 mL). The organic phase was dried with $MgSO_4$, concentrated in vacuo and purified by column chromatography (PET 40-60/EtOAc, gradient of increasing polarity) to yield pure compound as a pale yellow sticky solid (32 mg, 80%)

^{1}H NMR (400 MHz, Chloroform-*d*) δ 8.26 (d, *J* = 8.0 Hz, 4H), 7.67 (m, 12H), 7.46 – 7.42 (m, 4H), 7.30 (s, 4H), 7.16 – 7.09 (m, 8H), 5.54 (s, 8H), 4.89 (several broad singlets due to rotamers, 8H), 4.12 (several broad singlets due to rotamers, 8H), 2.37 (s, 2H), 1.33 (s, 36H), 1.32 (s, 36H).

^{13}C NMR (126 MHz, Chloroform-*d*) δ 169.86, 163.95, 152.28, 151.84, 143.47, 140.03, 133.61, 130.46, 128.94, 127.36, 123.46, 122.88, 122.36, 121.92, 78.25, 73.49, 54.90, 54.88, 39.98, 39.21, 34.91, 31.40.

HRMS (ES+): calcd for $C_{114}H_{130}N_{16}O_8$ 1851.02576 $[M+H]^+$, found 948.4997 $[M+2Na]^{2+}$.

FT-IR (ATR): 3274, 2959, 2924, 2867, 1740, 1639, 1602, 1504, 1454 cm^{-1}

Retention time: 2.41 min

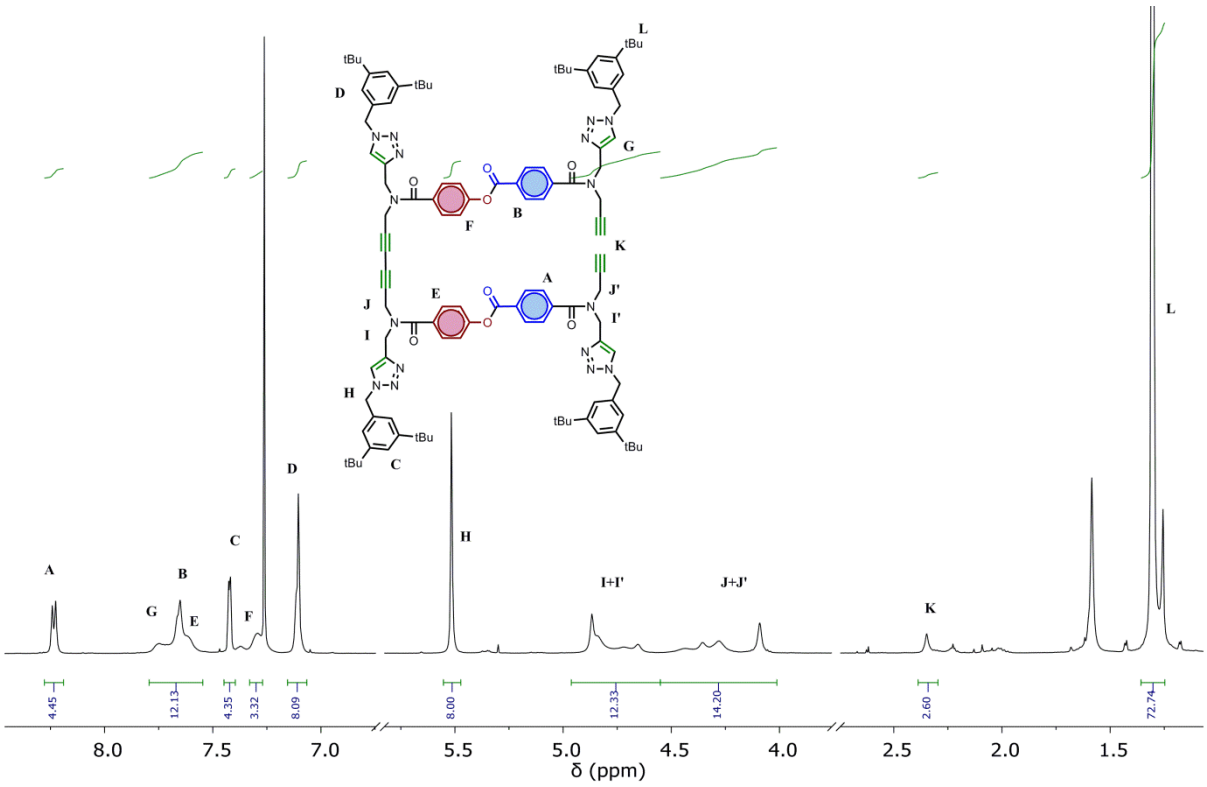
A
B
G
E
C
F
D
H
I+I'
J+J'
K
L
4.45
12.13
4.35
3.32
8.09
8.00
12.33
14.20
2.60
72.74
8.0
7.5
7.0
5.5
5.0
4.5
4.0
2.5
2.0
1.5
δ (ppm)

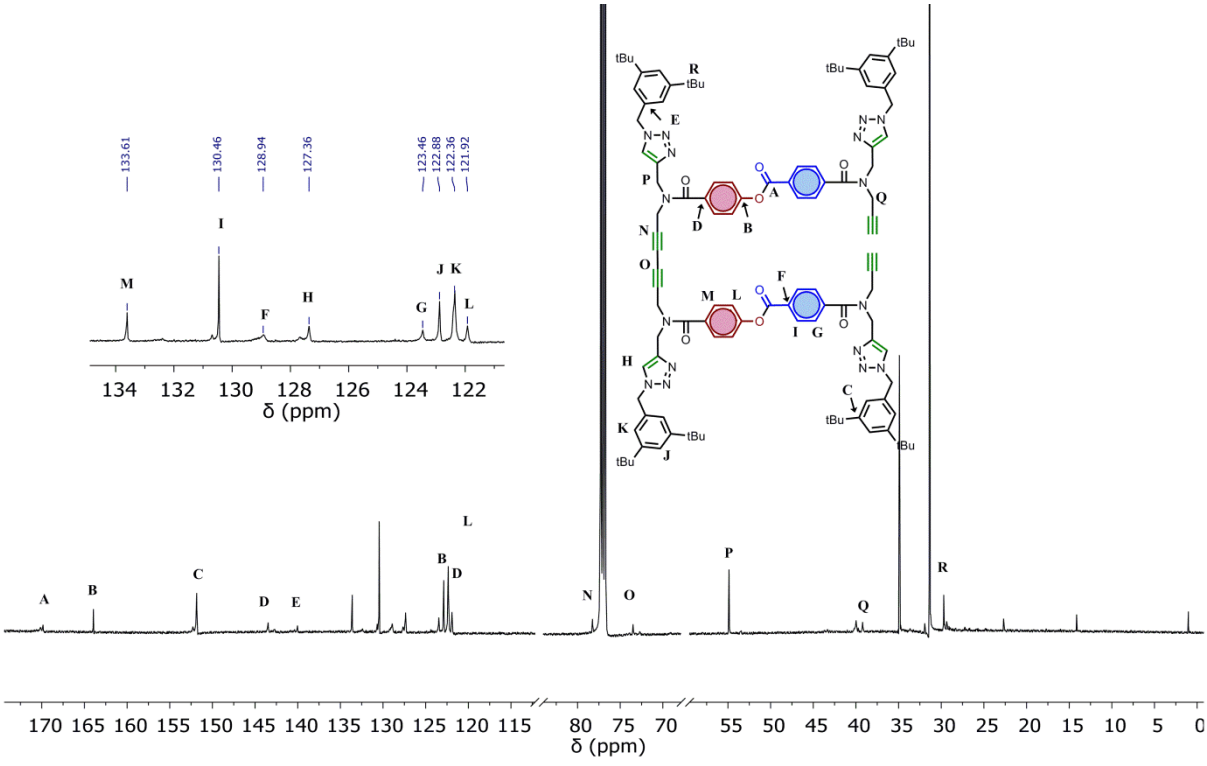
133.61
130.46
128.94
127.36
123.46
122.88
122.36
121.92
M
I
F
H
G
J K
L
134
132
130
128
126
124
122
δ (ppm)
A
B
C
D
E
L
B
D
N
O
P
Q
R
170 165 160 155 150 145 140 135 130 125 120 115
80 75 70
55 50 45 40 35 30 25 20 15 10 5 0
δ (ppm)

Synthesis of compound 3.19

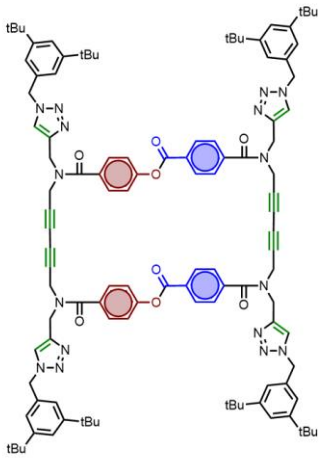

Compound **3.18** (10 mg, 0.005 mmol), $Pd(PPh_3)_2Cl_2$ (3.7 mg, 0.005 mmol), PPh_3 (3.9 mg, 0.015 mmol), and CuI (0.95 mg, 0.005 mmol) were dissolved in acetonitrile (108 mL). Et_3N (70 µL, 0.5 mmol) was added and the reaction was stirred for 1 h. After this time the reaction was neutralized with HCl 1M, diluted with water, and product reextracted with EtOAc. The organic solution was washed with brine (2 x 20 mL), dried with $MgSO_4$, filtered and dried in vacuo. The crude was purified via HPLC ($MeCN/H_2O$ gradient) to yield final compound as a dark yellow sticky solid (6.8 mg, 68%)

^{1}H NMR (500 MHz, Chloroform-*d*) δ 8.25 (d, *J* = 8.0 Hz, 4H), 7.70 – 7.64 (m, 8H), 7.45 – 7.41 (m, 4H), 7.36 – 7.30 (m, 8H), 7.12 (s, 8H), 5.52 (d, *J* = 4.2 Hz, 8H), 4.83 (two overlapping broad singlets due to rotamers, 8H), 4.25 (two overlapping broad singlets due to rotamers, 8H), 1.31 (d, *J* = 2.1 Hz, 72H).

^{13}C NMR (126 MHz, Chloroform-*d*) δ 151.84, 143.45, 143.21, 139.90, 130.55, 128.88, 127.30, 122.92, 122.87, 122.43, 121.90, 54.92, 54.88, 34.91, 31.40.

HRMS (ES+): calcd for $C_{114}H_{128}N_{16}O_8$ 1849.0101 $[M+H]^+$, found 947.4916 $[M+2Na]^{2+}$.

FT-IR (ATR): 2962, 2918, 2858, 1747, 1646, 1457 cm^{-1}

Retention time: 2.55 min

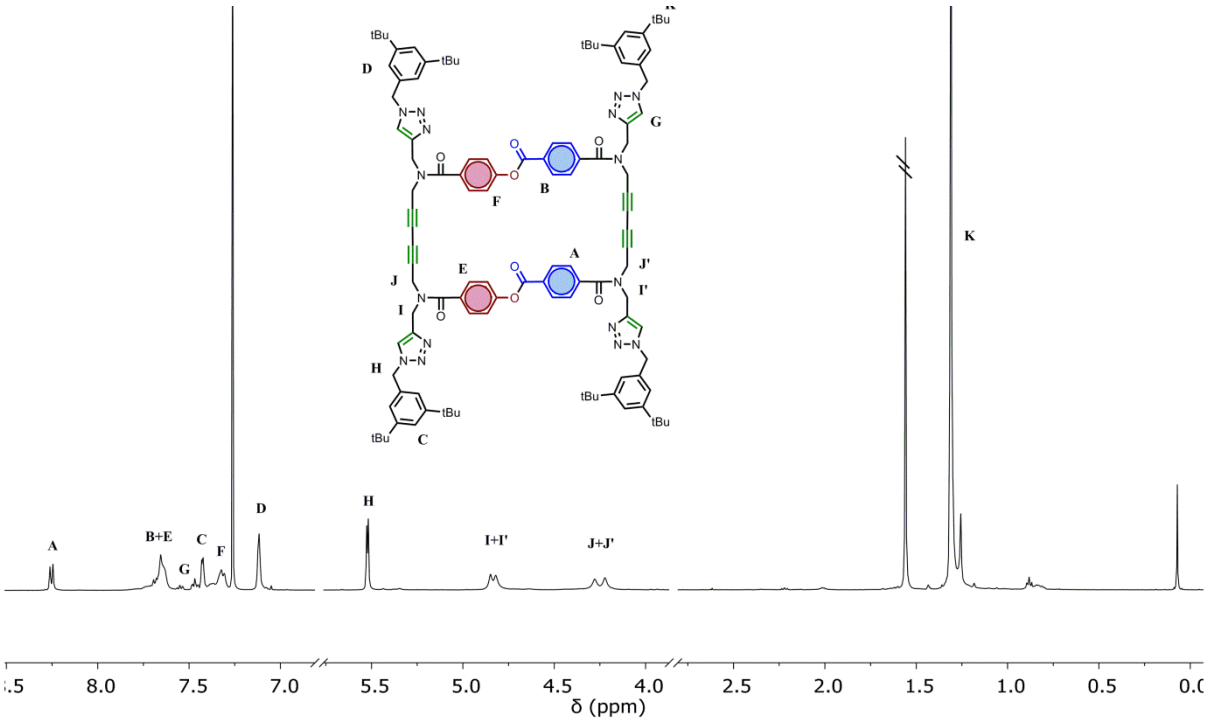
A
B+E
C
G
F
D
H
I+I'
J+J'
K
δ (ppm)

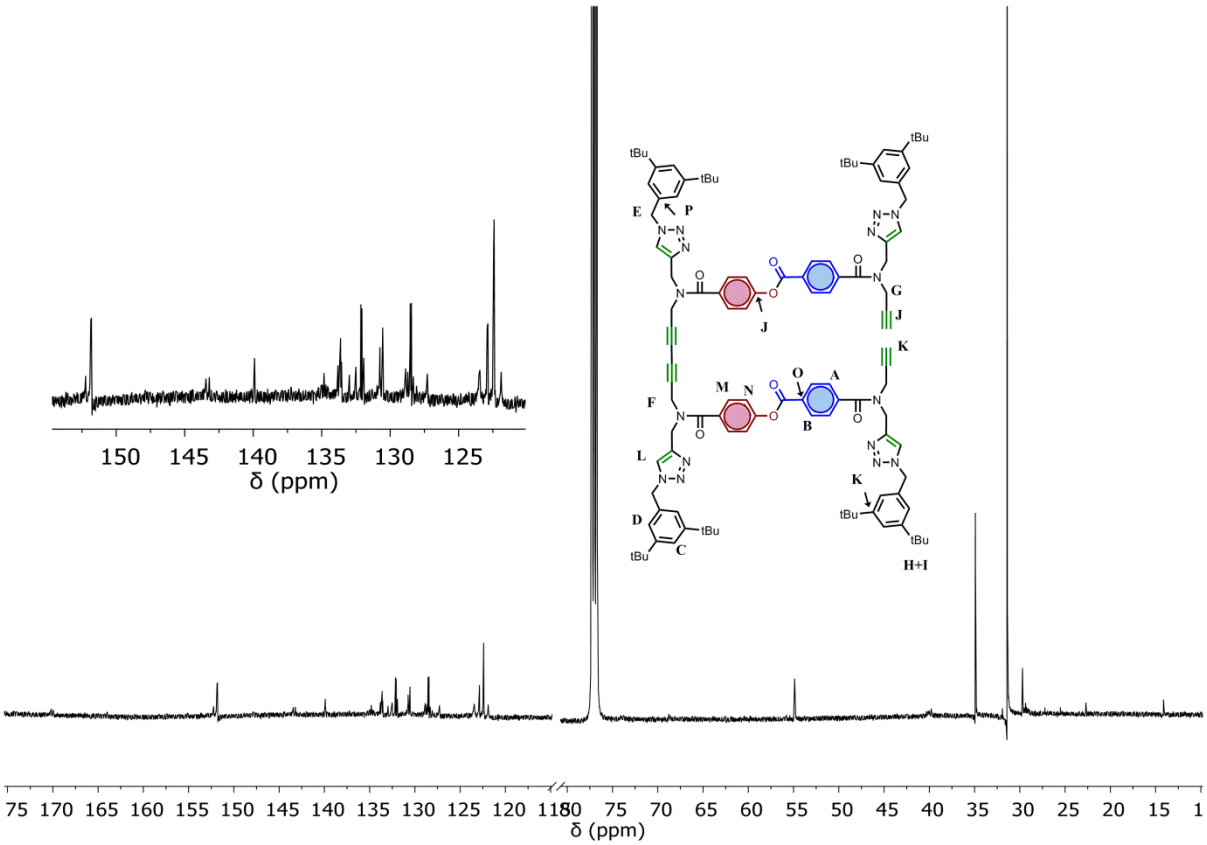
150 145 140 135 130 125
δ (ppm)
H+I
δ (ppm)

Synthesis of compound 20

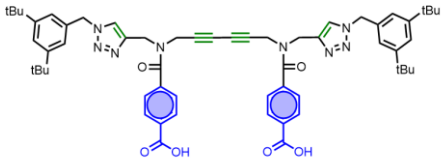

Compound **3.19** (4 mg, 0.01 mmol) was dissolved in THF (2 mL) and LiOH (0.26 mg, 0.006 mmol) dissolved in water (0.1 ml) was added dropwise. The reaction was followed by LCMS and quenched with HCl 1M when no starting material could be seen (30 min). The solution was diluted with water (5 mL), reextracted with EtOAc (2 x 15 mL) and the organic phase washed with brine (2 x 20 mL), dried with $MgSO_4$, and evaporated under vacuo. The crude was purified via column chromatography (PET 40-60/EtOAc, gradient of increasing polarity, flushed with MeOH) to yield final pure compound as a yellow sticky solid (2 mg, 95%)

^{1}H NMR (500 MHz, Chloroform-*d*) δ 8.13 (s, 4H), 7.68 (s, 2H), 7.55 (s, 4H), 7.41 (s, 2H), 7.11 (s, 4H), 5.51 (s, 4H), 4.83 (s, 4H), 4.16 (s, 4H), 1.29 (s, 36H).

^{13}C NMR (126 MHz, Chloroform-*d*) δ 151.82, 143.27, 133.58, 130.40, 127.00, 123.61, 122.87, 122.42, 54.90, 39.92, 34.89, 31.39.

HRMS (ES+): calcd for $C_{58}H_{67}N_8O_6$ 971.5184 $[M+H]^+$, found 971.5178 $[M+H]^+$.

Retention time (column 1): 1.92 min

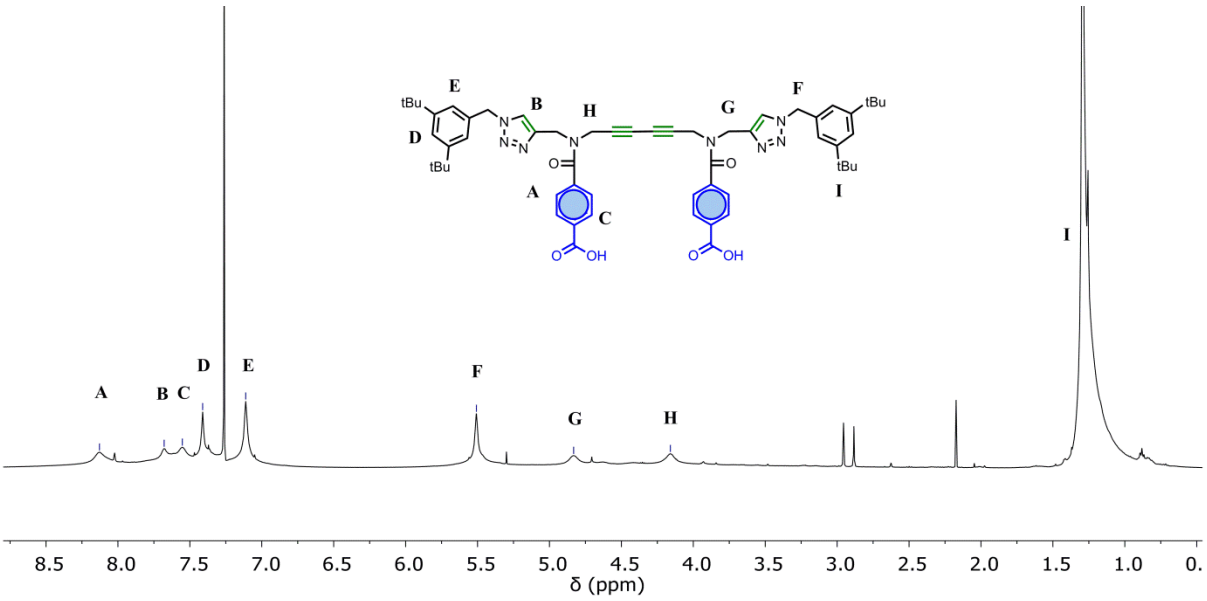
A
B C
D
E
F
G
H
I
8.5 8.0 7.5 7.0 6.5 6.0 5.5 5.0 4.5 4.0 3.5 3.0 2.5 2.0 1.5 1.0 0.
δ (ppm)

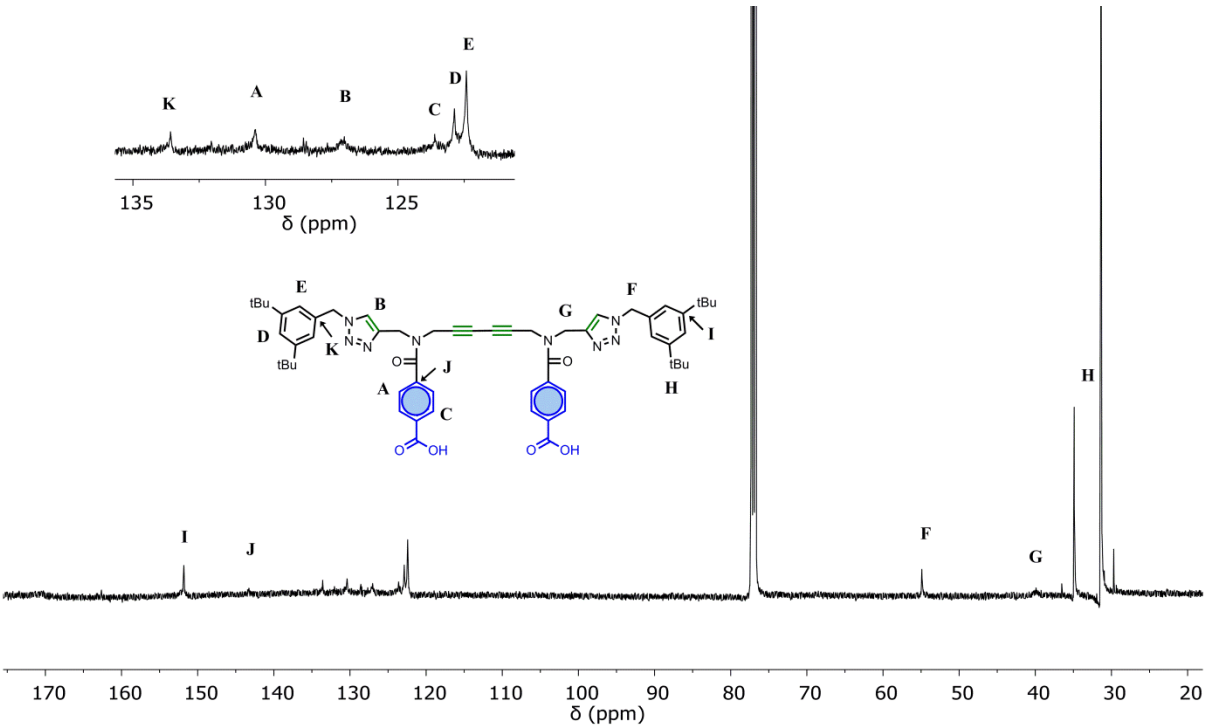
K
A
B
C
D
E
135 130 125
δ (ppm)
I
J
F
G
H
170 160 150 140 130 120 110 100 90 80 70 60 50 40 30 20
δ (ppm)

Synthesis of compound 3.21

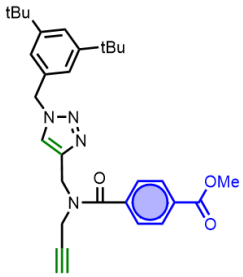

Compound **3.11** (600 mg, 0.91mmol) was dissolved in THF (30 mL) and the solution cooled in ice. TBAF (1M in THF, 1.1 ml) was added dropwise and the reaction was left stirring at room temperature for 20 min before adding HCl 1M until pH reached 3-4. Water was added (20 mL), the organic compound was reextracted with EtOAc (2 x 20 mL) and this organic phase washed with brine (2 x 20 mL), dried with $MgSO_4$, filtered and evaporated in vacuo to yield a yellow crunchy solid in quantitative yield.

^{1}H NMR (400 MHz, Chloroform-*d*) δ 8.08 (d, *J* = 7.9 Hz, 2H), 7.69 (br s, 1H), 7.55 (br s, 2H), 7.43 (d, *J* = 1.9 Hz, 1H), 7.11 (s, 2H), 5.52 (s, 2H), 4.86 (2 singlets due to two rotamers, 2H), 4.07 (2 singlets due to two rotamers, 2H), 3.93 (s, 3H), 2.34 (s, 1H), 1.31 (s, 18H).

^{13}C NMR (101 MHz, Chloroform-*d*) δ 166.22, 151.79, 139.12, 133.67, 131.67, 129.78, 127.09, 123.42, 122.81, 122.34, 78.30, 73.43, 54.83, 52.34, 39.95, 39.17, 34.88, 31.38.

HRMS (ES+): calcd for $C_{30}H_{36}N_4O_3$ 523.2685 $[M+Na]^+$, found 523.2674 $[M+Na]^+$.

FT-IR (ATR): 2962, 2870, 1725, 1641, 1517, 1453 cm^{-1}

Retention time: 1.65 min

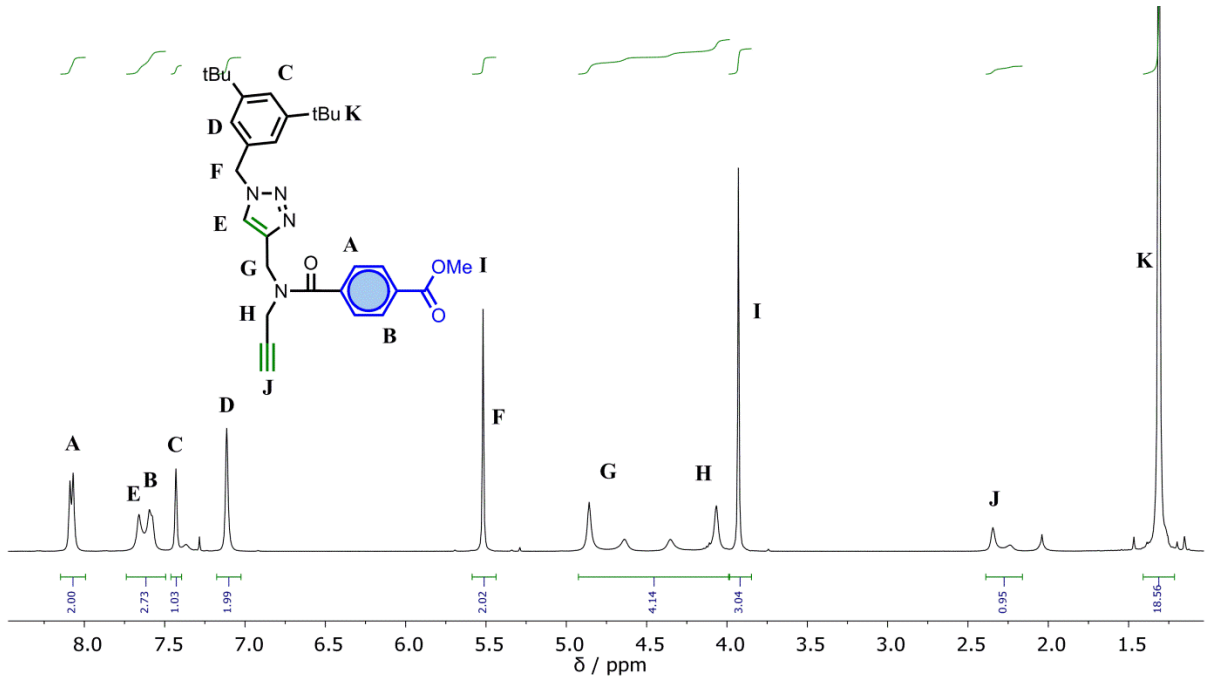
tBu
C
D
tBu K
F
N-N
N
E
G
O
A
OMe I
N
O
H
B
J
A
B
C
D
E
F
G
H
I
J
K
2.00
2.73
1.03
1.99
2.02
4.14
3.04
0.95
18.56
8.0
7.5
7.0
6.5
6.0
5.5
5.0
4.5
4.0
3.5
3.0
2.5
2.0
1.5
δ / ppm

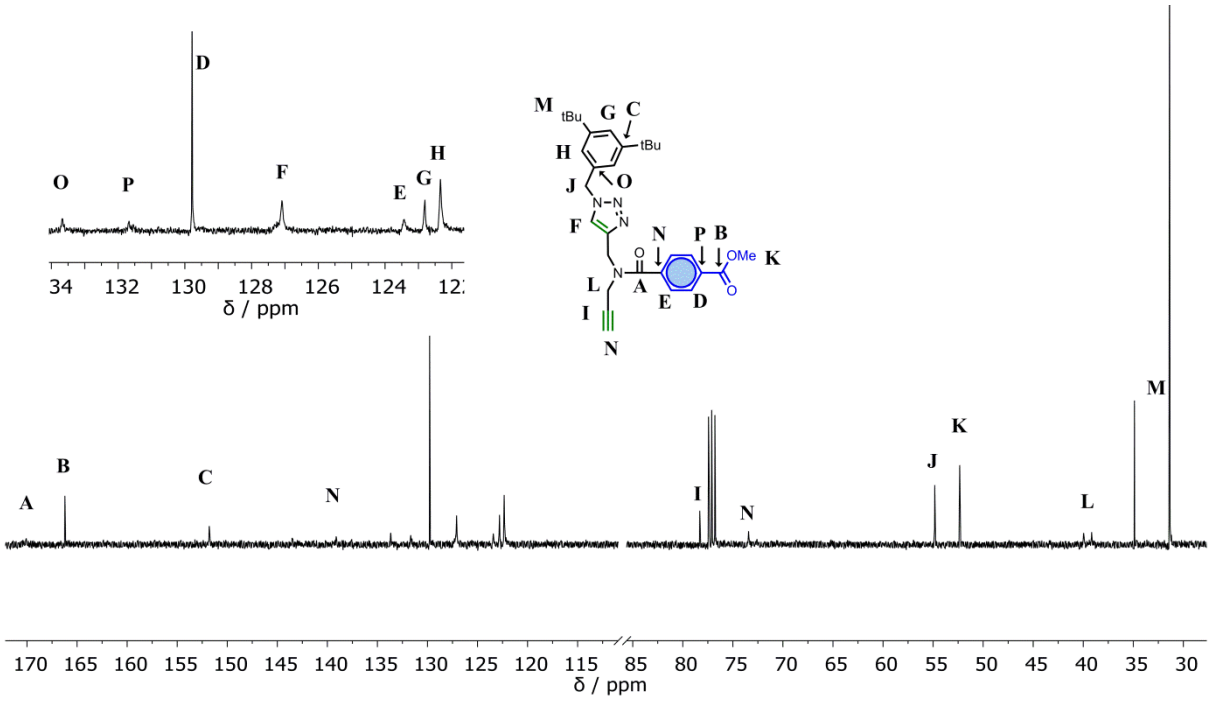
O
P
D
F
E
G
H
34
132
130
128
126
124
δ / ppm
M
tBu
G
C
H
tBu
J
O
F
N
P
B
N
OMe
K
L
A
E
D
I
N
A
B
C
N
I
N
J
K
L
M
170
165
160
155
150
145
140
135
130
125
120
115
85
80
75
70
65
60
55
50
45
40
35
30
δ / ppm

Synthesis of compound 3.22

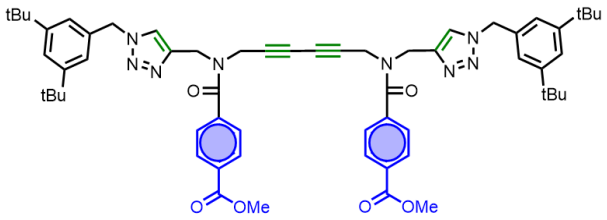

Compound **3.21** (200 mg, 0.4 mmol), $Pd(PPh_3)_2Cl_2$ (26 mg, 0.04 mmol), PPh_3 (30 mg, 0.12 mmol), and CuI (7.2 mg, 0.04 mmol) were dissolved in acetonitrile (20 mL). Et_3N (560 µL, 4 mmol) was added and the reaction was stirred overnight. After this time the reaction was neutralized with HCl 1M, diluted with water, and the product reextracted with EtOAc (2 x 20 mL). The combined organic phase was washed with brine (2 x 20 mL), dried with $MgSO_4$, filtered and dried in vacuo. The crude was purified via column chromatography (PET 40-60/EtOAc, gradient of increasing polarity) to yield the pure compound as a clear orange oil (174 mg, 87%)

^{1}H NMR (400 MHz, $CDCl_3$) δ 8.09 (broad singlet, 4H), 7.65 (broad singlet, 4H), 7.52 (broad singlet, 2H), 7.41 (s, 2H), 7.09 (s, 4H), 5.50 (s, 4H), 4.85 (2 singlets due to two rotamers, 4H), 4.15 (2 singlets due to two rotamers, 4H), 3.92 (s, 6H), 1.29 (s, 36H).

^{13}C NMR (101 MHz, $CDCl_3$) δ 169.69, 166.22, 151.84, 138.78, 133.54, 131.70, 129.91, 127.22, 127.04, 123.47, 122.90, 122.38, 73.72, 68.99, 54.89, 52.40, 43.48, 39.93, 34.90, 31.29.

HRMS (ES+): calcd for $C_{60}H_{70}N_8O_6$ 1021.5316 $[M+Na]^+$, found 1021.5300 $[M+Na]^+$.

FT-IR (ATR): 3050, 2968, 1724, 1645, 1436 cm^{-1}

Retention time: 2.12 min

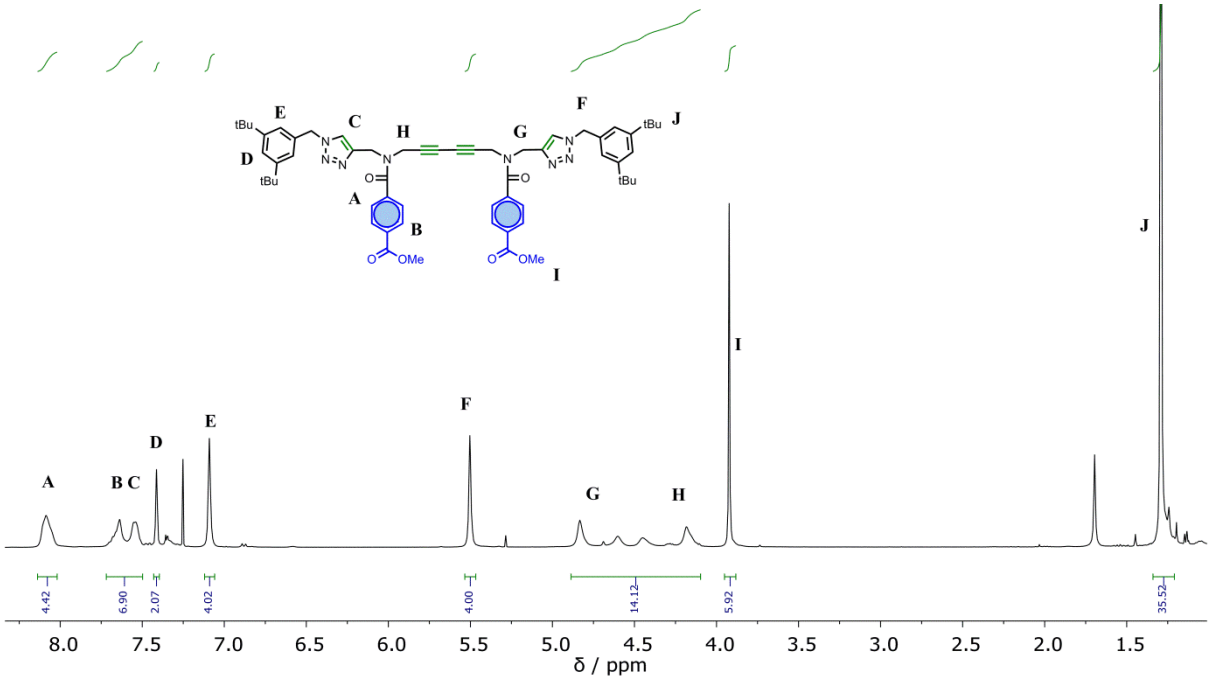
A
B C
D
E
F
G
H
I
J
4.42
6.90
2.07
4.02
4.00
14.12
5.92
35.52
8.0
7.5
7.0
6.5
6.0
5.5
5.0
4.5
4.0
3.5
3.0
2.5
2.0
1.5
δ / ppm

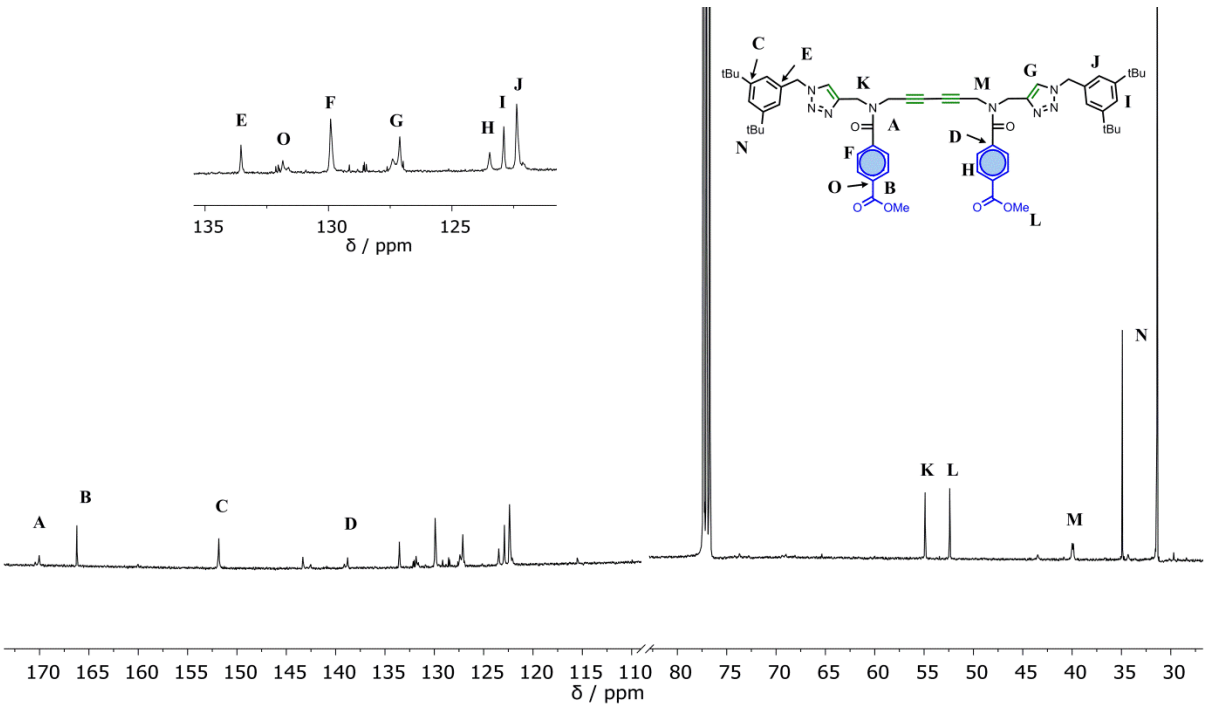
A
B
C
D
E
O
F
G
H
I
J
K L
M
N
135
130
125
δ / ppm
170 165 160 155 150 145 140 135 130 125 120 115 110 80 75 70 65 60 55 50 45 40 35 30
δ / ppm

Synthesis of compound 3.23

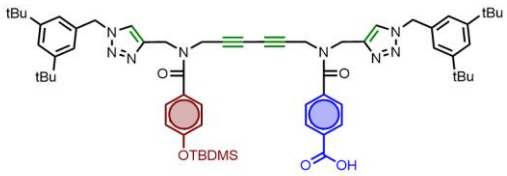

Compound **3.17** (10 mg, 0.011 mmol) was dissolved in THF (5 mL) and tert-butyldimethylsilyl chloride (4 mg, 0.025 mmol) and imidazole (6 mg, 0.088 mmol) were added, and the solution was stirred overnight. HCl 1M (10 mL) was added, and the solution was reextracted with EtOAc. The organic phase was washed with brine (2 x 20 mL), dried over $MgSO_4$, evaporated and dried under high vacuum to yield compound **3.23** as a yellow sticky solid (11 mg, quantitative yield). The product was carried forward without further purification.

^{1}H NMR (400 MHz, Chloroform-*d*) δ 8.10 (d, *J* = 8.0 Hz, 2H), 7.76 – 7.52 (m, 4H), 7.44 (s, 2H), 7.12 (s, 4H), 6.87 (d, *J* = 8.0 Hz, 2H), 5.53 (d, *J* = 4.2 Hz, 4H), 4.84 (overlapping broad singlets due to rotamers, 4H), 4.26 (overlapping broad singlets due to rotamers, 4H), 1.32 (m, 36H), 1.00 (s, 9H), 0.23 (s, 6H).

HRMS (ES+): calcd for $C_{63}H_{80}N_8O_5Si$ 1057.6099 $[M+H]^+$, found 1079.5889 $[M+Na^+]^+$.

Retention time: 2.39 min

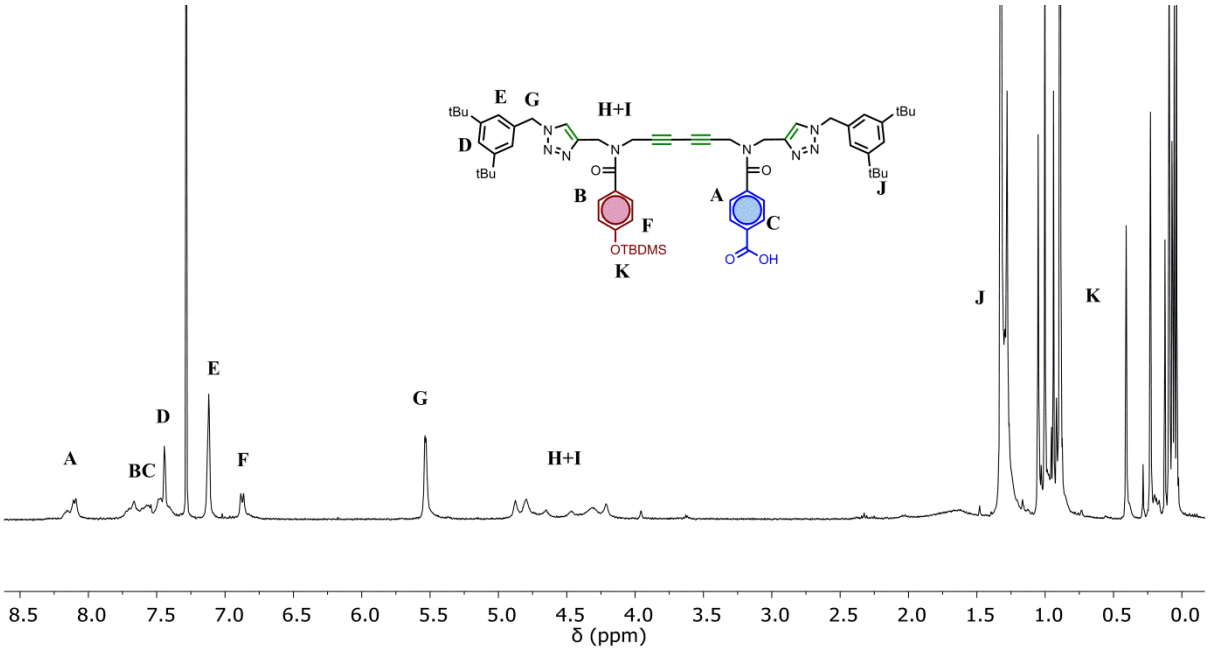

Synthesis of compound 3.24

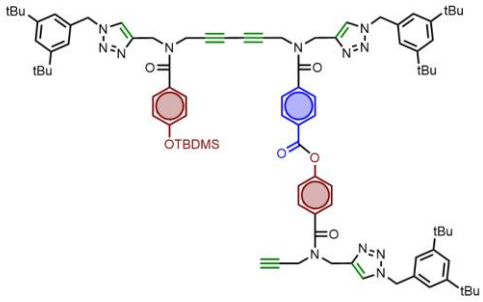

Compound **3.23** (8 mg, 0.007 mmol), compound **3.14** (3.5 mg, 0.008 mmol), EDC (1.5 mg, 0.008 mmol) and DMAP (1 mg, 0.008 mmol) were dissolved in dry DCM (5 mL) and stirred under N_2 until no starting material could be seen by LCMS. The crude was washed with HCl 1M (2 x 20 mL), and brine (2 x 20 mL). The organic phase was dried with $MgSO_4$, concentrated in vacuo and purified by column chromatography (PET 40-60/EtOAc, gradient of increasing polarity) to yield pure compound as a yellow sticky solid (8.8 mg, 84%)

^{1}H NMR (400 MHz, Chloroform-*d*) δ 840 – 8.18 (d, *J* = 8 Hz, 2H), 7.67 (multiplet, 8H), 7.44 (s, 3H), 7.13 (s, 4H), 7.12 (s, 2H), 6.87 (d, *J* = 8.1 Hz, 2H), 5.55 (s, 4H), 5.53 (s, 2H), 4.84 - 4.11 (overlapping broad singlets due to rotamers, 12H), 2.35 (s, 1H), 1.33 (s, 36H), 1.32 (s, 18H), 1.00 (s, 9H), 0.23 (s, 6H).

HRMS (ES+): calcd for $C_{91}H_{112}N_{12}O_6Si$ 1496.8597 $[M+H]^+$, found 1519.8431 $[M+Na]^+$.

Retention time (column 1): 2.62 min

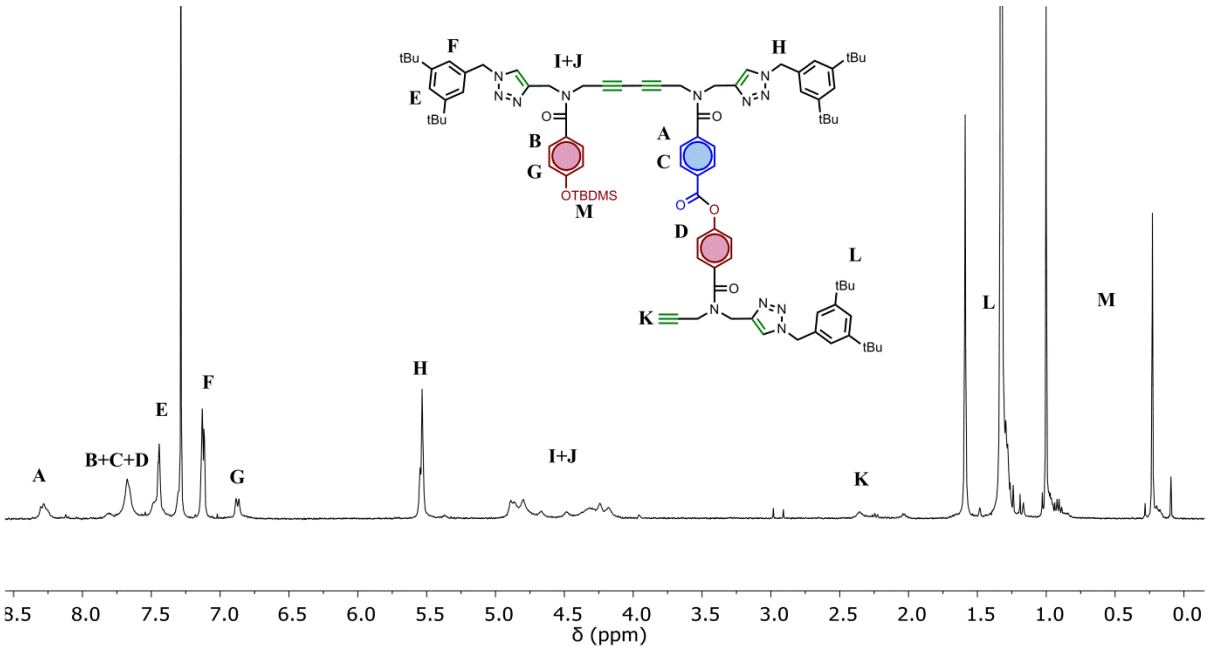

Synthesis of compound 3.25

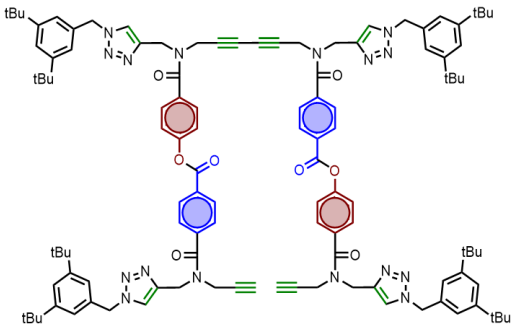

Compound **3.24** (7 mg, 0.0047 mmol) was dissolved in THF (5 mL) and the solution cooled in ice. Acetic acid (290 µL, 0.0055 mmol) and TBAF (1M in THF, 5.5 µL) were added and the reaction was left stirring at room temperature for 20 min before adding HCl 1M until pH reached 3-4. Water was added (20 mL), the organic compound was reextracted with EtOAc (2 x 20 mL) and this organic phase washed with brine (2 x 20 mL), dried with $MgSO_4$, filtered and evaporated in vacuo. The reaction crude, compound **3.13** (2.5 mg, 0.005 mmol), EDC (1.5 mg, 0.008 mmol) and DMAP (1 mg, 0.008 mmol) were dissolved in dry DCM (5 mL) and stirred under N_2 until no starting material could be seen by LCMS. The crude was washed with HCl 1M (2 x 20 mL), and brine (2 x 20 mL). The organic phase was dried with $MgSO_4$, concentrated in vacuo and purified by column chromatography (PET 40-60/EtOAc, gradient of increasing polarity) to yield pure compound as a yellow sticky solid (7.7 mg, 89% over the two steps)

^{1}H NMR (400 MHz, Chloroform-*d*) δ 8.26 (d, *J* = 8.7 Hz, 4H), 7.67 (s, 12H), 7.45 (d, *J* = 2.6 Hz, 4H), 7.13 (s, 8H), 5.54 (d, *J* = 3.1 Hz, 8H), 4.89 (s, 8H), 4.41 – 4.16 (m, 8H), 2.37 (s, 2H), 1.33 (s, 72H).

HRMS (ES+): calcd for $C_{114}H_{130}N_{16}O_8$ 1852.0336 $[M+H]^+$, found 948.4988 $[M+2Na^+]^{2+}$.

Retention time (column 1): 2.42 min

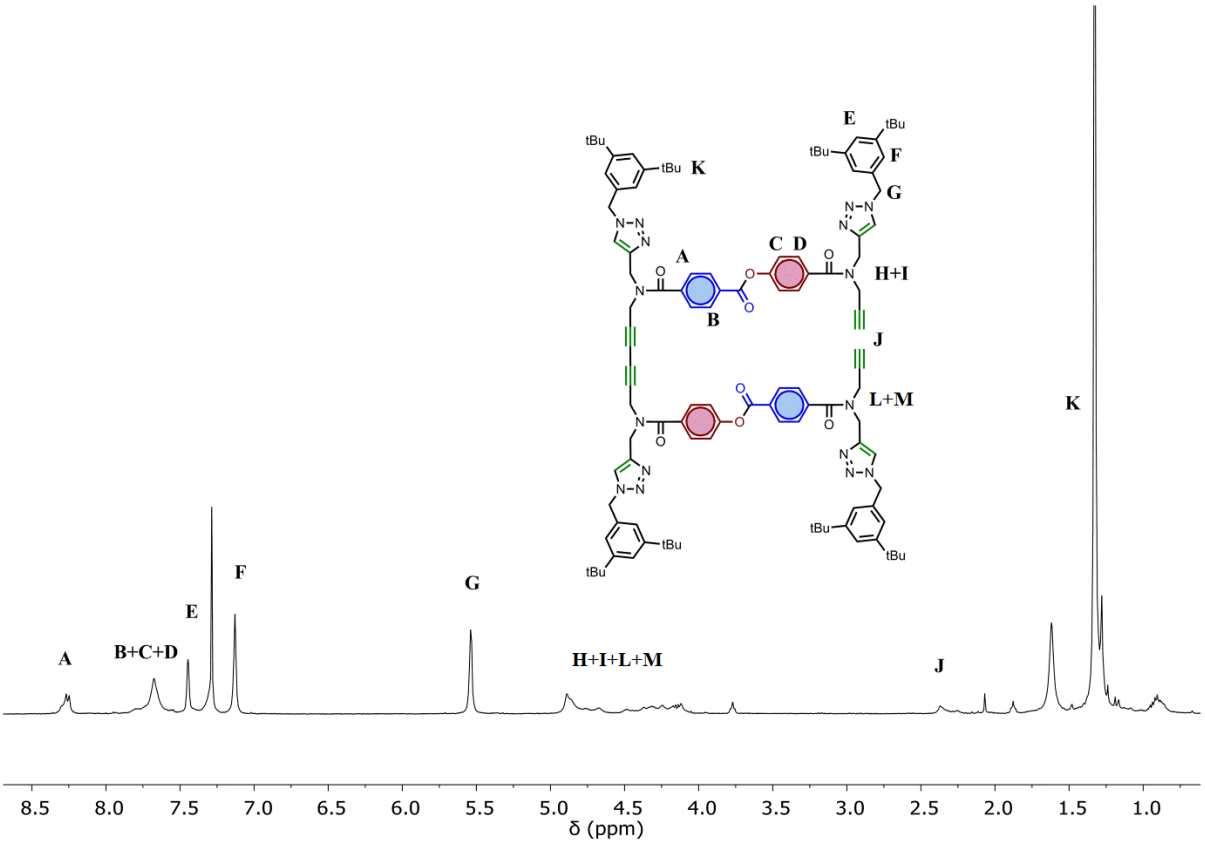
A
B+C+D
E
F
G
H+I+L+M
J
K
8.5
8.0
7.5
7.0
6.5
6.0
5.5
5.0
4.5
4.0
3.5
3.0
2.5
2.0
1.5
1.0
δ (ppm)

Synthesis of compound 3.26

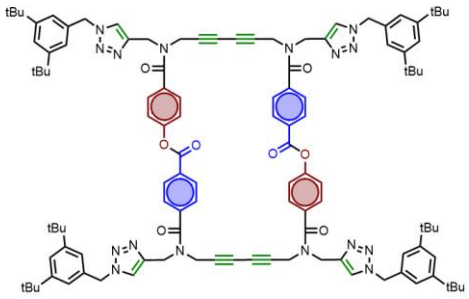

Compound **3.25** (3.5 mg, 0.002 mmol), $Pd(PPh_3)_2Cl_2$ (1.3 mg, 0.002 mmol), PPh_3 (1.4 mg, 0.006 mmol), and CuI (0.33 mg, 0.002 mmol) were dissolved in acetonitrile (38 mL). Et_3N (25 µL, 0.2 mmol) was added and the reaction was stirred for 1 h. After this time the reaction was neutralized with HCl 1M, diluted with water, and the product reextracted with EtOAc. The organic phase was washed with brine (2 x 20 mL), dried with $MgSO_4$, filtered and dried in vacuo. The crude was purified via HPLC ($MeCN/H_2O$) to yield final compound as a dark yellow sticky solid (2.5 mg, 72%)

^{1}H NMR (400 MHz, Chloroform-*d*) δ 8.30 (d, *J* = 7.9 Hz, 4H), 7.68 (s, 4H), 7.45 (s, 4H), 7.34 (s, 4H), 7.14 (s, 8H), 5.55 (s, 4H), 5.54 (s, 4H), 4.87 (s, 4H), 4.84 (s, 4H), 4.30 (s, 4H), 4.25 (s, 4H), 1.34 (s, 36H), 1.33 (s, 36H).

HRMS (ES+): calcd for $C_{114}H_{128}N_{16}O_8$ 1850.01793 $[M+H]^+$, found 947.4942 $[M+2Na]^{2+}$.

Retention time (column 1): 2.52 min

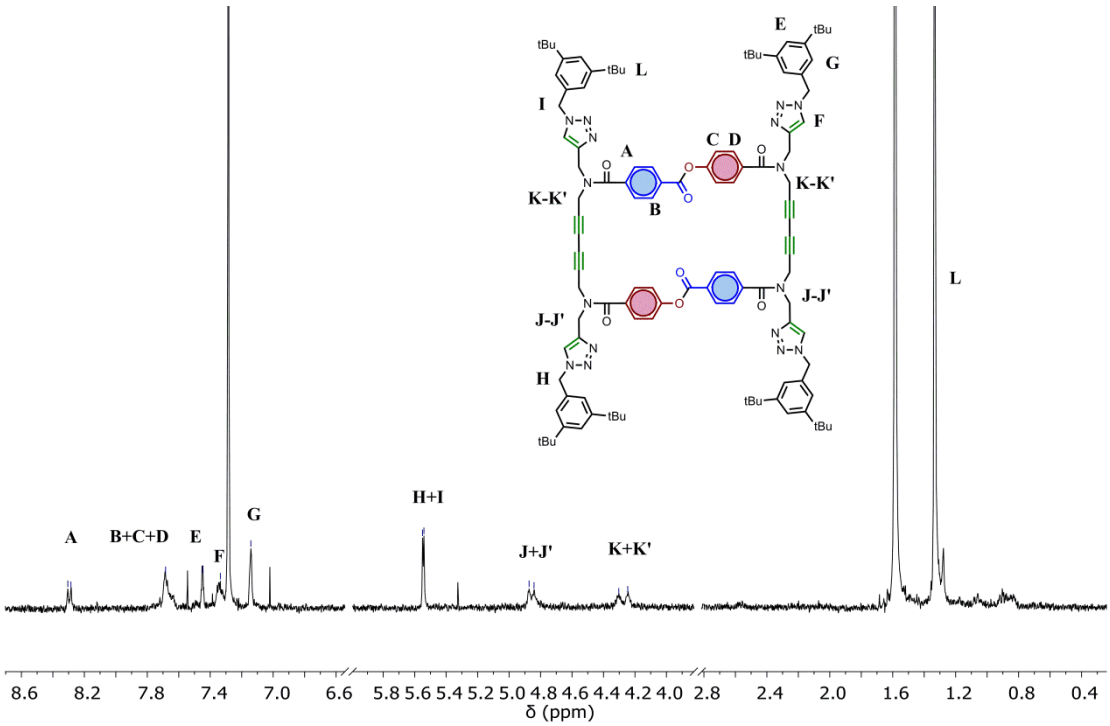
A
B+C+D
E
F
G
H+I
J+J'
K+K'
L
δ (ppm)

3.9 Bibliography

[1] R. Balamurugan, C-C. Chien, K-M. Wu, Y-H. Chiu and J-H. Liu, *Analyst*, 2013, 138, 1564-1569

Valentine's Day is coming up? Oh crap, I forgot to get a girlfriend again!"

Fry

4

Templated Replication of Homodimers

4.1 Introduction

Following the strategy described in Chapter 3, it would take two full cycles of synthesis of complementary strands to obtain material replication. Here we present a new design to achieve the same result in just a single cycle. (Figure 4.1).

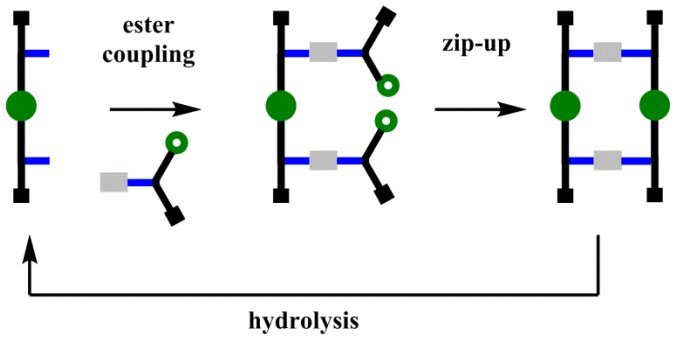

Figure 4.1. Schematic representation of the strategy to replicate a homodimer by introducing a spacer unit between the template and monomers. Blue bars represent carboxylic acid bases;

grey rectangles represent spacer units; green empty circles represent terminal alkynes; full green circles represent butadiyne links; black squares represent capping groups.

We introduced a spacer unit that acted as linkage between the mother strand and the daughter strand. Since our goal was making a daughter strand identical to the template, we designed the linkage to have symmetrical chemical handles, and to be complementary to the molecule being replicated, i.e. to replicate an acid, the spacer motif will be a bis-phenol derivative, and vice versa. (Figure 4.2). Therefore, instead of grafting onto the template just monomers, in the work described in this chapter we first coupled the monomers with spacers.

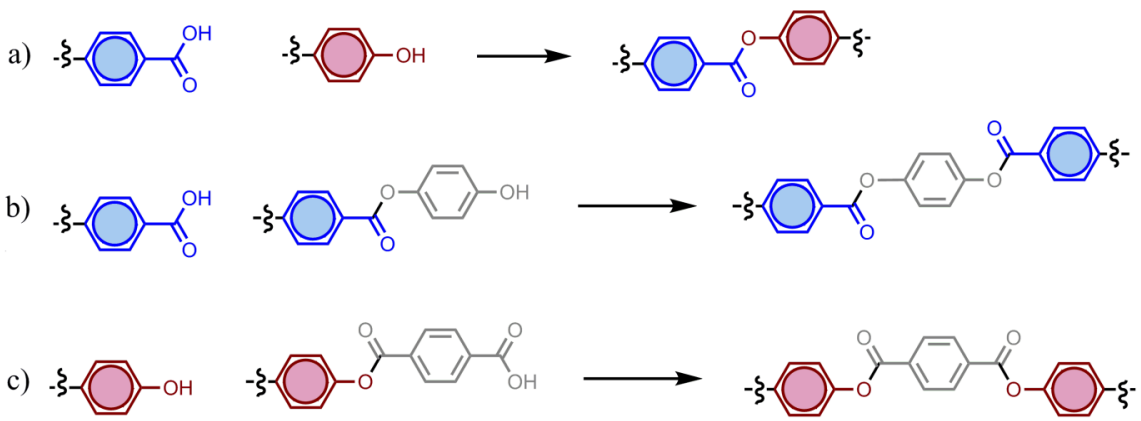

Figure 4.2. Different base-pairing strategies. (a) Template synthesis gives a complementary oligomer sequence. (b) Template synthesis to replicate an acid oligomer. (c) Template synthesis to replicate a phenol oligomer.

4.2 Synthesis of linker monomers

We first set out to synthesise the monomer with linker units attached that would later be grafted onto the template. To that effect, the capped-acid monomer introduced in Chapter 3 was coupled with mono-TBDMS-protected hydroquinone, and the resulting compound was subsequently deprotected to produce compound **4.3** (Scheme 4.1).

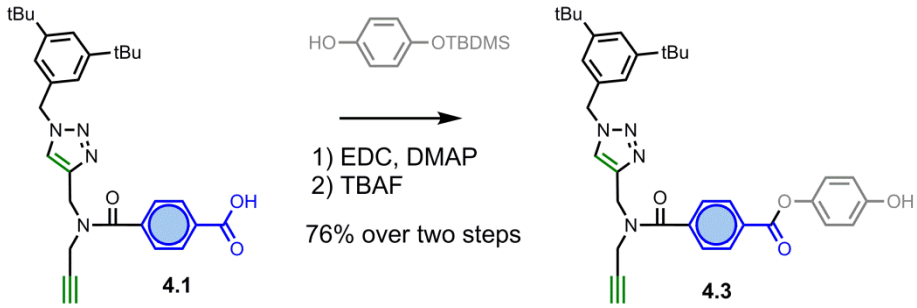

Scheme 4.1. Synthesis of the carboxylic acid linker monomer **4.3**.

When it came to the phenol replication, it was our intention to show an increase of material through spectroscopic techniques, after a succession of replication cycles. For that, we decided that the product of the first cycle had to be different from the initial template, and further replication cycles would amplify the signals corresponding to this first daughter strand. To do that we modified the capping group to a benzyl azide carrying a CF_3 unit. This will have a large effect on the polarity of the molecule and therefore the difference between these molecules will become apparent by UPLC. Moreover, the change of substitution in the ring will affect the ^1H NMR spectra (Figure 4.3): there is a slight shift in the benzyl CH_2 signal due to the different electron-donating and electron-withdrawing capabilities of the aromatic substituents.

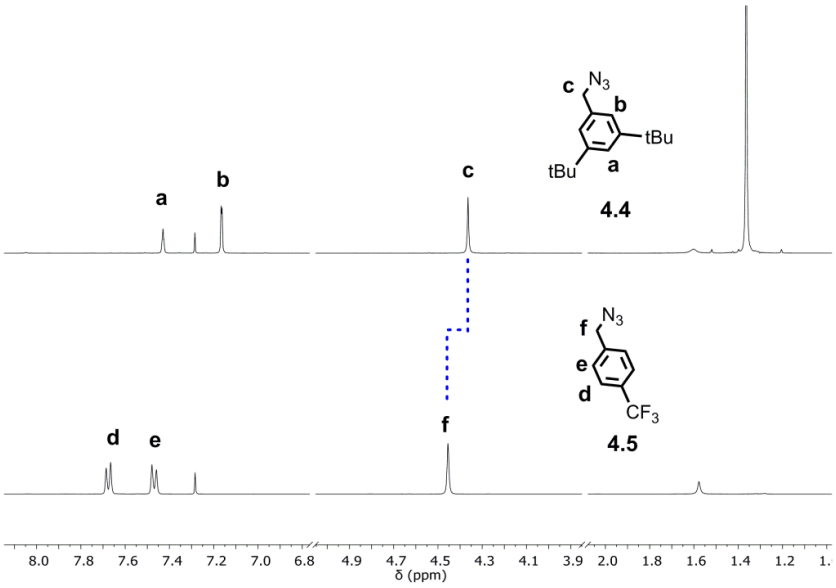

Figure 4.3. ^{1}H NMR spectra (400 MHz, $CDCl_3$ 298K, ca. 100 mM) of azides **4.4** and **4.5** showing the difference in the chemical shifts of the signals due the benzylic protons.

With that in mind, a new monomer unit was synthesized in a statistical reaction to produce the CF_3-capped phenol monomer **4.7** (Scheme 4.2), which was then reacted with a mono *t*-Bu ester derivative of terephthalic acid, before being deprotected with TFA to yield the linker monomer unit **4.9**.

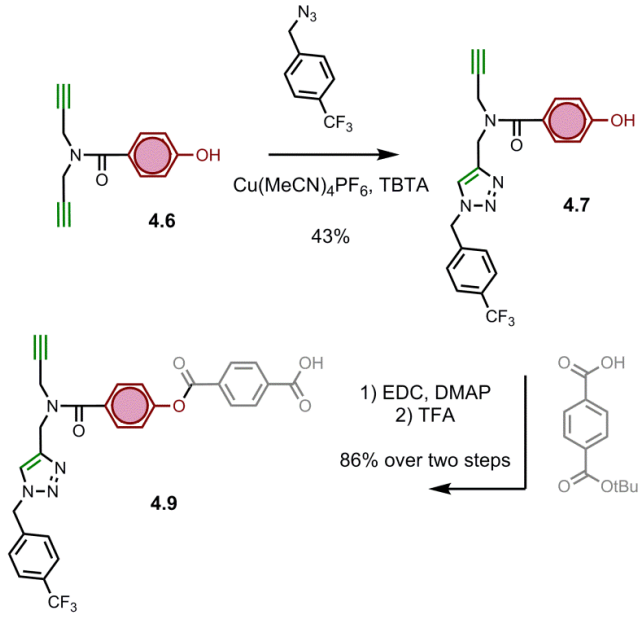

Scheme 4.2. Synthesis of the CF_3-capped phenol linker monomer **4.9**.

4.3 Synthesis of homodimer templates

The synthesis of phenol dimer was described in Chapter 3.

Synthesizing and purifying the carboxylic acid dimer template was non-trivial for a variety of reasons. Firstly, the free acid does not react under normal Glaser coupling conditions, due to copper complexation under the required basic conditions. It was decided to dimerise an ester and follow that with a hydrolysis reaction to yield the free acid molecule. But this strategy generated a second concern: the amide-propargyl bond proved to be unstable under basic conditions, so this process was in competition with ester hydrolysis in the presence of a base.

We decided to test three different ester monomers made with alcohols that have different pK_a values and therefore have different abilities as leaving groups. Two of them were introduced in the previous chapter and are presented here in Scheme 4.4 as compounds **4.11** and **4.12**. Compound **4.11** is a methyl ester and it is the least reactive of the three in hydrolytic conditions. **4.12** is an aromatic ester with an electronegative group in the para position of the aromatic ring, so it is especially good at stabilising the resulting phenolate after the hydrolysis. A third compound with a reactivity in between these two esters was prepared by esterifying the capped-acid monomer **4.1** with 4-tertbutyl phenol, producing compound **4.10**. (Scheme 4.3)

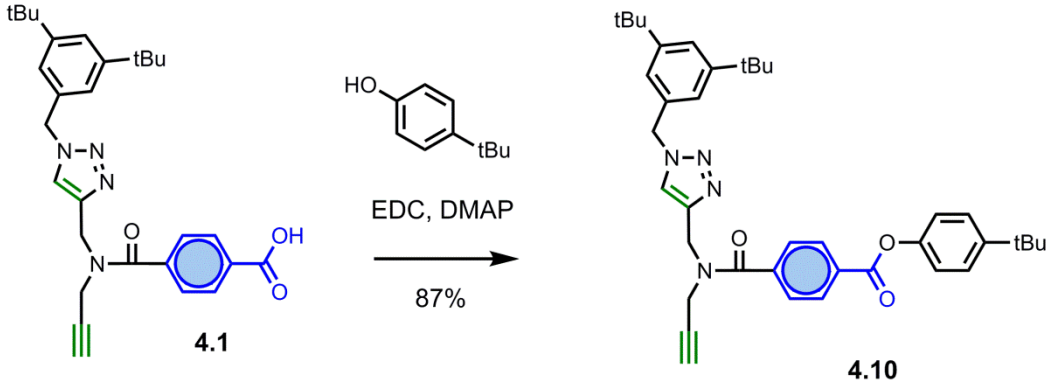

Scheme 4.3. Synthesis of the capped ester monomers **4.10.**

All three esters were then dimerised by Glaser-Hay coupling and hydrolysed in the same conditions (Scheme 4.4). A summary with the yield of every reaction can be found in Table 4.1. After the homocoupling of compound **4.11** to form dimer **4.13**, the molecule decomposed when exposed to 6 equivalents of LiOH. Only small amounts of final acid dimer were observed by UPLC (Figure 4.4a). The reaction had to be left overnight to see complete consumption of starting material.

Compound **4.10** was dimerised in the same conditions to form **4.14**. Its hydrolysis proceeded at a faster rate than that of **4.13**, but UPLC analysis of the reaction crude showed that still a substantial amount of decomposition products were produced (Figure 4.4b). Finally, we coupled **4.12** to form the dimer **4.15**. The material was hydrolysed and reacted to completion in an hour (Figure 4.4c). After a challenging purification, the acid dimer **4.16** was isolated in a 56% yield. The main decomposition product in all the hydrolysis reactions was determined to be the depropargylated version of the acid monomer, i.e. the base cleaved the propargyl-amide bond.

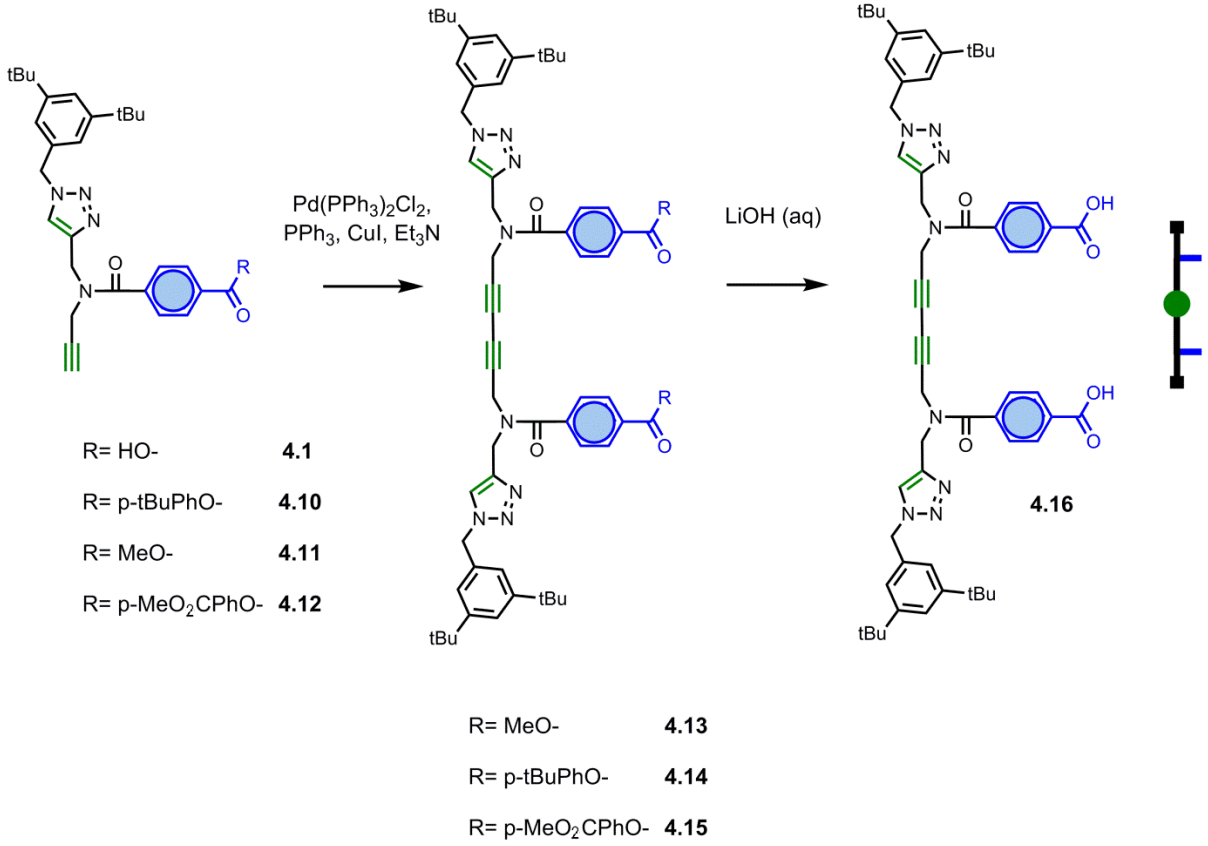

Scheme 4.4. Synthesis of the carboxylic acid homodimer template **4.17**. See Table 4.1 for reaction yields.

Table 4.1: Yields for dimerization and hydrolysis reactions shown in Scheme 4.4.

Starting Material	R	Dimerisation yield	Hydrolysis yield
4.1	HO-	-	-
4.10	p-tBuPhO-	84	-
4.11	MeO-	87	-
4.12	p-MeO_2CPhO-	70	56

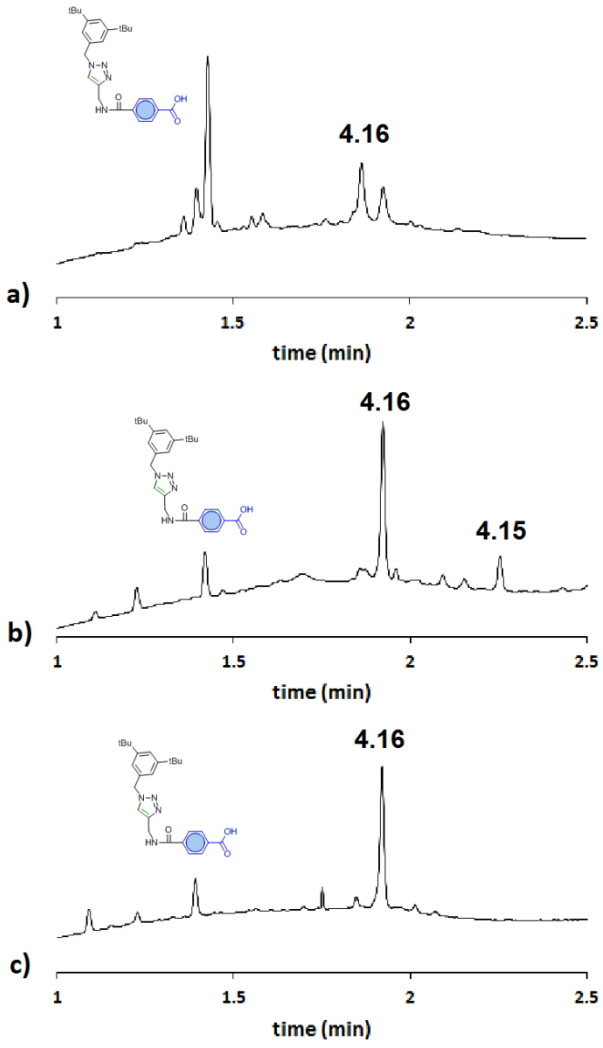

Figure 4.4. UPLC traces of the crude reaction mixtures obtained after treatment of (a) **4.13** overnight, (b) **4.14** for 90 min, (c) **4.15** for 60 min with aqueous 2M LiOH (6 eq.) in THF at room temperature. The carboxylic acid dimer product is **4.16**, and depropargylation gives the main side product indicated. The conditions of the UPLC method are as follows: Solvent A: Water +0.1%

Formic acid; Solvent B: Acetonitrile +0.1% Formic acid; Gradient of 0-2 minutes 5% - 100%B + 1 minute 100% B with re-equilibration time of 2 minutes. Flow rate: 0.6 ml/min; Column temperature of 40°C; Injection volume of 2 µL. The signal was monitored at 254 nm.

4.4 Template-directed replication of a carboxylic acid homodimer.

The esterification of **4.16** and **4.3**, the two necessary pieces to start the acid replication cycle, produced the pre-zip structure **4.17** (Scheme 4.5). Glaser Hay coupling between the two free alkynes of **4.17** produced macrocycle **4.18**, which upon purification was hydrolysed using an aqueous solution of LiOH in THF. This process produced two molecules of acid dimer **4.16**, starting from one acid template. Hence, this strategy potentially offers the opportunity to have exponential material amplification after successive replication cycles.

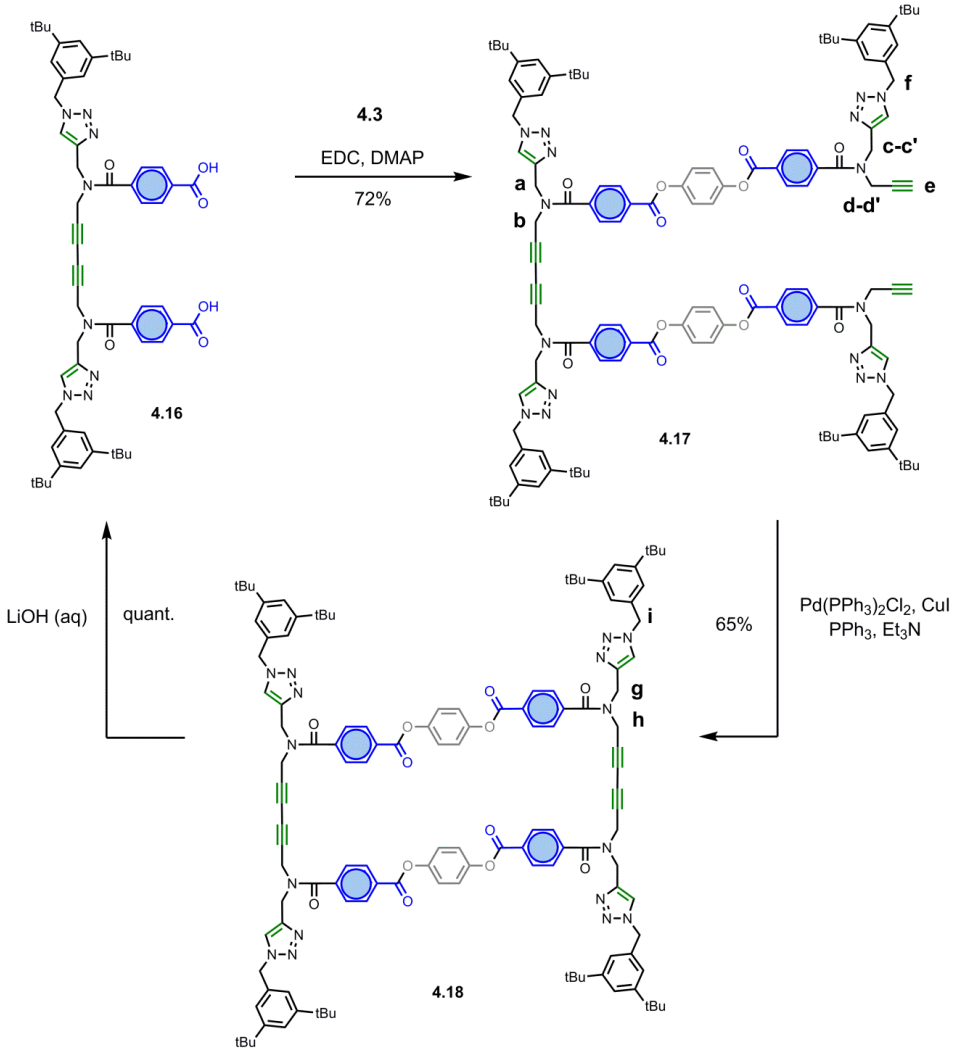

Scheme 4.5. Covalent template-directed replication of the carboxylic acid dimer **4.16**. The proton labelling scheme used in Figures 4.6 and 4.7 is shown.

Lower catalyst loading, though it would increase reaction times, would simplify considerably purification of **4.18**. As shown in Chapter 3, the phosphine ligand used in the zip-up reaction gets

partially oxidized and proceeds to elute during long periods of time, causing broad peaks in the UPLC trace. The UPLC traces in Figure 4.5 show starting material **4.17** peak at 1.88 min evolving into a peak at 1.92 min, due to the final closed macrocycle **4.18**. The masses of the initial and final peak were differentiated by 2 units in the +1 mass spectrum, 1 unit in the +2 and 0.6 units of mass in the triply charged adduct.

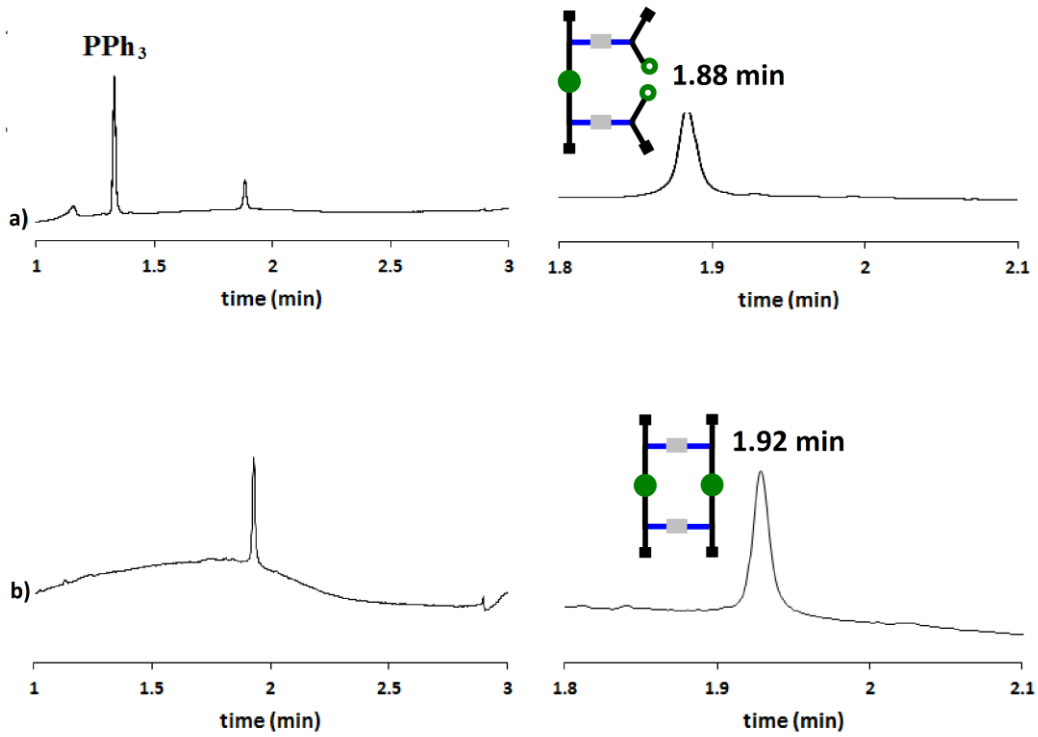

Figure 4.5. UPLC traces for the reaction of **4.18** (50 µM) with $Pd(PPh_3)_2Cl_2$ (1 eq.), PPh_3 (3 eq.), CuI (1 eq.), Et_3N (100 eq.) in MeCN at room temperature after (a) 0 min, with zoom of area of interest; and (b) 6h, with zoom of area of interest. The conditions of the UPLC method are as follows: Solvent A: Water +0.1% Formic acid; Solvent B: Acetonitrile +0.1% Formic acid; Gradient of 0-2 minutes 5% - 100%B + 1 minute 100% B with re-equilibration time of 2 minutes. Flow rate: 0.6 ml/min; Column temperature of 40°C; Injection volume of 2 µL. The signal was monitored at 254 nm.

4.18 was purified by HPLC and characterized by ^1H NMR spectroscopy. As with the macrocycles previously described, ring closure can be ascertained by looking at two regions of interest (Figure 4.6):

- The 4 to 5 ppm range, in which the propargyl CH_2 protons appear. In compound **4.17** there are four distinct environments (**a**-**b**, and **c**-**d**). Both **c** and **d** are split into nearly identical rotameric peaks, **c'** and **d'**. Unlike in the cases described in the previous chapter, the macrocycle **18** still seems to have rotamers that give rise to small peaks, **g'** and **h'**.
- At 2.4 ppm the alkyne proton **e** disappears.

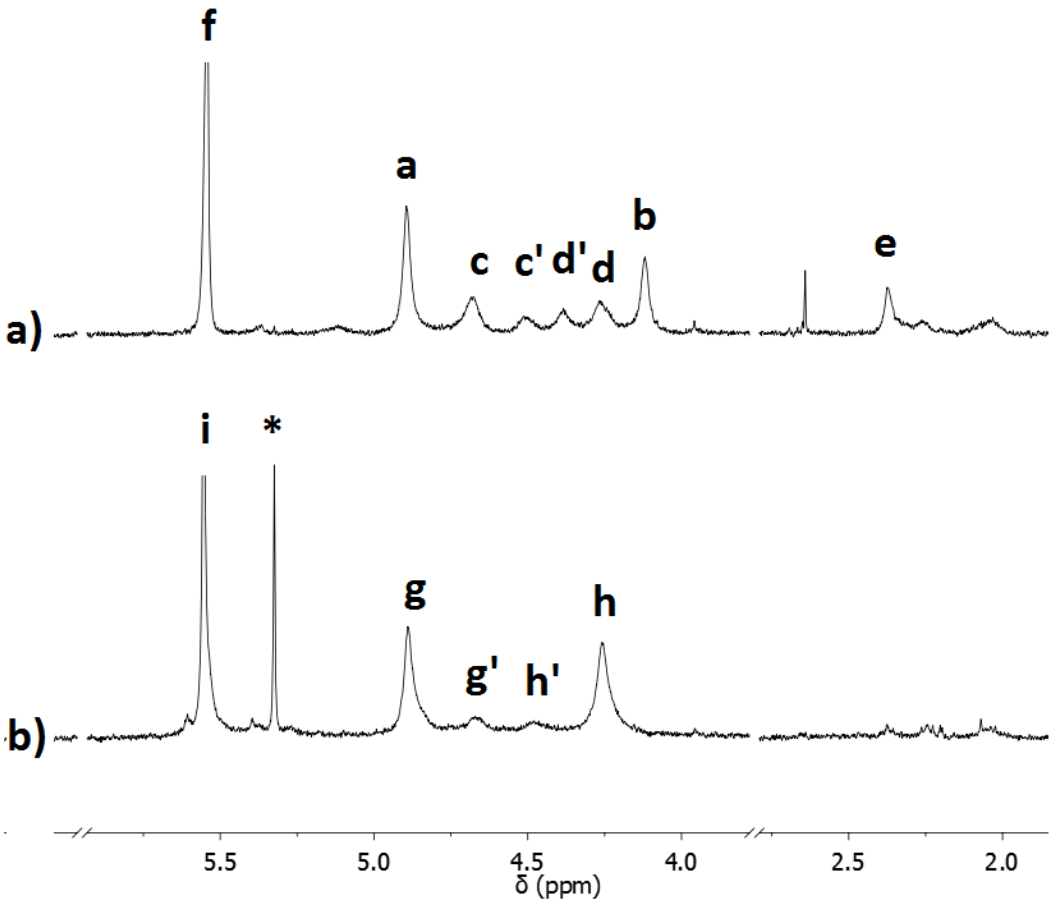

Figure 4.6: Partial ^{1}H NMR spectra (500 MHz, $CDCl_3$ 298K, ca. 5 mM) of (a) **4.17** and (b) **4.18** The asterisk indicates DCM impurity. The proton labelling scheme is shown in Scheme 4.5.

NOESY spectra highlight once more the different conformational isomerism presented by **4.17** and **4.18** (Figure 4.7). The exchange cross-peaks disappear upon ring closure, and no sign of **g'** and **h'** can be seen in the NOESY of **4.18**.

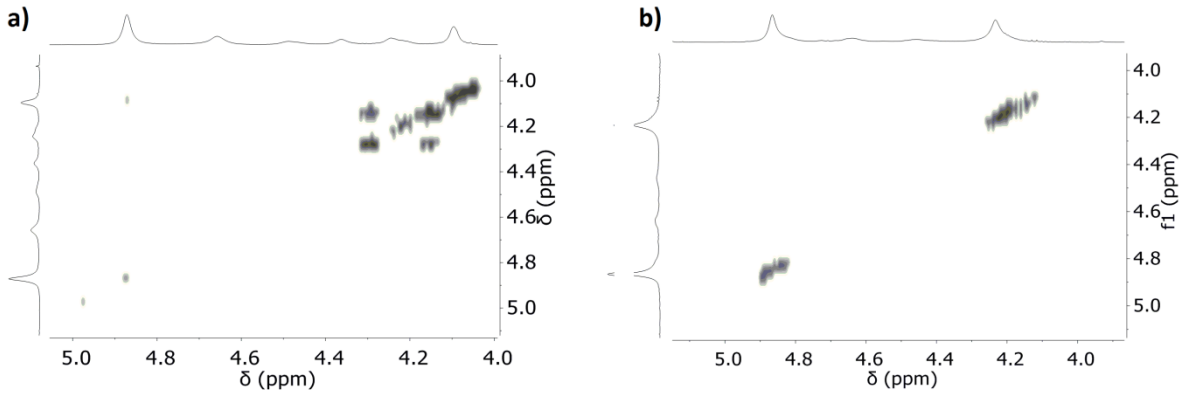

Figure 4. 7: 2D NOESY (500 MHz, $CDCl_3$, 298K, ca. 5 mM) spectra of (a) **17** and (b) **18**.

To finalize the replication cycle, compound **4.18** was hydrolysed into two acid dimers using 10 eq. of LiOH in water. The reaction was followed by UPLC and it was seen to go to completion in around 30 min, where the peak at 2.61 min completely disappeared and was substituted by another signal at 1.92 min, belonging to the acid dimer **4.16** (Figure 4.9).

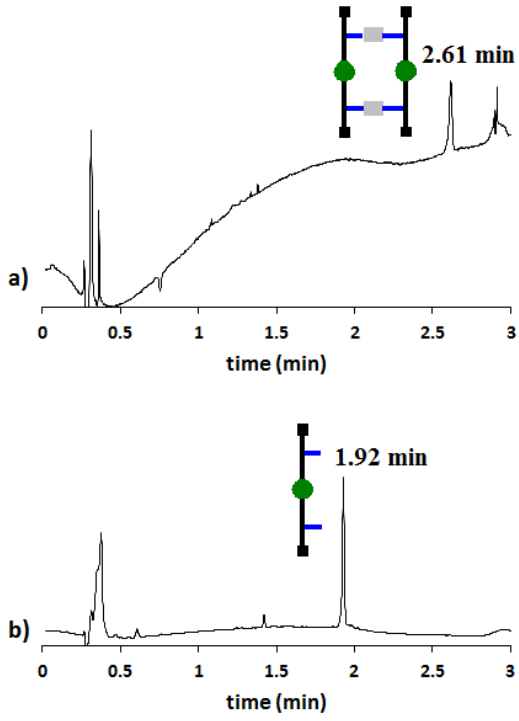

Figure 4.9: UPLC trace for the reaction of **4.18** with aqueous LiOH 2M (10 eq.) in THF at room temperature after (a) 0 min and (b) 30 min. The conditions of the UPLC method are as follows: Solvent A: Water +0.1% Formic acid; Solvent B: Acetonitrile +0.1% Formic acid; Gradient of 0-

2 minutes 5% - 100%B + 1 minute 100% B with re-equilibration time of 2 minutes. Flow rate: 0.6 ml/min; Column temperature of 40°C; Injection volume of 2 µL. The signal was monitored at 254 nm.

4.5 Template-directed replication of a phenol homodimer.

The phenol replication cycle is shown in Scheme 4.6. Phenol dimer **4.19** was reacted with the linker monomer **4.9** to produce the pre-zip structure **4.20**, which was subsequently zipped-up, yielding macrocycle **4.21**. When molecule **4.21** was hydrolysed it produced two different phenol dimers, the original template **4.19** and one capped with the CF_3-containing groups, compound **4.22.** This difference in capping between the dimers made them easily distinguishable by ^1H NMR spectroscopy and by UPLC.

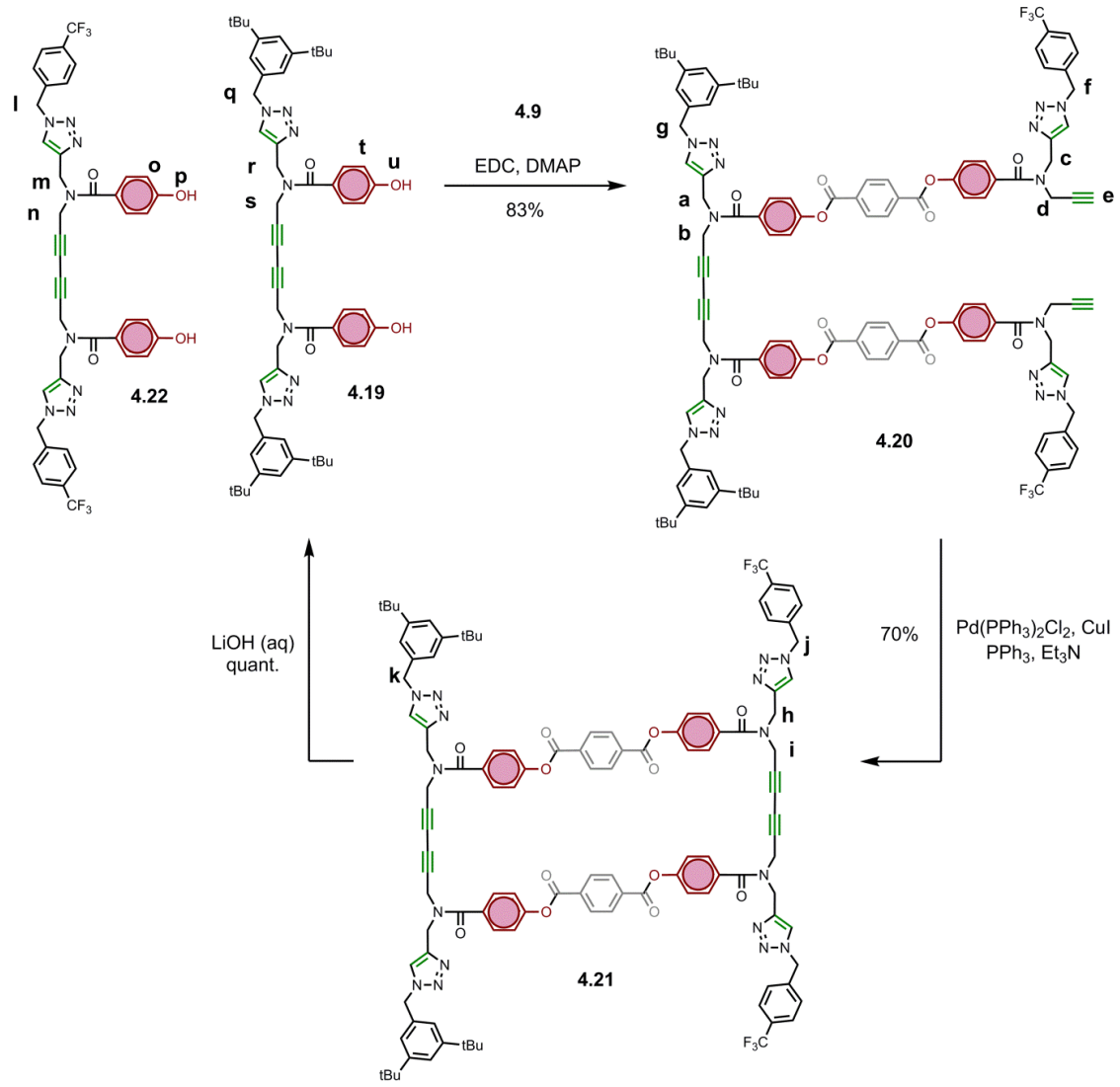

Scheme 4.6. Covalent template-directed replication of the phenol dimer **4.19.** The proton labelling scheme used in Figure 4.11 is shown.

Similarly to the previous ring closures, the pre-zip structure **4.20** was closed using palladium, copper and triphenyl phosphine as a ligand. The progress of the reaction was followed by UPLC (Figure 4.10). The peak of compound **4.20** at 1.73 min progressively disappeared, and a single peak appeared at 1.78 min, which after purification of the crude reaction mixture was identified as macrocycle **4.21**. Once more, the masses of **4.20** and **4.21** were differentiated by 2 units in the +1 peak in the mass spectrum, 1 unit in the +2 and 0.6 units of mass in the triply charged adduct.

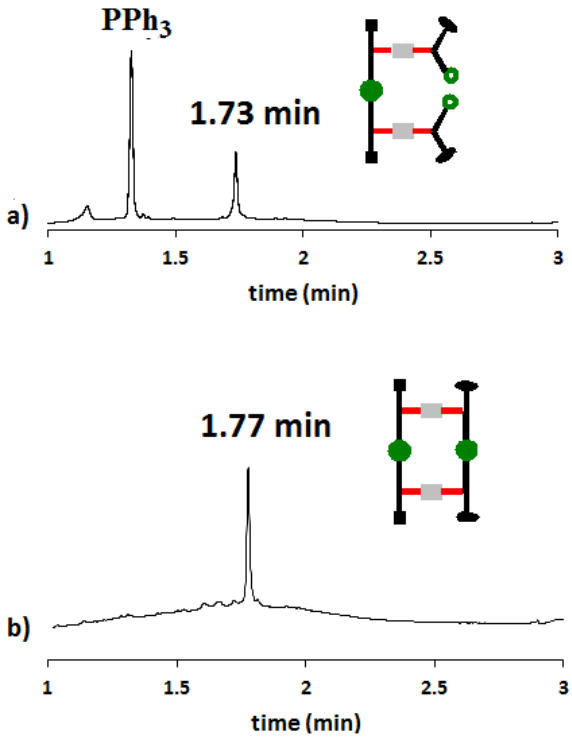

Figure 4.10. UPLC traces for the reaction of **4.20** (50 µM) with $Pd(PPh_3)_2Cl_2$ (1 eq.), PPh_3 (3 eq.), CuI (1 eq.), Et_3N (100 eq.) in MeCN at room temperature after (a) 0 min and (b) 6h. The conditions of the UPLC method are as follows: Solvent A: Water +0.1% Formic acid; Solvent B: Acetonitrile +0.1% Formic acid; Gradient of 0-2 minutes 5% - 100%B + 1 minute 100% B with re-equilibration time of 2 minutes. Flow rate: 0.6 ml/min; Column temperature of 40°C; Injection volume of 2 µL. The signal was monitored at 254 nm.

4.20 and **4.21** were characterised by ^1H NMR spectroscopy (Figure 4.11). The disappearance of the alkyne proton signal at 2.40 ppm was obvious. Moreover, it was noticeable that at 4.85 ppm **a** and **c** appear together both in **4.20**, while at 4.30 ppm there are two signals (**d-b**) with roughly the

same integration, which upon ring closure coalesce into a single peak (**i**). Finally, there are two different benzyl signals around 5.6 ppm (**f-g**), with similar intensity.

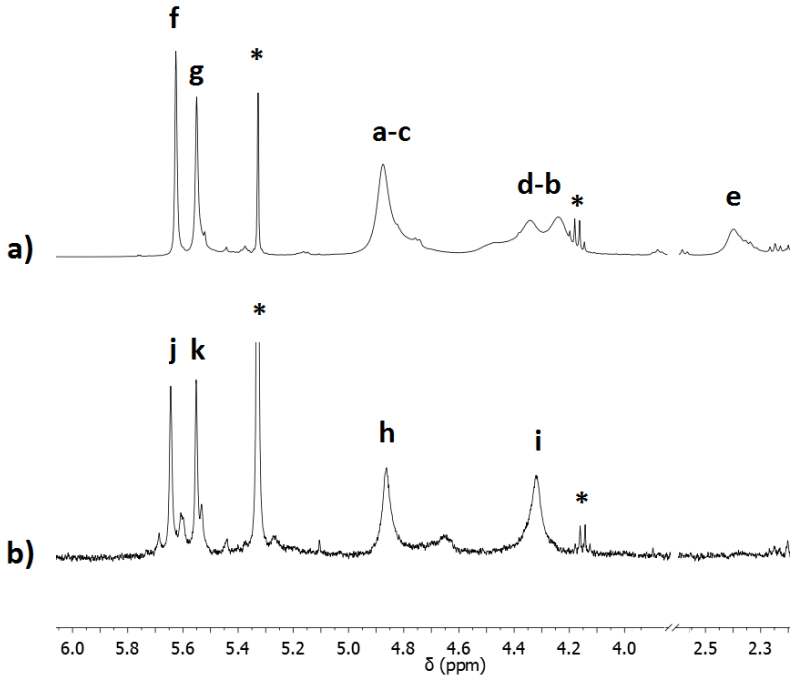

Figure 4.11. Partial ^{1}H NMR spectra (500 MHz, $CDCl_3$ 298K, ca. 5 mM) of (a) **4.20** and (b) **4.21**. The asterisks indicate DCM (5.3 ppm) and EtOAc (4.12 ppm) impurities. The proton labelling scheme is shown in Scheme 4.6.

The replication cycle was completed with a basic hydrolysis to produce the starting phenol dimer and the daughter strand dimer **4.22**. This converted the single UPLC peak at 2.19 min to two peaks corresponding to the two different dimers (Figure 4.12).

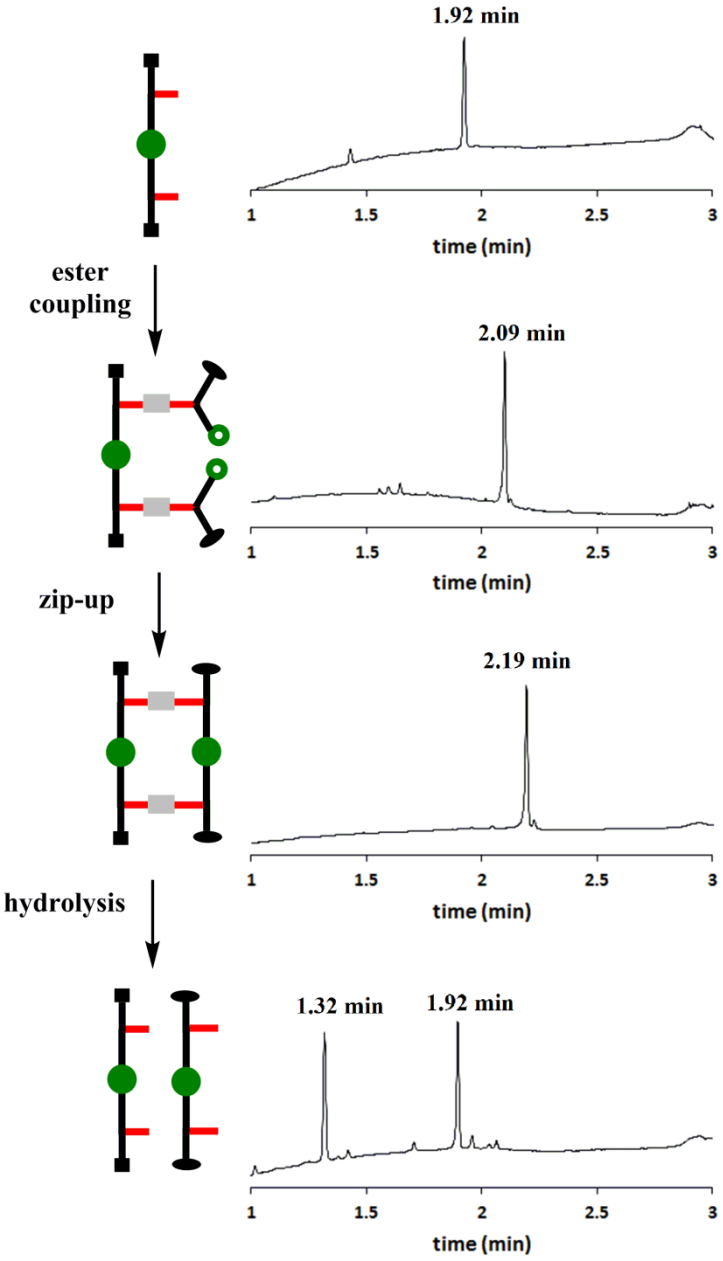

Figure 4.12: UPLC trace the crude reaction mixture of the replication cycle of the phenol dimer **4.19**. The conditions of the UPLC method are as follows: Solvent A: Water +0.1% Formic acid; Solvent B: Acetonitrile +0.1% Formic acid; Gradient of 0-2 minutes 5% - 100%B + 1 minute 100% B with re-equilibration time of 2 minutes. Flow rate: 0.6 ml/min; Column temperature of 40°C; Injection volume of 2 µL. The signal was monitored at 254 nm.

The CF_3-capped dimer **4.22** proved to be very insoluble, which led us to proceed with the characterization of the mixture in d_6-DMSO (Figure 4.13). ^{1}H NMR spectroscopy showed the maintenance of the integral ratio between the benzyl environments at around 5.6 ppm before (**j-k**)

and after (**l-q**) the hydrolysis. Moreover, a sharp phenol proton peak appears at 10 ppm (**p-u**), a peak that did not exist in the macrocycle **4.21**. Additionally, the appearance of the ortho protons to the phenol group at around 6.8 ppm (**t-o)** confirms the change in the electronic environment after the hydrolysis. Finally, it is worth noticing that thanks to the sharpening of the signals between 4 and 5 ppm caused by the change in solvent, we can observe the slightly different signals arising from the propargyl CH_2 protons of **4.19** and **4.22 (m-r**, **n-s)** (Figure 4.13b)

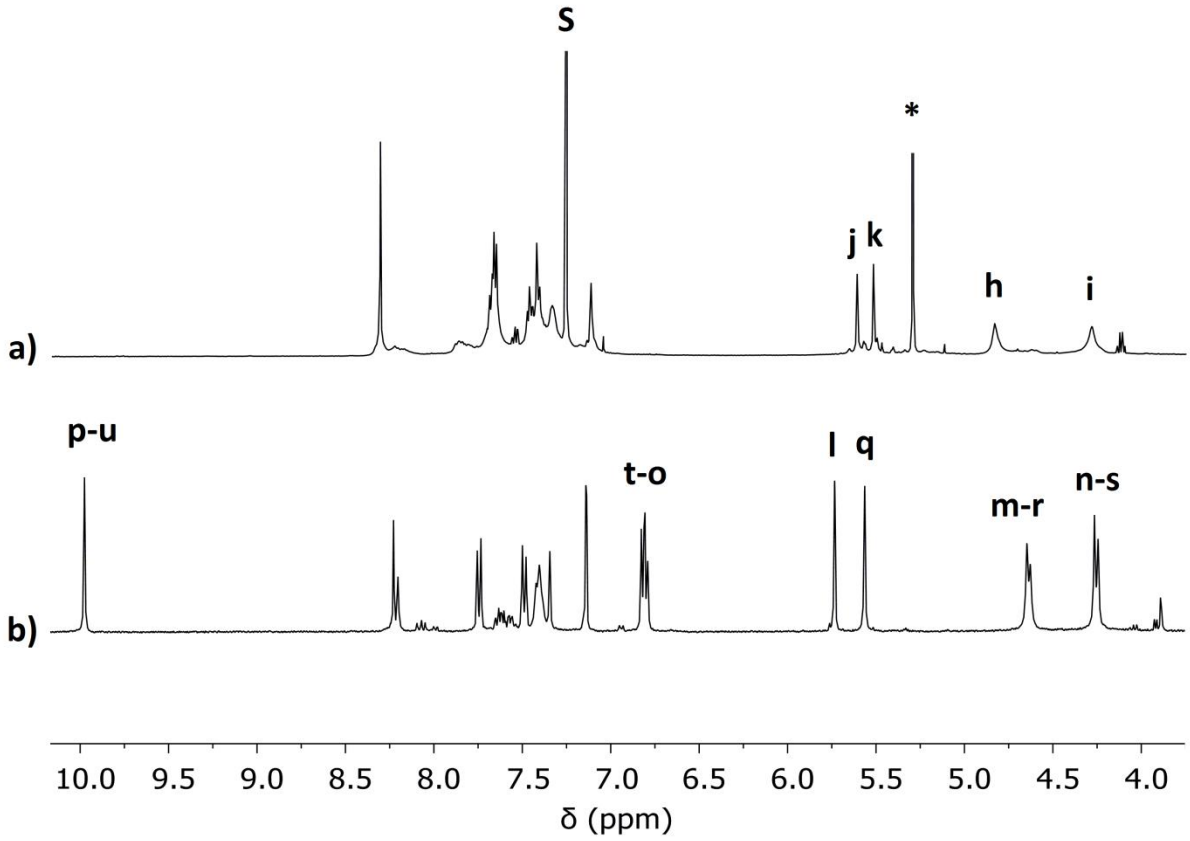

Figure 4.13: Partial ^{1}H NMR spectra of (a) **4.21**(500 MHz, $CDCl_3$ 298K, ca. 5 mM)) and (b) the crude product from the hydrolysis reaction that contains **4.19** and **4.22** (400 MHz, DMSO, 298K, ca. 5 mM). The asterisk indicates DCM impurity. The proton labelling scheme is shown in Scheme 4.6.

4.6 Conclusions

In this chapter we have developed the synthetic strategy to perform replication of oligomers in a single base-pair cycle, thanks to the introduction of a reciprocal spacing unit. We demonstrated the strategy with two different homodimers. Further works needs to be done optimizing the purification processes to ensure that true material amplification occurs during these cycles.

4.7 Experimental Section

General methods

All the reagents were obtained from commercial sources (Sigma-Aldrich, Alfa Aesar, Fisher Scientific and Fluorochem) and were used without further purification. Thin layer chromatography was carried out using with silica gel 60F (Merck) on aluminium. Flash chromatography was carried out on an automated system (Combiflash Rf+ or Combiflash Rf Lumen) using prepacked cartridges of silica (25µ or 50µ PuriFlash® Columns). ^{1}H and ^{13}C NMR spectra were recorded on either a Bruker AV3400 or AV3500 spectrometer at 298 K unless specifically stated otherwise. Residual solvent peak was used as an internal standard. All chemical shifts are quoted in ppm on the δ scale and the coupling constants expressed in Hz. Signal splitting patterns are described as follows: s (singlet), d (doublet), t (triplet), m (multiplet). FTIR spectra were recorded on a PerkinElmer Spectrum One FT-IR spectrometer. ES+ was carried out on a Waters LCT-TOF spectrometer or a Waters Xevo G2-S bench top QTOF machine. The LCMS analysis of samples was performed using Waters Acquity H-class UPLC coupled with a single quadrupole Waters SQD2. ACQUITY UPLC CSH C18 Column, 130Å, 1.7 µm, 2.1 mm X 50 mm was used as the UPLC column. The conditions of the UPLC method are as follows: Solvent A: Water +0.1% Formic acid; Solvent B: Acetonitrile +0.1% Formic acid; Gradient of 0-2 minutes 5% - 100%B + 1 minute 100% B with re-equilibration time of 2 minutes. Flow rate: 0.6 ml/min; Column temperature of 40 °C; Injection volume of 2 µL. The signal was monitored at 254 nm.

Synthesis of compound 4.2

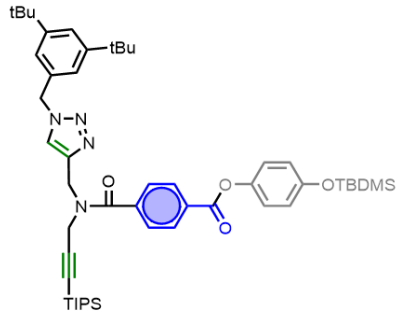

Compound **4.1** (150 mg, 0.38 mmol)**,** mono TBDMS protected hidroquinone (94 mg, 0.42 mmol), EDC (95 mg, 0.5 mmol) and DMAP (13 mg, 0.11 mmol) were dissolved in dry DCM (20 mL) and stirred under N_2 overnight. The crude solution was washed with HCl 1M (2 x 20 mL) and brine (2 x 20 mL). The organic phase was dried with $MgSO_4$, concentrated in vacuo and purified via column chromatography (PET 40-60/EtOAc, gradient of increasing polarity

) to yield final pure compound as a yellow oil (267 mg, 83%)

^{1}H NMR (400 MHz, Chloroform-*d*) δ 8.23 (d, *J* = 8.4 Hz, 2H), 7.72 (d, *J* = 8.4 Hz, 2H), 7.44 (t, *J* = 1.8 Hz, 1H), 7.14 (s, 2H), 7.09 (d, *J* = 8.9 Hz, 2H), 6.88 (d, *J* = 8.9 Hz, 1H), 5.52 (s, 2H), 4.87 (two singlets due to rotamers, 2H), 4.12 (two singlets due to rotamers, 2H), 1.33 (s, 18H), 1.10 (s, 21H), 1.01 (s, 9H), 0.23 (s, 6H).

^{13}C NMR (101 MHz, Chloroform-*d*) δ 169.90, 164.51, 153.45, 151.72, 144.74, 143.65, 139.86, 133.79, 131.25, 130.21, 127.36, 123.48, 122.77, 122.37, 122.26, 120.62, 101.97, 86.65, 54.79, 31., 25.69, 18.64, 18.18, 11.14, -4.43.

HRMS (ES+): calcd for $C_{50}H_{72}N_4O_4Si_2$ 871.4989 $[M+H]^+$, found 871.4981 $[M+H]^+$.

FT-IR (ATR): 2969, 2875, 1734, 1640, 1500, 1453, 1422 cm^{-1}

Retention time: 1.91 min (column 4)

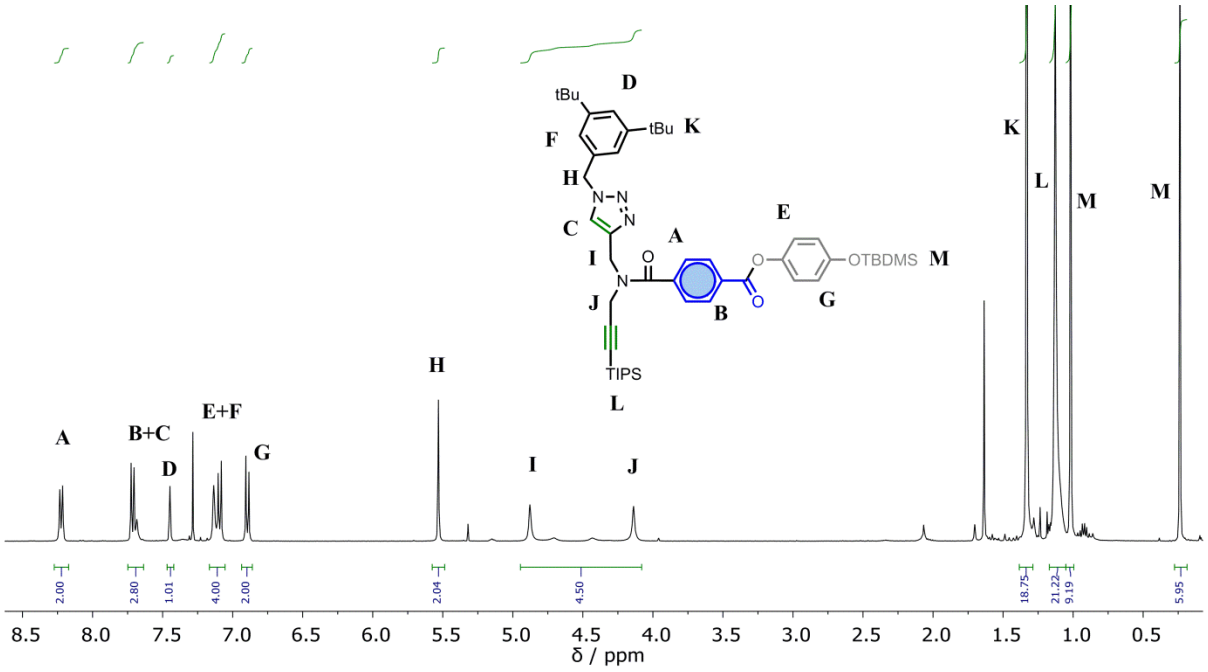
tBu
D
tBu K
F
H
N-N
N
C
I
A
E
O
OTBDMS M
N
O
O
J
B
G
TIPS
L
A
B+C
D
E+F
G
H
I
J
K
L
M
M
2.00
2.80
1.01
4.00
2.00
2.04
4.50
18.75
21.22
9.19
5.95
8.5 8.0 7.5 7.0 6.5 6.0 5.5 5.0 4.5 4.0 3.5 3.0 2.5 2.0 1.5 1.0 0.5
δ / ppm

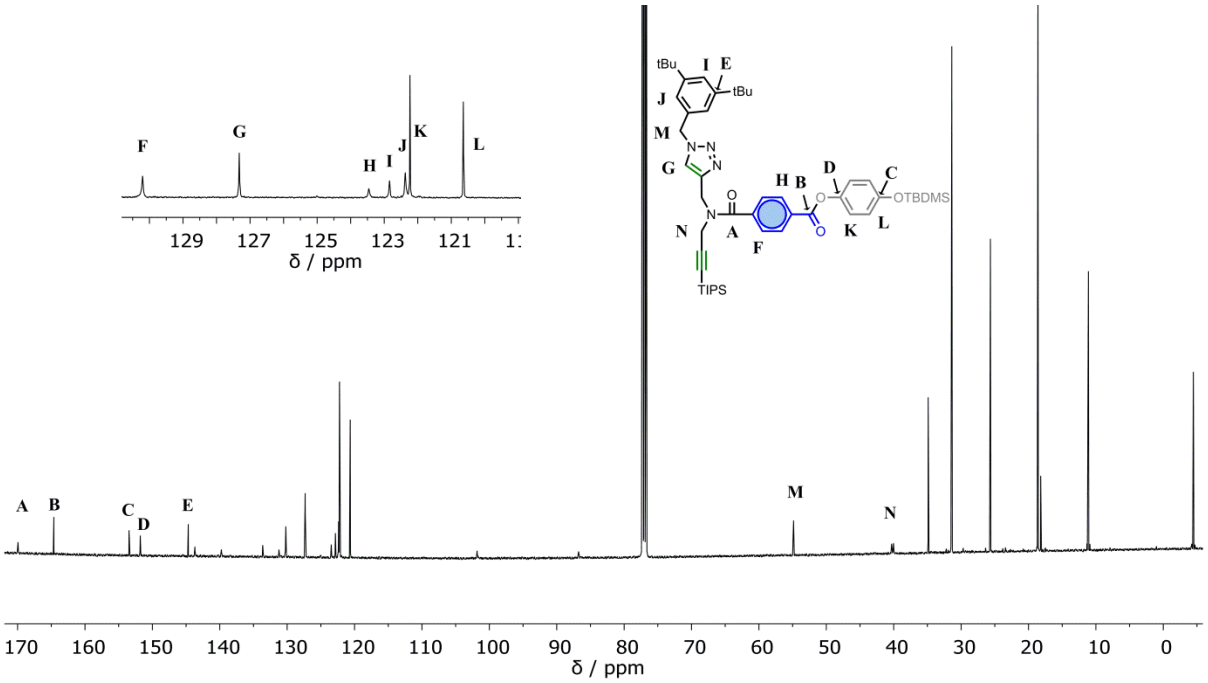
F
G
H
I
J
K
L
129 127 125 123 121
δ / ppm
tBu
I E
tBu
J
M
N-N
N
G
H B
D
C
O
OTBDMS
N
A
K
L
F
TIPS
A
B
C
D
E
M
N
170 160 150 140 130 120 110 100 90 80 70 60 50 40 30 20 10 0
δ / ppm

Synthesis of compound 4.3

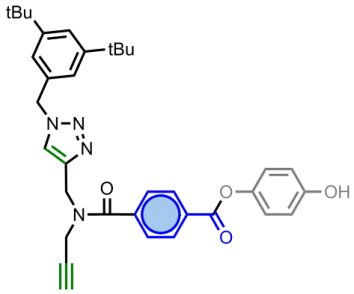

Compound **4.2** (200 mg, 0.23 mmol) was dissolved in THF (20 mL) and the solution cooled in ice. TBAF (1M in THF, 0.55 ml) was added dropwise and the reaction was left stirring at room temperature for 20 min before adding HCl 1M until pH reached 3. Water was added (20 mL), and the organic compound was reextracted with EtOAc (2 x 20 mL). This organic phase was washed with brine (2 x 20 mL), dried with $MgSO_4$, filtered and evaporated in vacuo before purifying it by column chromatography (PET 40-60/EtOAc, gradient of increasing polarity) to yield a yellow oil-ish solid (121 mg, 91%)

^{1}H NMR (400 MHz, *d*$_4$-methanol) δ 8.23 (s, 2H), 7.99 (d, *J* = 39.1 Hz, 1H), 7.68 (d, *J* = 8.2 Hz, 1H), 7.45 (s, 1H), 7.22 (s, 2H), 7.05 (d, *J* = 8.7 Hz, 2H), 6.85 (d, *J* = 8.7 Hz, 2H), 5.60 (s, 2H), 4.90 (two broad singlets due to rotamers, 2H), 4.05 (two broad singlets due to rotamers, 2H), 1.32 (s, 18H).

^{13}C NMR (100 MHz, *d*$_4$-methanol) δ 170.57, 164.87, 155.45, 151.73, 143.54, 135.01, 130.30, 127.04, 122.10, 121.96, 115.92, 77.88, 58.74, 54.54, 34.25, 30.39.

HRMS (ES+): calcd for $C_{35}H_{39}N_4O_4$ 579.2971 $[M+H]^+$, found 579.2976 $[M+H]^+$.

FT-IR (ATR): 3260, 2950, 2892, 1744, 1636, 1490, 1453, 1422 cm^{-1}

Retention time: 1.65 min

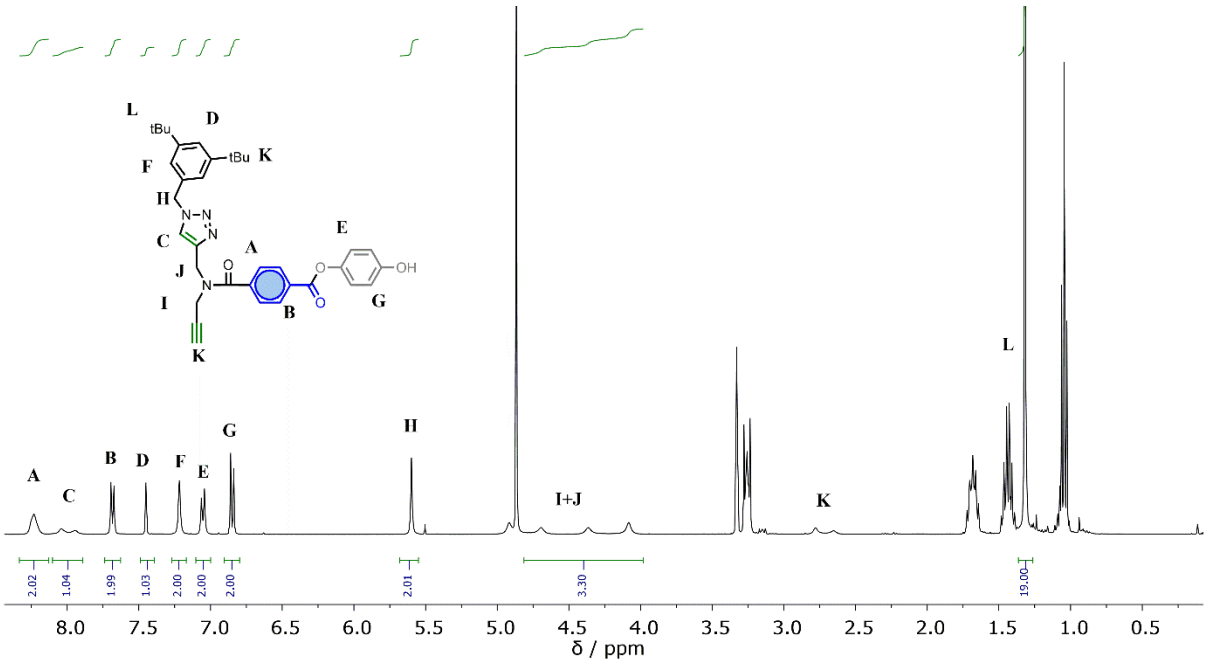
L
tBu
D
tBu
K
F
H
N
N
N
C
A
E
J
O
N
O
OH
I
B
G
K
A
C
B
D
F
E
G
H
I+J
K
L
2.02
1.04
1.99
1.03
2.00
2.00
2.00
2.01
3.30
19.00
8.0
7.5
7.0
6.5
6.0
5.5
5.0
4.5
4.0
3.5
3.0
2.5
2.0
1.5
1.0
0.5
δ / ppm

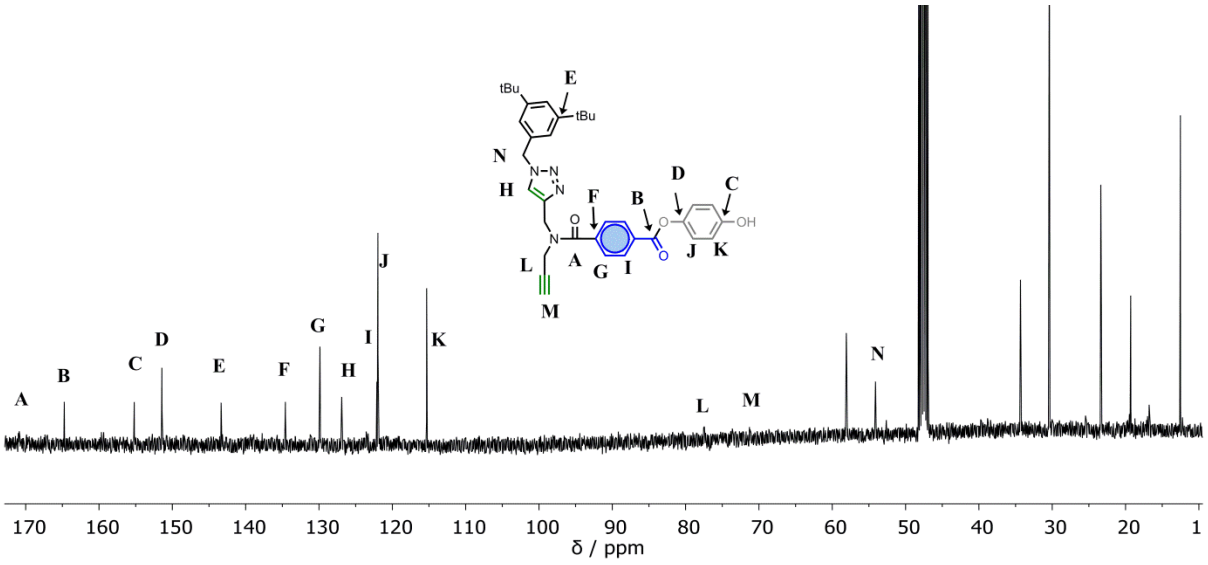
E
tBu
tBu
N
H
F
B
D
C
O
OH
N
A
G
I
J
K
L
M
A
B
C
D
E
F
G
H
I
J
K
L
M
N
170
160
150
140
130
120
110
100
90
80
70
60
50
40
30
20
1
δ / ppm

Synthesis of compound 4.4

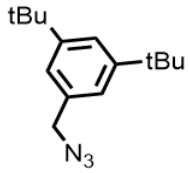

3,5-Ditertbutylbenzyl bromide (1.7 g, 5.9 mmol), and sodium azide (850 mg, 8.9 mmol) were dissolved in DMF (15 mL) and the solution was heated overnight at 100°C. After this time, the crude was diluted with EtOAc (30 mL), and washed with LiCl 5% (4 x 30 mL) and brine (2 x 20 mL). The organic phase was dried with $MgSO_4$, filtered and evaporated in vacuo before purifying it by column chromatography (PET 40-60/EtOAc, gradient of increasing polarity) to yield a clear oil (1.36 g, 94%)

^{1}H NMR (400 MHz, Chloroform-*d*) δ 7.43 (t, *J* = 1.8 Hz, 1H), 7.17 (d, *J* = 1.7 Hz, 2H), 4.37 (s, 2H), 1.37 (s, 18H).

^{13}C NMR (100 MHz, Chloroform-*d*) δ 151.40, 134.53, 122.39, 122.32, 55.52, 34.86, 31.43.

HRMS (ES+): calcd for $C_{15}H_{24}N_3$ 246.1970 $[M+H]^+$, found 246.1962 $[M+H]^+$.

FT-IR (ATR): 2962, 2870, 2097, 1608, 1469 cm^{-1}

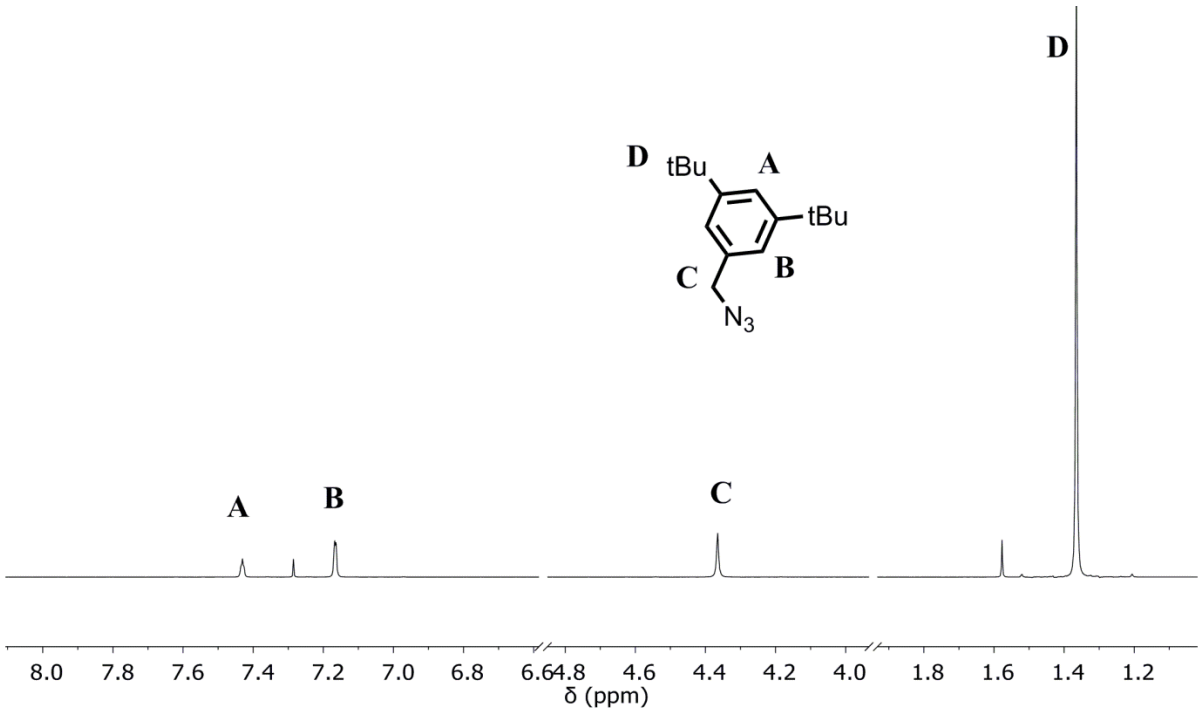
D
D
tBu
A
tBu
B
C
N3
A
B
C
D
8.0
7.8
7.6
7.4
7.2
7.0
6.8
6.6
4.8
4.6
4.4
4.2
4.0
1.8
1.6
1.4
1.2
δ (ppm)

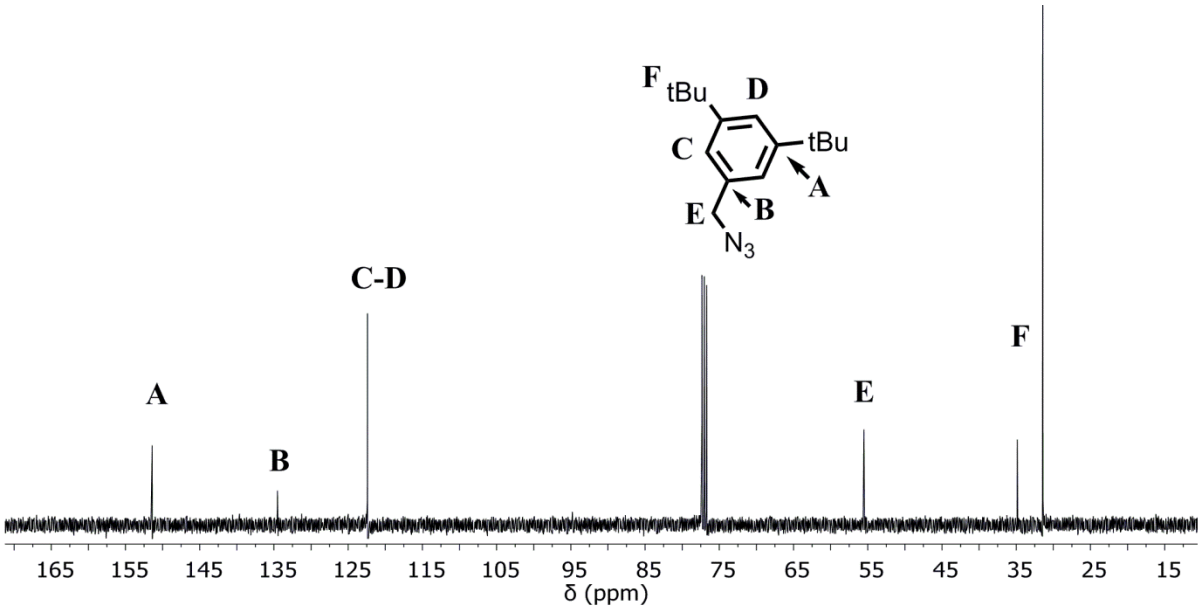
F
tBu
D
C
tBu
A
E
B
N3
C-D
A
B
E
F
165
155
145
135
125
115
105
95
85
75
65
55
45
35
25
15
δ (ppm)

Synthesis of compound 4.5

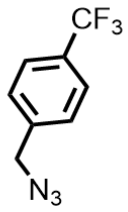

4-Trifluoromethylbenzyl bromide (1.5 g, 6.27 mmol), and sodium azide (902 mg, 9.4 mmol) were dissolved in DMF (15 mL) and the solution was heated overnight at 100°C. After this time, the crude was diluted with EtOAc (30 mL), and washed with LiCl 5% (4 x 30 mL) and brine (2x20 ml). The organic phase was dried with $MgSO_4$, filtered and evaporated in vacuo before purifying by column chromatography (PET 40-60/EtOAc, gradient of increasing polarity) to yield a clear oil (1.15 g, 91%)

^{1}H NMR (400 MHz, Chloroform-*d*) δ 7.68 (d, J = 8.0 Hz, 2H), 7.47 (d, J = 7.9 Hz, 2H), 4.45 (s, 2H).

^{13}C NMR (101 MHz, Chloroform-*d*) δ 139.39, 130.67, 128.26, 125.82 (q, J = 3.6 Hz), 54.10.

HRMS (ES+): calcd for $C_8H_6N_3F_3$ 201.0514 $[M+H]^+$, found 201.0515 $[M+H]^+$.

FT-IR (ATR): 2959, 2198, 1741, 1643 cm^{-1}

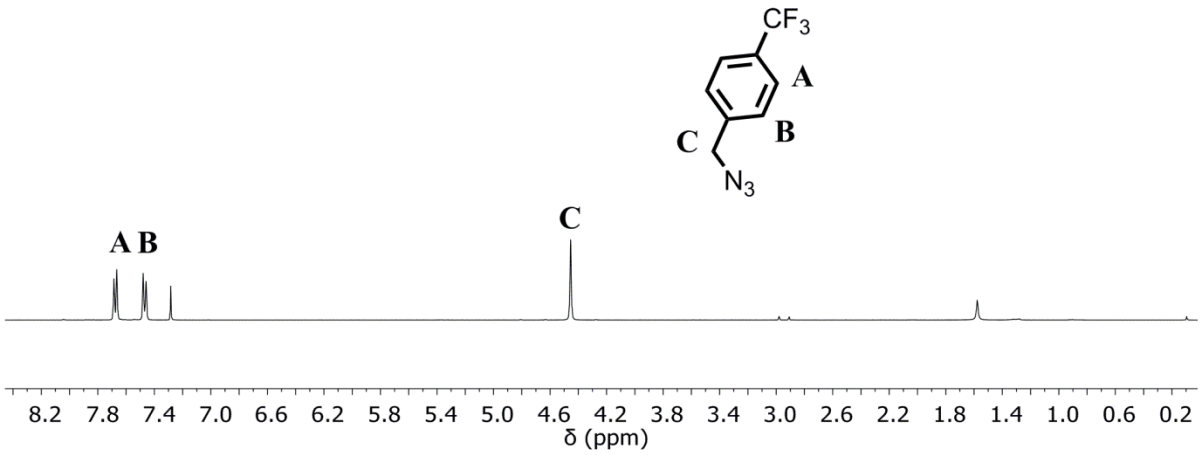
CF3
A
B
C
N3
A B
C
8.2 7.8 7.4 7.0 6.6 6.2 5.8 5.4 5.0 4.6 4.2 3.8 3.4 3.0 2.6 2.2 1.8 1.4 1.0 0.6 0.2
δ (ppm)

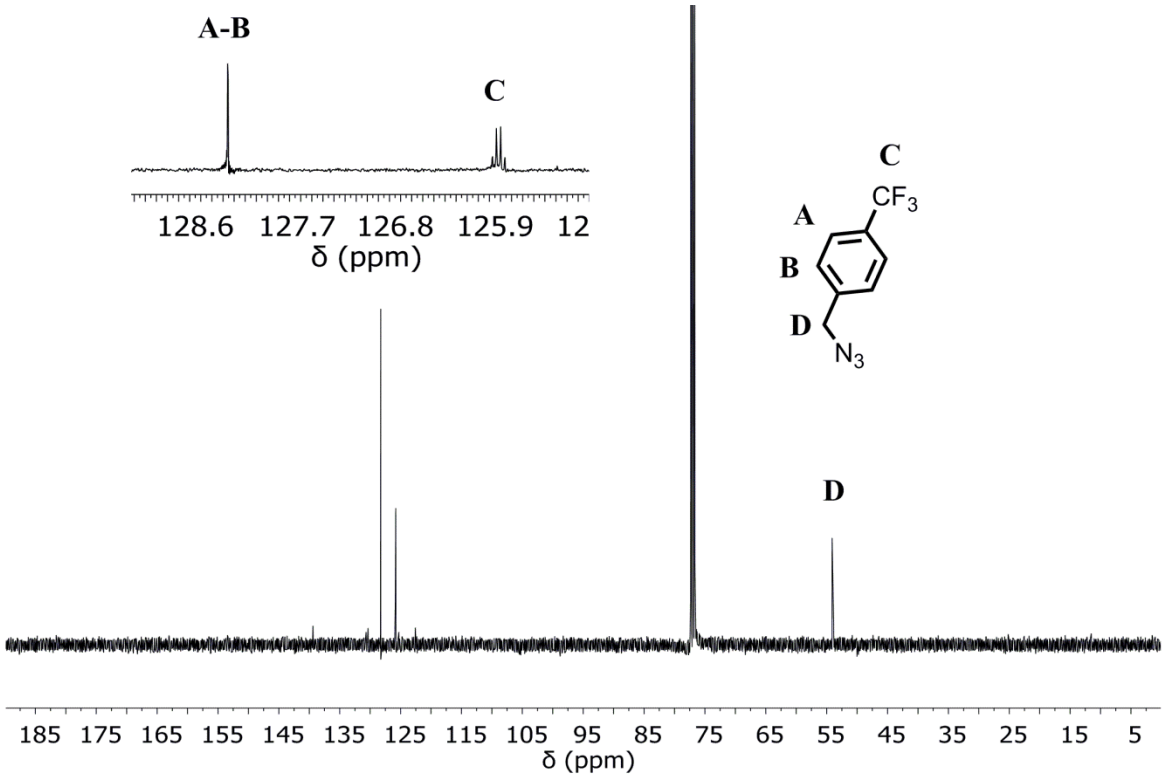
A-B
C
128.6 127.7 126.8 125.9 12
δ (ppm)
C
CF3
A
B
D
N3
D
185 175 165 155 145 135 125 115 105 95 85 75 65 55 45 35 25 15 5
δ (ppm)

Synthesis of compound 4.7

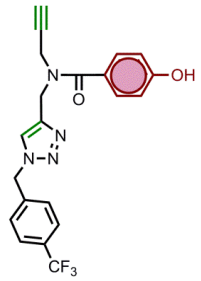

Compound **4.6** (500 mg, 2.4 mmol), $Cu(MeCN)_4PF_6$ (17.7 mg, 0.047 mmol) and TBTA (25.3 mg, 0.047 mmol) were dissolved in dry THF (400 mL) under a N_2 atmosphere. A solution of **5** (95 mg, 0.47 mmol) in dry THF (150 mL) was added dropwise and the solution was stirred overnight. The solution was concentrated in vacuo, redissolved in EtOAc and washed with brine (3 x 20 mL), dried with $MgSO_4$, filtered and evaporated. The crude oil was purified by column chromatography (PET 40-60/EtOAc, gradient of increasing polarity) to yield the pure compound as a yellow oil (83 mg, 43%).

^{1}H NMR (400 MHz, Chloroform-*d*) δ 7.66 (d, *J* = 8.0 Hz, 2H), 7.45 (d, *J* = 8.2 Hz, 2H), 7.41 (d, *J* = 8.0 Hz, 2H), 6.99 (s, 1H), 6.80 (d, *J* = 8.2 Hz, 2H), 5.60 (s, 2H), 4.82 (s, 2H), 4.21 (s, 2H), 2.35 (s, 1H).

^{13}C NMR (101 MHz, Chloroform-*d*) δ 158.37, 129.48, 128.29, 126.15, 115.45, 78.67, 53.58.

HRMS (ES+): calcd for $C_{21}H_{17}F_3N_4O_2$ 437.1201 $[M+Na]^+$, found 437.1199 $[M+Na]^+$.

FT-IR (ATR): 3290, 2921, 1614, 1507, 1457 cm^{-1}

Retention time: 1.09 min

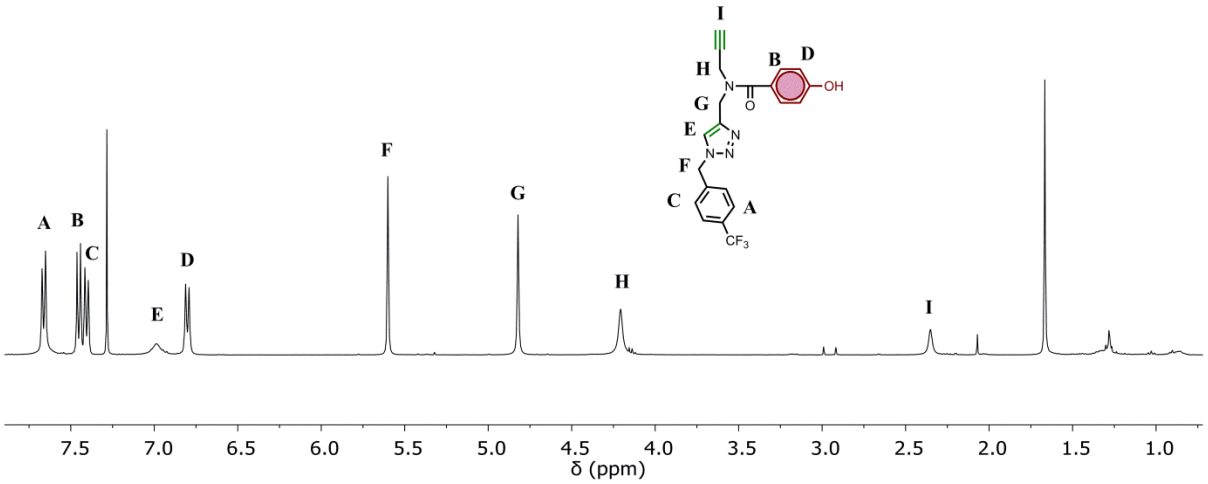
A
B
C
D
E
F
G
H
I
7.5
7.0
6.5
6.0
5.5
5.0
4.5
4.0
3.5
3.0
2.5
2.0
1.5
1.0
δ (ppm)
OH
CF3

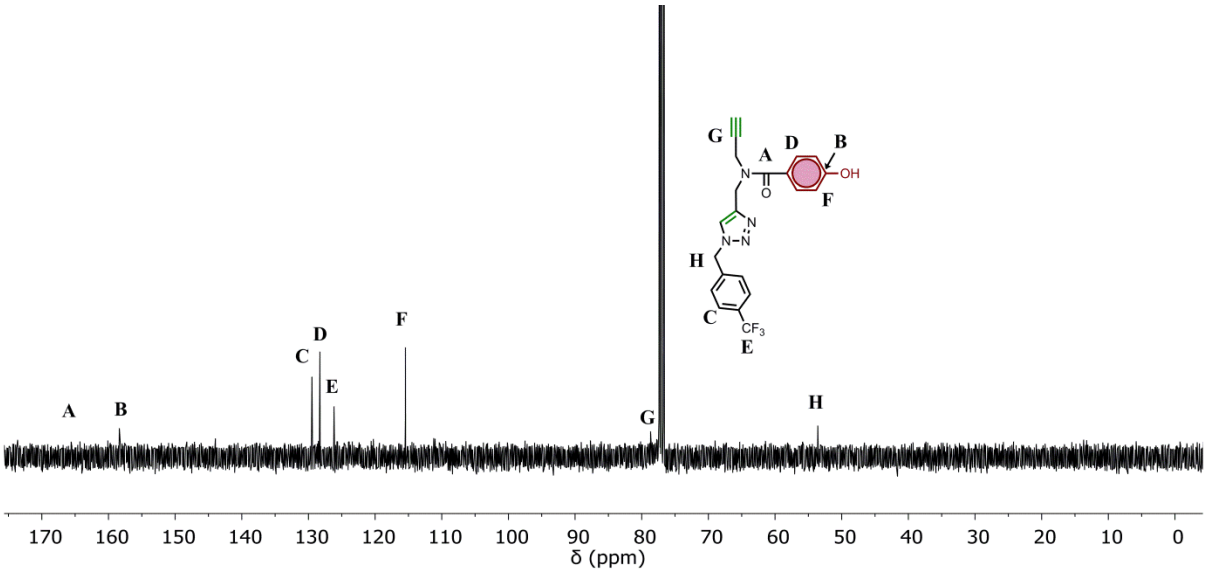
A
B
C
D
E
F
G
H
170
160
150
140
130
120
110
100
90
80
70
60
50
40
30
20
10
0
δ (ppm)
OH
CF3

Synthesis of compound 4.8

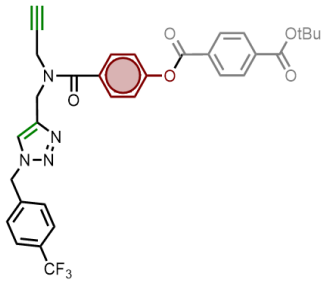

Compound **4.7** (70 mg, 0.17 mmol)**,** 4-(tert-butoxycarbonyl) benzoic acid (41 mg, 0.18 mmol), EDC (42 mg, 0.22 mmol) and DMAP (10 mg, 0.08 mmol) were dissolved in dry DCM (15 mL) and stirred under N_2 overnight. The crude solution was washed with HCl 1M (2 x 20 mL) and brine (2 x 20 mL). The organic phase was dried with $MgSO_4$, concentrated in vacuo and purified via column chromatography (PET 40-60/EtOAc, gradient of increasing polarity) to yield final pure compound as a pale yellow solid (90 mg, 86%)

^{1}H NMR (400 MHz, $CDCl_3$) δ 8.24 (d, *J* = 8.3 Hz, 2H), 8.13 (d, *J* = 8.4 Hz, 2H), 7.70 – 7.64 (m, 5H), 7.41 (d, *J* = 8.0 Hz, 2H), 7.31 (d, *J* = 8.1 Hz, 2H), 5.61 (s, 2H), 4.78 (s, 2H), 4.20 (s, 2H), 2.38 (s, 1H), 1.65 (s, 9H).

^{13}C NMR (101 MHz, $CDCl_3$) δ 170.43, 164.68, 164.17, 152.29, 144.34, 138.4, 136.67, 132.34, 131.28, 130.96, 130.01, 129.59, 128.88, 128.27, 126.11, 125.09, 123.87, 121.86, 82.01, 78.53, 73.38, 53.55, 39.58, 28.16.

HRMS (ES+): calcd for $C_{33}H_{29}N_4O_5F_3$ 619.2168 $[M+H]^+$, found 619.2167 $[M+H]^+$.

FT-IR (ATR): 3250, 2986, 2930, 2860, 1750, 1719, 1640, 1453, 1422 cm^{-1}

Retention time: 1.66 min

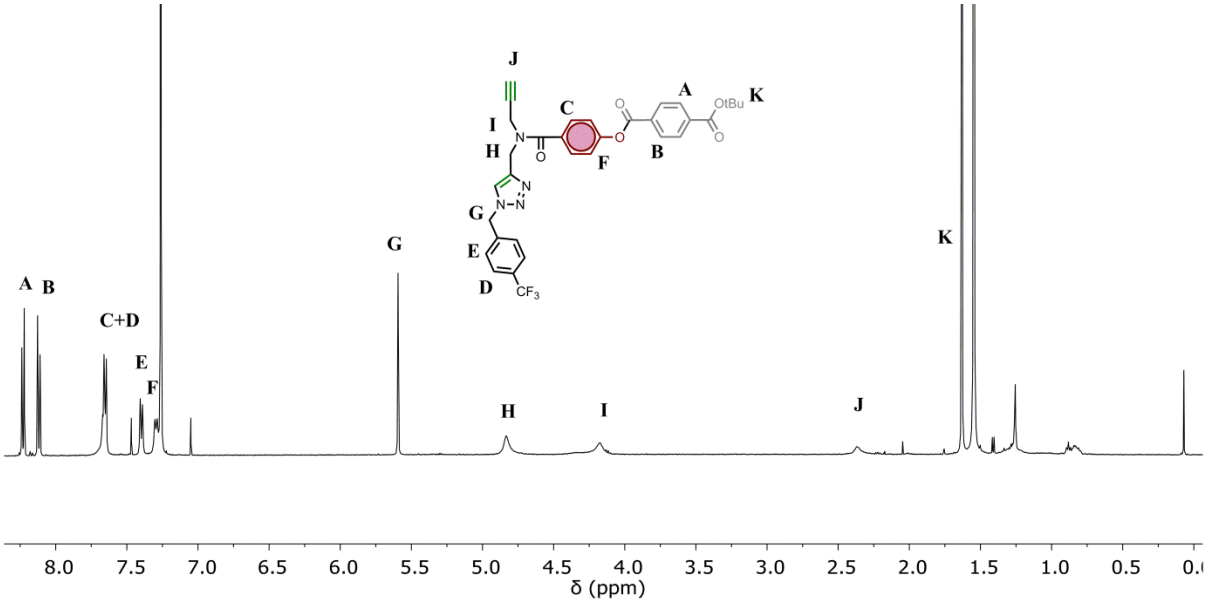
A B
C+D
E
F
G
H
I
J
K
8.0 7.5 7.0 6.5 6.0 5.5 5.0 4.5 4.0 3.5 3.0 2.5 2.0 1.5 1.0 0.5
δ (ppm)

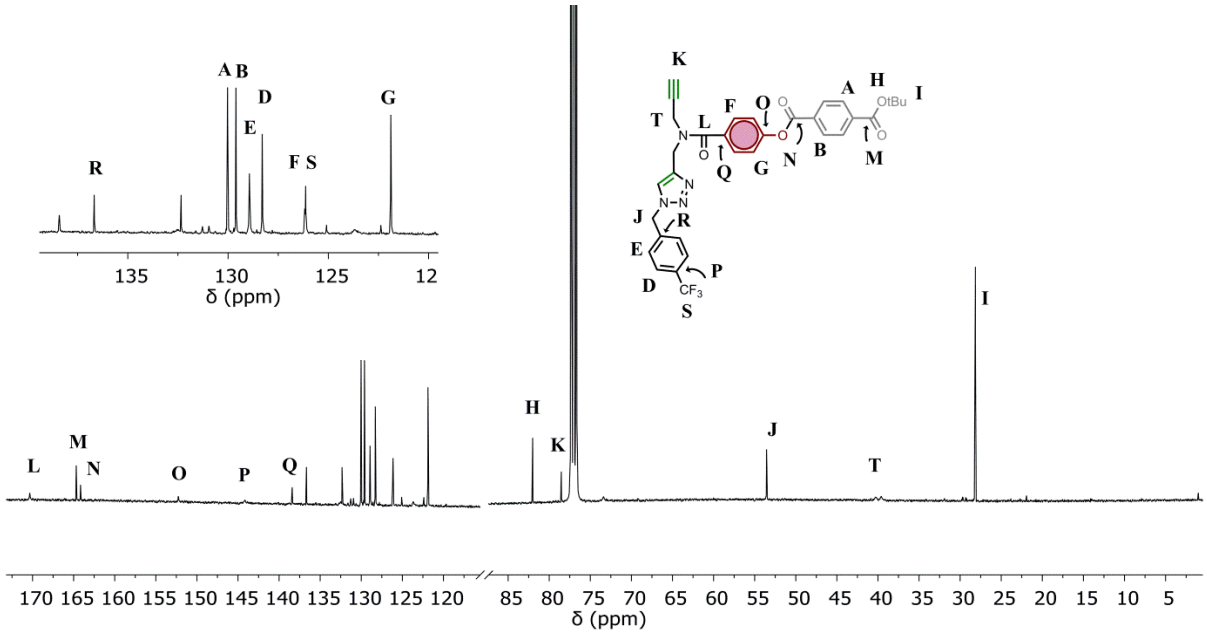
A B
D
E
F S
G
R
135 130 125 12
δ (ppm)
L
M
N
O
P
Q
H
K
J
T
I
170 165 160 155 150 145 140 135 130 125 120 85 80 75 70 65 60 55 50 45 40 35 30 25 20 15 10 5
δ (ppm)

Synthesis of compound 4.9

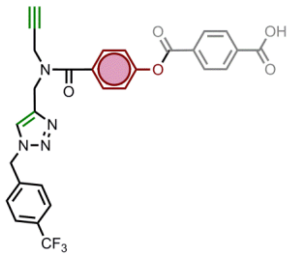

Compound **4.8** (60 mg, 0.097 mmol) was dissolved in DCM (10 mL) and TFA (2 mL) was added dropwise and the mixture was left stirring overnight. The solution was washed with water (2 x 20 mL) and brine (2 x 20 mL), dried with $MgSO_4$, filtered and evaporated to produce the final compound as an orange dense oil (53 mg, quantitative yield).

^{1}H NMR (400 MHz, d_4-methanol) δ 8.28 (d, *J* = 8.4 Hz, 2H), 8.20 (d, *J* = 8.4 Hz, 2H), 8.06 (broad s, 1H), 7.69 (m, 4H), 7.51 (d, *J* = 8.0 Hz, 2H), 7.38 (d, *J* = 7.8 Hz, 2H), 5.73 (s, 2H), 4.90 (s, 2H), 4.13 (s, 2H), 2.85 (s, 1H).

^{13}C NMR (100 MHz, d_4-methanol) δ 171.32, 167.14, 164.09, 152.41, 139.83, 135.47, 132.74, 130.36, 130.04, 129.75, 129.59, 128.35, 128.24, 125.51, 125.47, 121.84, 77.78, 52.77.

HRMS (ES+): calcd for $C_{29}H_{22}N_4O_5F_3$ 563.1542 $[M+H]^+$, found 563.1541 $[M+H]^+$.

FT-IR (ATR): 3250, 2903, 2812, 1750, 1736, 1632, 1453, 1422 cm^{-1}

Retention time: 1.32 min

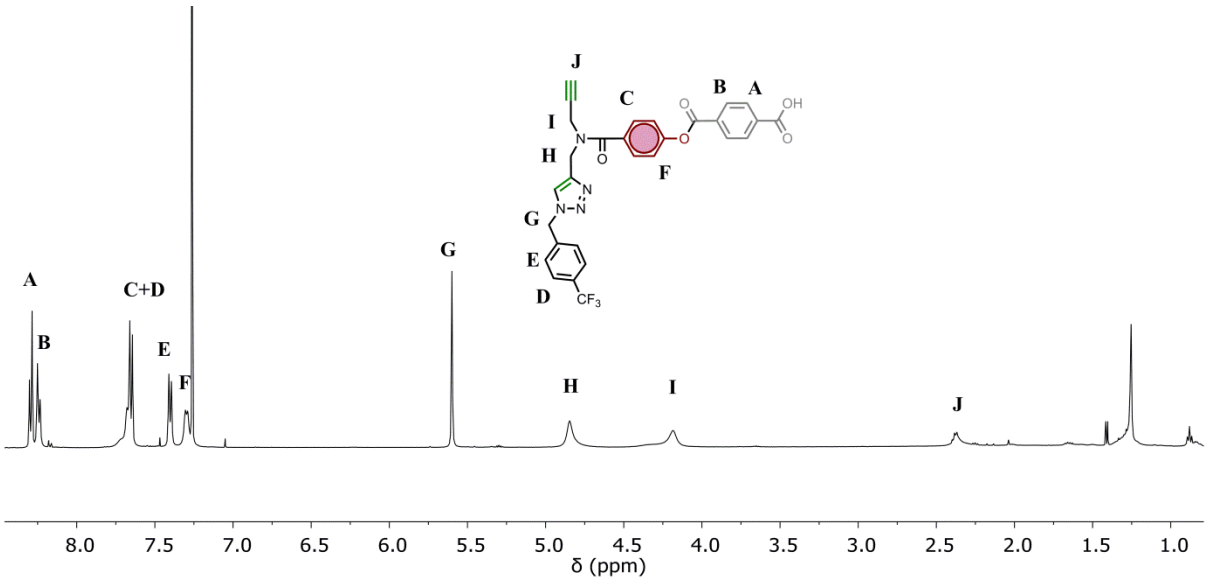
A
B
C+D
E
F
G
H
I
J
δ (ppm)

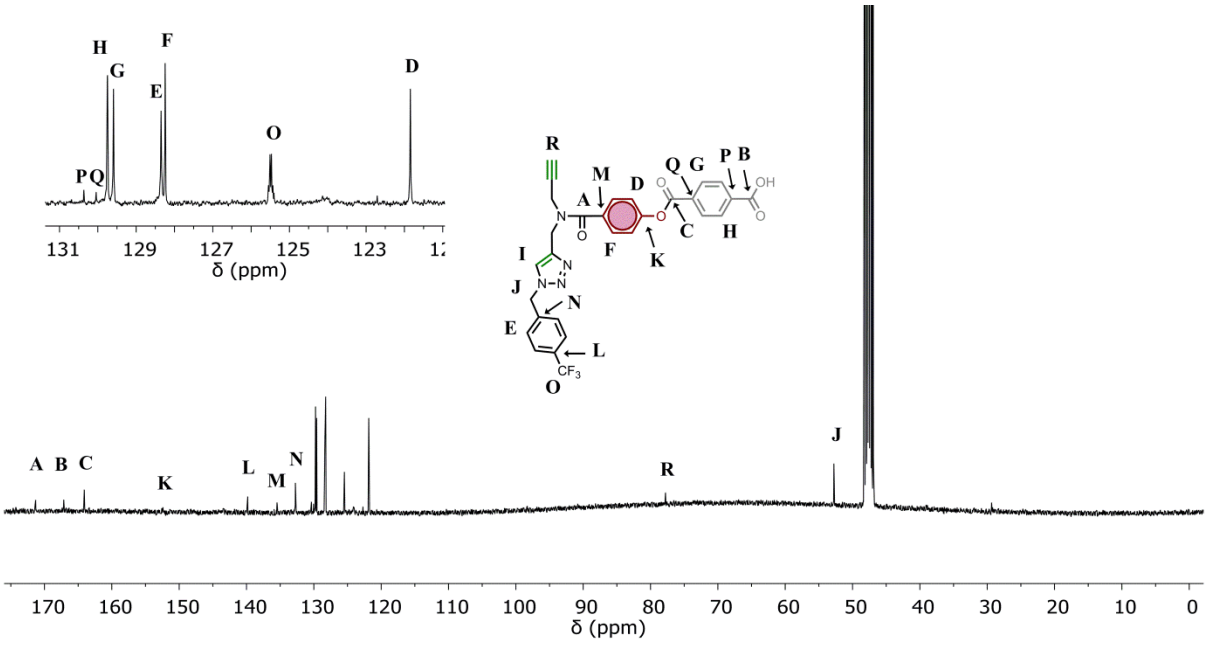
A B C
K
L
M
N
R
J
δ (ppm)

Synthesis of compound 4.10

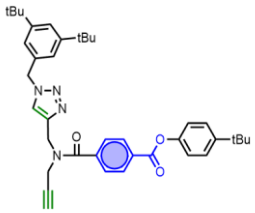

Compound **4.1** (48 mg, 0.10 mmol)**,** 4-tert-butyl phenol (17 mg, 0.11 mmol), EDC (25 mg, 0.13 mmol) and DMAP (4 mg, 0.03 mmol) were dissolved in dry DCM (15 mL) and stirred under N_2 overnight. The crude was washed with HCl 1M (2 x 20 mL), and brine (2 x 20 mL). The organic phase was dried with $MgSO_4$, concentrated in vacuo and purified by column chromatography (PET 40-60/EtOAc, gradient of increasing polarity) to yield pure compound as a yellow sticky solid (54 mg, 87%)

^{1}H NMR (500 MHz, Chloroform-*d*) δ 8.24 (d, *J* = 7.9 Hz, 2H), 7.68 – 7.62 (m, 3H), 7.47 – 7.41 (m, 3H), 7.15 – 7.08 (m, 4H), 5.52 (s, 2H), 4.87 (2 singlets due to two rotamers, 2H), 4.09 (2 singlets due to two rotamers, 2H), 2.34 (s, 1H), 1.35 (s, 9H), 1.31 (s, 18H).

^{13}C NMR (126 MHz, Chloroform-*d*) δ 169.91, 164.51, 151.82, 148.91, 148.37, 143.51, 139.65, 133.63, 130.36, 127.23, 126.44, 123.44, 122.38, 120.85, 78.28, 73.42, 54.87, 39.97, 39.20, 34.90, 34.52, 31.42, 31.38.

HRMS (ES+): calcd for $C_{39}H_{46}N_4O_3$ 641.3467 $[M+Na]^+$, found 641.3446 $[M+Na]^+$.

FT-IR (ATR): 3234, 2952, 2830, 1730, 1640 cm^{-1}

Retention time: 2.04 min

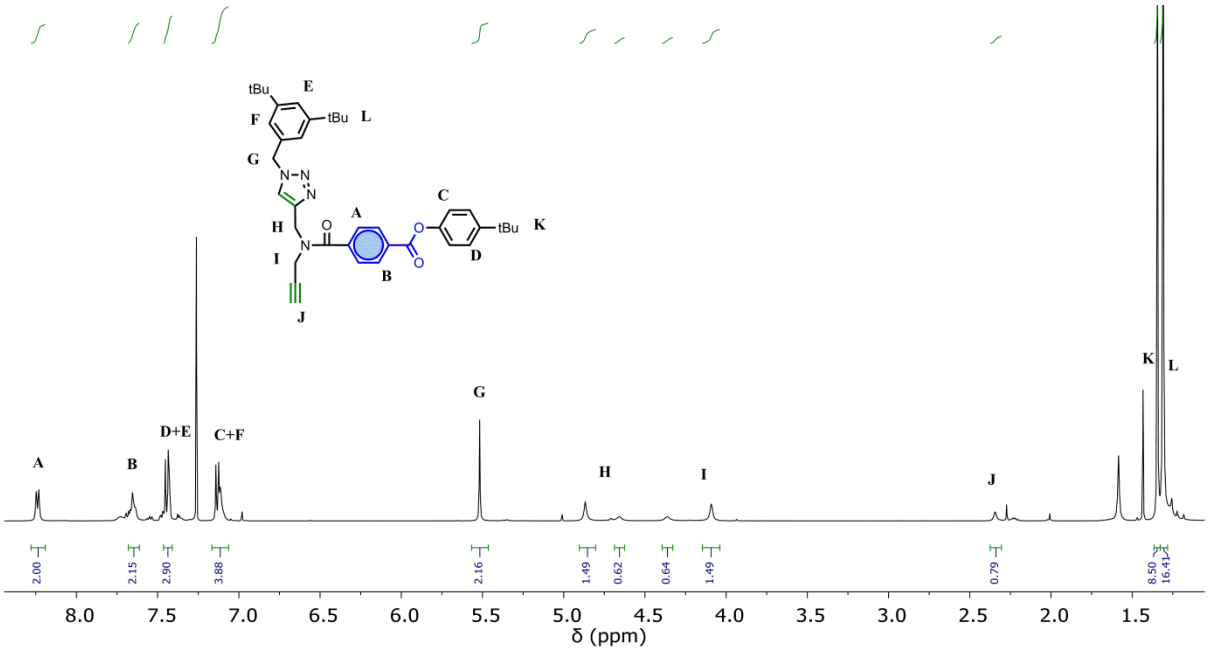
A
B
D+E
C+F
G
H
I
J
K
L
2.00
2.15
2.90
3.88
2.16
1.49
0.62
0.64
1.49
0.79
8.50
16.41
8.0
7.5
7.0
6.5
6.0
5.5
5.0
4.5
4.0
3.5
3.0
2.5
2.0
1.5
δ (ppm)

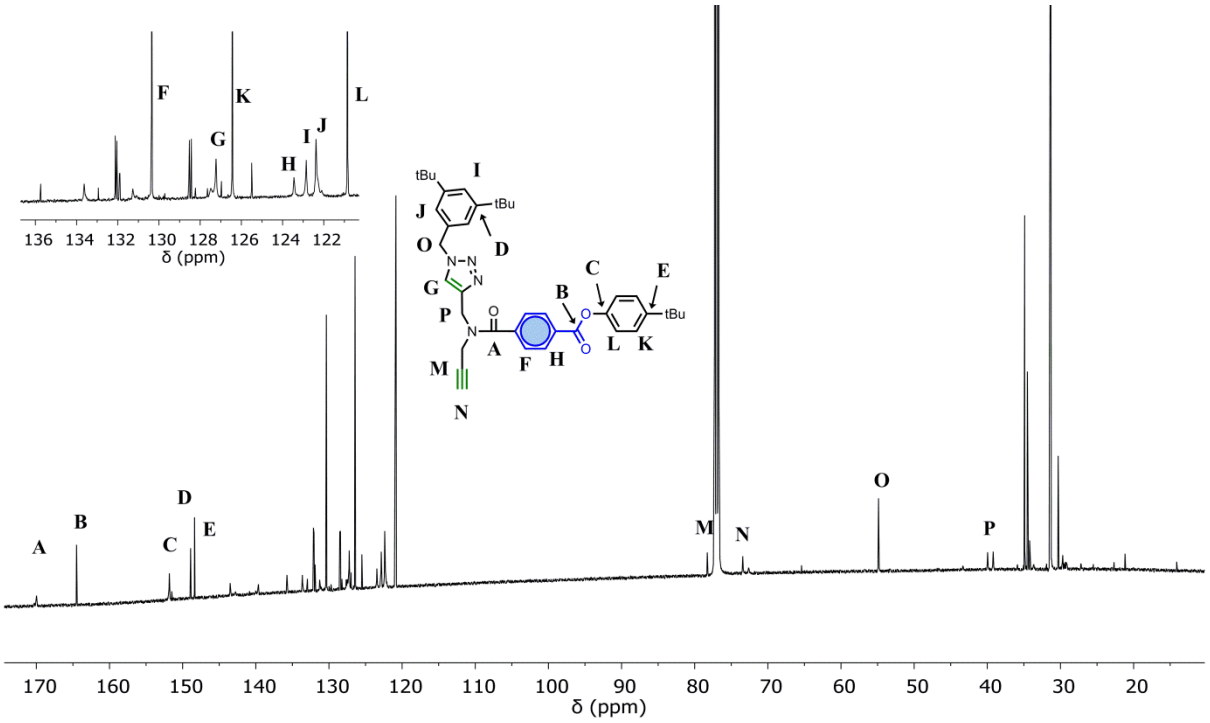
F
K
G
I
J
H
L
136 134 132 130 128 126 124 122
δ (ppm)
A
B
C
D
E
M
N
O
P
170 160 150 140 130 120 110 100 90 80 70 60 50 40 30 20
δ (ppm)

Synthesis of compound 4.14

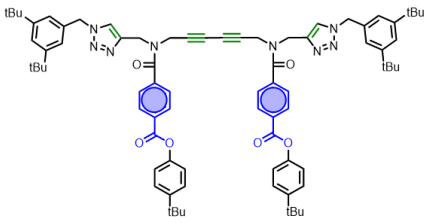

Compound **4.10** (45 mg, 0.073 mmol), $Pd(PPh_3)_2Cl_2$ (5.1 mg, 0.007 mmol), PPh_3 (5.5 mg, 0.021 mmol), and CuI (1.4 mg, 0.007 mmol) were dissolved in acetonitrile (10 mL). Et_3N (100 µL, 0.73 mmol) was added and the reaction was stirred overnight. After this time the reaction was neutralized with HCl 1M, diluted with water, and the product reextracted with EtOAc. The organic solution was washed with brine (2 x 20 mL), dried with $MgSO_4$, filtered and dried in vacuo. The crude was purified via column chromatography (PET 40-60/EtOAc, gradient of increasing polarity) to yield the pure compound as a clear orange oil (38 mg, 84%)

^{1}H NMR (400 MHz, Chloroform-*d*) δ 8.28 (s, 4H), 7.75 – 7.63 (m, 6H), 7.49 – 7.42 (m, 6H), 7.20 – 7.12 (m, 28H), 5.54 (s, 4H), 4.89 (s, 4H), 4.25 (s, 4H), 1.37 (s, 18H), 1.33 (s, 36H).

HRMS (ES+): calcd for $C_{78}H_{90}N_8O_6$ 1257.6881 $[M+Na]^+$, found 1257.6832 $[M+Na]^+$.

FT-IR (ATR): 3224, 2950, 2935, 2830, 1728, 1640 cm^{-1}

Retention time: 2.59 min

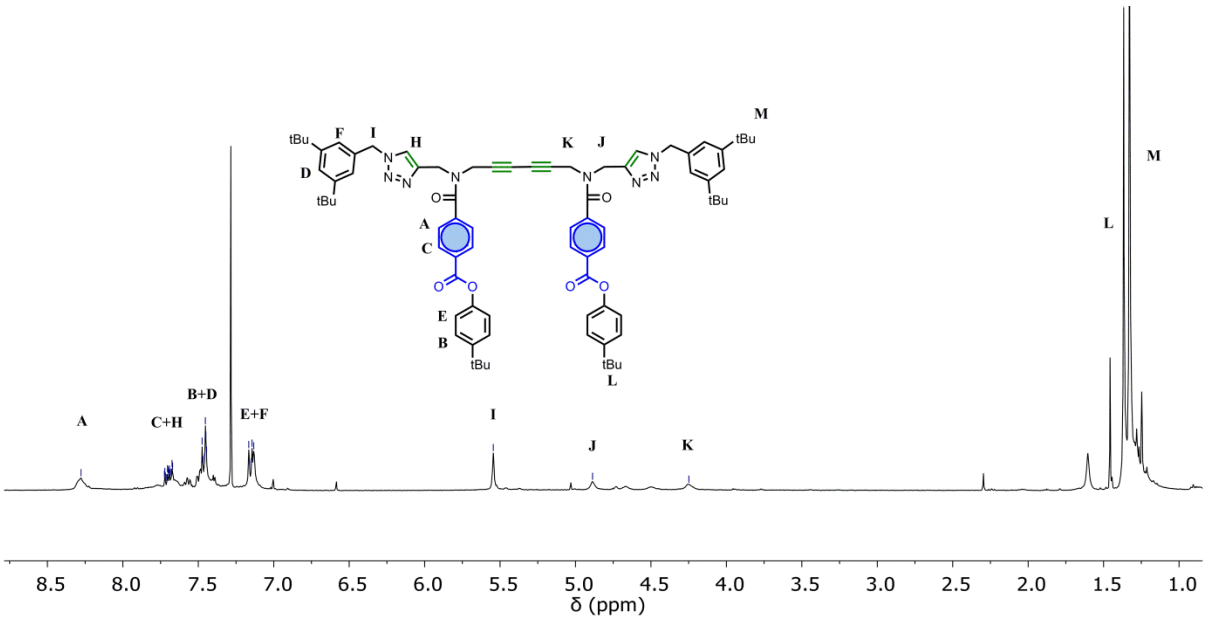
A
C+H
B+D
E+F
I
J
K
L
M
8.5
8.0
7.5
7.0
6.5
6.0
5.5
5.0
4.5
4.0
3.5
3.0
2.5
2.0
1.5
1.0
δ (ppm)

Synthesis of compound 4.15

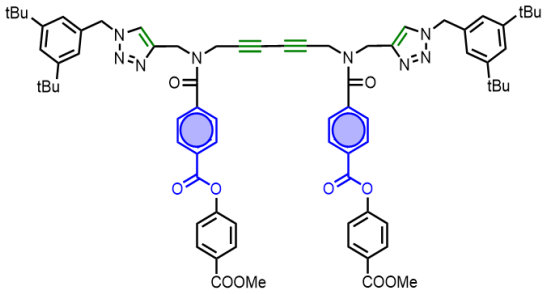

Compound **4.12** (70 mg, 0.11 mmol), $Pd(PPh_3)_2Cl_2$ (8 mg, 0.011 mmol), PPh_3 (9 mg, 0.033 mmol), and CuI (2 mg, 0.011 mmol) were dissolved in acetonitrile (10 mL). Et_3N (150 µL, 1.1 mmol) was added and the reaction was stirred overnight. After this time the reaction was neutralized with HCl 1M, diluted with water, and the product reextracted with EtOAc. The organic solution was washed with brine (2 x 20 mL), dried with $MgSO_4$, filtered and dried in vacuo. The crude was purified via column chromatography (PET 40-60/EtOAc, gradient of increasing polarity) to yield the pure compound as a clear orange oil (48 mg, 70%)

^{1}H NMR (500 MHz, Chloroform-*d*) δ 8.25 (d, *J* = 20.9 Hz, 4H), 8.17 – 8.08 (m, 4H), 7.77 (s, 2H), 7.65 – 7.61 (m, 4H), 7.43 (d, *J* = 1.8 Hz, 2H), 7.34 – 7.29 (m, 4H), 7.11 (s, 4H), 5.52 (s, 4H), 4.86 (two singlets due to rotamers, 2H), 4.23 (two singlets due to rotamers, 2H), 3.94 (s, 3H), 1.30 (s, 36H).

^{13}C NMR (126 MHz, Chloroform-*d*) δ 170.16, 166.25, 163.76, 154.31, 151.85, 143.23, 139.73, 133.52, 131.27, 130.56, 127.37, 123.45, 122.91, 122.38, 121.63, 54.91, 52.25, 39.93, 34.90, 31.38.

HRMS (ES+): calcd for $C_{74}H_{78}N_8O_{10}$ 1239.5919 $[M+H]^+$, found 1239.5922$[M+H]^+$.

FT-IR (ATR): 3050, 2968, 1747, 1722, 1643, 1602, 1510 cm^{-1}

Retention time: 2.21 min

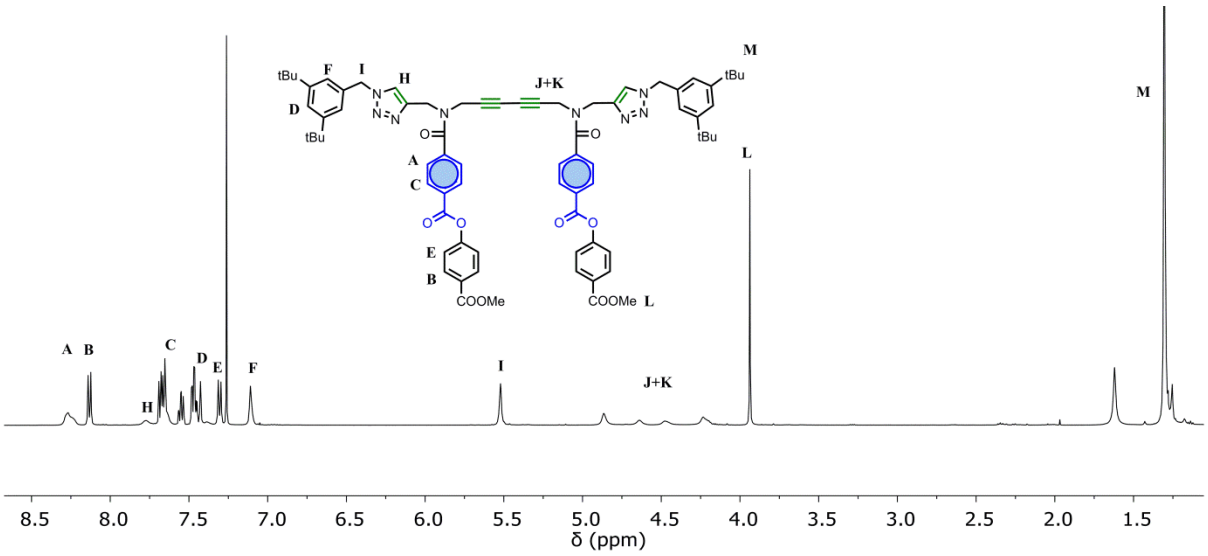
A B
C
D E
F
H
I
J+K
L
M
COOMe
δ (ppm)

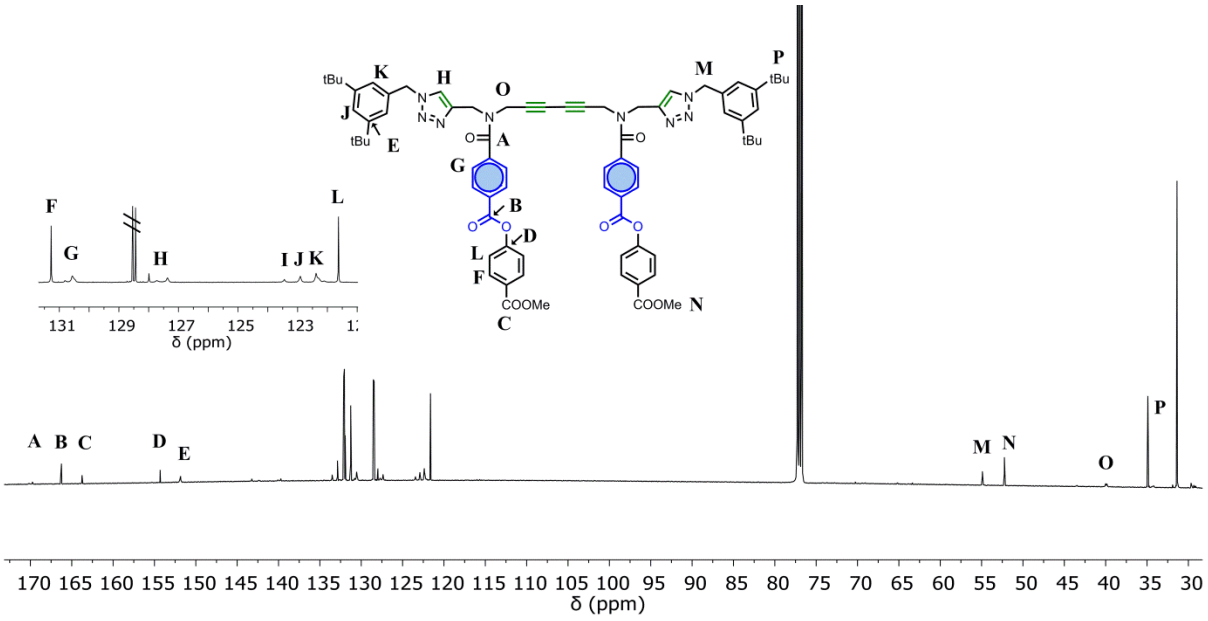
F
G
H
I J K
L
δ (ppm)
A B C
D E
M N
O
P
δ (ppm)

Synthesis of compound 4.16

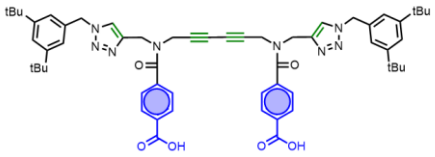

Compound **4.15** (20 mg, 0.016 mmol) was dissolved in THF (5 mL) and LiOH (6.7 mg, 0.16 mmol) dissolved in water (1 mL) was added dropwise. The reaction was followed by LCMS and quenched with HCl 1M when no starting material could be seen (45-60 min). The solution was diluted with water (10 mL), extracted with EtOAc (2x15 ml) and the organic phase washed with brine (2x20 ml), dried with $MgSO_4$, and evaporated under vacuo. The crude was purified via column chromatography (PET 40-60/EtOAc, gradient of increasing polarity) to yield final pure compound as a yellow sticky solid (8.5 mg, 56%)

^{1}H NMR (500 MHz, Chloroform-*d*) δ 8.13 (s, 4H), 7.68 (s, 2H), 7.55 (s, 4H), 7.41 (s, 2H), 7.11 (s, 4H), 5.51 (s, 4H), 4.83 (s, 4H), 4.16 (s, 4H), 1.29 (s, 36H).

^{13}C NMR (126 MHz, Chloroform-*d*) δ 151.82, 143.27, 133.58, 130.40, 127.00, 123.61, 122.87, 122.42, 54.90, 39.92, 34.89, 31.39.

HRMS (ES+): calcd for $C_{58}H_{67}N_8O_6$ 971.5184 $[M+H]^+$, found 971.5178 $[M+H]^+$.

FT-IR (ATR): 2965, 1703, 1645, 1570, 1463 cm^{-1}

Retention time: 1.92 min

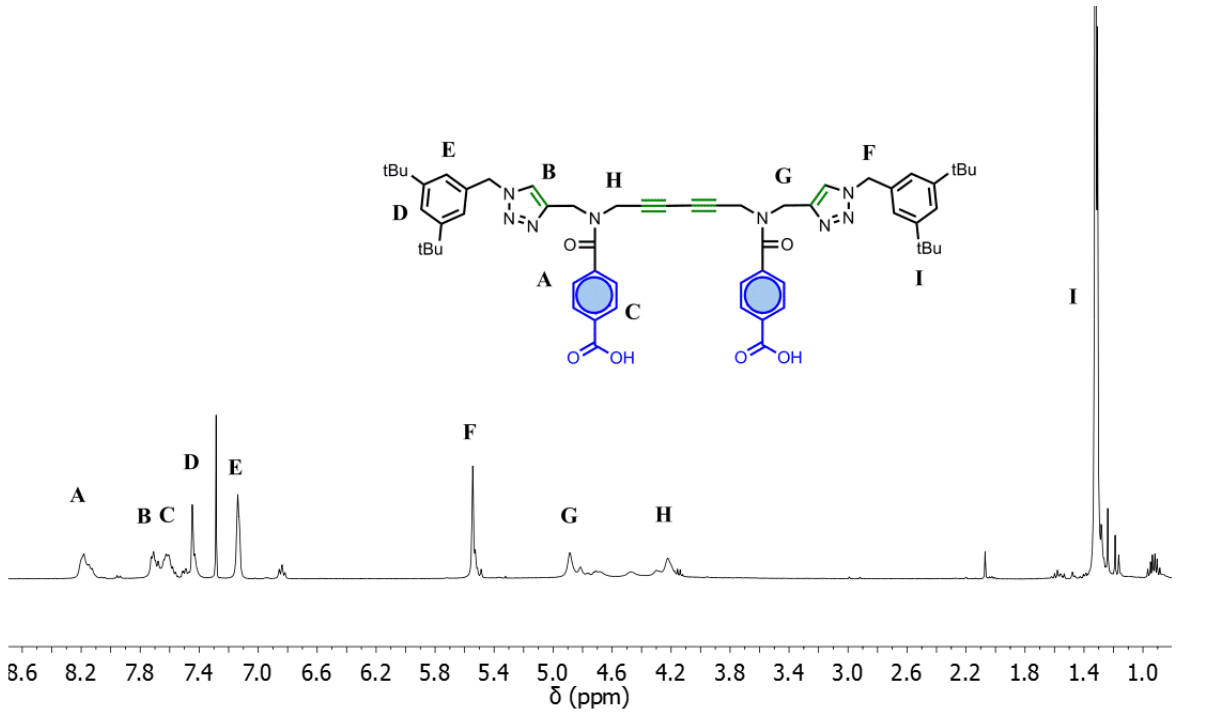
E
tBu
D
tBu
B
H
G
F
tBu
tBu
A
C
I
I
O
OH
F
D
E
A
B C
G
H
8.6 8.2 7.8 7.4 7.0 6.6 6.2 5.8 5.4 5.0 4.6 4.2 3.8 3.4 3.0 2.6 2.2 1.8 1.4 1.0
δ (ppm)

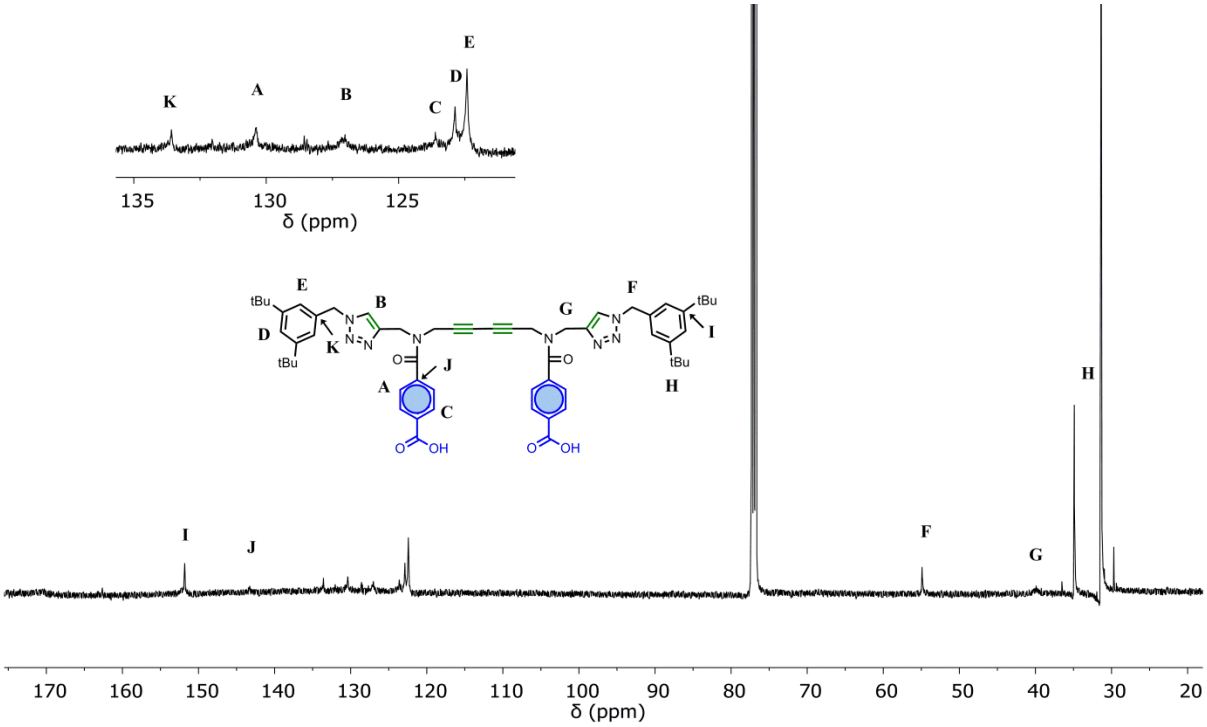
E
D
K
A
B
C
135
130
125
δ (ppm)
E
tBu
D
tBu
B
K
F
G
tBu
I
A
J
C
H
I
J
F
G
H
170 160 150 140 130 120 110 100 90 80 70 60 50 40 30 20
δ (ppm)

Synthesis of compound 4.17

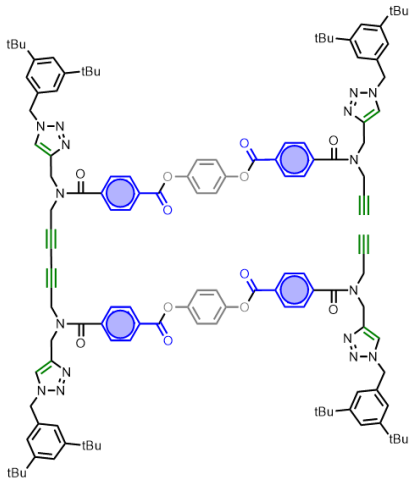

Compound **4.16** (6 mg, 0.006 mmol)**,** compound **4.3** (8.5 mg, 0.014 mmol), EDC (3 mg, 0.016 mmol) and DMAP (2 mg, 0.16 mmol) were dissolved in dry DCM (5 mL) and stirred under N_2 until no starting dimer could be seen by LCMS. The crude solution was washed with HCl 1M (2 x 20 mL) and brine (2 x 20 mL). The organic phase was dried with $MgSO_4$, concentrated in vacuo and purified via column chromatography (PET 40-60/EtOAc, gradient of increasing polarity) to yield final pure compound as a yellow oil (9 mg, 72%)

^{1}H NMR (500 MHz, Chloroform-*d*) δ 8.25 (d, *J* = 8.0 Hz, 8H), 7.76 (s, 4H), 7.66 (s, 8H), 7.43 (d, *J* = 2.0 Hz, 4H), 7.30 (s, 4H), 7.12 (s, 8H), 5.52 (d, *J* = 2.2 Hz, 8H), 4.76 (m, 4H), 4.17 (m, 4H), 2.35 (s, 2H), 1.31 (s, 72H).

^{13}C NMR (126 MHz, Chloroform-*d*) δ 164.19, 151.83, 148.33, 130.39, 127.32, 123.45, 122.88, 122.64, 122.39, 78.27, 73.48, 54.92, 40.01, 34.92, 31.40.

HRMS (ES+): calcd for $C_{128}H_{138}N_{16}O_{12}$ 2092.0758 $[M+H]^+$, found 1068.5204 $[M+2Na^+]^{2+}$.

FT-IR (ATR): 3265, 2936, 2859, 1736, 1640, 1593 cm^{-1}

Retention time: 2.41 min

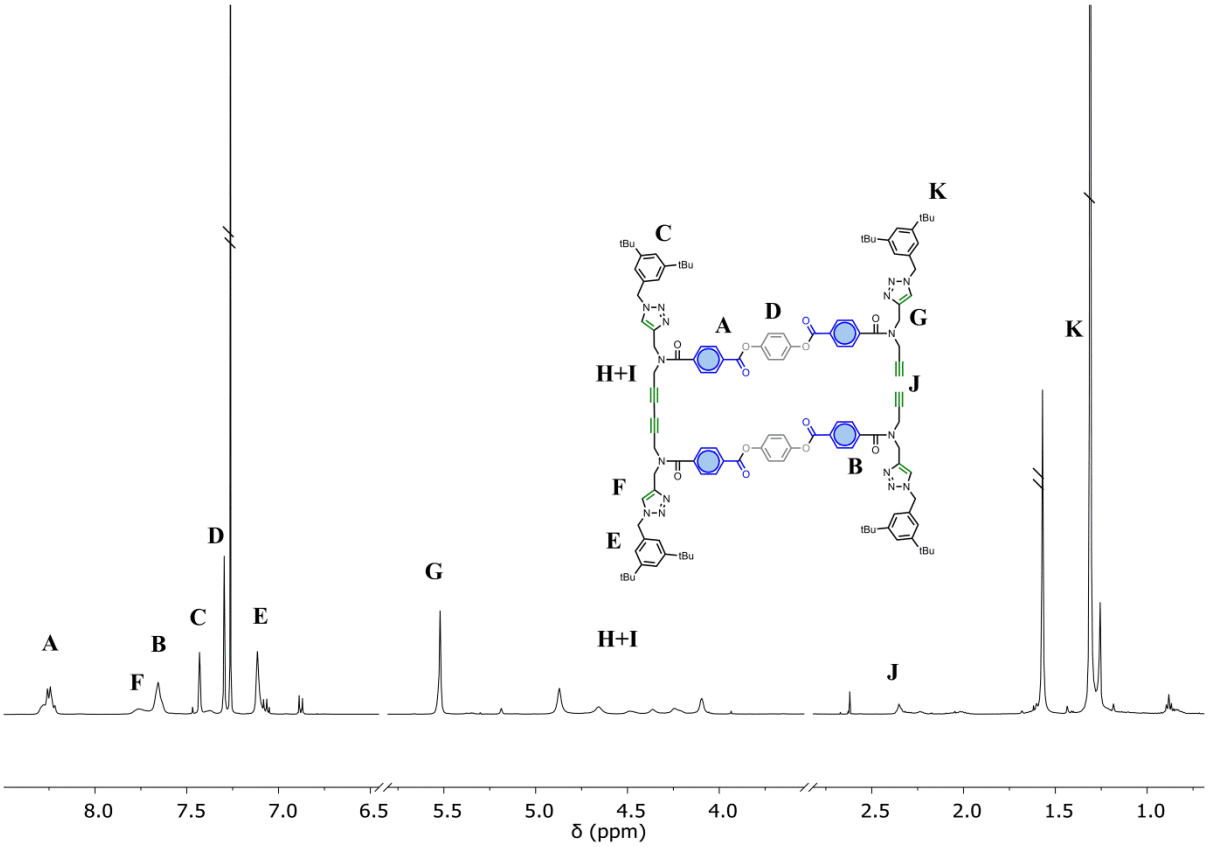
A
B
F
C
D
E
G
H+I
J
K
8.0
7.5
7.0
6.5
5.5
5.0
4.5
4.0
2.5
2.0
1.5
1.0
δ (ppm)

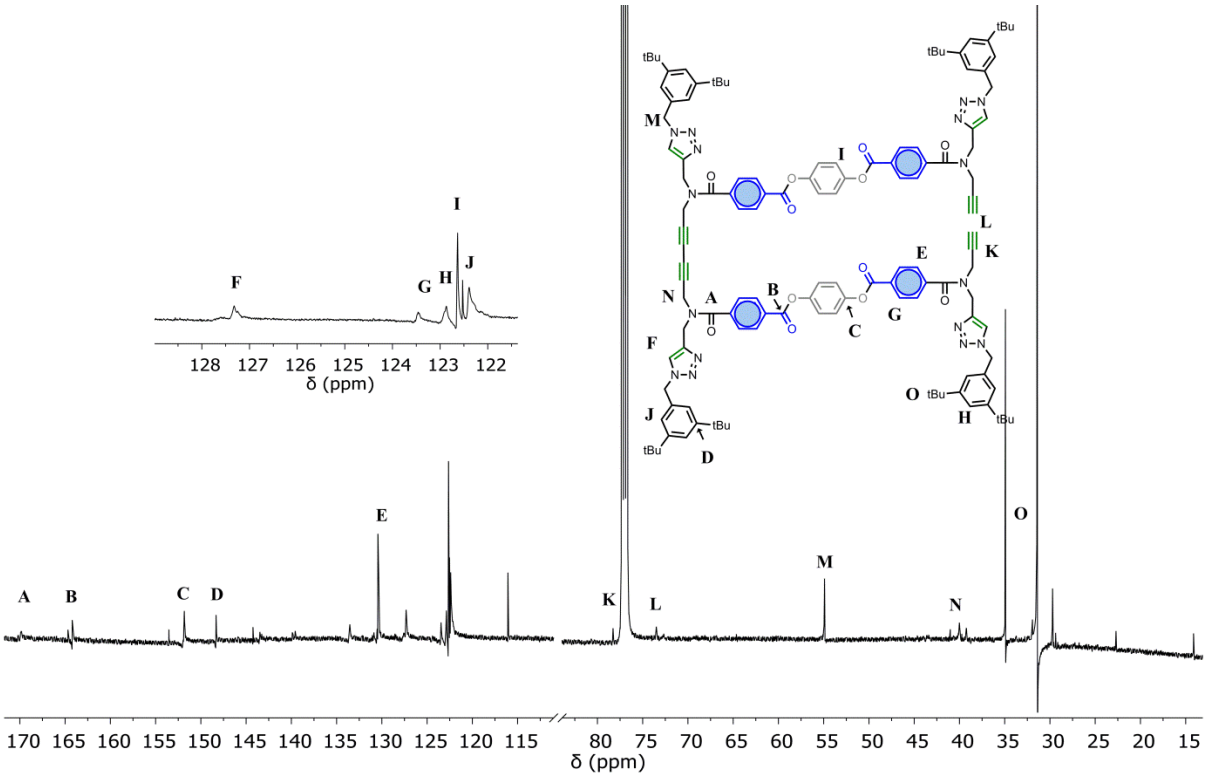
A
B
C
D
E
F
G
H
I
J
K
L
M
N
O
128
127
126
125
124
123
122
δ (ppm)
170
165
160
155
150
145
140
135
130
125
120
115
80
75
70
65
60
55
50
45
40
35
30
25
20
15
δ (ppm)

Synthesis of compound 4.18

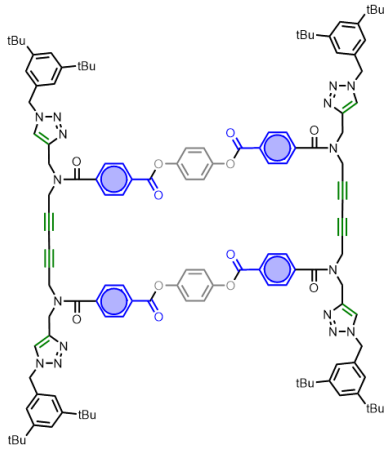

Compound **4.17** (7mg, 0.003 mmol), $Pd(PPh_3)_2Cl_2$ (2.4 mg, 0.003 mmol), PPh_3 (2.8 mg, 0.009 mmol), and CuI (0.7 mg, 0.003 mmol) were dissolved in acetonitrile (67 mL). Et_3N (46 µL, 0.3 mmol) was added and the reaction was stirred overnight. After this time the reaction was neutralized with HCl 1M, diluted with water, and the product reextracted with EtOAc. The organic solution was washed with brine (2 x 20 mL), dried with $MgSO_4$, filtered and dried in vacuo. The crude was purified via HPLC ($MeCN/H_2O$ gradient) to yield final compound as a dark yellow sticky solid (4.5 mg, 65%)

^{1}H NMR (500 MHz, Chloroform-*d*) δ 8.28 (d, *J* = 8.0 Hz, 8H), 7.67 (m, 12H), 7.43 (t, *J* = 1.8 Hz, 4H), 7.28 (s, 8H), 7.13 (s, 8H), 5.53 (s, 8H), 4.87 (s, 4H), 4.23 (s, 4H), 1.32 (s, 72H).

^{13}C NMR (126 MHz, Chloroform-*d*) δ 169.8, 164.29, 151.86, 148.34, 143.25, 139.66, 133.58, 132.14, 132.06, 130.54, 127.36, 123.49, 122.91, 122.74, 122.44, 54.92, 31.41, 29.71.

HRMS (ES+): calcd for $C_{128}H_{136}N_{16}O_{12}$ 209.0602 $[M+H]^+$, found 1045.5346 $[M+2H]^{2+}$.

FT-IR (ATR): 3230, 2945, 2860, 1741, 1637, 1570 cm^{-1}

Retention time: 2.61 min

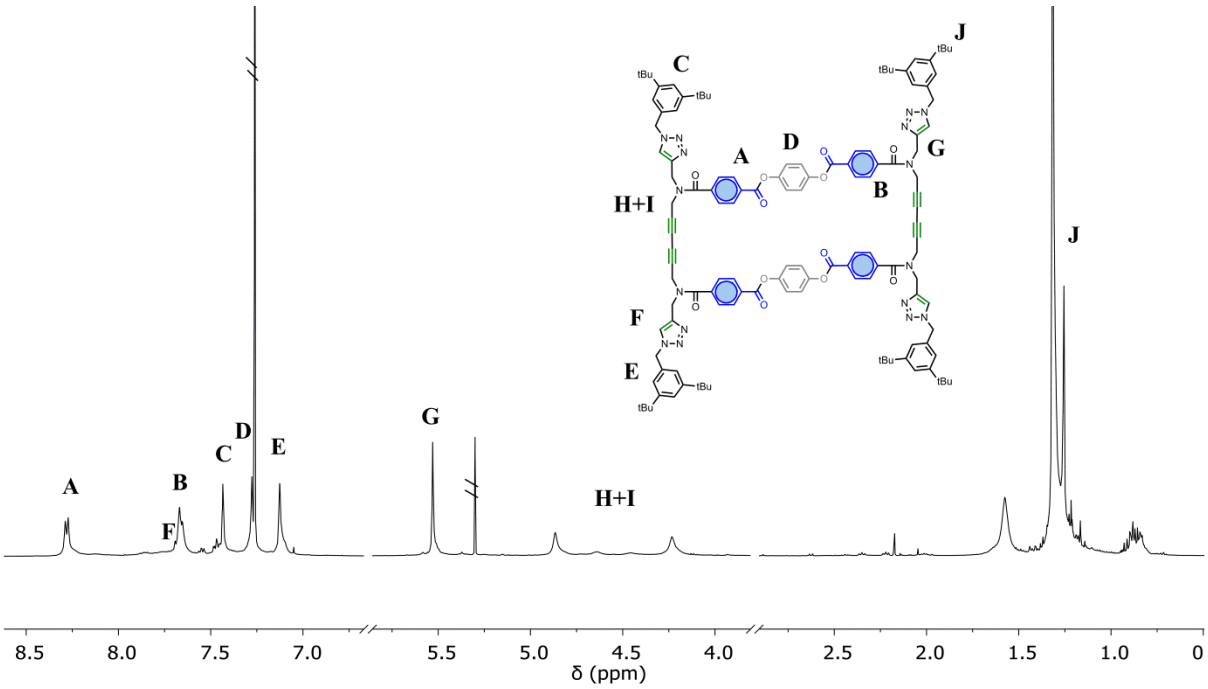
A
B
F
C
D
E
G
H+I
J
8.5 8.0 7.5 7.0 5.5 5.0 4.5 4.0 2.5 2.0 1.5 1.0 0
δ (ppm)

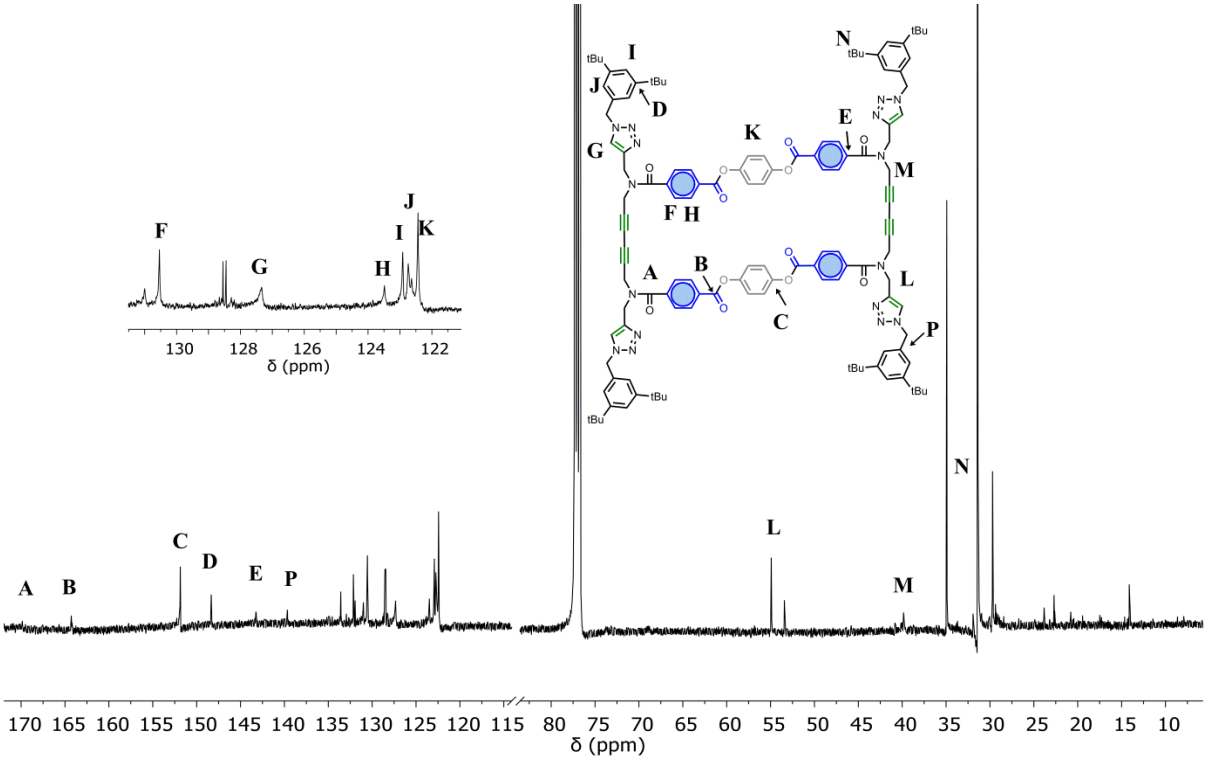
A
B
C
D
E
P
L
M
N
F
G
H
I
J
K
170 165 160 155 150 145 140 135 130 125 120 115 80 75 70 65 60 55 50 45 40 35 30 25 20 15 10
δ (ppm)
130 128 126 124 122
δ (ppm)

Synthesis of compound 4.20

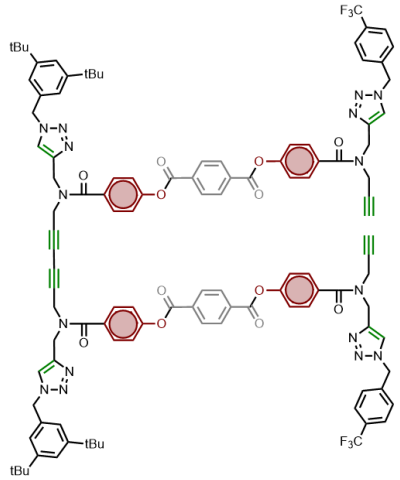

Compound **4.19** (6 mg, 0.006 mmol)**,** compound **4.9** (8.5 mg, 0.015 mmol), EDC (3 mg, 0.016 mmol) and DMAP (2 mg, 0.16 mmol) were dissolved in dry DCM (5 mL) and stirred under N_2 until no starting dimer could be seen by LCMS. The crude solution was washed with HCl 1M (2 x 20 mL) and brine (2 x 20 mL). The organic phase was dried with $MgSO_4$, concentrated in vacuo and purified via column chromatography (PET 40-60/EtOAc, gradient of increasing polarity) to yield final pure compound as a yellow oil (9.9 mg, 83%)

^{1}H NMR (500 MHz, Chloroform-*d*) δ 8.36 (s, 8H), 7.75 – 7.63 (m, 16H), 7.44 (d, *J* = 4.8 Hz, 4H), 7.41 (s, 2H), 7.34 (d, *J* = 8.3 Hz, 8H), 7.13 (d, *J* = 1.8 Hz, 4H), 5.62 (s, 4H), 5.54 (s, 4H), 4.86 (s, 8H), 4.22 (s, 8H), 2.39 (s, 2H), 1.33 (s, 36H).

^{13}C NMR (126 MHz, Chloroform-*d*) δ 170.28, 163.82, 152.19, 151.86, 138.43, 133.82 – 133.48 (m), 130.41, 129.00, 128.30, 126.24 – 125.70 (m), 122.90, 122.37, 121.83, 78.53, 54.88, 53.56, 34.91, 31.40.

HRMS (ES+): calcd for $C_{128}H_{138}N_{16}O_{12}$ 2003.8002 $[M+H]^+$, found 1024.3841 $[M+2Na]^{2+}$.

FT-IR (ATR): 3327, 2944, 2905, 2843, 1750, 1656 cm^{-1}

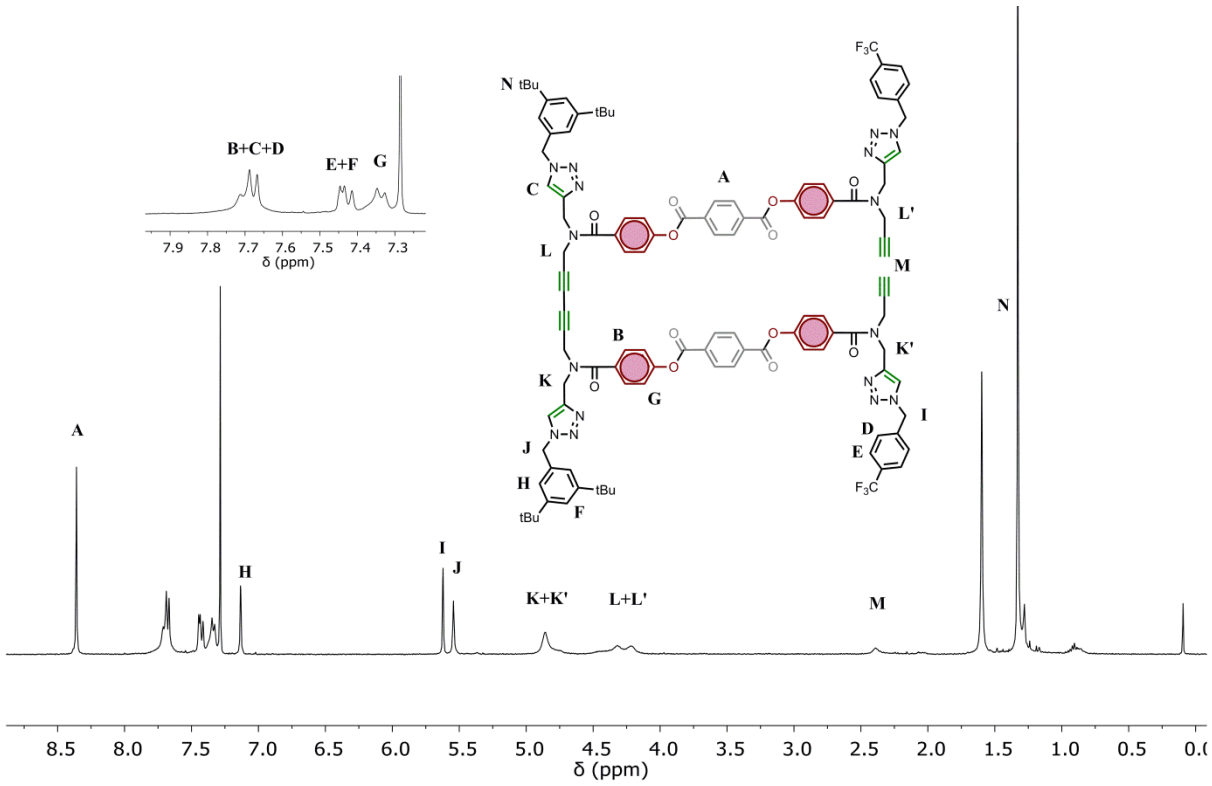
B+C+D
E+F
G
7.9 7.8 7.7 7.6 7.5 7.4 7.3
δ (ppm)
A
H
I
J
K+K'
L+L'
M
N
8.5 8.0 7.5 7.0 6.5 6.0 5.5 5.0 4.5 4.0 3.5 3.0 2.5 2.0 1.5 1.0 0.5
δ (ppm)

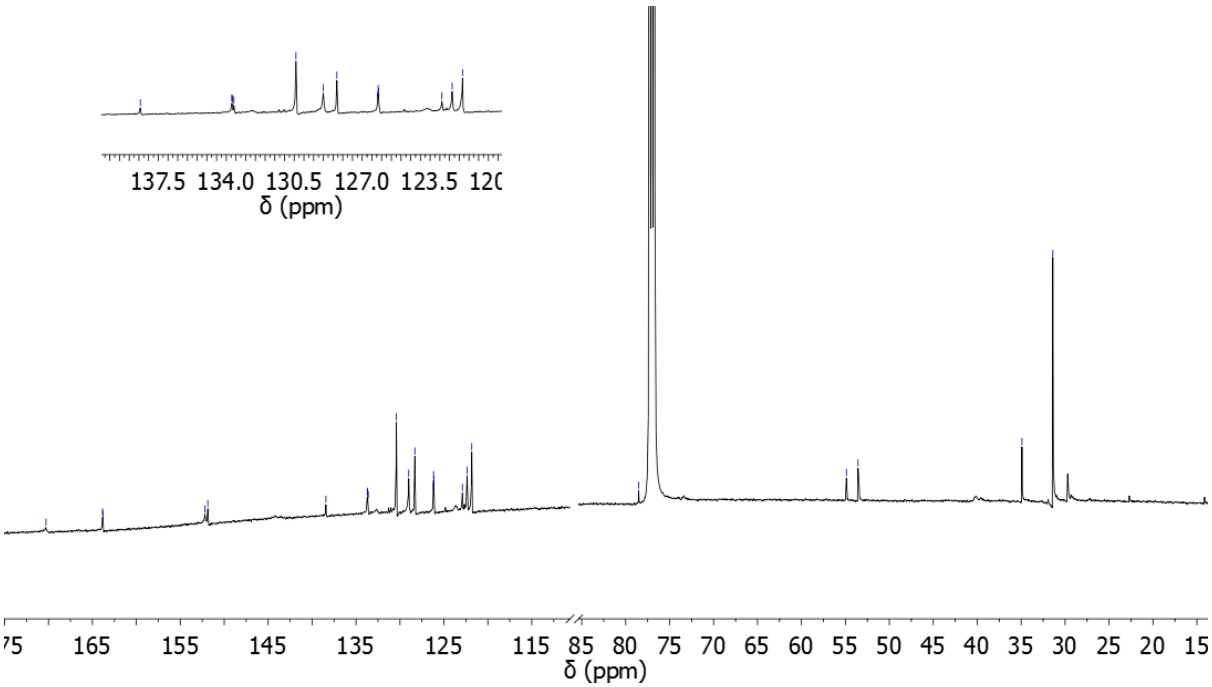
137.5 134.0 130.5 127.0 123.5
δ (ppm)
165 155 145 135 125 115 85 80 75 70 65 60 55 50 45 40 35 30 25 20 15
δ (ppm)

Synthesis of compound 4.21

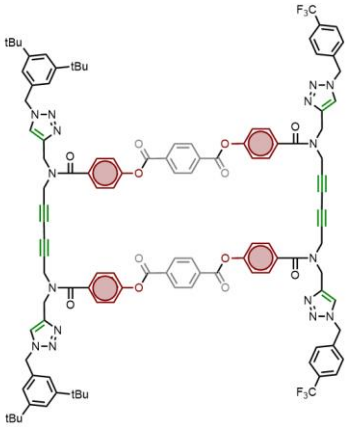

Compound **4.20** (6 mg, 0.003 mmol), $Pd(PPh_3)_2Cl_2$ (2.4 mg, 0.003 mmol), PPh_3 (2.8 mg, 0.009 mmol), and CuI (0.7 mg, 0.003 mmol) were dissolved in acetonitrile (67 mL). Et_3N (46 µL, 0.3 mmol) was added and the reaction was stirred overnight. After this time the reaction was neutralized with HCl 1M, diluted with water, and product reextracted with EtOAc. The organic solution was washed with brine (2 x 20 mL), dried with $MgSO_4$, filtered and dried in vacuo. The crude was purified via HPLC ($MeCN/H_2O$ gradient) to yield final compound as a dark yellow sticky solid (4.2 mg, 70%)

^{1}H NMR (500 MHz, Chloroform-*d*) δ 8.31 (s, 8H), 7.85 (s, 4H), 7.73 – 7.61 (m, 12H), 7.53 – 7.39 (m, 6H), 7.34 (s, 8H), 7.12 (d, *J* = 1.9 Hz, 4H), 5.62 (s, 4H), 5.52 (s, 4H), 4.84 (s, 8H), 4.29 (s, 8H), 1.31 (s, 36H).

^{13}C NMR (126 MHz, Chloroform-*d*) δ 164.05, 152.32, 151.78, 132.13, 130.44, 128.5, 128.45, 128.39, 122.90, 122.37, 121.83, 53.42, 34.91, 31.40.

HRMS (ES+): calcd for $C_{128}H_{138}N_{16}O_{12}$ 2001.7845 $[M+H]^+$, found 1023.3746 $[M+2Na]^{2+}$.

FT-IR (ATR): 3063, 2975, 1744, 1646, 1504, 1460, 1422 cm^{-1}

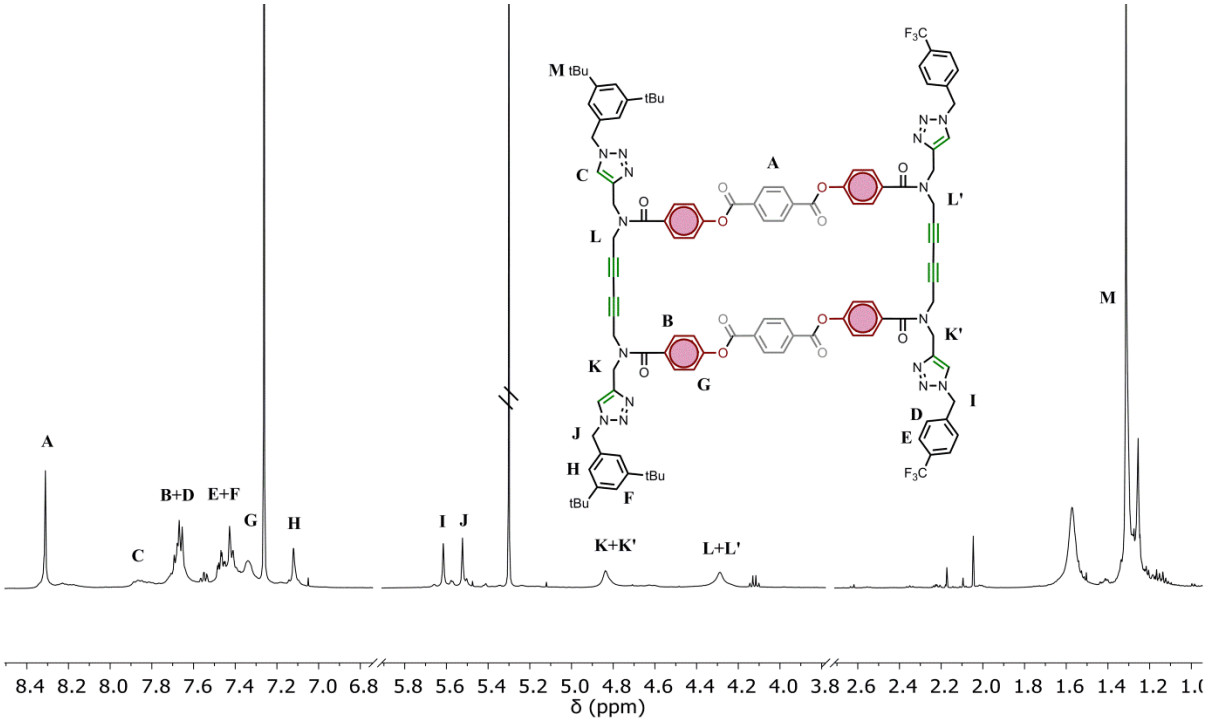
A
B+D
E+F
G
H
C
I
J
K+K'
L+L'
M
δ (ppm)

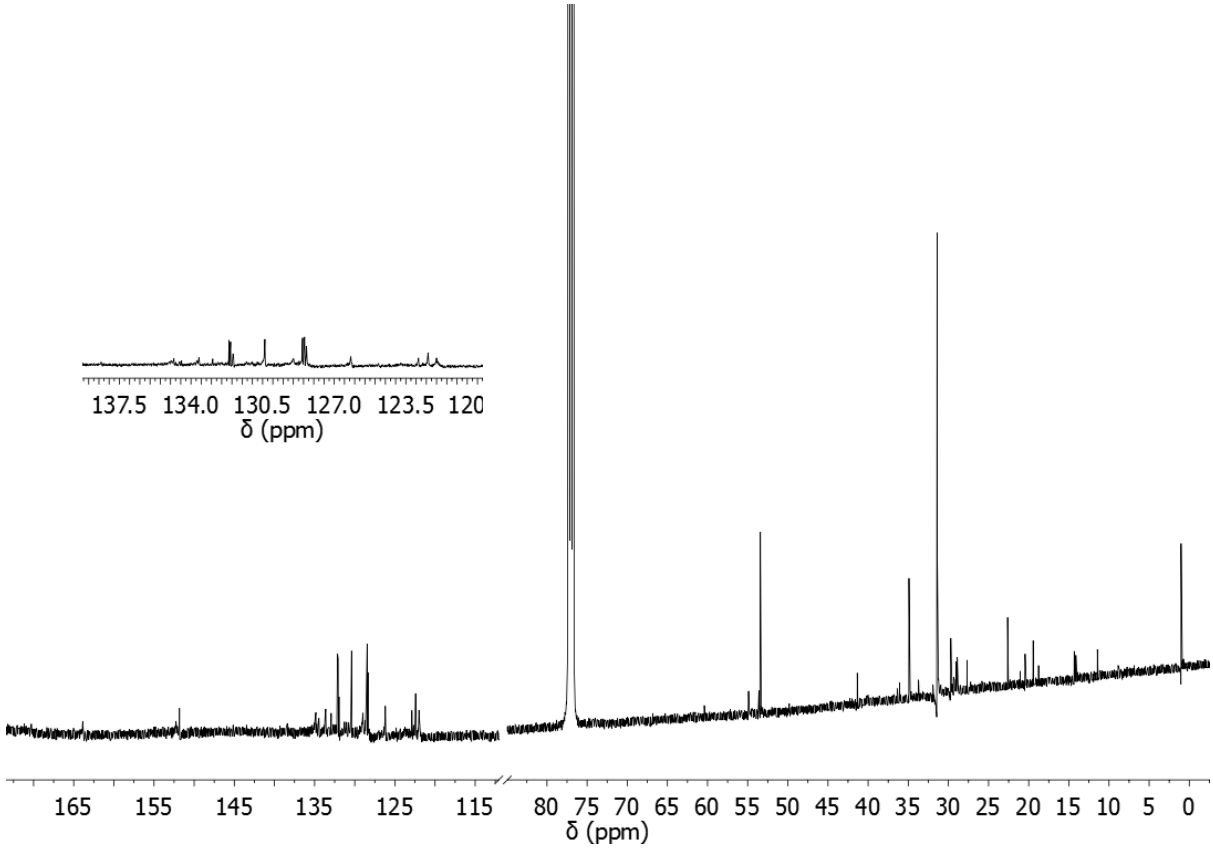
137.5 134.0 130.5 127.0 123.5 120
δ (ppm)
165 155 145 135 125 115 80 75 70 65 60 55 50 45 40 35 30 25 20 15 10 5 0
δ (ppm)

"Come on, the army doesn't want deadbeat 14-year olds. They want deadbeat 18-year olds"

Frank Murphy

5

Synthesis and Characterization of Supramolecular Polymer Nanoparticles

5.1 Introduction

Biopolymers found in Nature, such as DNA and proteins, present highly specific functionalities that are associated with their tertiary and quaternary structures.[1-3] Scientists have long tried to create mimics of natural systems in the laboratory.[4-6] In the case of proteins, their three-dimensional arrangement depends on the specific amino acid sequence of the extended chain.[7] Inspired by this fact, research on sequence-specific polymerizations continues to grow in its pursuit of polymeric chains with perfectly defined sequences[8-9], but other alternatives, to create synthetic protein-like

objects have also been explored. One approach that has become particularly appealing is the design of functional single-chain polymer nanoparticles (SCPNs)[10-12].

SCPNs are polymer chains that are typically synthesized via a living polymerization technique incorporating pendant units that can interact with each other. When these interactions occur in an intramolecular fashion the chain collapses on itself forming folded discrete objects. Several types of folding interactions have been studied, but they generally can be divided in two categories: i) covalent (non-reversible[13-14] and dynamic[15-16]) and ii) supramolecular.[17] Among the latter, a particularly appealing structural motif is benzene-1,3,5-tricarboxamides (BTAs), which interact with each other via trifold hydrogen bonds. When free in solution BTAs stack on top of each other and form helical aggregates.[18] When appended to polymer chains, their aggregation causes the polymer to fold into a compartmentalized object.[19] SCPNs folded via hydrogen bonding offer the advantages of dynamism and adaptability when presented with certain external stimuli, such as changes of temperature or polarity.[20] Though still in its infancy, the SCPN field has produced systems able of catalyzing reactions,[21-23] sensing[24] or even targeting and imaging tumors in vivo.[25] But examples of materials that present both functionality that can be tuned in response to external stimuli and biocompatibility are still scarce. Accordingly, we sought to study the reactivity and the aggregation behavior of biodegradable polycarbonate chains that fold via dynamic supramolecular interactions in organic solvents.

The folding of several polymeric backbones has been studied,[26] including that of polyacrylates, polynorbornenes and poly(dimethyl siloxanes).[27] In this work, we use a strategy presented by Hedrick and co-workers for the synthesis of a polycarbonate precursor functionalized with an activated ester (Poly(MTC-OC_6F_5))[28]. This type of polymer is interesting for a number of reasons: i) it can be synthesized from cyclic monomers via Ring Opening Polymerization (ROP),[29] a methodology that yields living polymers with very low polydispersity (PDI < 1.1); ii) it is easily post functionalized at room temperature in a matter of hours with successive additions of primary amines (Figure 5.1), which opens the possibility of obtaining a variety of functional materials; iii) the composition of the chains can be easily quantified by ^{1}H NMR peak integration due to well-resolved, diagnostic signals; iv) and most importantly, it is biodegradable and biocompatible,[30-31] which, when put together with the promising possibilities in the biomedical field offered by the folding of polymer chains,[32] makes the polycarbonate backbone a very attractive target for the synthesis of SCPNs. Furthermore, the resulting polymeric chains only required precipitation as

purification method, unlike previous systems presented in the Meijer group, in which several days of dialysis were necessary to remove the outgoing pentafluorophenol from the polymer precursor.

We proceeded to characterize these systems by ^{1}H NMR spectroscopy, gel permeation chromatography (GPC), IR and circular dichroism (CD) in solvent mixtures of different polarities. CD represents one of the main techniques used to characterize systems that form chiral supramolecular aggregates.[33] The extent to which the molecules stack forming helices can be determined depending on the intensity of the Cotton effect. This signal will be positive or negative depending on the handedness of the helix, which is determined by the stereochemistry of the chiral atom of the molecule. Since BTAs interact via triple H-bonds, the factors that affect these interactions will affect the size of the helices and, therefore, the CD signal. Higher concentration, lower polarity and lower temperatures give rise to stronger signals, and vice versa. To confirm that BTAs aggregate in multiple domains instead of a single stack when they are appended to a polymer, as has previously been reported by the Meijer group,[34] we perform sergeant and soldiers experiments by functionalizing a set of polymers with chiral and achiral mixtures of BTA.

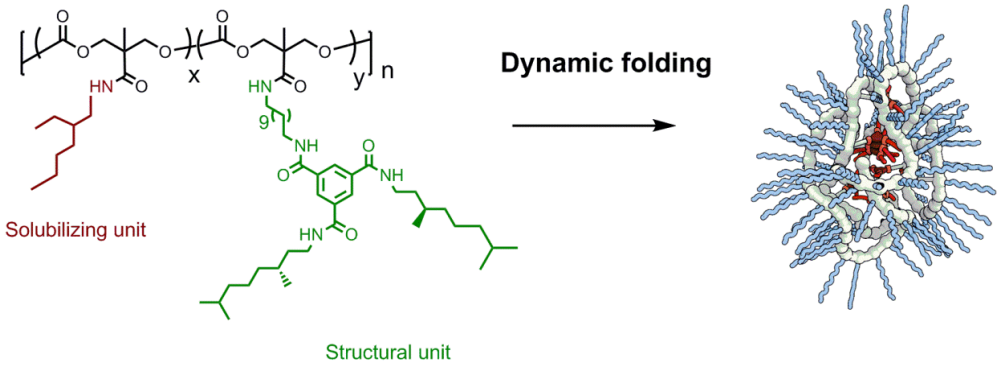

Figure 5.1. BTA-functionalized polycarbonate materials folding into polymer nanoparticles.

5.2 BTA synthesis

The synthesis of both chiral and achiral BTA-NH_2 **5.9** and **5.10** started with a statistical reaction of 1,3,5-benzenetricarbonyl chloride with a 2:1 mixture of two different primary amines (Scheme 5.1): i) a chiral amine acting as solubilizing chain, that will determine the handedness of the BTA stacks; ii) and one with a primary alcohol at the end of the molecule where further chemical processes could be undertaken (compound **5.2**). The reaction produces a mixture of aromatic products with different substitutions. Careful chromatographic separation rendered four fractions of increasing polarity, from the trialkyl-substituted BTA molecule to the triol substituted one. BTA alcohols **5.3-5.4** were then tosylated, to generate **5.5** and **5.6**, before being subjected to nucleophilic attack with potassium phthalimide to produce molecules **5.7-5.8**. The final reduction with hydrazine produced the desired chiral and achiral BTA-NH_2, **5.9** and **5.10** respectively.

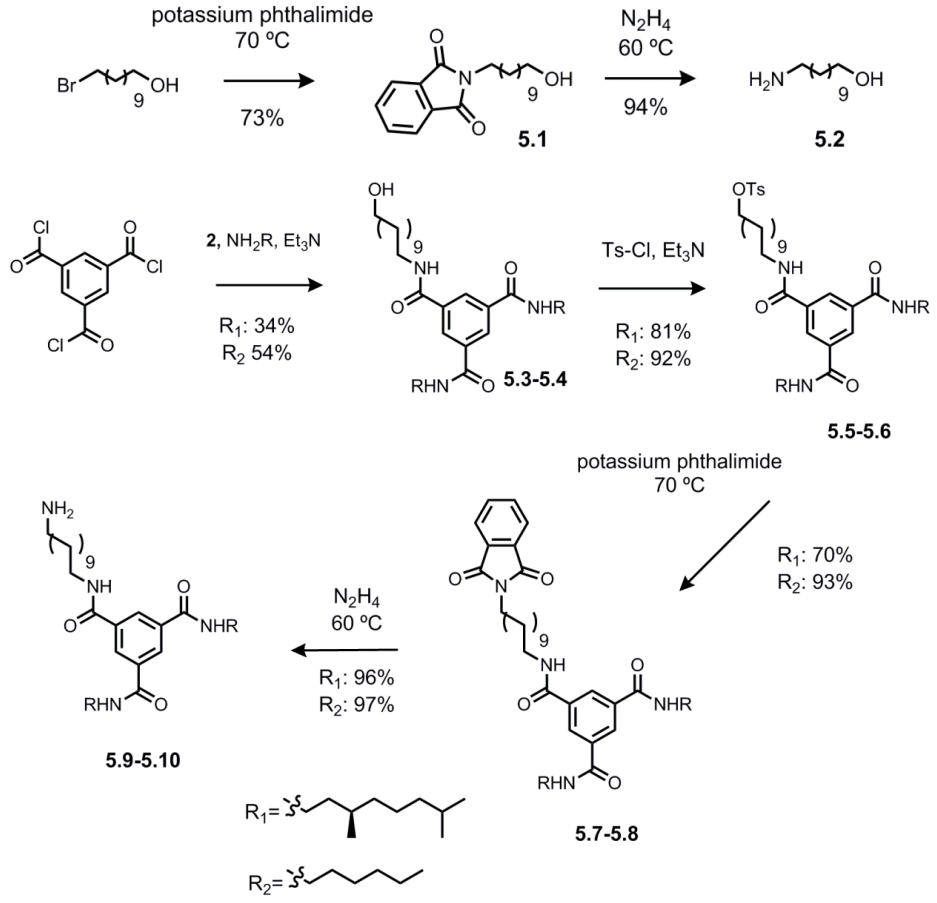

Scheme 5.1. Synthesis of chiral BTA-NH_2 **5.9** and achiral BTA-NH_2 **5.10**.

5.3 Polycarbonate synthesis

In order synthesize the precursor-polycarbonate **P0**, the cyclic monomer **5.11** had to be prepared (Scheme 5.2). The synthesis involved simple mixing and overnight stirring of the propionic acid derivative and bis(pentafluorophenyl) carbonate. After re-crystallization, monomer **5.11** was suspended in DCM with triflic acid and 4-methylbenzyl alcohol as the reaction initiator. The suspension was reacted at room temperature inside a glove box until the mixture turned clear. At that point the vial was taken out from the glove box and the polymer was precipitated into cold ether before centrifuging and drying in the oven rendering the precursor-polycarbonate, **P0**.

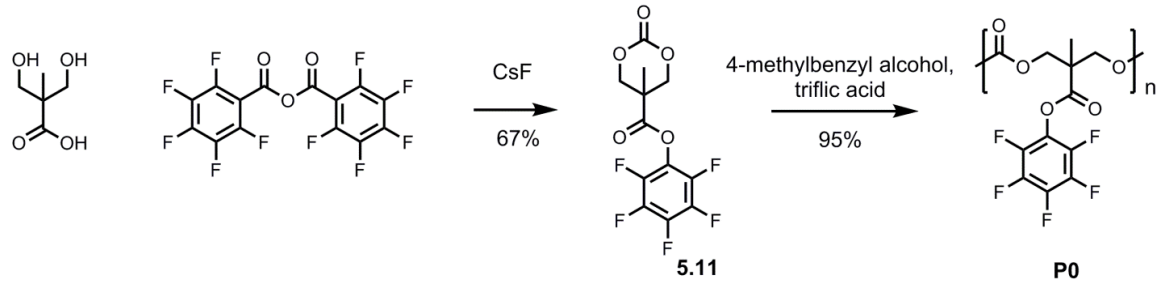

Scheme 5.2. Synthesis of polycarbonate precursor **P0**.

The easy and quick postfunctionalization of the precursor-polycarbonate **P0** was one of the reasons why this backbone and method is so attractive for the synthesis of functional materials. **P0** was dissolved in dry THF along with triethylamine, and the primary amines were added sequentially (Scheme 5.3). Each amine was left reacting for two hours before the addition of the next one. We made a set of polymers with variable quantities of two components: i) a BTA with an eleven-carbon chain and a primary amine on the end (BTA-NH_2, compound **5.9**); and ii) a short, branched alkyl chain to promote the solubility of the polymers in solvents apolar enough for the BTA stack. It had been observed in previous works in the Meijer group that high percentages of BTA within the same polymeric chain induced intermolecular aggregation.[19] With this in mind we decided to limit the amount of BTA to a maximum of 20%.

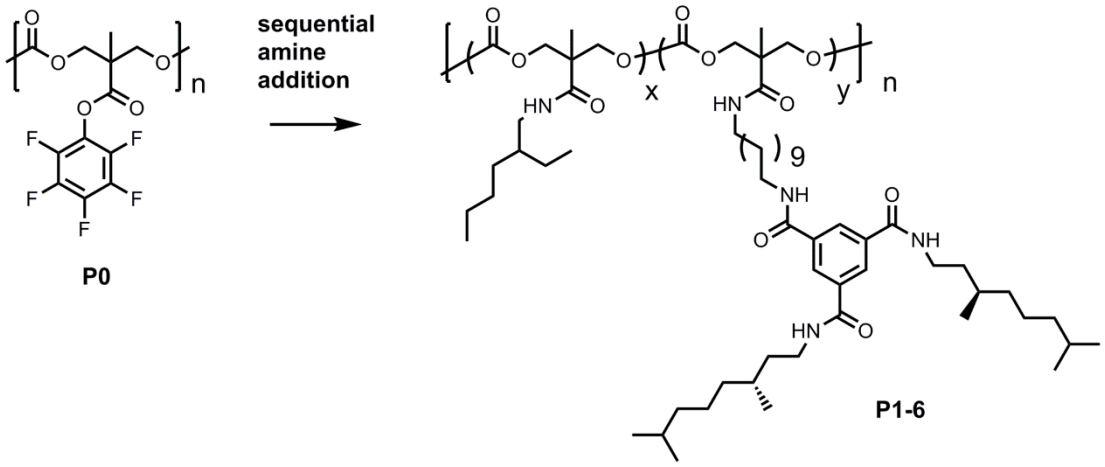

Scheme 53. Synthesis of polymer Series 1 (**P1-P6**) through sequential addition of amines to **P0**. Increasing quantities of BTA-NH_2 **5.9** are added onto the different polymers of the series. Detailed polymer composition can be found in Table 5.1.

The samples were characterized by THF-GPC (Figure 5.2, Table 5.1), which showed that the polymerization of the carbonate cyclic monomer is a living process which produces very narrowly dispersed molecules. Moreover, the sequential addition of amines and reaction for short periods of times at room temperature barely affects the dispersity of the molecules, suggesting that there are no problems with transesterification, as was the case in some of our early experiments with higher temperatures and longer reaction times. Finally, the good agreement in the NMR-calculated M_n of all the chains and the obtained from GPC measurements suggests that proton signal integration is a reliable method to assess absolute content of polymer chains. Detailed information about polymer composition and molecular weights can be found in Table 5.1.

Table 5.1. Composition, molecular weight and dispersity of polymer Series 1.

Series 1 Polymer ID	**% BTA**	$M_{n,\,GPC}$[a] **(kDa)**	$M_{n,\,NMR}$[b] **(kDa)**	$Đ$[a]
P0	-	30.4	38.0	1.05
P1	0	29.4	31.6	1.06
P2	3	27.7	33.4	1.16
P3	7	32.5	35.9	1.07
P4	9	32.9	37.4	1.09
P5	14	34.3	40.8	1.11
P6	16	35.3	41.4	1.08

[a] Analyzed with GPC in THF at 40ºC using PS standards.

[b] Calculated from NMR integration with the DP of **P0** being calculated from polymerization conversion and monomer to initiator ratio. Formula used:

$$Mn\ NMR = \sum \frac{DP\ (\boldsymbol{P0})\ x\ \%i\ x\ Mwi}{100}$$

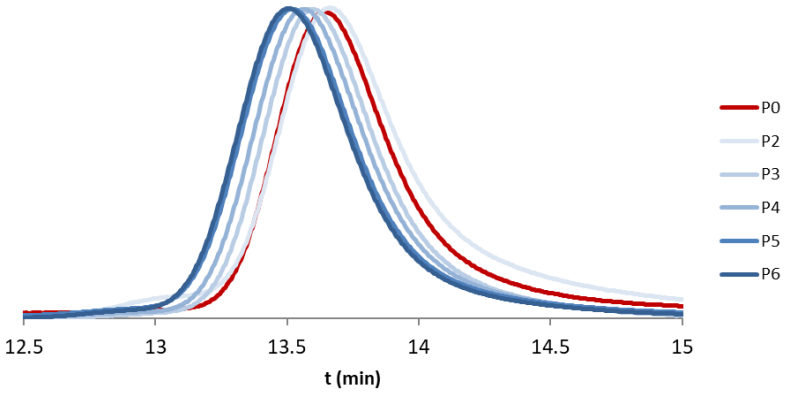

Figure 5.2. GPC traces of Series 1 polymers. From highest BTA content (P6, darkest shade of blue) to lowest content (P2, lightest shade). The precursor polymer is coloured red (P0)

5.3. Polycarbonate synthesis

^{1}H NMR spectroscopy provides an easy characterization method to determine the exact polymer content of **P1-P6**. Spectra of all samples can be found in the experimental section (Figure S2-S5). Figure 5.3 depicts how we deduced that one of our polymers had a 16% BTA content through comparison of the integration of the backbone signal (**c**) at 4.28 ppm (4 ^{1}H) with the broad signal that appeared at around 8.34 ppm (**a**) corresponding to the three protons of the BTA moiety. Since **a** integrates to 0.47 ^{1}H it indicates that ca. 16% of the repetitive units of the polymer are functionalized with BTA. This was corroborated by the integration of the broad signal (**d**) at 3.44 ppm, which corresponds to the three methylene units that surround the core of the pendant BTAs. This signal integrates to double that of the aromatic BTA signals, 0.99 ^{1}H. Other characteristic signals include **(b)** at 6.04 ppm, a broad singlet corresponding to the amide proton of the backbone, and **(e-e')**, another broad signal at 3.20 ppm that correspond to the methylene protons next to the amide functionalities from the backbone. The second characteristic signal on the backbone (**f**) and the rest of the aliphatic signals from the 2-ethyl-hexyl units and the BTA side chains appear between 0.5 and 1.7 ppm.

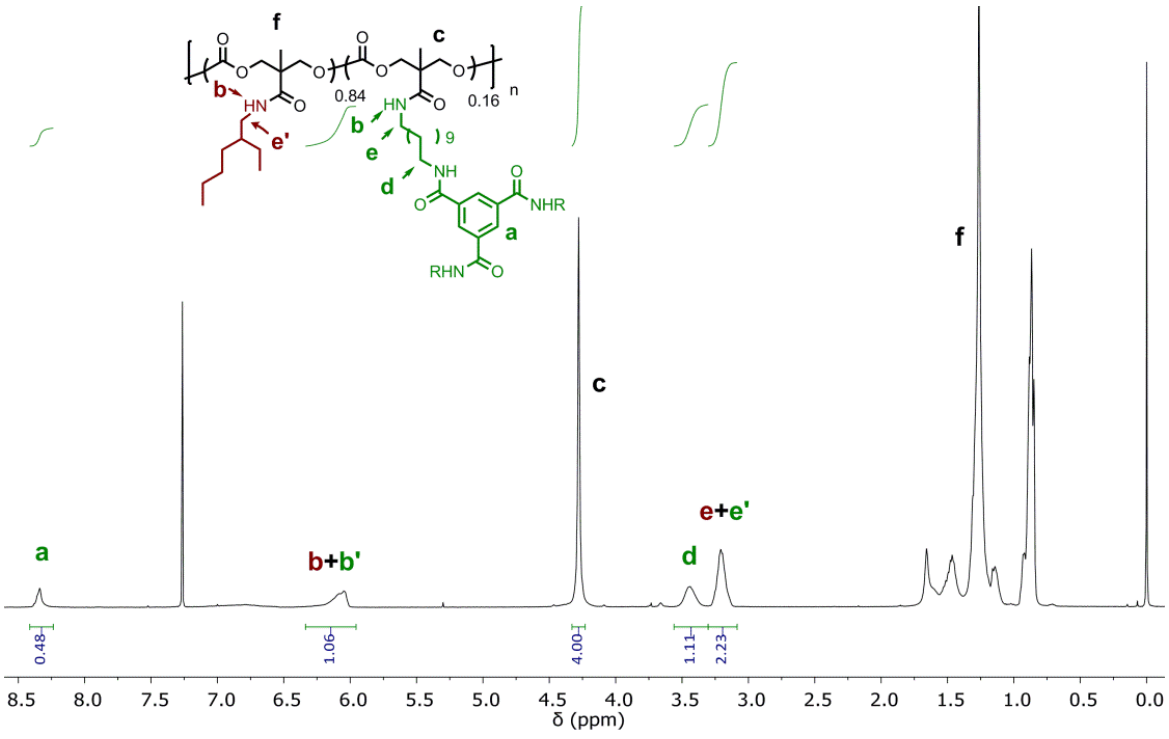

Figure 5.3. ^{1}H NMR (400 MHz, Chloroform-*d*, 298 K) of **P6** with signal integration to determine polymer composition

Moreover, ^{1}H NMR spectra and FTIR measurements (Figure 5.4) were acquired after the first functionalization for two polymers of the series (**P2** and **P6**). However, during these additional measurements we observed lower BTA functionalization yields than we would have expected, perhaps due to stopping the reaction and precipitating the material instead of allowing the reaction to continue during the addition of the second amine (Table S1). The NMR spectra allowed us to see the change in chemical signals attributable to the backbone methylene and methyl groups shift from 4.5 and 1.5 ppm (**c'** and **f'**) to 4.3 and 1.3 ppm (**c** and **f**), respectively, as the polymer was functionalized. The first step of the functionalization was confirmed by the appearance of CH_2-N from the BTA amides and the newly-formed amides along the backbone (**d** and **e**, respectively). The final functionalization, to install the solubilizing groups, resulted in the diagnostic increase in intensity of the methylene signal at 3.2 ppm (**e-e'**). By FT-IR spectroscopy, the appearance of the C=O signals of the amides ca. 1600 cm^{-1}, the C-H from the aliphatic chains of the solubilizing groups and the BTA side chains and the N-H from the amides were all consistent with functionalization. We also observed no ^{19}F NMR resonances in the final products, which is consistent with full conversion of the pentafluorophenyl ester units and purification of the polymer (Figure S1).

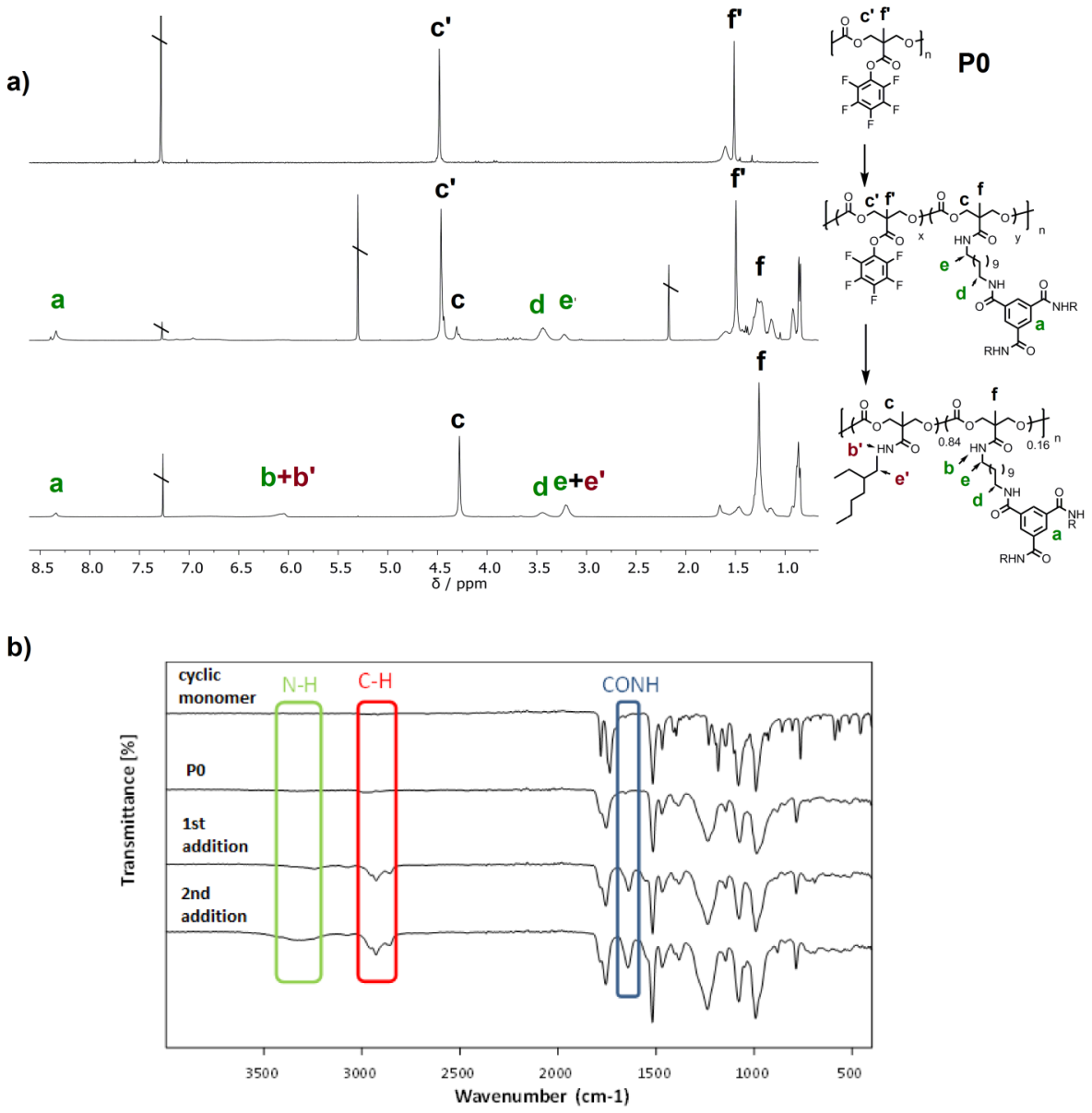

Figure 5.4. (a) Step by step ^{1}H NMR (400 MHz, Chloroform-d, 298 K) and (b) FT-IR characterization of **P2**.

5.4 Polymer Folding

Circular dichroism represents one of the main techniques used to characterize systems in which there are chiral BTAs present. The extent to which the molecules stack forming helices can be determined depending on the intensity of the Cotton effect. This signal will be positive or negative depending on the handedness of the helix, which is determined by the stereochemistry of the chiral atom of the molecule. Since BTAs interact via triple H-bonds, the environmental factors that induce changes in these interactions will have an effect on the size of the helices and the Cotton Effect they present. Higher concentration, lower polarity and lower temperatures give rise to stronger signals, while lower concentration, increased polarity and higher temperature decrease or even eliminate the signal.

The following experiments were conducted at room temperature and at a fixed BTA concentration of 50 μM. This made sure that any difference in signal when measuring the polymer series going from **P2** to **P6** was solely due to the variable percentage of BTA within the chain, not to the total amount present in solution (i.e. bigger quantities of BTA in the same chain stack in longer helices which in turn produce more intense CD signals). A typical sample was prepared as follows: **P1-P6** were dissolved in dichloroethane (DCE) to form a stock solution, and this was sonicated at 40 ºC for 45 min. Aliquots of this solution were then taken and diluted with the appropriate amount of methylcyclohexane (MCH) to form solution with different polarities and a total concentration of BTA of 50 μM. The samples were then immediately measured. In previous works it was observed that BTA-containing materials presented a maximum of absorbance at 223 nm.[35] However, these materials absorbed UV light strongly below 230 nm, thus we only consider the CD effect above 230 nm.

Figure 5.6a shows the measurement of **P6.** Decreased polarity (i.e. a higher percentage of MCH, lighter shades of red in the graph) facilitates aggregation along the chain, which translates into a more intense Cotton effect. The same applies for **P2-P5** at the whole range of wavelengths measured (Figures S6-S9**).** This can be seen summarized in Figure 5.6b, which depicts the Cotton effect at 230 nm for all the polymer series at different MCH percentages. Furthermore, when the Cotton effect of all the chains was compared for the MCH/DCE 70/30 (v/v) solvent mixture and room temperature measurement at 230 nm, it was observed that the CD signal increased proportionally with the percentage of BTA within a chain (Figure 5.6c).

We further probed the aggregation of these materials through the acquisition of melting curves (Figure 5.6d). It is expected that the CD signal decreases in intensity as temperature is increased due to the unfavourability of H-bond interactions at high temperature, which ultimately disrupts the formation of helical aggregates. The CD intensity was monitored at 230 nm as the temperature of the solution was increased from 10 °C to 80 °C. The polymers functionalized with a higher content of pendant BTA (lighter shades of green in the graph) exhibited higher melting temperatures since the initial amount of BTA stacking was bigger.

We interpret these findings as follows: i) first, that either bigger aggregates or more domains of smaller stacks were formed when chains had a higher BTA content, as it has been reported in Meijer's previous work,[34] and ii) there was not inter-polymer aggregation between different chains in solution. If there were, one would not expect to observe Cotton effects proportional to BTA content, but a more or less uniform measurement for all samples, given that the amount of BTA in solution was the same in all the experiments.

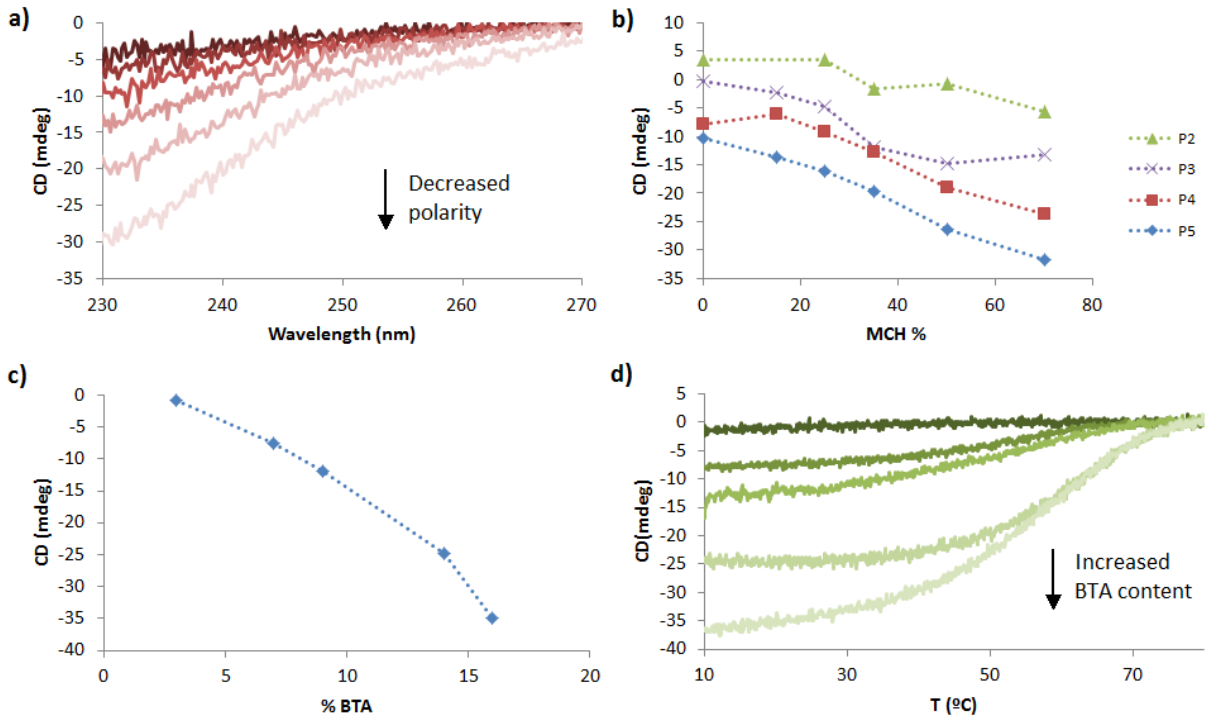

Figure 5.6. CD spectra taken of different BTA-containing polycarbonates. **a)** Cotton effect observed on the **P6** polymer chain at different MCH/DCE mixtures: i) 70% MCH (lightest shade of red); ii) 50% MCH; iii) 35% MCH; iv) 25% MCH; v) 15% MCH; vi) 0% MCH (darkest shade

of red); **b)** Cotton effect measured at 230 nm for the rest of the set, at different solvent polarities; **c)** Linear relation between Cotton effect measured at 230 nm for the 70% MCH sample and BTA percentage within a polymer chain; **d)** Melting curves of the polymer series, Cotton effect measured at 230 nm: i) **P6** (lightest shade of green); ii) **P5**; iii) **P4**; iv) **P3**; v) **P2** (darkest shade of green).

5.5 Sergeant and Soldiers Experiments.

To further study the importance of domain formation within the polymer chain, as opposed to aggregation in a unique helical stack, Sergeant and Soldiers studies were performed on this polycarbonate backbone. To that effect, an achiral BTA-NH_2 analogue was synthesized (compound **5.10**, Scheme 5.1) and a set of polymer chains containing both chiral and achiral BTA were prepared (Scheme 5.4). The total BTA functionalization (chiral + achiral) was aimed at 10%, and chains with increasing percentages of chiral units were made (from **P7** with a 10% chiral BTA relative content, to **P15** with a 90% chiral BTA relative content) (Table 5.2, Table S2).

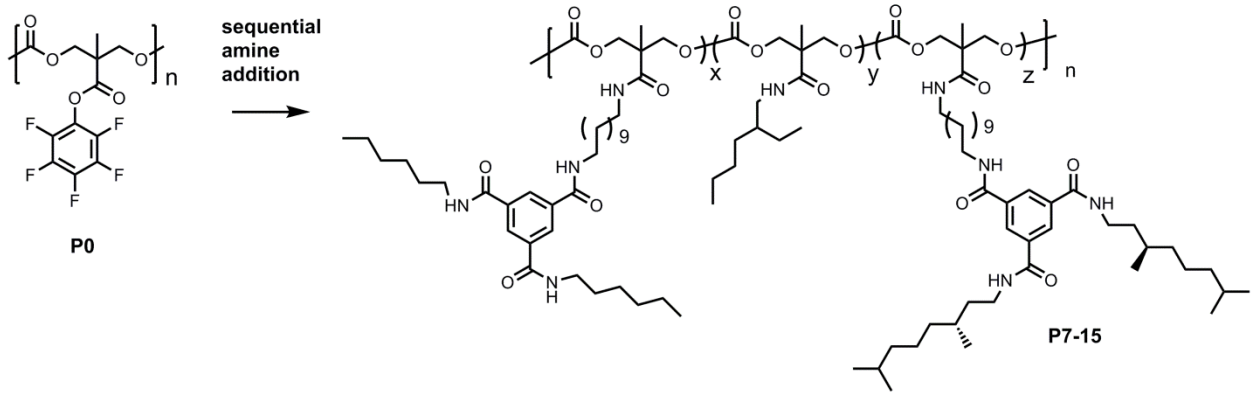

Scheme 5.4. Synthesis of polymer Series 2 (**P7-P15)** through sequential addition of amines to **P0.** Polymers in the series contain variable mixtures of chiral BTA-NH_2 (compound **5.9**) and achiral BTA-NH_2 (compound **5.10**). Detailed polymer composition can be found in Table 5.2.

Table 5.2. Total BTA functionalization and relative chiral BTA functionalization of polymer Series 2.

Series 2 Polymer ID	**Total BTA functionalization[1]**	**Relative % of chiral BTA[2]**
P7	8%	10
P8	8%	20
P9	9%	30
P10	9%	40
P11	7%	50
P12	7%	60
P13	8%	70
P14	8%	80
P15	9%	90

[1]Percentage of the polymer chain functionalized with BTA units (the rest up to 100% being solubilizing alkyl chains), i.e. (z+x)/(x+y+z)

[2]Percentage of chiral BTA with respect to the total BTA content (the rest up to 100% being achiral BTA), i.e. z/(z+x)

This set of polymers was characterized by THF-GPC, ^{1}H NMR spectroscopy and CD (Table S3, Figures S10-S11) and it was found that the total helicity, (i.e. the ratio of the CD signal of a chain containing chiral and achiral BTA to the CD signal of a chain containing only chiral-BTA in the same percentage) was almost linear with the amount of chiral BTA (Figure 5.7, Figure S11, Table S4). This proportionality, also observed in previous sergeant and soldiers experiments conducted by the Meijer group on SCPN systems, further confirmed that BTAs aggregate in a multi-domain fashion within the polymer chain with little communication between domains.

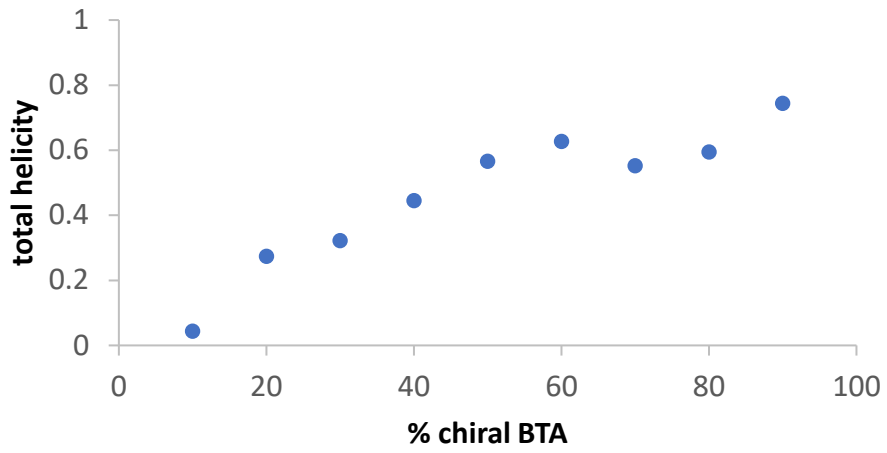

Figure 5.7. Relationship between net helicity and content of chiral-BTA. Cotton effect measured at 230 nm and 298 K in MCH/DCE 70/30 (v/v).

For perspective, when BTAs are free in solution, they behave cooperatively and only 5% of chiral BTA is necessary to induce chiral amplification on a helical stack formed by achiral BTAs, i.e. one molecule of chiral BTA induces chirality on 20 molecules of achiral BTA.[35] In contrast, in our experiments BTAs interact with each other while being attached to a polymer backbone. This translates into a loss of cooperative behavior in favor of a linear relationship between chiral content and CD signal, i.e. higher contents of chiral BTA within the polymer chain produce proportionally higher signals.

5.6 Conclusions

In this work we prepared a series of supramolecular SCPNs that fold due to the presence of triple H-bond interactions between pendant BTA units that stack forming chiral helices. They were made by simple amidation of an activated ester polycarbonate precursor synthesized via ROP in a living fashion ($Đ < 1.1$). The use of this backbone is very appealing since it has been proven to be biodegradable and biocompatible. The behavior of these particles was studied by means of CD under varying solvent polarity and temperature. Furthermore, sergeant and soldiers experiments with a polymer set containing both chiral and achiral BTAs in different percentages were performed, confirming that there is little cooperativity in the BTA stacking when appended to a polymer and that they form multiple small aggregates in domains along the polymer chain.

5.7 Experimental Section

Chemicals

Azobisisobutyronitrile (AIBN) was recrystallized from methanol. All other chemicals were obtained from Aldrich and used as received. All solvents were obtained from Biosolve, Acros or Aldrich. Dry DCM, THF, and DMF were tapped off a distillation setup which contained molsieves. $CHCl_3$ was dried over molecular sieves and triethylamine was stored on KOH pellets. (S)-(-)-Citronellol was purchased from Aldrich and converted into the corresponding (S)-3,7-dimethyloctan-1-amine according to a described procedure.[36]

Characterization methods.

Ultraviolet-visible (UV/Vis) and circular dichroism (CD) measurements were performed on a Jasco J-815 spectropolarimeter where the sensitivity, time constant and scan rate were chosen appropriately. Corresponding temperature-dependent measurements were performed with a PFD-425S/15 Peltier-type temperature controller with a temperature range of 263-383 K and adjustable temperature slope: in all cases a temperature slope of 1 K/min was used. All measurements were performed at a fixed BTA concentration of 50 μM. ^{1}H and ^{13}C NMR spectra were recorded at 298 K on a Varian Mercury Vx 400 MHz, where chemical shifts were determined with respect to tetramethylsilane (TMS) as an internal reference. THF-SEC-measurements were performed on a Shimadzu-system with two Agilent Technology columns in series (PLgel 5 mm mixed C [200–2 000 000Da] and PLgel 5 mm mixed D [200–40 000 Da]) and equipped with a RI detector (Shimadzu RID-10A) and a PDA detector (Shimadzu SPD-M10A), with THF as eluent at a constant flowrate of 1.0 mL min^{-1}. The system was calibrated with polystyrene (PS) samples with a range of 580–100,000 Da (Polymer Laboratories).

Synthesis of compound 5.1

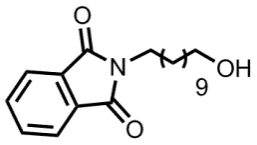

11-Bromo-1-undecanol (11.5 g, 45.8 mmol) and potassium phthalimide (11.0 g, 59.0 mmol) were dissolved in DMF (200 ml) and heated at 70ºC under argon overnight. The crude solution was evaporated, redissolved in EtOAc and washed with water (x2) and brine (x3). The organic phase was dried with $MgSO_4$ and evaporated in vacuo, to yield the product as a white solid (11.2 g, 77%). ^{1}H-NMR (400 MHz, Chloroform-*d*): δ 7.84 (d-d, 2H, *J* = 3.2 Hz, aromatic), 7.71 (dd, 2H, *J* = 3.2 Hz, aromatic), 3.67 (t, 2H, *J* = 7.2 Hz, CH_2N), 3.63 (t, 2H, *J* = 5.6 Hz, CH_2OH), 1.67 (t, 2H, *J* = 7.2 Hz), 1.56 (t, 2H, *J* = 5.6 Hz) 1.4-1.2 (m, 14H, aliphatic protons). The ^{1}H spectrum matches the literature.[36]

Synthesis of compound 5.2

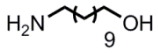

Compound **5.1** (24.5 g, 77.2 mmol) was dissolved in THF (200 ml) and hydrazine monohydrate (15.0 ml, 309.0 mmol) was added to the solution and the mixture was refluxed overnight under argon. The reaction crude was evaporated, suspended in chloroform and NaOH 1M and transferred to a separating funnel (this had to be done in three separate batches). Several washes with NaOH 1M were made, and the aqueous phase was reextracted with chloroform. The organic phase was dried with $MgSO_4$ and evaporated in vacuo to yield the product as a white solid (13.5 g, 93%). ^{1}H-NMR (400 MHz, Chloroform-*d*): δ = 3.6 (t, *J* = 6.6 Hz, 2H, CH2OH), 2.6 (t, *J* = 7 Hz, 2H, -CH_2NH_2), 1.6-1.0 (m, 18H, aliphatic protons).). The ^{1}H spectrum matches the literature.[36]

Synthesis of chiral BTA-OH, compound 5.3

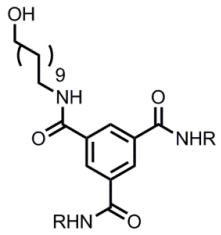

(S)-3,7-Dimethyloctan-1-amine (7.8 g, 49.7 mmol), **5.2** (4.7 g, 24.8 mmol) and triethylamine (13.7 g, 135.4 mmol) were dissolved in dry chloroform (300 mL) and put under argon. To this solution, while cooled with an ice bath, was added dropwise a solution of 1,3,5-benzenetricarbonyl trichloride (5.4 g, 20.2 mmol) in chloroform (50 mL). The mixture was left stirring overnight at room temperature. The crude was evaporated, redissolved in EtOAc and washed with HCl 1M (x2) and brine (x3). The organic phase was dried with $MgSO_4$ and evaporated in vacuo. The crude was purified by column chromatography ($CHCl_3$/EtOAc gradient of increasing polarity) Final product was obtained as a light yellow sticky solid (4.5 g, 34%). ^{1}H-NMR (400 MHz, Chloroform-*d*): δ 8.35 (s, 2H, aromatic), 8.33 (s, 1H, aromatic), 6.66 (t, J = 5.6 Hz , 3H, NH), 6.60 (t, J = 5.4 Hz , 2H, NH) 3.63 (t, J = 6.6 Hz, 2H, OCH_2), 3.48 (m, 6H, $NHCH_2$-, 1.8-0.8 (m-m, 38H, aliphatic protons). The ^{1}H spectrum matches the literature. [36]

Synthesis of achiral BTA-OH, compound 5.4

Hexylamine (4.6 g, 45 mmol), compound **5.2** (4.2 g, 22.5 mmol) and triethylamine (18.5 ml, 13.0 mmol) were dissolved in dry chloroform (300 ml) and put under argon. To this solution, while cooled to 0 °C, was added dropwise a solution of 1,3,5-benzenetricarbonyl trichloride (5 g, 18.76 mmol) in chloroform (50 ml). The mixture was left stirring overnight at room temperature. The crude was evaporated, redissolved in EtOAc and washed with HCl 1M (x2) and brine (x3). The organic phase was dried with $MgSO_4$ and evaporated in vacuo. The crude was purified by column chromatography ($CHCl_3$/EtOAc gradient of increasing polarity). Final product was obtained as a light yellow sticky solid (5.5 g, 54%). ^{1}H-NMR (400 MHz, Chloroform-*d*): δ 8.34 (s, 3H, aromatic), 7.47 (broad s, 3H, NH), 3.59 (t, J = 6.6 Hz, 2H, OCH_2-), 3.43 (m, 6H, -$NHCH_2$-), 1.8-0.8 (m-m, aliphatic protons). The ^{1}H spectrum matches the literature. [36]

Synthesis of chiral BTA-tosylate, compound 5.5

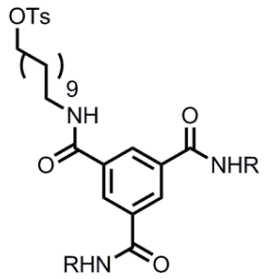

Compound **5.3** (2.0 g, 3.0 mmol) and triethylamine (0.9 ml, 6.1 mmol) were dissolved in dry DCM (40 ml) and this solution was cooled in an ice bath. A solution of tosyl chloride (870 mg, 4.6 mmol) in dry DCM (12 ml) was added dropwise and the solution was left stirring for 2 days at room temperature. The crude was washed with HCl 1M (x2) and brine (x3), dried with $MgSO_4$ and evaporated in vacuo. The crude mixture was purified by column chromatography (DCM/EtOAc gradient of increasing polarity). Final product was isolated as a slightly dark yellow sticky solid (2 g, 81 %). ^{1}H-NMR (400 MHz, Chloroform-*d*): δ 8.33 (s, 3H, aromatic), 7.78 (d, *J* = 7.9 Hz, 2H), 7.34 (d, *J* = 7.9 Hz, 2H), 6.7 (t, *J* = 5.6 Hz , 1H, NH), 6.65 (t, *J* = 5.4 Hz , 2H, NH), 4.01 (t, *J* = 6.5 Hz, 2H, OCH_2-) 3.47 (m, 6H, -$NHCH_2$-), 1.8-0.8 (m-m, 38H, aliphatic protons). The ^{1}H spectrum matches the literature. [36]

Synthesis of achiral BTA-tosylate, compound 5.6

Compound **5.4** (4 g, 7.3 mmol) and pyridine (2.4 ml, 29.8 mmol) were dissolved in dry DCM (100 ml) and this solution was cooled in an ice bath. A solution of tosyl chloride (1.8 g, 9.5 mmol) in dry DCM (50 mL) was added dropwise and the solution was left stirring for 2 days at room temperature. The crude was washed with HCl 1M (x2) and brine (x3), dried with $MgSO_4$ and evaporated in vacuo. The crude mixture was purified by column chromatography (DCM/EtOAc gradient of increasing polarity) Final product was isolated as a slightly dark yellow sticky solid (4.7 g, 92 %). ^{1}H-NMR (400 MHz, Chloroform-*d*): δ 7.99 (broad s, 3H, aromatic), 7.73 (d, *J* = 7.9 Hz, 2H), 7.30 (d, *J* = 7.9 Hz, 2H), 7.23 (broad s, 3H, NH), 3.97 (t, *J* = 6.5 Hz, 2H, OCH_2-) 3.24 (broad s, 6H, -$NHCH_2$-), 1.8-0.8 (m-m, aliphatic protons). The ^{1}H spectrum matches the literature. [36]

Synthesis of chiral BTA-phthalimide, compound 5.7

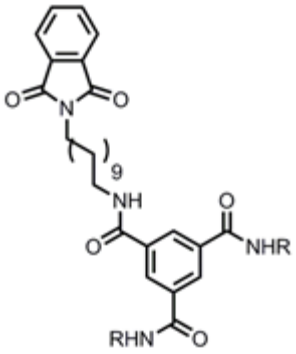

Compound **5.5** (1.9 g, 2.4 mmol) and potassium phthalimide (622 mg, 3.4 mmol) were dissolved in DMF (30 ml) and the solution was heated at 70 ºC overnight under argon. The crude solution was evaporated under vacuum, re-dissolved in EtOAc and washed with water (x2) and brine (x3). The organic phase was dried with $MgSO_4$ and evaporated in vacuo. The crude solid was purified by column chromatography (DCM/EtOAc gradient of increasing polarity) to obtain the desired product as a yellow solid (1.75 g, 93%). ^{1}H-NMR (400 MHz, Chloroform-*d*): δ = 7.78 (d, *J* = 8 Hz, 2H), 7.34 (d, *J* = 8 Hz, 2H), 7.30 (b, 3H, NH), 4.01 (t, *J* = 6.5 Hz, 2H, OCH_2), 3.26 (b, 6H, NH-CH2), 1.90 ~ 0.85 (m, 56H, aliphatic protons). The ^{1}H spectrum matches the literature. [21]

Synthesis of achiral BTA-phthalimide, compound 5.8

Compound **5.6** (1.4 g, 2 mmol) and potassium phthalimide (407 mg, 2.2 mmol) were dissolved in DMF (30 mL) and the solution was heated at 70ºC overnight under argon. The crude solution was evaporated in vacuo, redissolved in EtOAc and washed with water (x2) and brine (x3). The organic phase was dried with $MgSO_4$ and evaporated in vacuo. The crude solid was purified by column chromatography (DCM/EtOAc gradient of increasing polarity) to obtain the desired product as a yellow solid (1.3 g, 93%). ^{1}H-NMR (400 MHz, Methanol-d_4): δ = 8.38 (s, 3H), 7.85 (m, 7H), 7.30 (b, 3H, NH), 4.61 (broad s, 8H) 1.90 ~ 0.85 (m, aliphatic protons). The ^{1}H spectrum matches the literature. [36]

Synthesis of chiral BTA-NH_2, compound 5.9

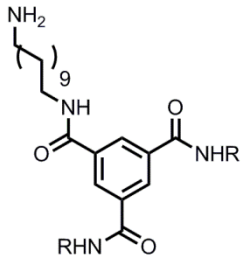

Compound **5.7** (1.8 g, 2.2 mmol) was dissolved in THF (50 mL) and hydrazine monohydrate (4.0 mL, 90 mmol) was added to the solution and the mixture was refluxed overnight under argon. The crude solution was evaporated and re-dissolved in chloroform and NaOH 1M. The organic phase was washed with NaOH 1M (x2) and brine (x3), and the aqueous phase was re-extracted with chloroform (x2). The combined organic phases were dried with $MgSO_4$ and evaporated in vacuo to yield the pure product as a light green sticky solid (1.4 g, 96%). ^{1}H-NMR (400 MHz, Chloroform-*d*): δ = 8.17 (b, 3H, aromatic), 7.32 (broad triplet, 1H, NH), 7.27 (broad triplet, 2H, NH), 3,41 (m, 6H, NH-CH_2), 2.67 (b, 2H, NH_2-CH_2), 1.78 ~0.85 (m, 56H, aliphatic protons). The ^{1}H spectrum matches the literature. [21]

Synthesis of achiral BTA-NH_2, compound 5.10

Compound **5.8** (1 g, 1.4 mmol) was dissolved in THF (50 mL). Hydrazine monohydrate (4 mL, 90 mmol) was added to the solution and the mixture was refluxed overnight under argon. The crude solution was evaporated, and re-dissolved in chloroform and NaOH 1M. The organic phase was washed with NaOH 1M (x2) and brine (x3), and the aqueous phase was reextracted with chloroform (x2). The combined organic phases were dried with $MgSO_4$ and evaporated in vacuo to yield the pure product as a light green sticky solid (750 mg, 97%). ^{1}H-NMR (400 MHz, Chloroform-*d*): δ = 7.9 (broad singlet, 3H, aromatic), 7.84 (broad singlet, 3H, NH), 3,41 (m, 6H, NH-CH_2), 2.67 (b, 2H, NH_2-CH_2), 1.78 ~0.85 (m, 56H, aliphatic protons). The ^{1}H spectrum matches the literature. [36]

Synthesis of compound 5.11

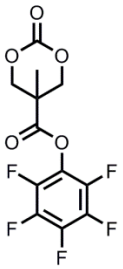

3-Hydroxy-2-(hydroxymethyl)-2-methyl propionic acid (3.0 g, 22.4 mmol), bis(pentafluorophenyl) carbonate (22.0 g, 55.9 mmol) and cesium fluoride (680 mg, 4.5 mmol) were dissolved in dry THF and stirred overnight under argon. The THF was removed in vacuo, and the solid crude was dissolved in DCM. A white precipitate appeared (this being pentafluorophenol), and it was filtered off before evaporating in vacuo the DCM. Hexane was added to the crude reaction mixture, and then decanted (it obtains a pink coloration in the process). The remaining solid was dissolved in DCM, washed with $NaHCO_3$ (x2), brine (x2), dried with $MgSO_4$, and the organic phase evaporated in vacuo to obtain a slightly pink solid. This solid was purified by recrystallization in a mixture of EtOAc and hexane to obtain the final product as a white solid (4.8 g, 67%) ^{1}H-NMR (400 MHz, Chloroform-d): δ = 4.85 (d, J = 11.0 Hz, 2H), 4.38 (d, J = 11.0 Hz, 2H), 1.55 (s, 3H). The ^{1}H spectrum matches the literature. [28]

Synthesis of precursor-polycarbonate P0

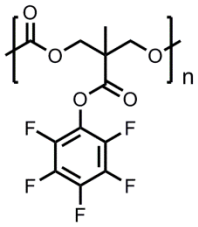

The reaction was carried out inside a glove-box. The cyclic carbonate monomer (**7**) (1.0 g, 3.07 mmol) and 4-methylbenzyl alcohol (3.0 mg, 0.03 mmol) were dissolved in DCM (2 mL). Trifluoromethane sulfonic acid (3.9 mg, 0.026 mmol) was weighed with the tip of a pipette in a separate vial, dissolved in DCM (1 mL) and added to the monomer mixture. The vial was capped, and the insoluble slurry was left stirring until it went completely into solution (24-48 h). The vial was extracted from the glove-box, and the solution was precipitated in cold ether, centrifuged and

decanted. This process was repeated twice. The final solid was dissolved in DCM, transferred to a vial and dried in the vacuum oven overnight at 60ºC to yield the final compound as a crunchy white-pink solid (950 mg, 95%). ^{1}H-NMR (400 MHz, Chloroform-*d*): δ = 4.48 (s, 4H), 1.51 (s, 3H). M_n = 30.4 kDa. *Đ* = 1.05. The ^{1}H spectrum matches the literature.[28]

General procedure for the synthesis of Series 1 polymer materials.

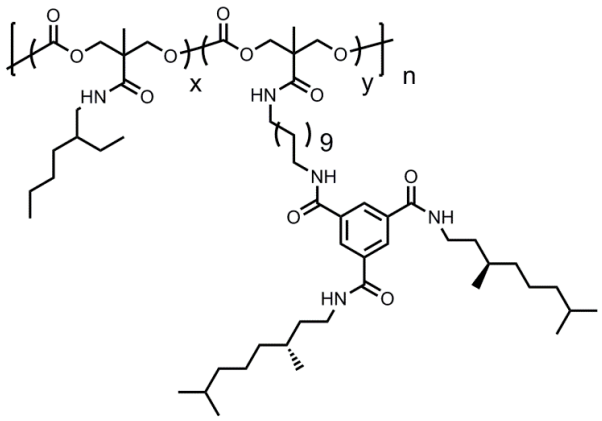

P0 (100 mg, 0.315 mmol) was dissolved in dry THF (4 mL) and left stirring under argon. BTA-amine (see table below) and DIPEA (48 mg, 0.378 mmol) were dissolved in dry THF (2 mL) in a vial and added dropwise to the polymer solution. The mixture was stirred at room temperature under argon for 1-2 h. After this time, 2-ethylhexyl amine (48 mg, 0.378 mmol) was dissolved in dry THF (1 ml) in a vial and added dropwise to the polymer solution. The mixture was stirred at room temperature under argon for 2-3 h. The crude solution was precipitated in cold ether, centrifuged and decanted. This process was repeated twice. The final solid was dissolved in DCM, transferred to a vial and dried in the vacuum oven overnight at 60ºC to yield the final compound as a flaky yellow solid (appearance dependent on BTA content).

Table S1: Series 1 functionalization

Polymer	Eq. of BTA[1]	m BTA (mg)	Mmol	% BTA[2]
P1	0	0	0	0
P2	0.05	10.3	0.016	3
P3	0.07	14.5	0.022	7
P4	0.1	20.7	0.032	9
P5	0.15	29.0	0.044	14
P6	0.2	33.1	0.050	16

[1] Number of equivalents of BTA-NH_2 added to the reaction mixture with respect to the repeat monomeric unit of the polycarbonate precursor. [2] Percentage of functionalization achieved determined by ^{1}H-NMR and confirmed by THF-GPC.

Figure S1: Example ^{19}F NMR (400 MHz, Chloroform-*d*, 298 K) of a polymer from Series 1, showing that amine functionalization went to completion and no pentafluorphenol groups were still appended on the polymer backbone

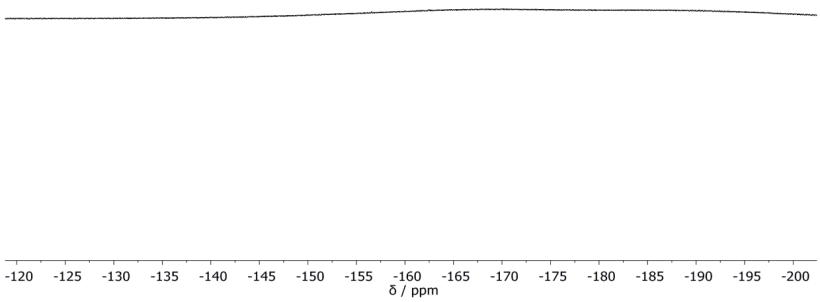

Figures S2-S5: ^{1}H NMR (400 MHz, Chloroform-*d*, 298 K) of polymer Series 1.

P2

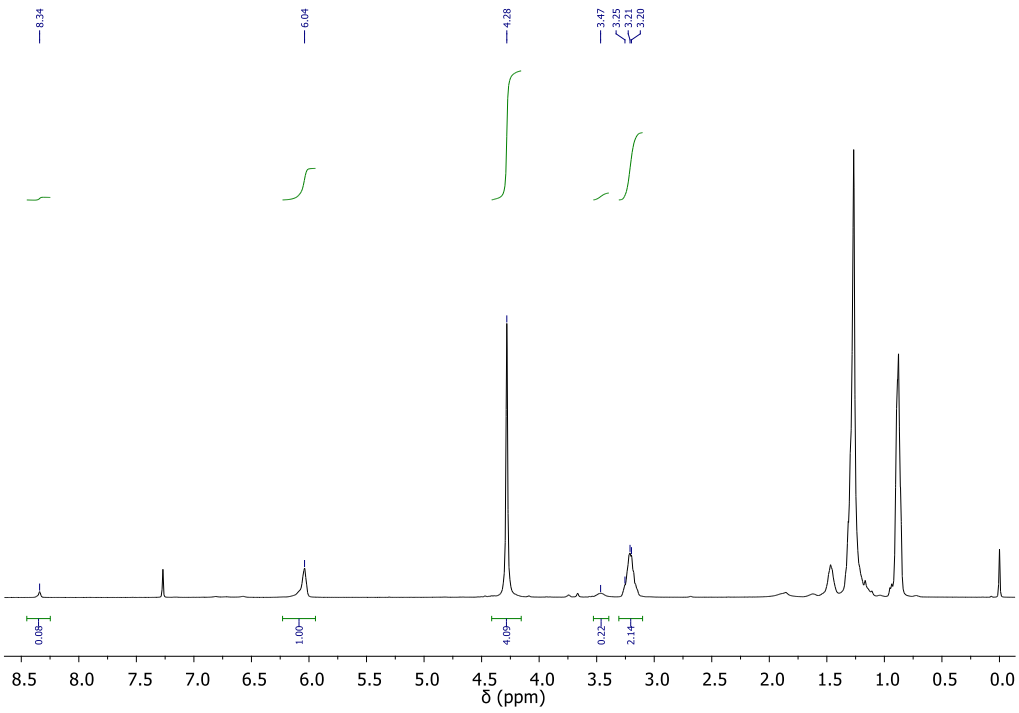

P3

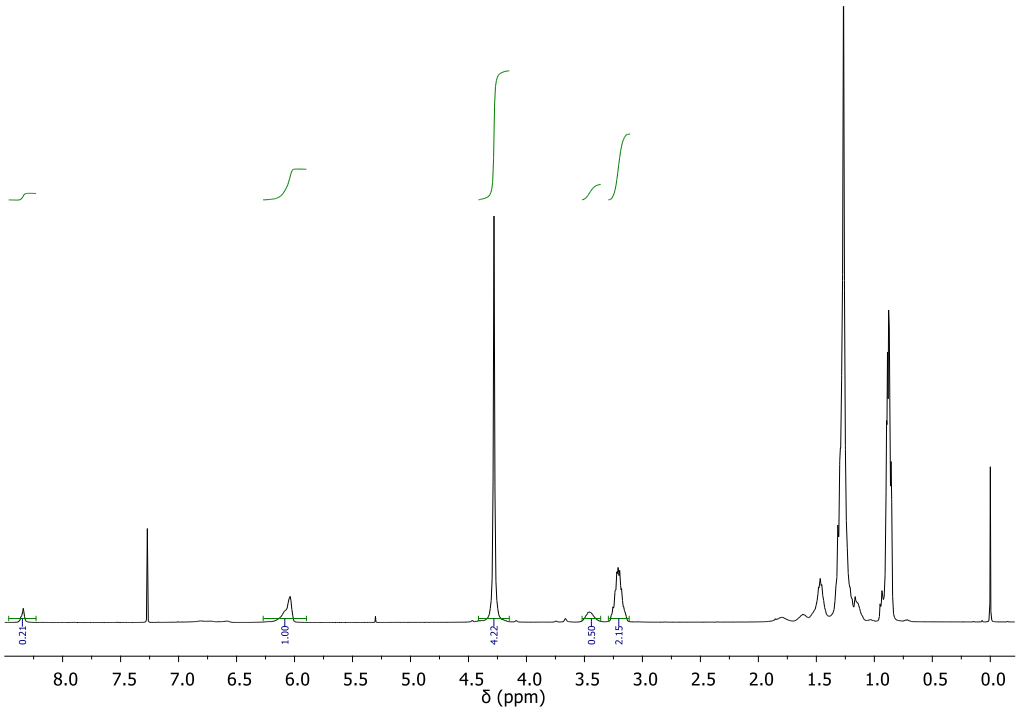

P4

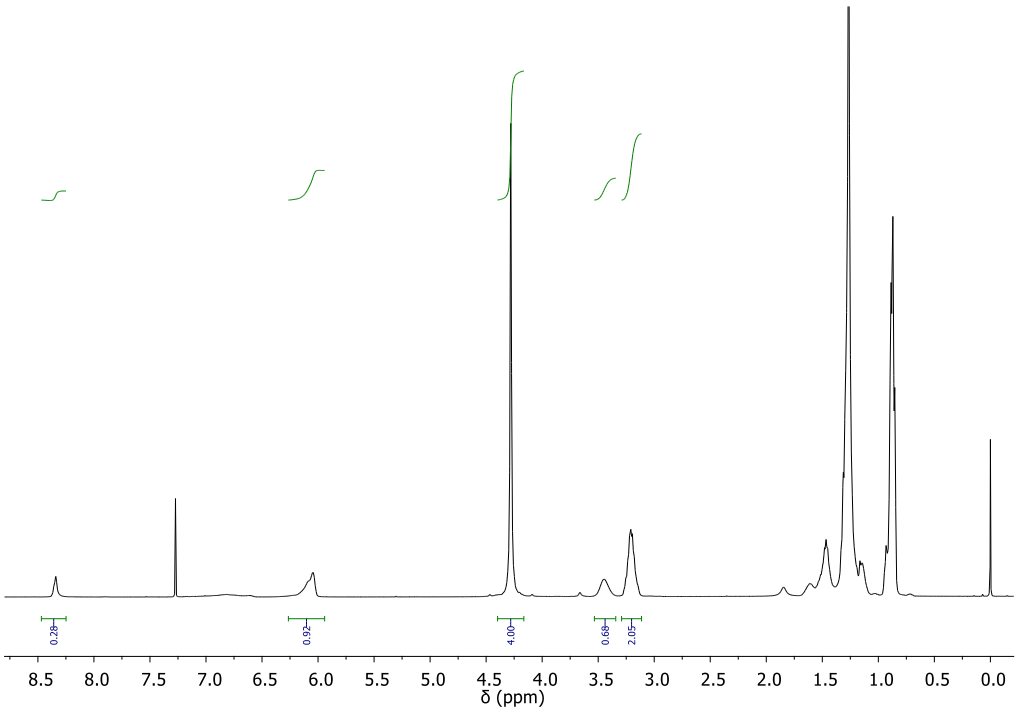
0.28
0.92
4.00
0.68
2.05
8.5 8.0 7.5 7.0 6.5 6.0 5.5 5.0 4.5 4.0 3.5 3.0 2.5 2.0 1.5 1.0 0.5 0.0
δ (ppm)

P5

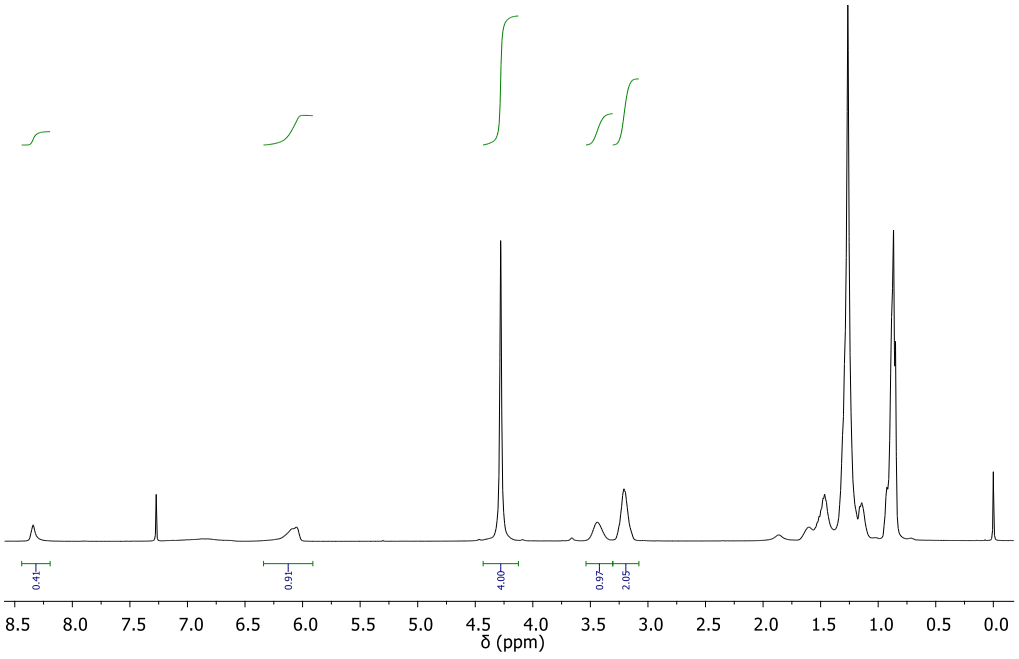
0.41
0.91
4.00
0.97
2.05
8.5 8.0 7.5 7.0 6.5 6.0 5.5 5.0 4.5 4.0 3.5 3.0 2.5 2.0 1.5 1.0 0.5 0.0
δ (ppm)

Figures S6-S9. CD spectra of Polymer Series 1 in MCH/DCE mixtures, recorded at 298 K.

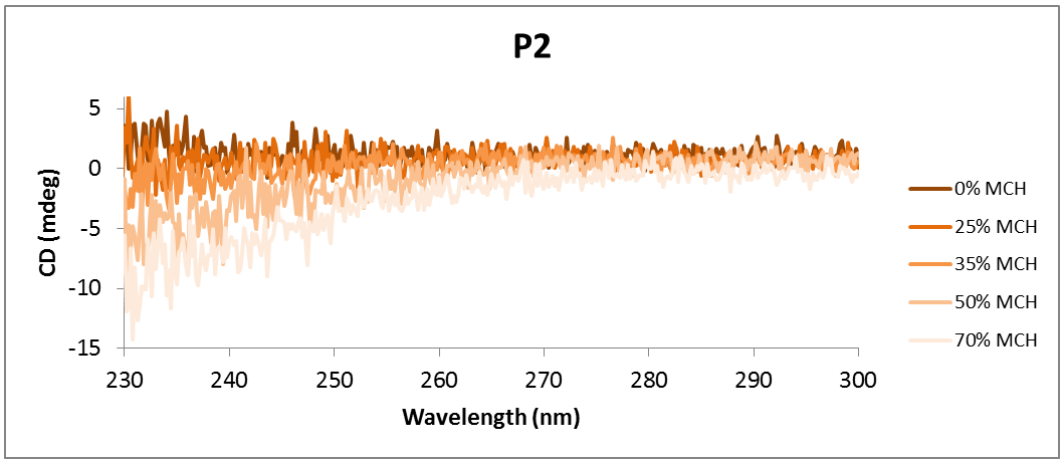

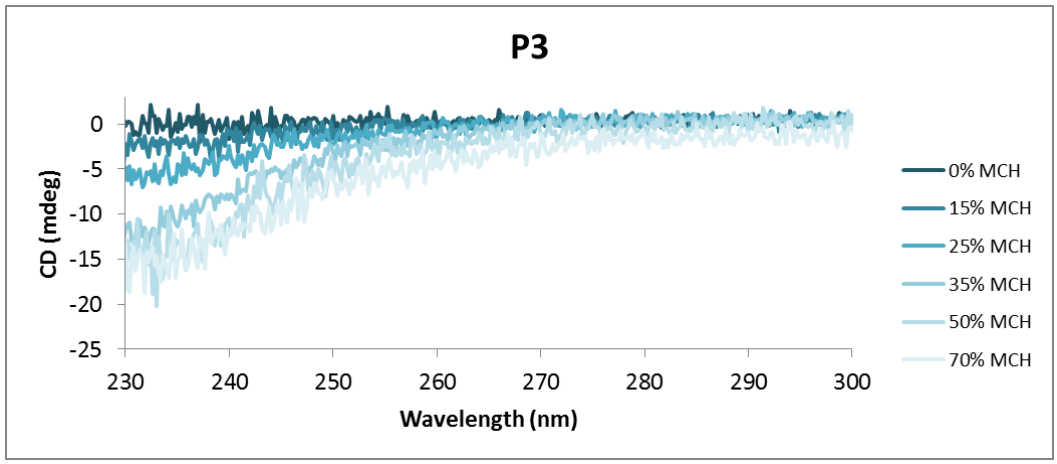

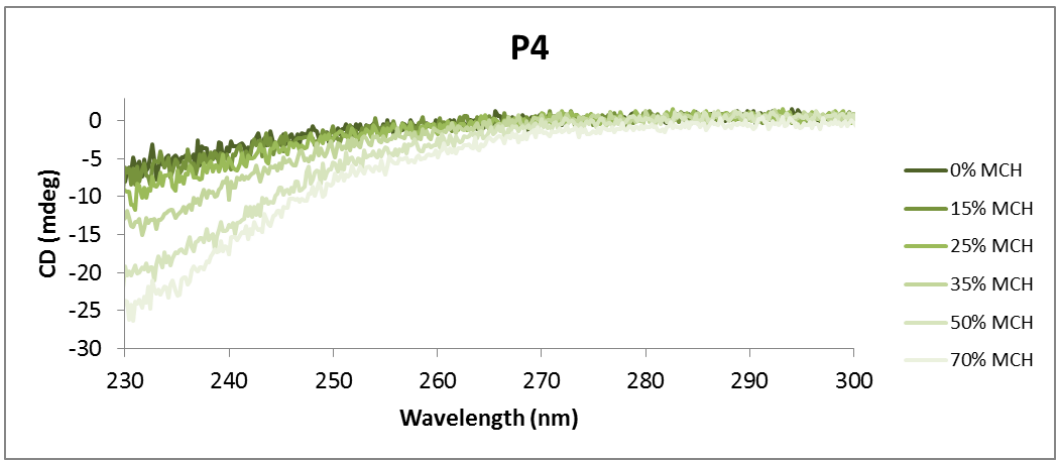

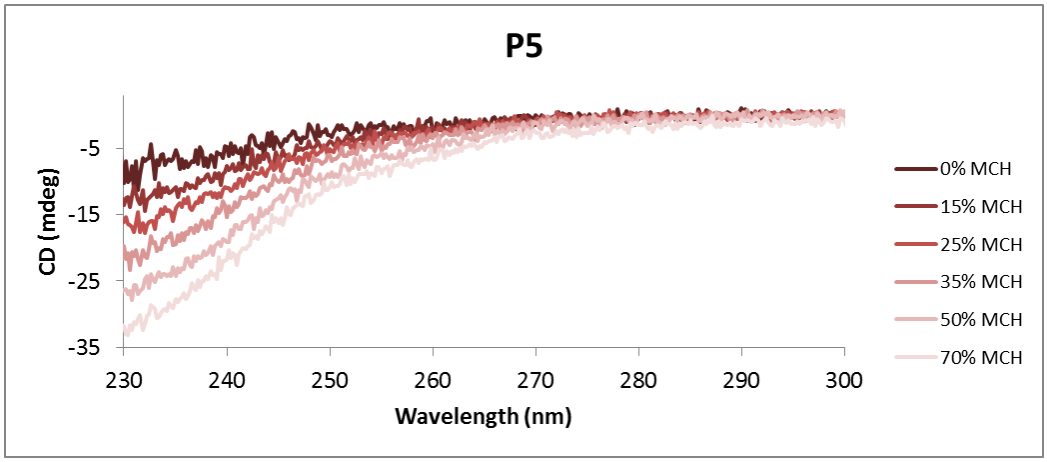

General procedure for the synthesis of Series 2 polymer materials.

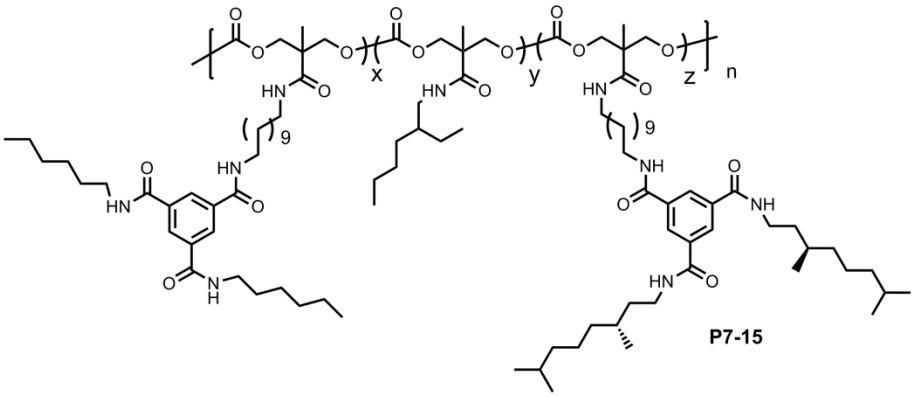

P0 (50 mg, 0.16 mmol) was dissolved in dry THF (2 mL) and left stirring under argon. Chiral and achiral BTA-amine mixtures (see table below) and DIPEA (24 mg, 0.19 mmol) were dissolved in dry THF (1ml) in a vial and added dropwise to the polymer solution. The mixture was stirred at room temperature under argon for 1-2 h. After this time, 2-ethylhexyl amine (24 mg, 0.19 mmol) was dissolved in dry THF (1 ml) in a vial and added dropwise to the polymer solution. The mixture was stirred at room temperature under argon for 2-3 h. The crude solution was precipitated in cold ether, centrifuged and decanted. This process was repeated twice. The final solid was dissolved in DCM and dried in the vacuum oven overnight at 60 ºC to yield the final compound as a flaky yellow solid (appearance dependent on BTA content).

Table S2. Series 2 functionalization.

Polymer	Eq. of chiral BTA[1]	m chiral BTA (mg)	Eq. of achiral BTA[1]	m chiral BTA (mg)	Total BTA functionalization[2]
P7	0.01	1.1	0.09	7.8	9%
P8	0.02	2.1	0.08	7.0	8%
P9	0.03	3.2	0.07	6.1	7%
P10	0.04	4.2	0.06	5.2	7%
P11	0.05	5.3	0.05	4.4	7%
P12	0.06	6.3	0.04	3.5	9%
P13	0.07	7.3	0.03	2.6	9%
P14	0.08	8.4	0.02	1.7	7%
P15	0.09	9.4	0.01	0.9	8%

[1] Number of equivalents of BTA-NH_2 added to the reaction mixture with respect to the repetitive monomeric unit of the polycarbonate precursor. [2] Percentage of functionalization achieved determined by ^{1}H NMR and confirmed by THF-GPC.

Table S3: Molecular weight and polydispersity obtained by THF GPC (40ºC)

	$M_{n,\,GPC}$[a] (kDa)	$Đ$[a]
P0’	10.4	1.13
P7	10.5	1.16
P10	11.7	1.10
P12	11.7	1.10
P15	12.4	1.09

	$M_{n,\,GPC}$[a] (kDa)	$Đ$[a]
P0	38.0	1.05
P8	33.7	1.05
P9	33.4	1.05
P11	30.8	1.09
P13	30.7	1.09
P14	29.5	1.12

[a] Analyzed with GPC in THF at 40ºC using PS standards.

Note: Some experiments had to be repeated and a second **P0’** with a different M_n was used. This did not affect the overall conclusion of the experiment since the Cotton Effect of a polymeric material is indifferent to the DP of the material. The percentage of chiral BTA within the chain is what determines CD signal strength.[37]

Figure S10. CD spectra of Polymer Series 2 in MCH/DCE 70/30 v/v, recorded at 298 K.

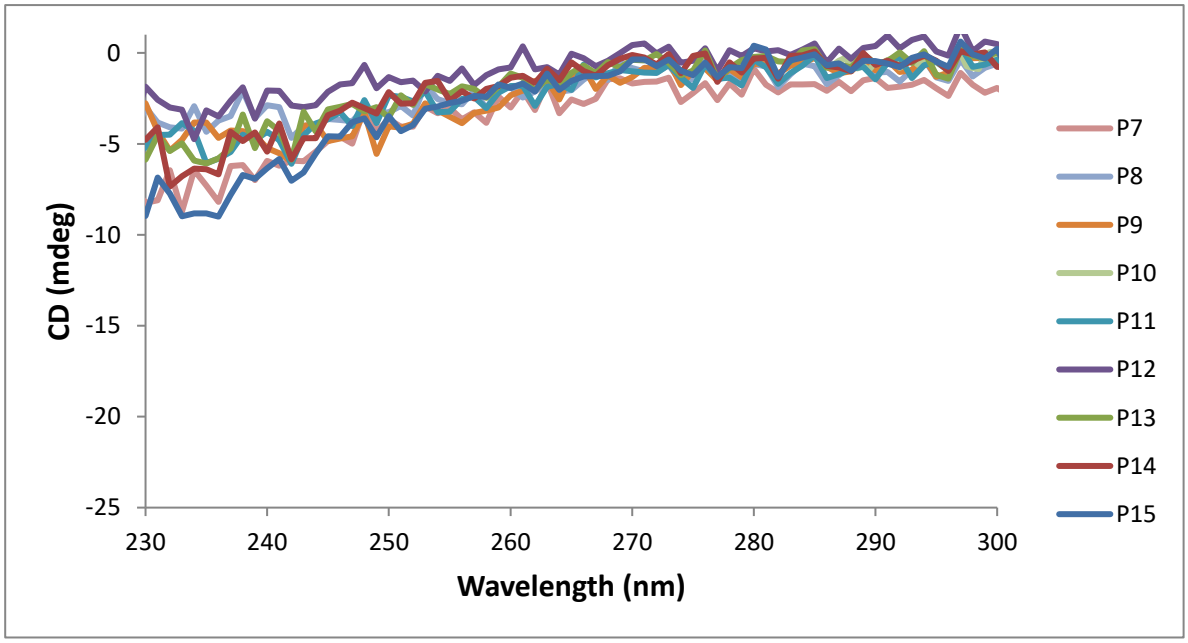

Total helicity calculation

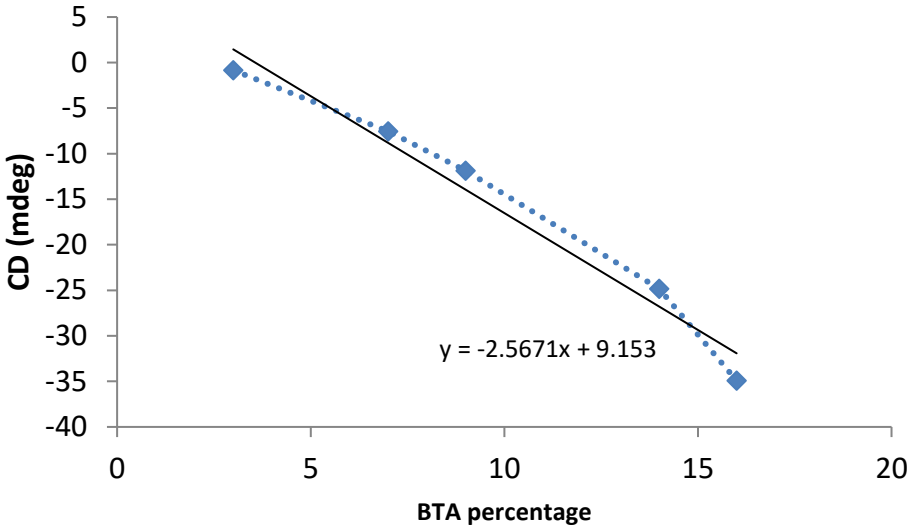

Figure S11. Calibration curve relating the amount of chiral BTA present in a polymer chain and the Cotton Effect observed at 230 nm.

Table S4. Total helicity calculation.

Polymer ID	Total BTA functionalization[2]	Cotton Effect observed (234 nm)	Expected Cotton Effect for 100% chiral BTA (mdeg)	Total helicity
P7	8%	-0.47	-10.7	0.043925234
P8	8%	-2.93657	-10.7	0.274445794
P9	9%	-3.82958	-11.86	0.32289882
P10	9%	-5.28502	-11.86	0.445617201
P11	7%	-4.28569	-7.56	0.566890212
P12	7%	-4.74205	-7.56	0.627255291
P13	8%	-5.91387	-10.7	0.552698131
P14	8%	-6.36661	-10.7	0.59501028
P15	9%	-8.82788	-11.86	0.744340641

5.8 Bibliography

[1] A. W. Bosman, H. M. Janssen and E. W. Meijer, *Chem. Rev*., 1999, 99, 1665–1688.

[2] C. B. Anfinsen, *Science*, 1973, 181, 223-231.

[3] C. M. Dobson, *Nature*, 2003, 426, 884-890.

[4] G.Guichard, G., Huc, I., *Chemical Communications*, 2011, 47, 5933-5941.

[5] Dennis E. Discher and Adi Eisenberg, *Science*, 2002, 297, 967-973.

[6] E. Stross, G. Iadevaia, D. Núñez-Villanueva and C. A. Hunter, *J. Am. Chem. Soc.*, 2017, 139, 12655-12663.

[7] M. I. Sadowski and D. T. Jones, *Current Opinion in Structural Biology*, 19, 2009, 357-362.

[8] J.-F. Lutz, M. Ouchi, D. R. Liu and M. Sawamoto, *Science*, 2013, 341.

[9] J.-F. Lutz, *Macromol*. *Rapid Commun*. 2017, 38, 170058.

[10] S. Mavila, O. Eivgi, I. Berkovich and N. G. Lemcoff, *Chem. Rev*. 2016, 116, 878−961

[11] M. Ouchi, N. Badi, J.-F. Lutz and M. Sawamoto, *Nat. Chem*., 2011, 3, 917–924

[12] M. Artar , E. Huerta , E. W. Meijer , A. R. A. Palmans , in *Sequence-Controlled Polymers: Synthesis, Self-Assembly, and Properties*, American Chemical Society , USA, 2014 , p. 313.

[13] E. Harth, B. Van Horn, V. Y. Lee, D. S. Germack, C. P. Gonzales, R. D. Miller and C. J. Hawker, *J. Am. Chem. Soc*., 2002, 124, 8653–8660.

[14] C. F. Hansell, A. Lu, J. P. Patterson, and R. K. O'Reilly, *Nanoscale* 2014, 6, 4102−4107.

[15] B. S. Murray and D. A. Fulton, *Macromolecules*, 2011, 44, 7242–7252.

[16] A. W. Jackson , and D. A. Fulton , *Polym. Chem*. 2013 , 4, 31-45.

[17] E. J. Foster, E. B. Berda, and E. W. Meijer, *J. Am. Chem. Soc*. 2009, 131, 6964−6966.

[18] S. Cantekin, T. F. A. de Greef, and A. R. A. Palmans, *Chem. Soc. Rev.*, 2012, 41, 6125-6137.

[19] G. M. ter Huurne, L. N. J. de Windt, Y. Liu, E. W. Meijer, I. K. Voets, and A. R. A. Palmans, *Macromolecules,* 2017, 50, 8562-8569

[20] T. Mes, M. M. J. Smulders, A. R. A. Palmans, and E. W. Meijer *Macromolecules* 2010, 43, 1981-1991.

[21] Y. Liu, T. Pauloehrl, S. I. Presolski, L. Albertazzi, A. R. A. Palmans, and E. W. Meijer, *J. Am. Chem. Soc,* 2015, 137, 13096−13105.

[22] M. Artar, E. R. J. Souren, T. Terashima, E. W. Meijer, and A. R. A. Palmans, *ACS Macro Lett*. 2015, 4, 1099−1103

[23] Y. Liu, S. Pujals, P. J. M. Stals, T. Paulöhrl, S. I. Presolski, E. W. Meijer, L. Albertazzi, and A. R. A. Palmans, *J. Am. Chem. Soc,* 2018, 140, 3423-3433.

[24] M. A. J. Gillissen, I. K. Voets, E. W. Meijer, and A. R. A. Palmans, *Polym. Chem*. 2012, 3, 3166−3174.

[25] A. B. Benito, M. K. Aiertza, M. Marradi, L. Gil-Iceta, T. Shekhter Zahavi, B. Szczupak, M. Jiménez-González, T. Reese, E. Scanziani, L. Passoni, M. Matteoli, M. De Maglie, A. Orenstein, M. Oron-Herman, G. Kostenich, L. Buzhansky, E. Gazit, H.-J. Grande, V. Gómez-Vallejo, J. Llop and I. Loinaz, *Biomacromolecules,* 2016, 17, 3213–3221.

[26] P. J. M. Stals, M. A. J. Gillissen, R. Nicolaÿ, A. R. A. Palmans and E. W. Meijer, *Polym. Chem*., 2013, 4, 2584.

[27] M.L. Ślęczkowski, E.W. Meijer, and A.R.A. Palmans, *Macromol. Rapid Commun*., 2017, 38, 1700566.

[28] A. C. Engler, J. M. W. Chan, D. J. Coady, J. M. O'Brien, H. Sardon, A. Nelson, D. P. Sanders, Yi Y. Yang, and J. L. Hedrick *Macromolecules* 2013, 46, 1283-1290.

[29] Dove, A.P., *Chemical Communications*, 2008, 48, 6446-6470.

[30] Z. Y. Ong, D. J. Coady, J. P. K. Tan, Y. Li, J. M. W. Chan, Y. Y. Yang, and J. L. Hedrick, *J. Polym. Sci. Part A: Polymer Chemistry*, 2016, 54, 1029–1035.

[31] W. Chin, C. Yang, V. W. L. Ng, Y. Huang, J. Cheng, Y. W. Tong, Da. J. Coady, W. Fan, J. L. Hedrick, and Y. Y. Yang *Macromolecules* 2013, 46, 8797-8807.

[32] A. P. P. Kröger, and J. M. J. Paulusse, *Journal of Controlled Release*, 2018, 286, 326–347.

[33] J. H. K. K. Hirschberg, L. Brunsveld, A. Ramzi, J. A. J. M. Vekemans, R. P. Sijbesma, and E. W. Meijer, *Nature*, 2000, 407,167–170.

[34] N. Hosono, A. R. A. Palmans, and E. W. Meijer, *Chem. Commun*., 2014, 50, 7990-7993.

[35] M. M. J. Smulders, P. J. M. Stals, T. Mes, T. F. E. Paffen, A. P. H. J. Schenning, A. R. A. Palmans and E. W. Meijer, *J. Am. Chem. Soc*., 2010, 132, 620-626.

[36] T. Terashima, T. Mes, T. F. A. De Greef, M. A. J Gillissen, P. Besenius, A. R. A. Palmans, and E. W. Meijer, *J. Am. Chem. Soc*. 2011, 133, 4742-4745.

[37] P. M. Satals, M. A. J. Gillissent, T. F. E. Paffent, T. F. A de Greef, P. Lindner, E. W. Meijer, A. R. A. Palmans, I. Voets, *Macromolecules*, 2014, 47, 2947–2954.

"Laura! Clear out my schedule. I have to push a boulder up a hill and then have it roll over me time and time again with no regard for my well-being"

Princess Carolyn

6

Environmental Molecular Adaptation of Supramolecular Polymer Nanoparticles

6.1 Introduction

Shape, derived from sequence, determines function in the natural word. This was concluded decades ago by researchers like Perutz,[1] whose research on haemoglobin proved that among vertebrate species the tertiary and quaternary structures of the protein had remained pretty much the same between species, despite having suffered numerous amino acid replacements throughout evolution.

Scientists have tried to make synthetic mimics of natural systems for decades,[2-4] and in doing so have put a lot of emphasis on sequence control. Indeed, the field of polymer science has evolved towards obtaining perfectly defined macromolecules, from insertion of single monomer units[5] to more and more refined solid-phase strategies,[6] with Lutz spearheading the movement.[7-9] But in this pursuit of preparing artificial protein-like objects another strategy has gained traction over the past few years: the field of Single Chain Polymer Nanoparticles (SCPNs).[10-12]

In it, a polymer chain synthesized by a living polymerization technique folds on itself, or aggregates with other chains, via the interactions between units grafted along the chain. In doing so it creates a confined three-dimensional space. This well-defined space is reminiscent of the active sites found

in enzymes.[13] SCPNs have found some early applications as catalysts of organic reactions in aqueous media making use of such hydrophobic pockets created by the polymer folding.[14] Despite the SCPN field being relatively new, other promising applications, such as sensing,[15] or imaging[16] in the biomedical field, have been explored.

The nature of the folding interactions determines the type of SCPN created: i) covalent (with fixed or reversible bonds)[17-20] or ii) supramolecular.[21] Supramolecular SCPNs present the advantage of being dynamic and adaptable to their environment. The Meijer group has investigated the use of benzene-1,3,5-tricarboxamide (BTA), a chemical moiety that interacts with other BTA molecules via a three-fold hydrogen bond. When free in solution BTAs form columnar helices,[22] and when grafted to a polymeric chain they promote backbone folding in the process of forming the supramolecular stacks.[23] Researchers in the Meijer group have reported that topological differences in BTA-containing SCPNs affect the folding behavior, and that once the BTA is attached to the polymer chain there is very little communication between non-neighboring units on the same chain.[24] This lack of cooperativity reflects the formation of small stacks in individual domains along the chain.

The importance of shape, laid out by Anfinsen 45 years ago,[25] gave rise to the well-known "Thermodynamic Hypothesis", which claims that the three-dimensional structure of a protein in its native state in normal physiological conditions will be the one with the lowest Gibbs free energy. In other words, proteins fold in the most stable way possible. In this work we take inspiration from Anfinsen's dogma and we let the BTAs find the most thermodynamically stable conformation in different environmental conditions (Figure 6.1). By allowing BTA interactions to be the deciding factor on the final primary, secondary and tertiary structures of the system after post-functionalization, we create a polymeric material whose final characteristics will be dependent on the environment. The system will be able to adapt to the medium.

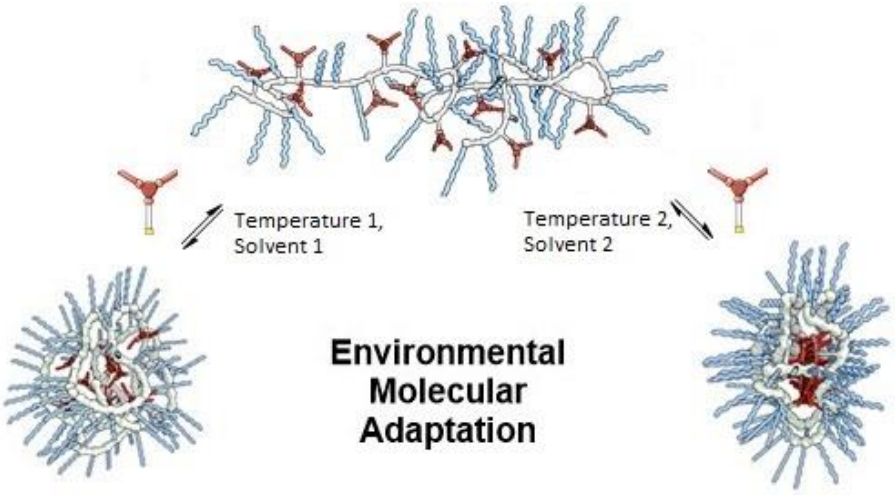

Figure 6.1. Schematic representation of a polymer chain being reversibly post-functionalized under different environmental conditions. Changes in temperature and solvent polarity affect the interactions between BTAs which gives raise to supramolecular systems with different characteristics. Red trigonal shapes represent BTAs, blue wavy lines represent solubilizing chains and white lines represent the polymer backbone.

To this effect, a polymer material was post-functionalized via the sequential addition of three different primary amines. One of them was a "fixed" BTA moiety that was irreversibly appended onto the backbone (Figure 6.2). After this, a proportion of "mobile" BTAs was incorporated onto the polymer in a reversible way, making use of dynamic covalent chemistry (Diels-Alder in this case).[26-27] The reversible incorporation was studied by means of ^{1}H NMR spectroscopy and circular dichroism (CD).[28] Once the chemistry was developed, some studies into molecular adaptation were conducted, varying the reaction conditions in which the "mobile" BTAs were incorporated (i.e. temperature and solvent polarity). This was done under the premise that "fixed" and "mobile" BTA will interact and form helical columns at a faster rate than the Diels Alder reaction, so changes in the conditions that affect the stacking will affect the final sequence and topology of the polymer.

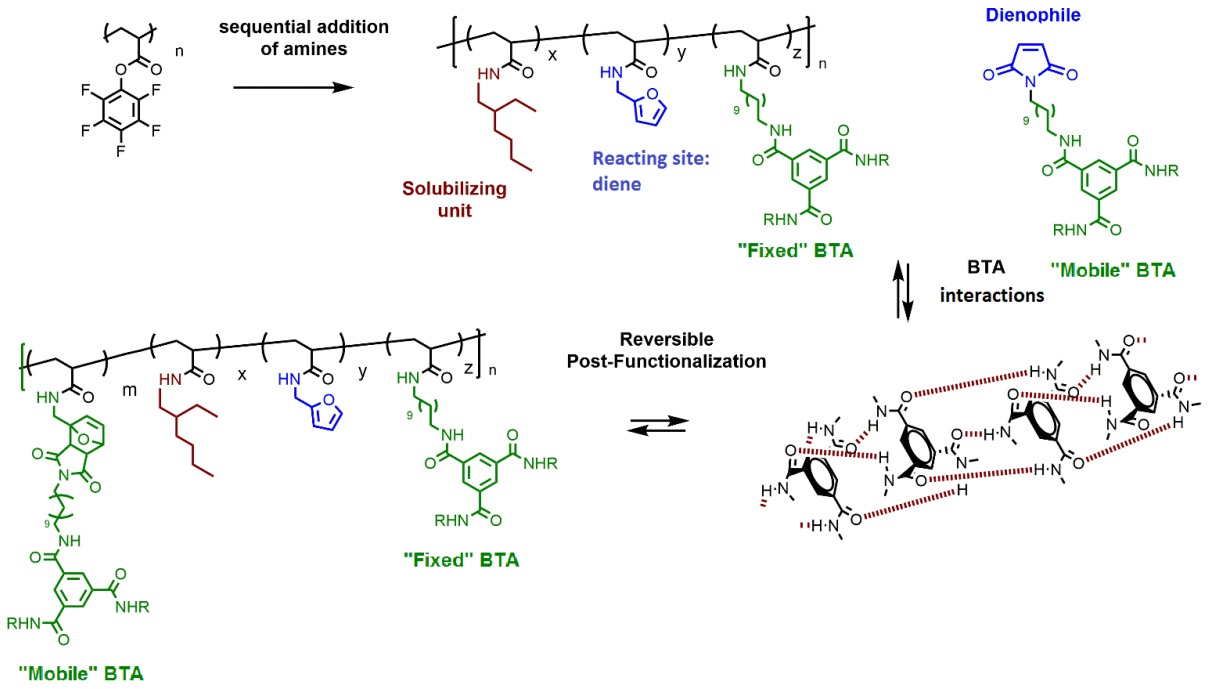

Figure 6.2. General strategy for the synthesis of supramolecular polymer nanoparticles with reversibly-attached BTA units. The polymer materials will comprise a solubilizing amine (red), a structural amine ("fixed" BTAs, green) and a reacting site for the reversible chemistry (diene, blue). "Mobile" BTAs will have a dienophile to react reversibly with the polymer backbone.

6.2 Polycarbonate backbone

We wanted to use the polycarbonate backbone studied in Chapter 5 to study the environmental molecular adaptation of polymer nanoparticles. To that effect, two series of polymers were synthesized following the same procedure laid out in Chapter 5 (Scheme 6.1). The polymer nanoparticles comprised three different modules: i) BTA-NH_2 with a chiral chain to make the system CD active and provide a structural unit that will promote the folding of the polymer chains (full synthesis and characterization provided in Chapter 5); ii) 2-ethylhexyl amine as solubilizing units for organic solvents; iii) and furfuryl amine to act as reacting site (diene) in the reversible Diels-Alder reaction with which the polymer will be post-functionalized. Two series of polymers were synthesized: series A (5% solubilizing unit), and Series B (20% solubilizing unit).

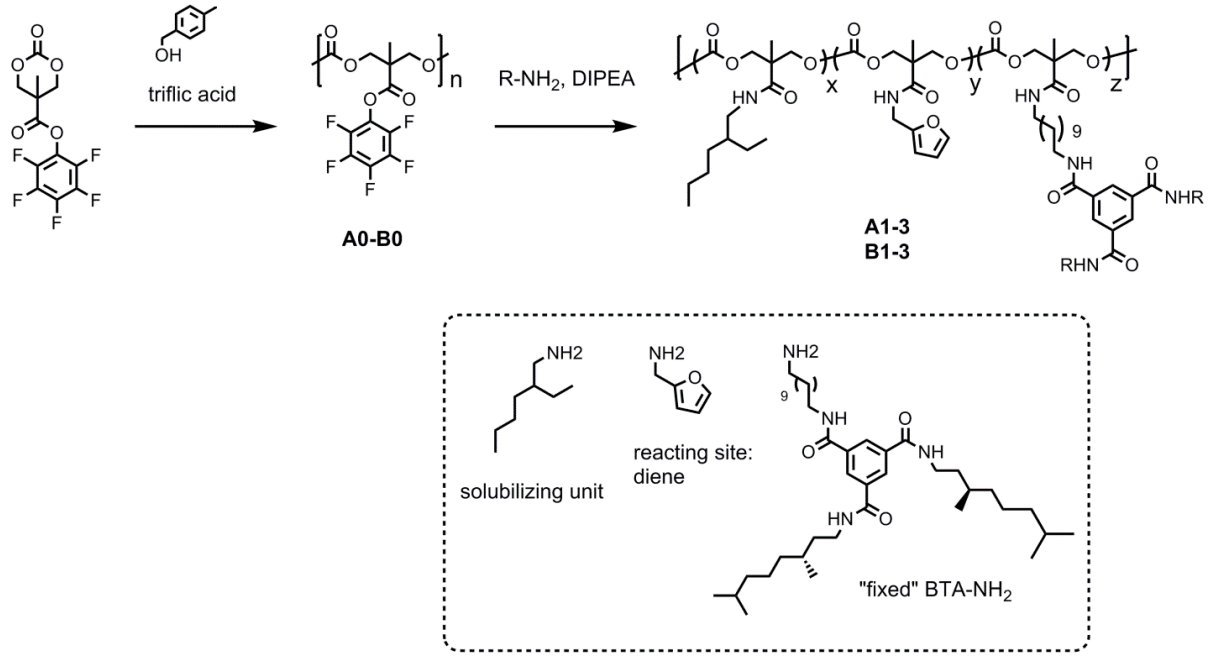

Scheme 6.1. Synthesis and post-functionalization of polymer Series A and B. Series A contains a 5% functionalization of solubilizing units. Series B contains a 20% functionalization of solubilizing units. The polymers are functionalized with variable BTA-NH_2 percentages, from 0% BTA (**A1** and **B1**) to 15 % BTA (**A3** and **B3**). Detailed polymer composition can be found in Table 6.1.

Both series of polymers were characterized by THF-GPC (Table 6.1, Figure 6.3), revealing that the very low polydispersity of the precursor polymer was maintained after the sequential functionalization. Detailed information about polymer composition and molecular weights can be found in Table 6.1.

Table 6.1. Composition, molecular weight and dispersity of polymer Series A and B.

Polymer	**x**	**y**	**z**	$M_{n,\,NMR}$[a] **(kDa)**	$M_{n,\,GPC}$[c] **(kDa)**	**Đ**[c]
A0	-	-	-	24.7[b]	20.4	1.09
A1	0.05	0.95	0	18.3	15.2	1.04
A2	0.05	0.90	0.05	21.2	17.4	1.08
A3	0.05	0.80	0.15	24.6	20.0	1.04
B0	-	-	-	37.8	30.4	1.05
B1	0.2	0.80	0	28.3	25.0	1.04
B2	0.2	0.75	0.05	31.8	26.8	1.07
B3	0.2	0.65	0.15	38.3	30.4	1.06

[a] Calculated from NMR integration with the DP of **A0** and **B0** being calculated from polymerization conversion and monomer to initiator ratio. Formula used:

$$Mn\ NMR = \sum \frac{DP\ (\boldsymbol{A0} - \boldsymbol{B0})\ x\ \%i\ x\ Mwi}{100}$$

[b] Calculated from polymerization conversion and monomer to initiator ratio.

[c] Analyzed with GPC in THF at 40ºC using PS standards.

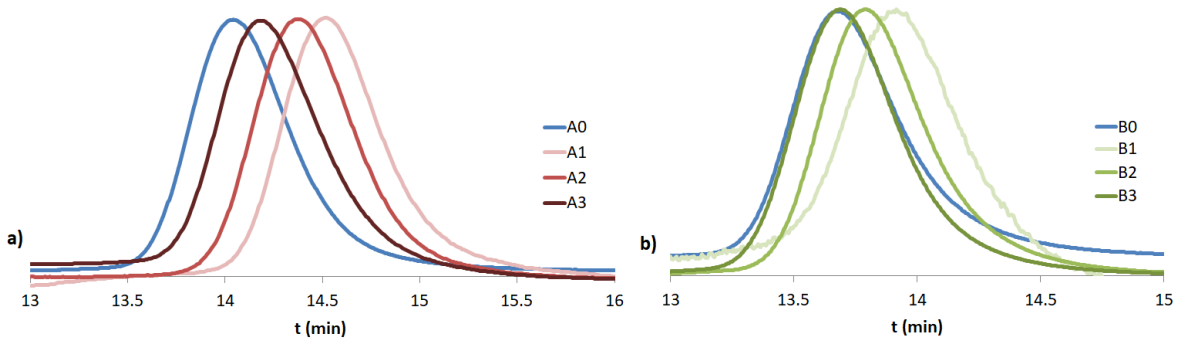

Figure 6.3. GPC traces of (a) Series A; and (b) Series B polymers. From highest BTA content (**A3**, darkest shade of red, and **B3**, darkest shade of green) to lowest content (**A1** and **B1**, lightest shade of red and green respectively). The precursor polymers **A0** and **B0** are colored blue.

^{1}H NMR spectroscopy provides an easy characterization of the exact polymer composition by integrating with respect to the backbone signal (**f**) at 4.28 ppm (4^{1}H) (Figure 6.4, Figures S1-S6). At around 8.34 ppm a broad signal appears (**a**) corresponding to the three protons of the BTA moiety. A second distinct signal from the BTA moiety comes from the six methylene protons that surround the BTA core, and it appears as a broad peak at 3.44 ppm (**g**). Signals coming from the furan recognition unit are the three alkene protons (**b**, **c** and **d**) at 7.31, 6.28 and 6.18 ppm respectively, and the CH_2-N protons at 4.4 ppm (**e**). The second signal from the backbone and the rest of the aliphatic signals from the 2-ethyl-hexyl units and the BTA side chains fall in the region between 0.5 and 1.7 ppm.

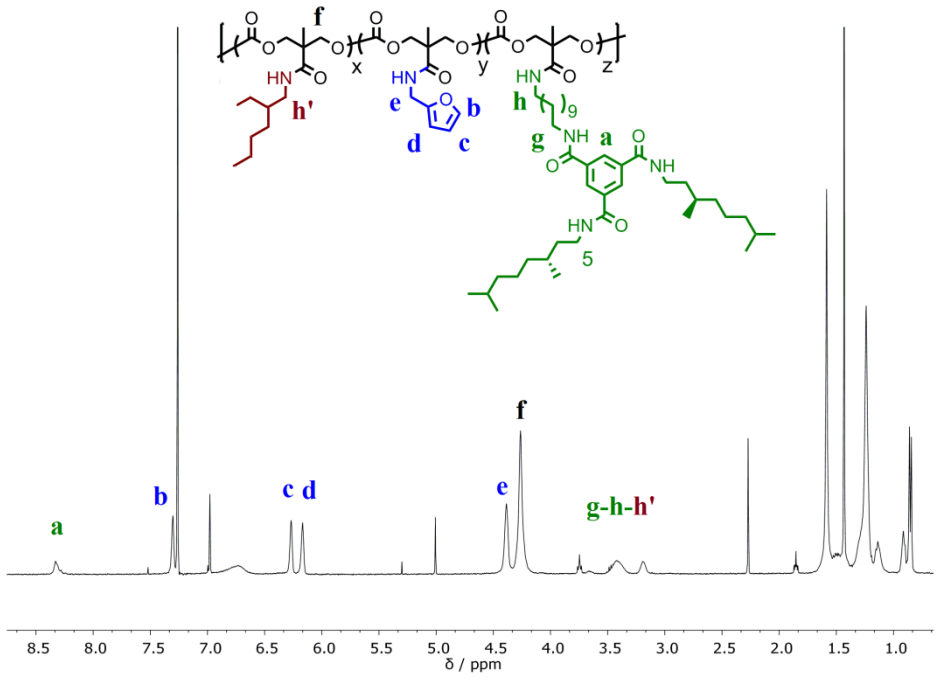

Figure 6.4. ^{1}H NMR (400 MHz, Chloroform-d, 298 K) spectrum of a polymer **B2**.

BTA-maleimide synthesis

BTA-maleimide **6.4** was synthesized by reacting BTA-tosylate **6.1** with compound **6.2** in DMF. This produced compound **6.3**, a BTA that was deprotected by performing a retro Diels-Alder at high temperature to obtain product **6.4** (Scheme 6.2).

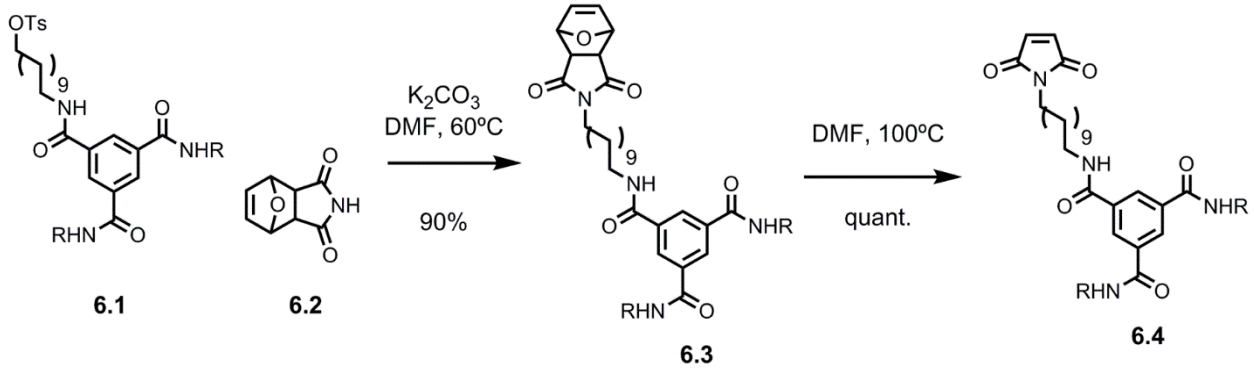

Scheme 6.2. Synthesis of BTA-maleimide **6.4**.

The post-functionalization of the polymer chains was achieved by mixing and heating **B1** and BTA-maleimide **6.4** at 50 ºC in THF to form **B4**. The reaction could be easily followed by ^{1}H NMR

spectroscopy, thanks to the appearance of the distinctive BTA aromatic protons at 8.4 ppm, while the rest of the signals remained unchanged (Figure 6.5).

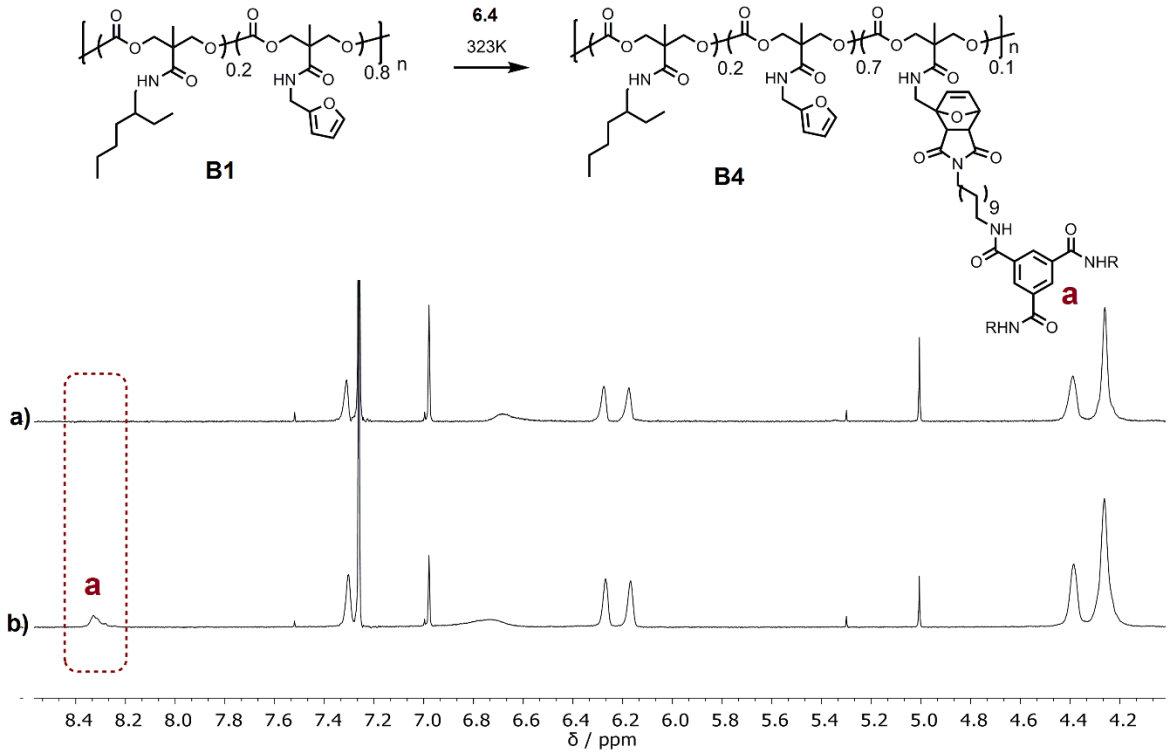

Figure 6.5: Post-functionalization of **B1** with BTA-maleimide **6.4**. ^{1}H NMR (400 MHz, Chloroform-d, 298K). Spectrum (a) shows the starting material **B1** and spectrum (b) depicts **B4** and the appearance of aromatic protons after the post-functionalization reaction.

This demonstrated that this polycarbonate backbone is a great scaffold for the synthesis of functional materials. The reversible introduction of different functional groups onto a polymer backbone offers the possibility of preparing materials with tunable properties.[29]

Unfortunately, none of the materials from Series A and Series B was soluble in solvent mixtures apolar enough to obtain a measurable Cotton Effect. The samples produced solutions that turned cloudy after sonication. This led to unreliable Cotton effect measurements. There were several possibilities to overcome this issue: i) increasing the percentage of solubilizing chains, which would in turn decrease the number of available reacting sites for the Diels-Alder process along the polymer backbone; ii) increasing the carbon count by modifying synthetically the furfuryl amine unit (i.e. longer alkylic chains would increase the polymers' solubility in organic solvents); iii) or changing the polymer backbone to one known to be more soluble.

We decided in favor of this last possibility and set out to synthesize equivalent molecules with an acrylate backbone.

6.3 Polyacrylate backbone

To create polyacrylate nanoparticles via post-functionalization reactions an acrylate precursor **C0** had to be synthesized (Scheme 6.3). First, the synthesis of the acrylate monomer **6.5** was achieved via the slow addition of a solution of acryloyl chloride in DCM into a solution of pentafluorophenol and triethylamine in DCM. **6.5** was then reacted via RAFT polymerization using AIBN as initiator and 4-cyano-4-((phenylcarbonothioyl)thio)pentanoic acid as chain transfer agent. After precipitation, a pink polymer **C0** with a DP of around 100 was obtained.

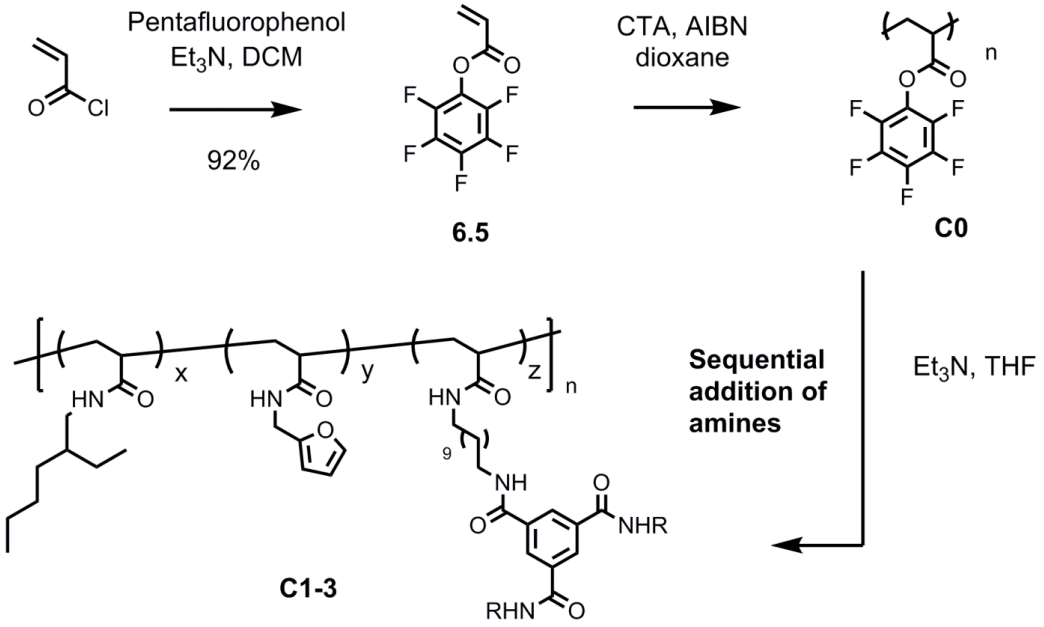

Scheme 6.3. Synthesis and post-functionalization of polymer Series C (20% solubilizing unit). The polymers are functionalized with variable BTA-NH_2 percentages, from 0% BTA (**C1**) to 15% BTA (**C3**). Detailed polymer composition can be found in Table 6.2.

C0 was post-functionalized in THF at 50 °C by the sequential addition of the three primary amines previously discussed: commercially available 2-ethylhexyl amine and furfuryl amine, and BTA-NH_2. Three polymers were made: **C1** (0% BTA, 20% solubilizing unit, 80% furan), **C2** (5% BTA, 20% solubilizing unit, 75% furan), **C3** (15% BTA, 20% solubilizing unit, 80% furan). All the samples were characterized by THF-GPC (Table 6.2, Figure 6.6). The polydispersity of the molecules in this polymer series was higher than those shown by the polycarbonate products in

Series A and B. This was particularly clear for **C1**, which appears to have a broad shoulder indicating a wider distribution of polymer lengths. The discrepancy between theoretical and experimental M_n can in principle be explained by the different nature of these acrylamide-derived materials, and the polystyrene standard used to calibrate the GPC.

Table 6.2: composition, molecular weight and dispersity of polymer Series C.

Polymer	**x**	**y**	**z**	$\boldsymbol{M}_{\mathbf{n,\ theoretical}}$ **(kDa)**	$\boldsymbol{M}_{\mathbf{n,\ GPC}}$[c] **(kDa)**	**Đ**[c]
C0	-	-	-	23.3[a]	16.0	1.16
C1	0.20	0.80	0	15.4[b]	10.7	1.32
C2	0.20	0.75	0.05	18.1[b]	14.7	1.27
C3	0.20	0.65	0.15	23.6[b]	13.7	1.25

[a] Formula used

$$Mn\ theoretical\ (\boldsymbol{C0}) = \left(\frac{[M]0}{[RAFT]0}\ x\ monomer\ conversion\ x\ Mw\ (monomer)\right) + Mw\ (RAFT\ agent)$$

[b] Calculated from monomer conversion (DP (**C0)**). Formula used:

$$Mn\ = \sum \frac{DP\ (\boldsymbol{C0})\ x\ \%i\ x\ Mwi}{100}$$

[c] Analyzed with GPC in THF at 40ºC using PS standards.

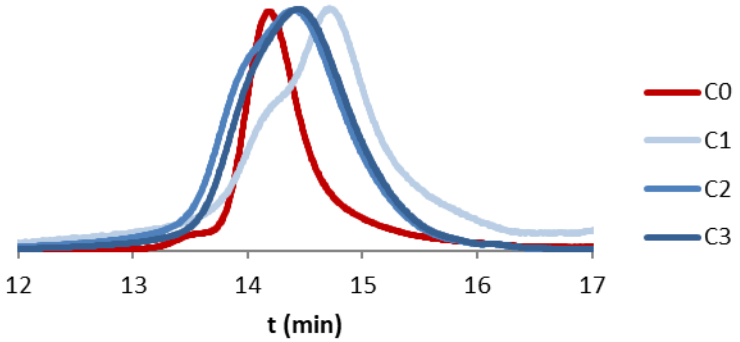

Figure 6.6. GPC traces of polyacrylate series. From highest BTA content (**C3**, darkest shade blue) to lowest content (**C1**, lightest). The precursor polymer **C0** is colored red.

The successive amine additions were monitored by ^{19}F NMR spectroscopy (Figure 6.7) to follow the incorporation of the amines and the release of pentafluorophenol. The precursor polymer presents broad signals, but as it is functionalized and the pentafluorophenol is released as a side product of the reaction, the decreasing broad peaks and the appearing sharp peaks can be compared. It is noteworthy the variation in chemical shift of the pentafluorophenol signals as it is released from the backbone. These signals are sensitive to environmental changes, such as polarity or concentration, and they have been seen to shift similarly in previous sequential postfunctionalizations. After the last functionalization step, when all the polymer chain has been reacted, only sharp signals are present. This pentafluorophenol must be removed from the crude solid by dialyzing in THF during a period of 72 hours, changing the solvent twice in the process. A final clean ^{19}F NMR spectrum indicates a successful functionalization and purification (i.e. there is no pentafluorophenol left appended on the backbone nor free in solution after the dialysis).

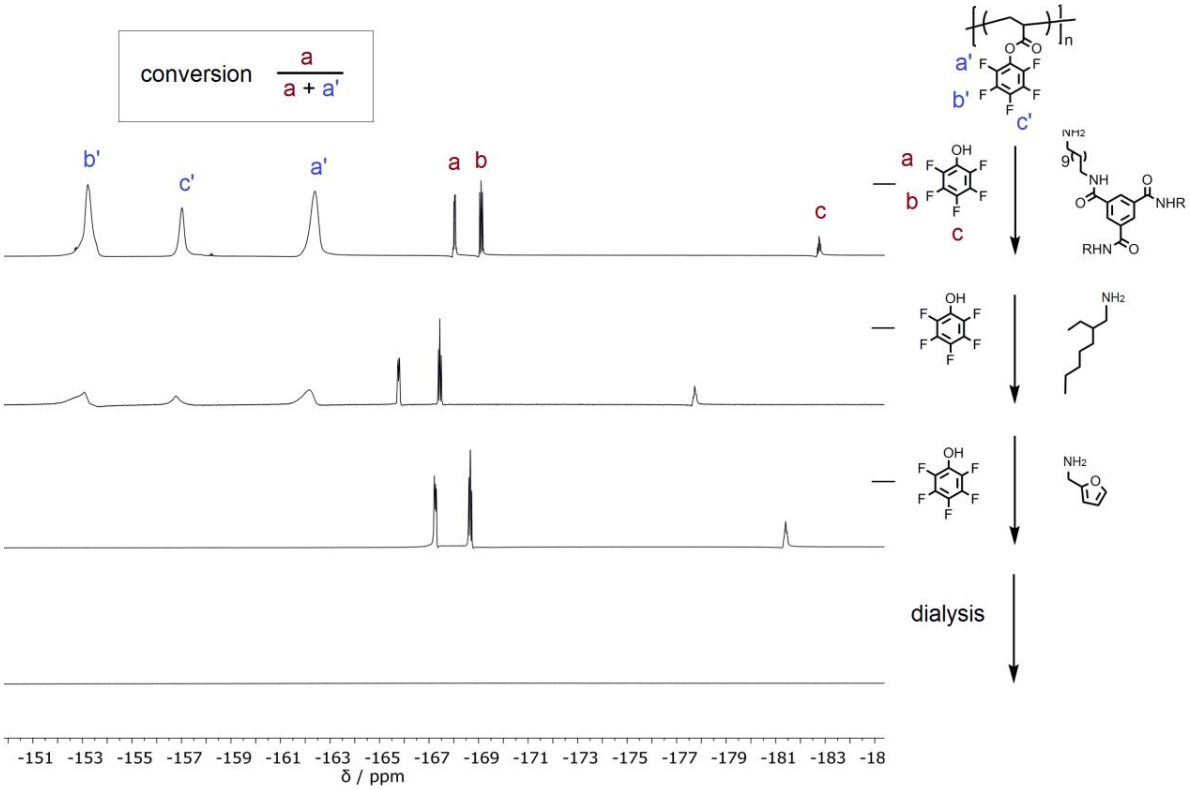

Figure 6.7. ^{19}F NMR spectra (400 MHz, Chloroform-d, 298 K) of the sequential amine additions onto **C0**.

This sequential functionalization could also be followed by IR spectroscopy (Figure 6.8). As was the case with the polycarbonate, we can observe the appearance of the carbonyl and N-H peaks from the amides, and the C-H from the side chains.

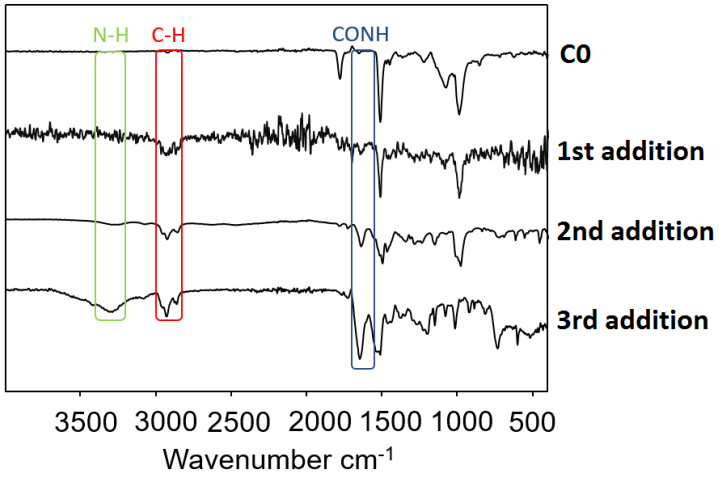

Figure 8. IR spectra of the sequential amine substitutions onto **C0**.

Unlike with polycarbonates, ^{1}H NMR spectroscopy of the acrylate derivatives only allows a qualitative characterization of the content of the polymer chain (Figure 6.9, Figures S7-S9). There are signals that can be assigned to the different moieties, but the integration is difficult due to their broadness and their overlap with other signals.

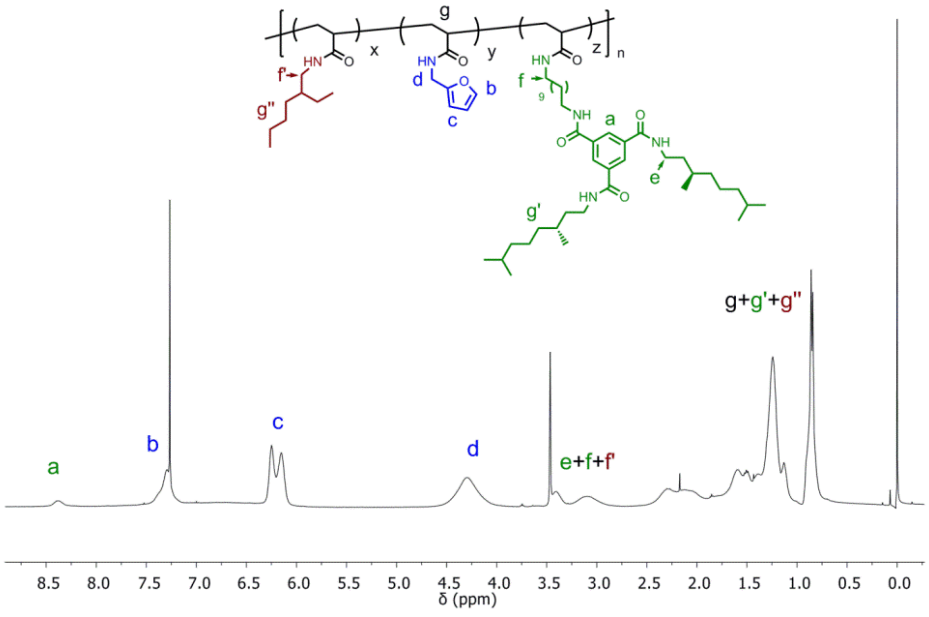

Figure 6.9. ^{1}H NMR (400 MHz, Chloroform-*d*, 298 K) spectrum of **C2**.

Reversible post-functionalization

To test the reversible addition of BTA-maleimide **6.4** onto the acrylate backbone, **C2** was reacted with 2 equivalents of **6.4** in chloroform at 50ºC. After 24 h, the mixture was precipitated in cold ether and analyzed by ^{1}H NMR spectroscopy (Figure 6.10a, Figure S10). There were two clear indicators that some functionalization had taken place: i) the appearance of a signal around 5.2 ppm that corresponds to the single proton of the furan-maleimide adduct; ii) and a proportional increase in the integral of the three aromatic protons of the BTA moiety. The extent of functionalization was unclear, though, since accurate proton integration is complicated in this system due to the broadness of the signals and the lack of a backbone signal that could be used as reference.

The samples for CD characterization were prepared following the procedure described in chapter 5. The solvent mixture for these measurements was MCH/DCE (70/30 v/v). The results of the measurements can be found in Figure 6.10b. **C2** gave a signal of just a few mdeg (blue trace). This was explained by its small BTA content. After the functionalization with BTA-maleimide **6.4** had taken place to form **C4**, the signal increased by several mdeg (yellow trace). This corroborated that some Diels-Alder reaction had occurred and that there were more BTA moieties present in the polymer backbone forming helical stacks. After heating **C4** in DMF at 95ºC overnight the signal went back to its original value, i.e. the BTA-maleimide had detached from the polymer (green trace).

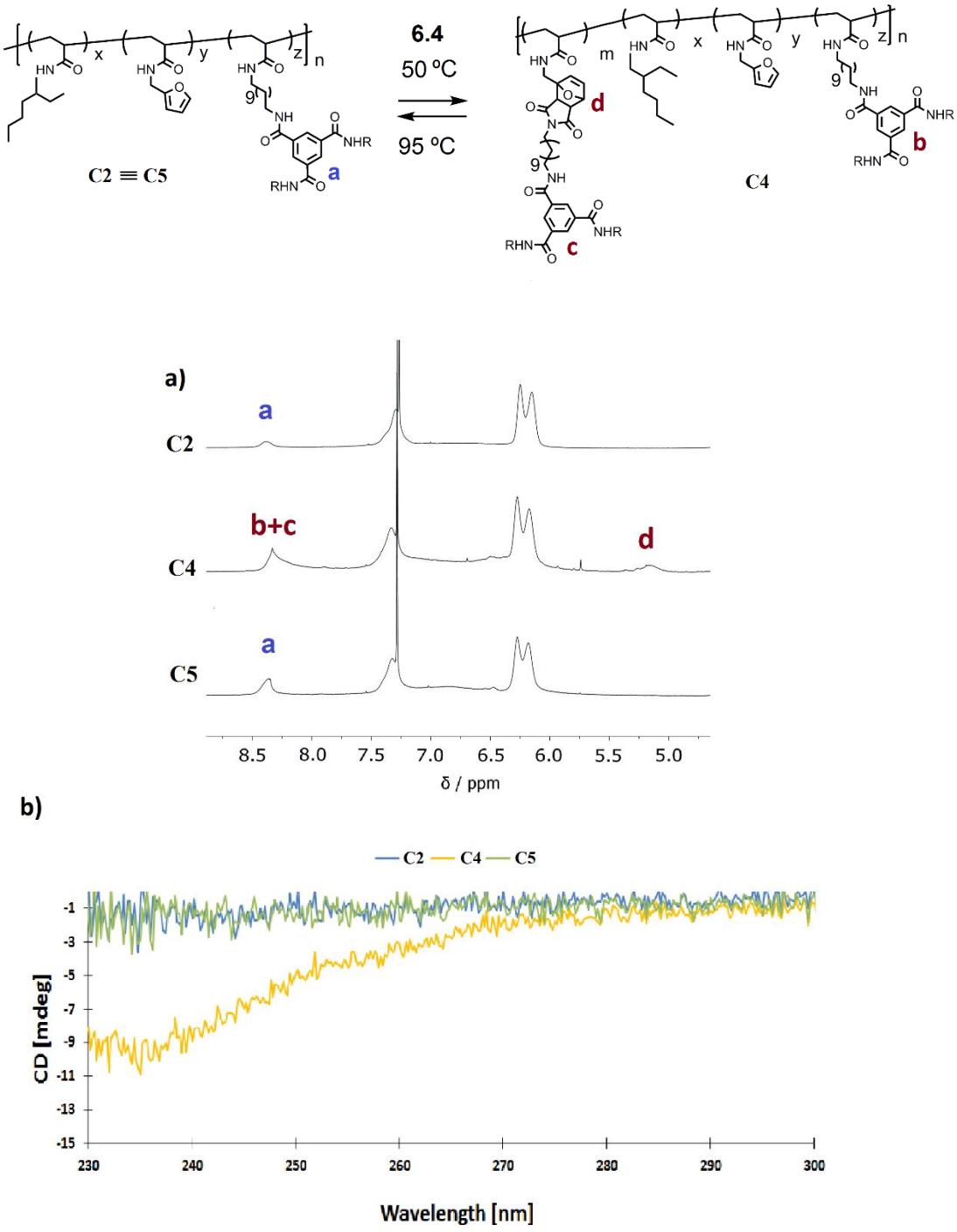

Figure 6.10. (a) ^{1}H NMR (400 MHz, $CDCl_3$, 298K) spectra and (b) CD spectra (MCH/DCE 70/30 v/v, 298 K) of the starting material (**C2)**, the material after the reaction with "mobile" BTA **6.4** (**C4**), and again after the reversible reaction (**C5**).

To prove that the CD signal decrease after the BTA detachment was not an effect of material degradation caused by exposure to high temperatures, we dissolved **C3** in DMF and subjected it to

the same reaction conditions that we used with **C4**. After that, the polymer was prepared to be measured by CD. We observed that there was not a significant difference in the signal of the material before and after heating overnight (Figure 6.11). This fact helped us conclude that the changes in the measurements seen in Figure 6.10b were caused by the removal of the "mobile" BTA.

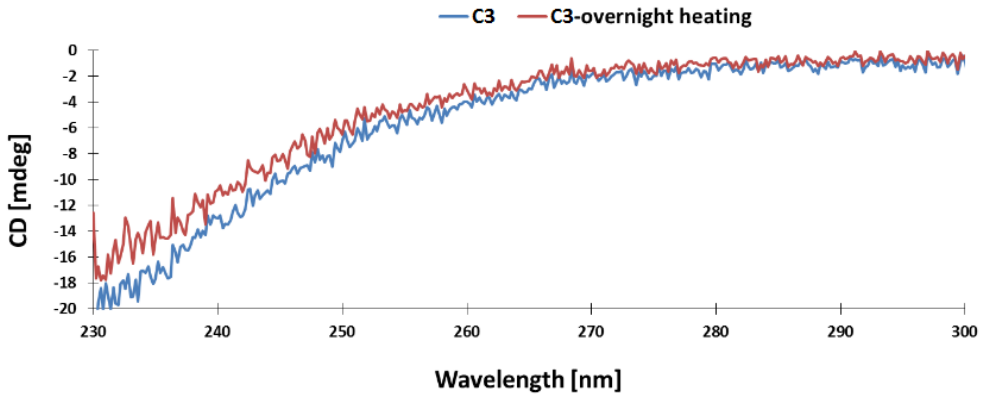

Figure 6.11. CD spectra (MCH/DCE 70/30 v/v, 298 K) of **C3** before and after heating overnight at 95ºC.

What was clear from these measurements was that we could not assess the extent of the functionalization reaction. In order to make sure that all the BTA-maleimide **6.4** reacted with the polymer chains, the reaction conditions would need to be optimized. The retro Diels-Alder to remove the "mobile" BTA from the materials, on the other hand, could easily be followed by the loss of the signal corresponding to the furan-maleimide adduct at 5.2 ppm and a decrease in the integral of the aromatic BTA signal

6.4 Environmental molecular adaptation

Reaction progression

In order to conduct the adaptation experiments it was important to know exactly the amount of BTA-maleimide that was being introduced in the polymer chain during the Diels-Alder reaction i.e. we needed to be certain that the reaction was going to completion. To do that, **C2** and BTA-maleimide **6.4** were reacted together and ^{1}H NMR spectra were measured as the reaction progressed. Figure 6.12 shows the different signs that indicate the full disappearance of free BTA-maleimide from solution and its incorporation onto the polymer backbone. They are: i) the disappearance of the alkene peak from the maleimide at 6.7 ppm; ii) the incorporation of the sharp aromatic signal from the BTA core at 8.4 ppm into the broad signal of the BTAs attached to the polymer chain; iii) and the broadening and merging with the baseline of the three amide protons, which where perfectly resolved at 6.5 ppm when compound **6.4** was free in solution.

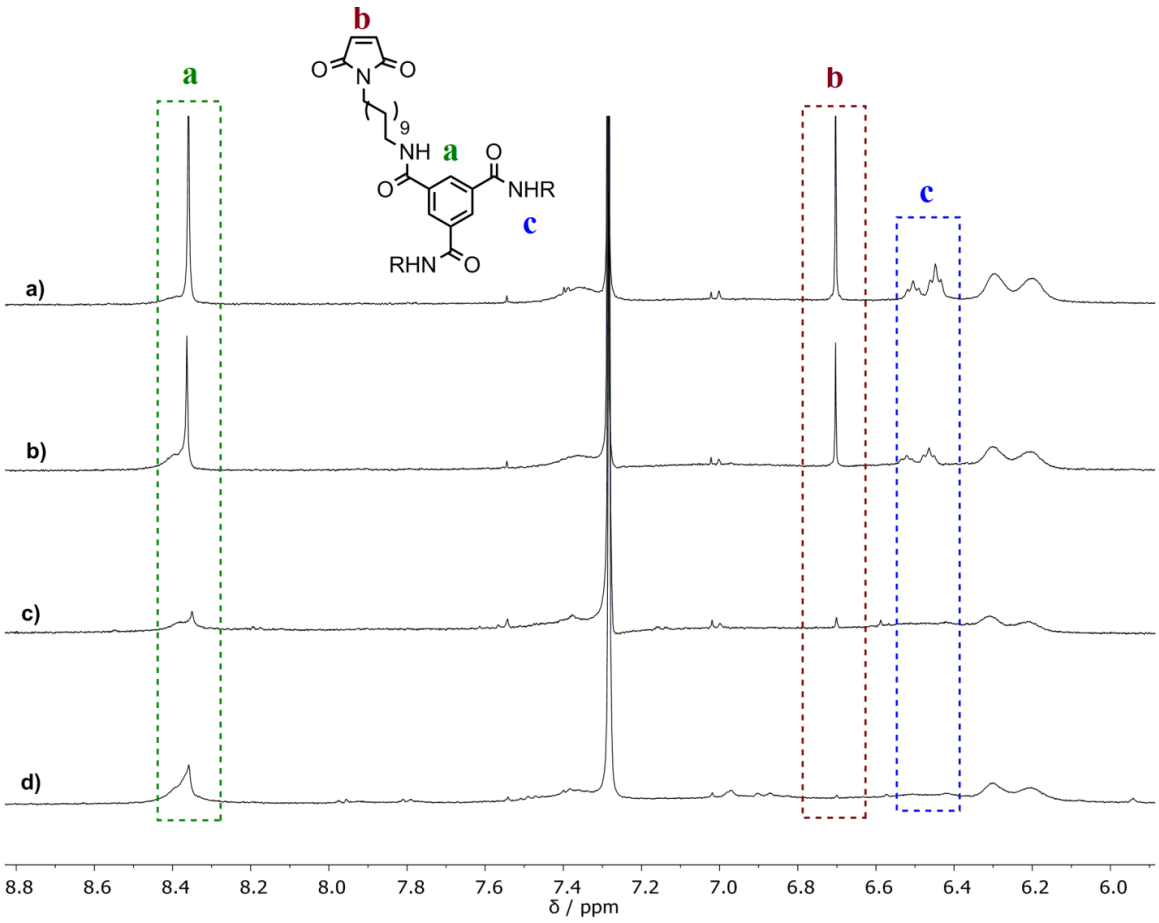

Figure 6.12. ^{1}H NMR (400 MHz, $CDCl_3$, 298K) spectra showing the progression of the reaction between **C2** and **6.4** at (a) 0 h; (b) 40 h; (c) 63 h; (d) 88 h. The disappearance of the signals of compound **6.4** indicates its attachment onto the polymer backbone and its disappearance from solution.

Once we knew how to assess that the attachment of BTA-maleimide had gone to completion, we were in position to perform the environmental adaptation experiments by repeating the post-functionalization in different reaction conditions.

Adaptation experiments

To perform the adaptation experiments we wanted to couple **C2** and BTA-maleimide **6.4** together in a range of different conditions of temperature and solvent polarity. The idea behind this was that the interactions between the "fixed" BTA and the "mobile" BTA would be affected by the temperature and polarity of the environment. If those interactions and, as a direct consequence, the BTA supramolecular helices, vary between conditions, the "mobile" BTA sequence along the chain will change with the environment. Different primary structures would produce different secondary and tertiary structures, and we hoped to measure that using spectroscopic techniques. To that effect, 5 mg of **C2** (5% BTA content) were reacted with 1.7 mg of BTA-maleimide **6.4** (2 eq with respect to BTA within the polymer) to give polymer chains with a total quantity of BTA equivalent to that of **C3** (15% BTA content)**.** Two sets of experiments were done: i) those in which the effects of performing the Diels-Alder reaction at different temperature were studied, while maintaining the solvent polarity constant across reactions; ii) and those in which we changed the solvent to study the effects of changing environment polarity, while keeping the reaction temperature constant (Table 6.3). All reactions were monitored until completion (Figure S11).

Table 6.3. Range of temperatures and solvent mixtures for coupling reactions between **C2** and BTA-maleimide **6.4**.

	Reaction solvent (MCH/DCE)	**T(°C)**
Constant solvent polarity	80/20	30
	80/20	35
	80/20	40
	80/20	50
Constant temperature	90/10	35
	80/20	35
	70/30	35
	60/40	35
	50/50	35
	0/100	35

We proceeded to measure the samples by CD, starting with the experiments performed at constant solvent polarity. The four samples were prepared for CD measurements following the same procedure utilized before. The stock solutions in DCE presented good solubility, but there were some solubility problems once the dilutions with MCH were carried out. The measurements gave lower signal intensity than expected, but still showed a clear tendency: the materials synthesized at higher temperatures presented lower Cotton Effect, despite all the samples having the same composition and concentration (Figure 6.13).

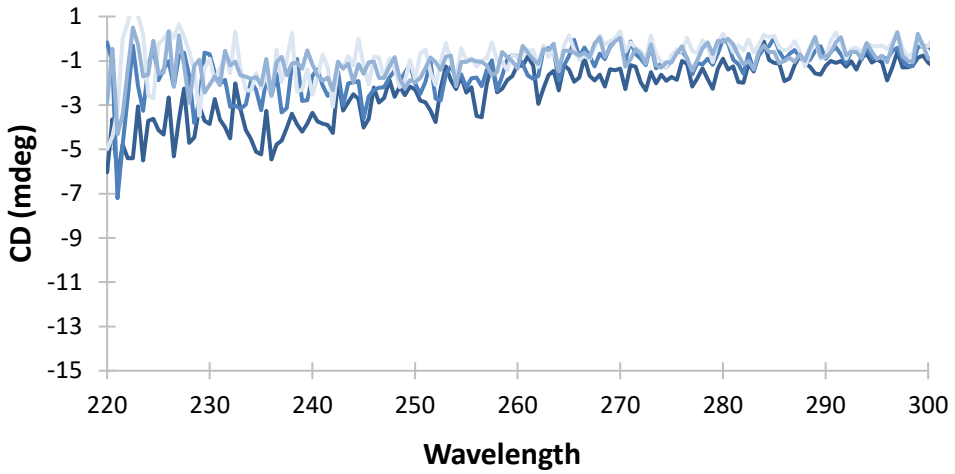

Figure 6.13: CD spectra (MCH/DCE 70/30 v/v, 298 K) of materials synthesized in MCH/DCE 80/20 mixture at different reaction temperatures: i) 30 ºC (darkest shade of blue); ii) 35 ºC; iii) 40 ºC; iv) 50 ºC (lightest shade of blue).

We then tried to measure the samples prepared at variable solvent polarity, but none of them was soluble enough in DCE to prepare the stock solutions. This was interesting for two reasons: i) they were similar materials to **C3** (the only difference being the presence of the Diels-Alder adduct in some side chains); ii) and this set of polymers made at constant temperature had the same composition as the ones made at constant solvent polarity, shown in Figure 6.13. The solubility of the similar materials made in different environments changed drastically.

6.5 Conclusions

In this work we prepared a set of supramolecular SCPNs that fold due to triple H-bond interactions between BTA pendant units that stack forming chiral helices. They were made by post-functionalization of a polyacrylate bearing an activated ester synthesized by RAFT polymerization. The materials were characterized by CD, GPC and ^{1}H NMR spectroscopy. They contained BTA as structural units and furan as reacting units for further post-functionalization as a way of obtaining functional materials that respond to external stimuli and that can be modified reversibly via dynamic covalent chemistry. This was done by reaction of one of the polymers with a mobile BTA carrying a maleimide unit, forming a Diels-Alder adduct. This reaction was reversible, as was observed by CD and ^{1}H NMR spectroscopy. Moreover, the same reaction was conducted at different temperature and polarity conditions to give materials that, despite having the exact same composition, presented different properties. While some of them did not dissolve in the conditions required to perform the measurements, others were measured by CD and showed a correlation between the temperature at which they had been synthesized and the CD signal: those made at lower temperature presented a slightly bigger Cotton Effect. We hypothesize that this would be a sign of environmental adaptation: the improved interactions between the fixed BTA and the mobile BTA directed the positioning of the incoming molecules, giving them a more thermodynamically stable primary and secondary structure, which led to changes in CD. More experiments need to be done to confirm this. We would need to make sets of polymers with improved solubility properties, to make sure that all the samples are soluble during the adaptation experiments. Besides, it would be of great interest correlating changes in the way the materials are created, and their CD signals, with conformational changes. For that purpose, Small-angle neutron scattering (SANS) and Dynamic Light Scattering (DLS) would be of great interest.

6.6 Experimental Section

Chemicals

Azobisisobutyronitrile (AIBN) was recrystallized from methanol. All other chemicals were obtained from Aldrich and used as received. All solvents were obtained from Biosolve, Acros or Aldrich. Dry DCM, THF, and DMF were tapped off a distillation setup which contained molsieves. $CHCl_3$ was dried over molsieves and triethylamine was stored on KOH pellets. (S)-(-)-Citronellol was purchased from Aldrich and converted into the corresponding (S)-3,7-dimethyloctan-1-amine according to a described procedure.[1]

Characterization methods.

Ultraviolet-visible (UV/Vis) and circular dichroism (CD) measurements were performed on a Jasco J-815 spectropolarimeter where the sensitivity, time constant and scan rate were chosen appropriately. Corresponding temperature-dependent measurements were performed with a PFD-425S/15 Peltier-type temperature controller with a temperature range of 263-383 K and adjustable temperature slope, in all cases a temperature slope of 1 K/min was used. Fluorescence measurements were performed on a Jasco FP-6500 spectrofluorometer. ^{1}H and ^{13}C NMR spectra were recorded at 25 ℃ on a Varian Mercury Vx 400 MHz, where chemical shifts were determined with respect to tetramethylsilane (TMS) as an internal reference. THF-SEC-measurements were performed on a Shimadzu-system with two Agilent Technology columns in series (PLgel 5 mm mixed C [200–2 000 000Da] and PLgel 5 mm mixed D [200–40 000 Da]) and equipped with a RI detector (Shimadzu RID-10A) and a PDA detector (Shimadzu SPD-M10A), with THF as eluent at a constant flowrate of 1.0 mL min-1. The system was calibrated with polystyrene (PS) samples with a range of 580–100,000 Da (Polymer Laboratories).

.

General procedure for the synthesis of polymer Series A and B

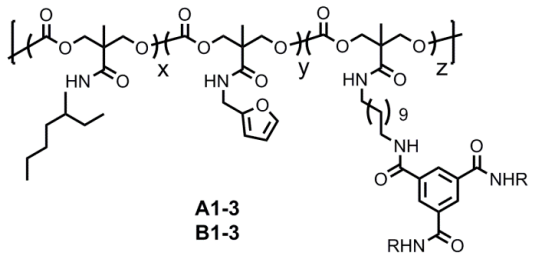

Polycarbonate (**A0** for Series A and **B0** for Series B) (100 mg, 0.315 mmol) was dissolved in dry THF (4 mL) and left stirring under argon. BTA-NH_2 (see table below) and DIPEA (48 mg, 0.378 mmol) were dissolved in dry THF (2 mL) and added dropwise to the polymer solution. The mixture was stirred at room temperature under argon for 1 h. After this time, the aliphatic amine (2 mg, 0.016 mmol for Series A, 7.9 mg, 0.063 mmol for Series B) was dissolved in dry THF (1 mL) in a vial and added dropwise to the polymer solution. The mixture was stirred at room temperature under argon for another hour. To finish the functionalization, furfurylamine (31 mg, 0.315 mmol) was dissolved in dry THF (1 mL) and added dropwise to the solution, which was stirred for a further 2 hours. The crude solution was precipitated in cold ether, centrifuged and decanted. This process was repeated twice. The final solid was dried in the vacuum oven overnight at 60ºC to yield the final compound as a crumbly yellow solid (appearance dependent on BTA content).

Polymer	**Eq. of alkyl amine[1]**	**m alkyl amine (mg)**	**Eq. of BTA[1]**	**m BTA (mg)**
A1	0.05	2.0	0	0
A2	0.05	2.0	0.05	10.3
A3	0.05	2.0	0.20	41.3
B1	0.20	8.1	0	0
B2	0.20	8.1	0.05	10.3
B3	0.20	8.1	0.20	41.3

[1] Number of equivalents added to the reaction mixture with respect to the repeat monomeric unit of the polycarbonate precursor

Figures S1-S6: ^{1}H NMR (400 MHz, Chloroform-d, 298 K) of polymer Series A and B.

A1

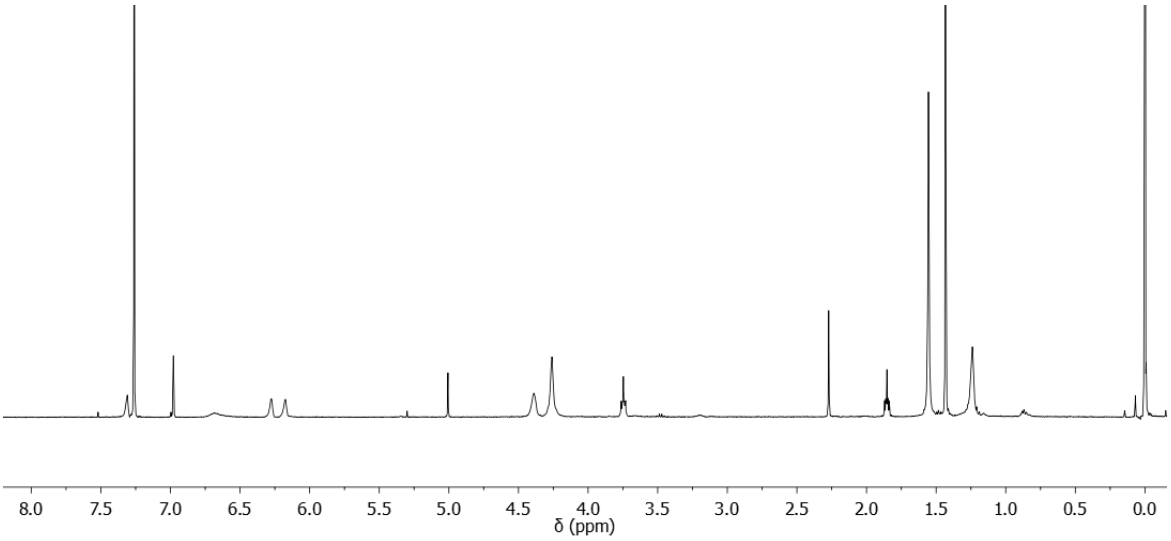
8.0
7.5
7.0
6.5
6.0
5.5
5.0
4.5
4.0
3.5
3.0
2.5
2.0
1.5
1.0
0.5
0.0
δ (ppm)

A2

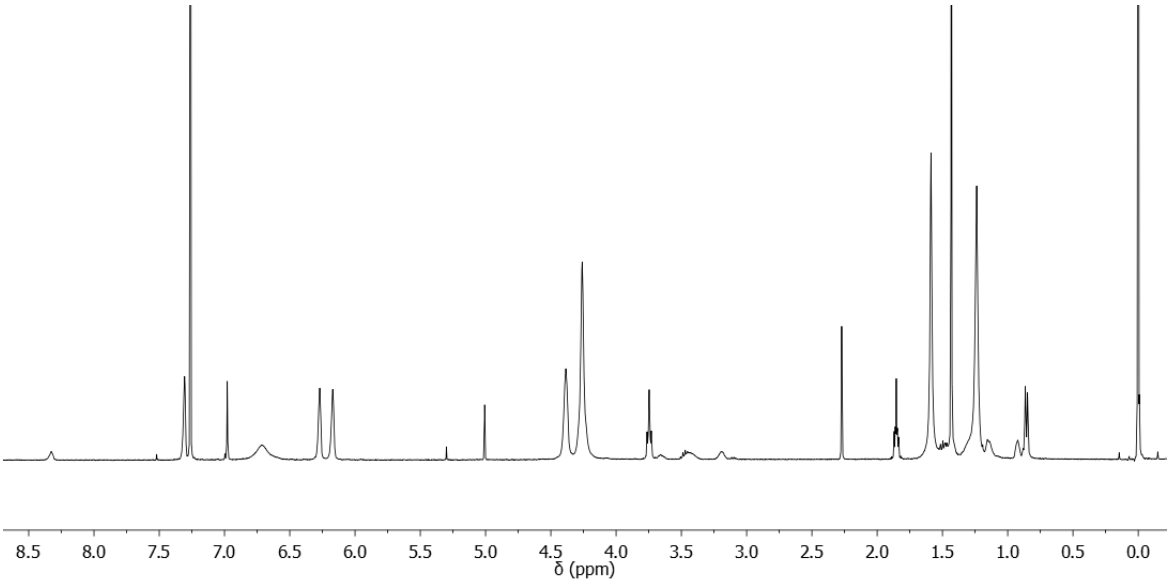
8.5
8.0
7.5
7.0
6.5
6.0
5.5
5.0
4.5
4.0
3.5
3.0
2.5
2.0
1.5
1.0
0.5
0.0
δ (ppm)

A3

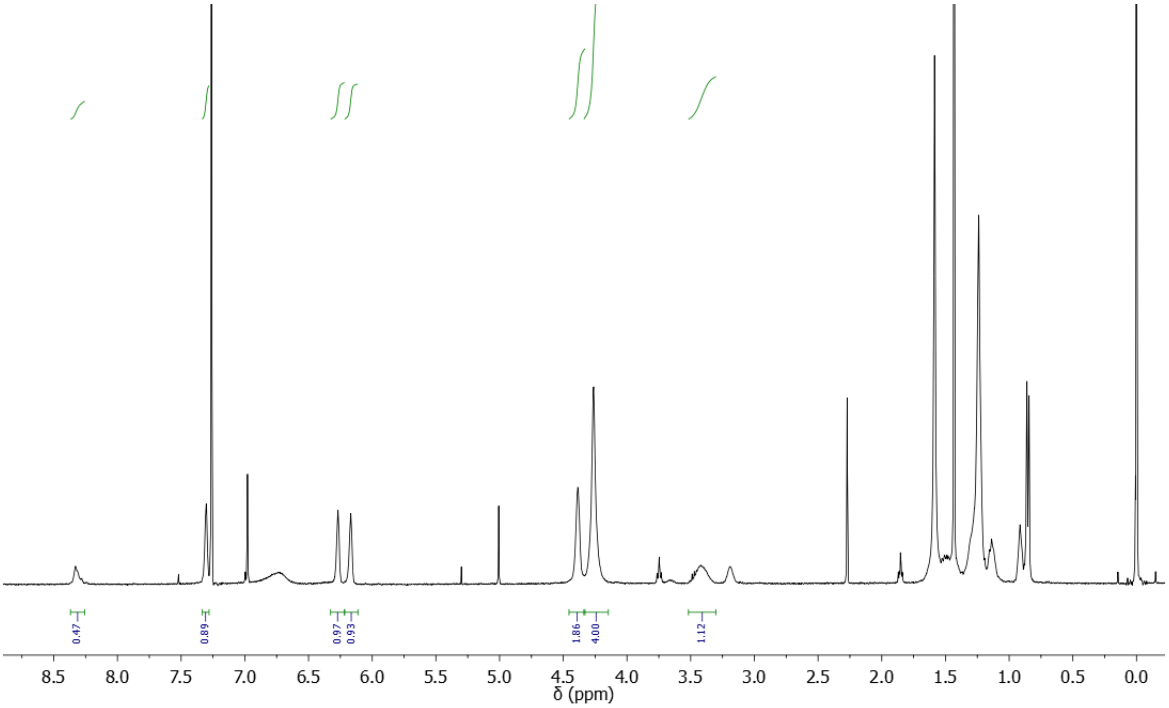
0.47
0.89
0.97
0.93
1.86
4.00
1.12
8.5 8.0 7.5 7.0 6.5 6.0 5.5 5.0 4.5 4.0 3.5 3.0 2.5 2.0 1.5 1.0 0.5 0.0
δ (ppm)

B1

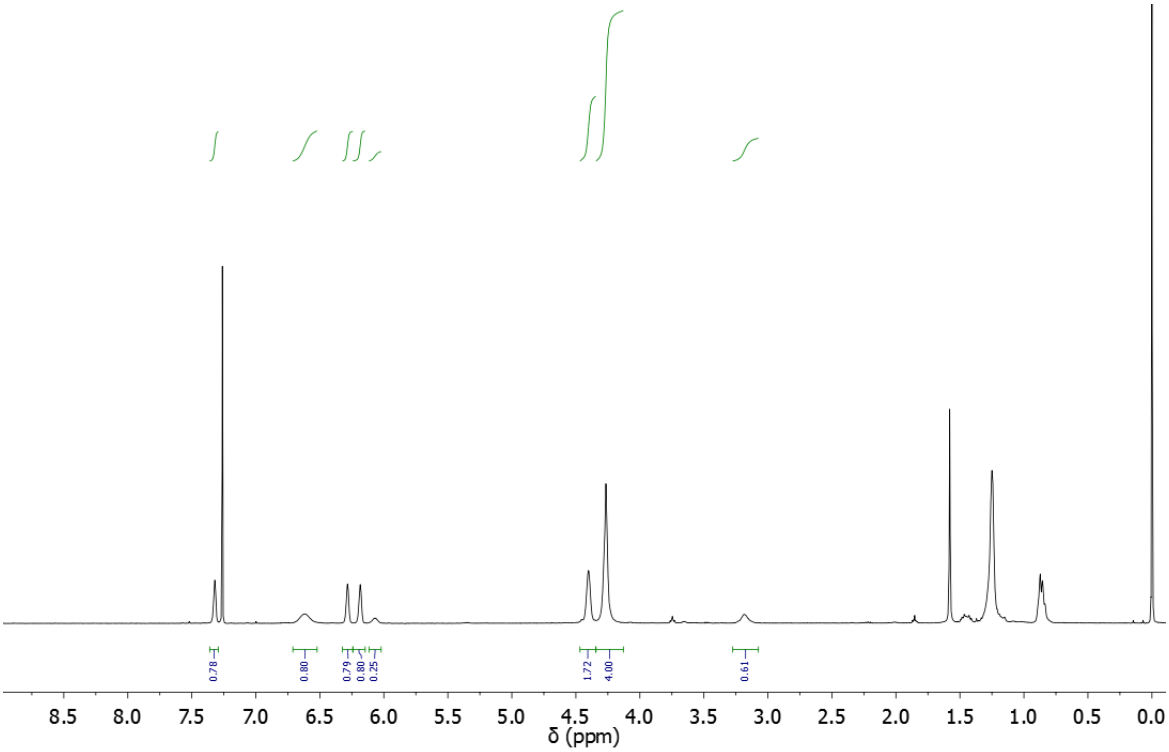
0.78
0.80
0.79
0.80
0.25
1.72
4.00
0.61
8.5 8.0 7.5 7.0 6.5 6.0 5.5 5.0 4.5 4.0 3.5 3.0 2.5 2.0 1.5 1.0 0.5 0.0
δ (ppm)

B2

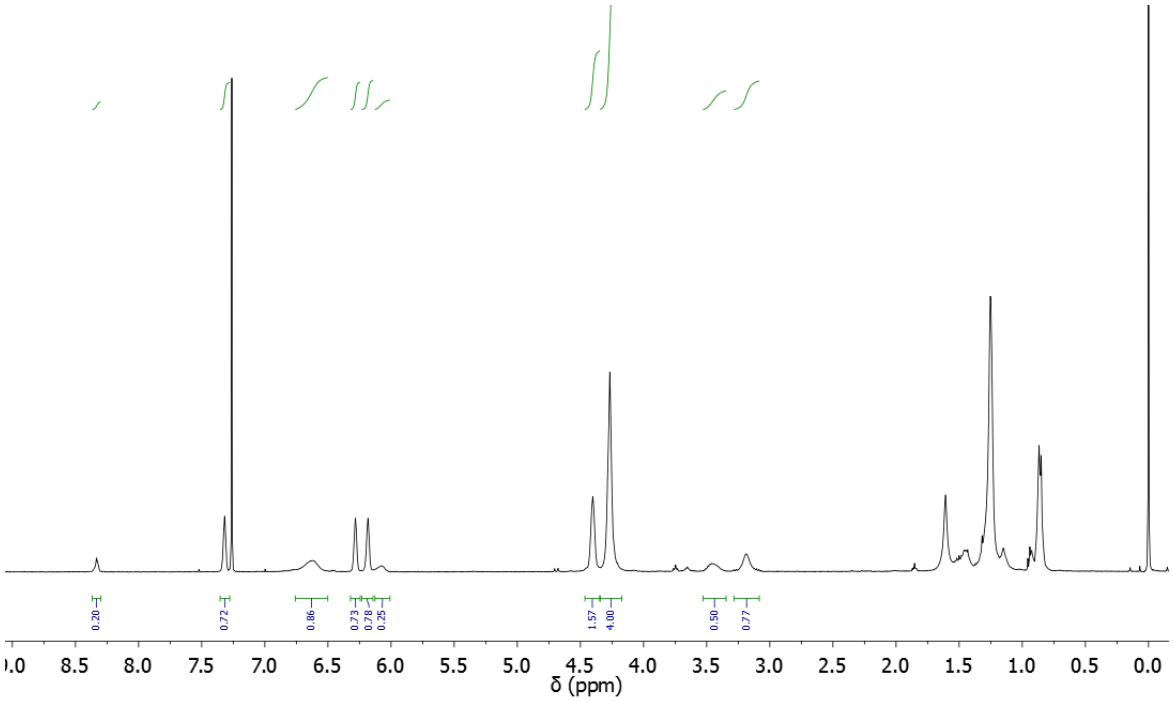
0.20
0.72
0.86
0.73
0.78
0.25
1.57
4.00
0.50
0.77
8.5 8.0 7.5 7.0 6.5 6.0 5.5 5.0 4.5 4.0 3.5 3.0 2.5 2.0 1.5 1.0 0.5 0.0
δ (ppm)

B3

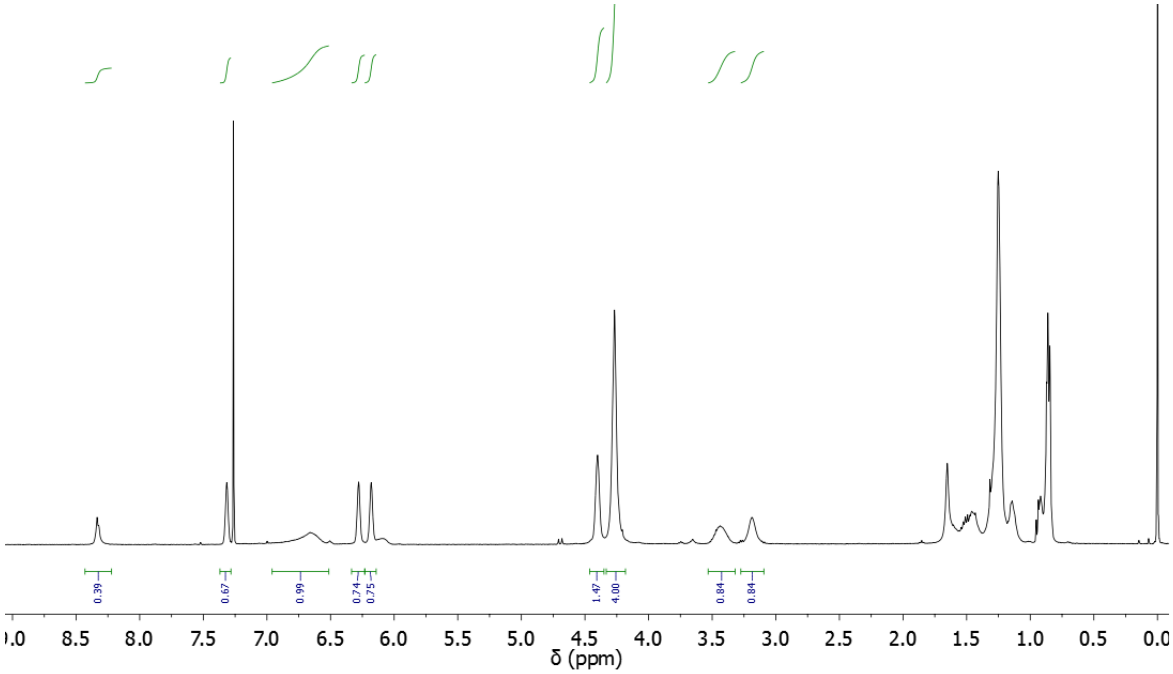
0.39
0.67
0.99
0.74
0.75
1.47
4.00
0.84
0.84
8.5 8.0 7.5 7.0 6.5 6.0 5.5 5.0 4.5 4.0 3.5 3.0 2.5 2.0 1.5 1.0 0.5 0.0
δ (ppm)

Synthesis of compound 6.3

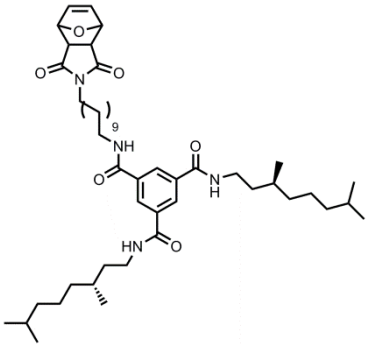

BTA-OTs (compound **6.1**, 400 mg, 0.50 mmol), oxanorbornene imide (compound **6.2**, 120 mg, 0.60 mmol) and K_2CO_3 (124 mg, 0.90 mmol) were dissolved in DMF (50 mL) and heated at 60°C overnight. The crude solution was carefully neutralized with HCl 1M and diluted with EtOAc (100 mL). The organic layer was washed with LiCl 5% (3 x 20 mL), water (2 x 20 mL) and brine (2x 20 mL), dried with $MgSO_4$ and concentrated in vacuo before purification by column chromatography (DCM/MeOH, gradient of increasing polarity) to yield pure compound **6.3** as a viscous, yellow material (362 mg, 90%)

^{1}H NMR (400 MHz, Chloroform-*d*) δ 8.28 (s, 3H), 7.08 (t, *J* = 5.5 Hz, 1H), 7.02 (t, *J* = 5.6 Hz, 2H), 6.49 (s, 2H), 5.23 (s, 2H), 3.42 (m, 8H), 2.84 (s, 2H), 1.70 – 0.76 (m, 56H).

^{13}C NMR (100 MHz, Chloroform-*d*) δ 176.41, 166.03, 136.51, 135.25, 128.03, 80.87, 47.42, 40.38, 39.23, 38.97, 38.52, 36.58, 27.52, 26.97, 26.59, 24.62.

FT-IR (ATR): 3243, 2053, 2928, 2858, 1725, 1640, 1551, 1466 cm^{-1}

HRMS (ES+): calcd for $C_{48}H_{77}N_4O_6$ 805.5843 $[M+H]^+$, found 805.5851 $[M+H]^+$.

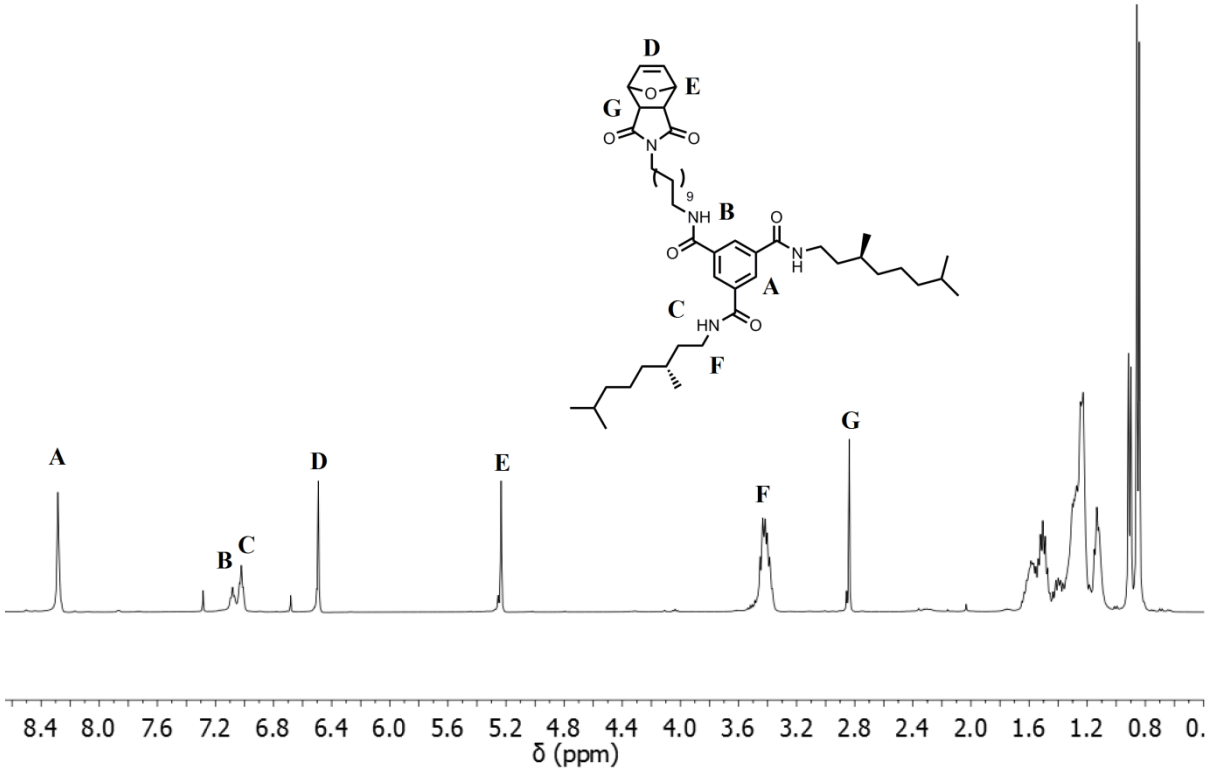
D
E
G
O
N
O
9
NH
B
O
O
N
H
A
C
HN
O
F
A
B
C
D
E
F
G
8.4 8.0 7.6 7.2 6.8 6.4 6.0 5.6 5.2 4.8 4.4 4.0 3.6 3.2 2.8 2.4 2.0 1.6 1.2 0.8 0.
δ (ppm)

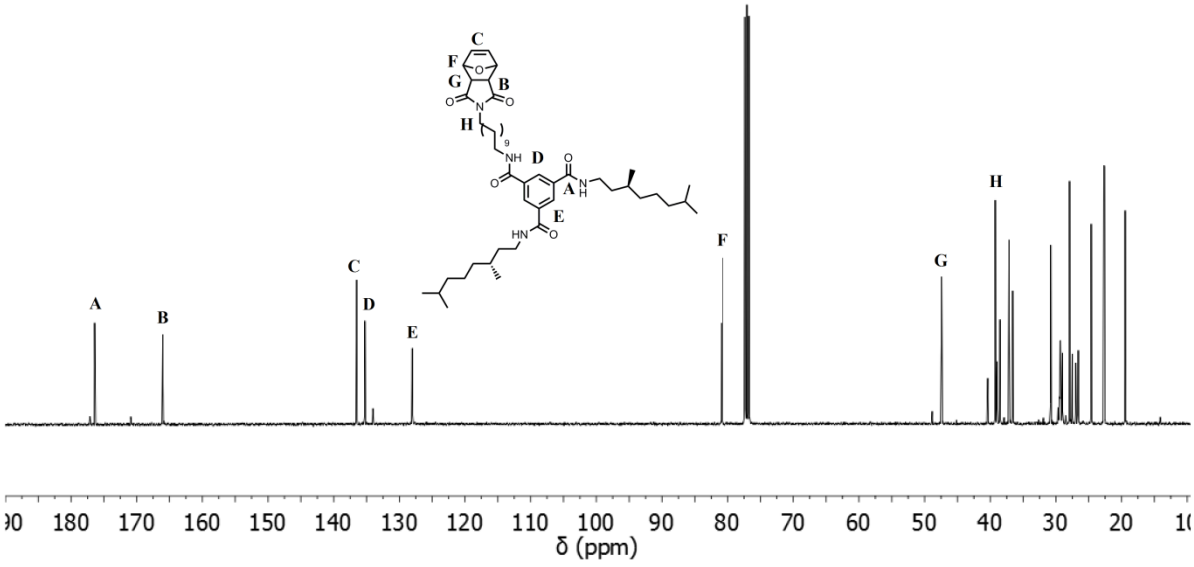
C
F
G
B
O
N
H
9
NH
D
O
A
N
H
E
HN
O
A
B
C
D
E
F
G
H
90 180 170 160 150 140 130 120 110 100 90 80 70 60 50 40 30 20 10
δ (ppm)

Synthesis of compound 6.4

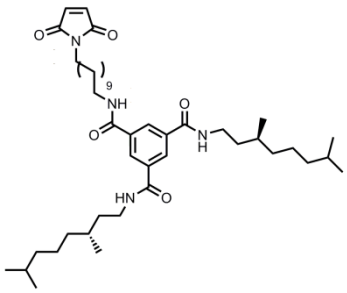

Compound **6.3** (120 mg, 0.15 mmol) was dissolved in DMF (20 mL) and heated overnight at 100°C with a condenser attached but open to the atmosphere to allow the evaporation of furan. Once cool, the crude solution was diluted with EtOAc (50 mL), and the mixture was washed with LiCl 5% (3 x 20 mL), water (2 x 20 mL) and brine (2 x 20 mL). The organic layer was then dried with $MgSO_4$ and evaporated in vacuo to yield pure compound **6.4** as a sticky, pale solid (110 mg, quantitative yield).

^{1}H NMR (400 MHz, Chloroform-*d*) δ 8.32 (s, 3H), 6.81 (t, *J* = 5.5 Hz, 1H), 6.77 (t, *J* = 5.6 Hz, 2H), 6.68 (s, 2H), 3.4 (m, 8H), 1.70 – 0.79 (m, 56H).

^{13}C NMR (101 MHz, Chloroform-*d*) δ 170.01, 167.14, 136.87, 135.43, 127.31, 39.29, 38.42, 37.15, 36.45, 30.90, 28.49, 27.93, 27.11, 25.82, 22.70, 22.58, 19.42.

FT-IR (ATR): 2959, 2930, 2858, 1700, 1659, 1526 cm^{-1}

HRMS (ES+): calcd for $C_{44}H_{73}N_4O_5$ 737.5581 $[M+H]^+$, found 737.5571$[M+H]^+$.

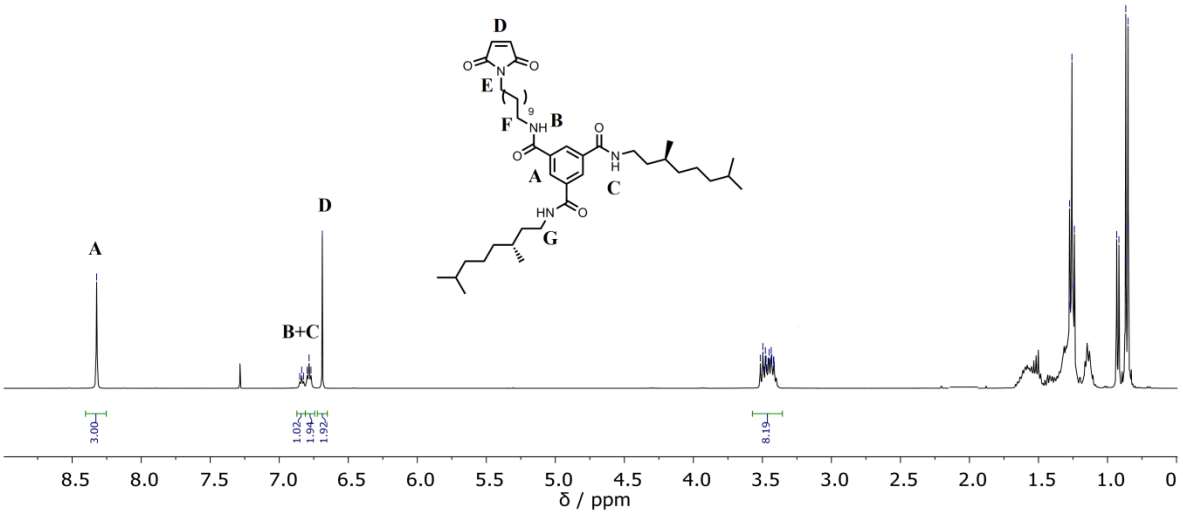
A
B+C
D
3.00
1.02
1.94
1.92
8.19
δ / ppm

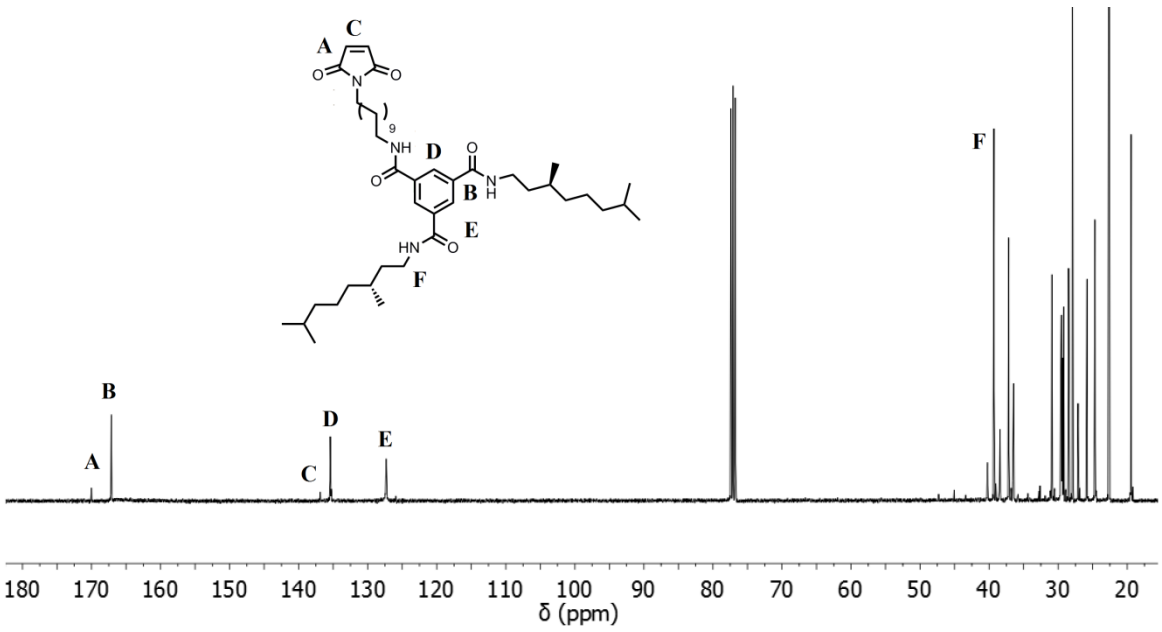
A
B
C
D
E
F
δ (ppm)

Synthesis of B4

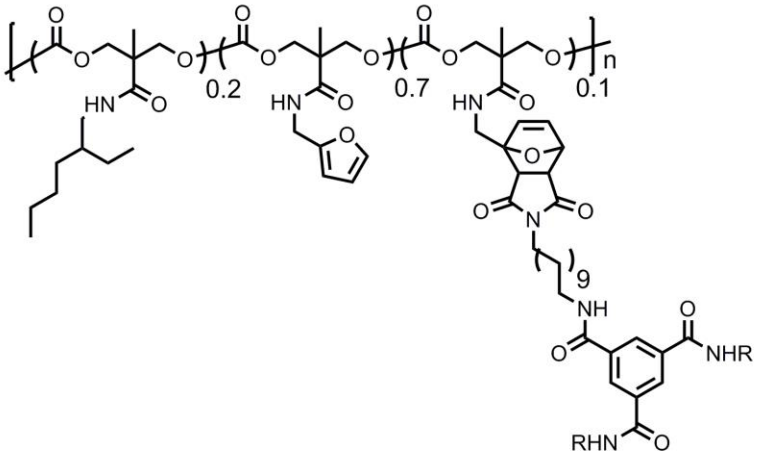

B1 (20 mg, 0.082 mmol) and compound **6.4** (5.3 mg, 0.008 mmol) were dissolved in THF (2 mL) and heated overnight at 50 °C. After this time, the crude solution was precipitated in cold ether, centrifuged and decanted. This process was repeated twice. The final solid was dried in the vacuum oven overnight at 60ºC to yield the final compound as a crumbly yellow solid. ^{1}H NMR (400 MHz, Chloroform-*d*) δ 8.39 (s, 0.3H), 7.34 (s, 0.7 H), 6.72 (s, 1 H), 6.30 (s, 0.7 H), 6.20 (s, 0.7 H), 4.42 (s, 1.4H), 4.29 (s, 4 H), 3.47 (s, 1H), 1.26 (s), 0.88 (s).

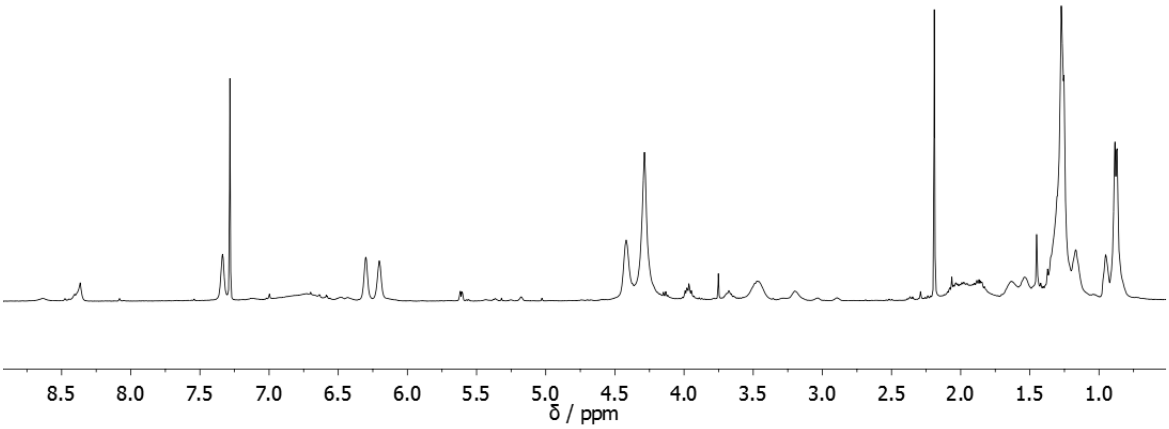

Synthesis of compound 6.5

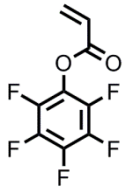

Pentafluorophenol (8.97 g, 48.73 mmol) was dissolved in dry DCM and several cycles of vaccum/N_2 were performed. Triethylamine (8.2 mL, 58.48 mmol) was added and the mixture was cooled in ice. A solution of acryloyl chloride (5.3 g, 58.48 mmol) in dry DCM was added dropwise and the mixture was stirred for 3h. Once the reaction went to completion, the solvent was evaporated in vacuo and the crude was redissolved in EtOAc. The solution was washed with HCl 1M (2 x 30mL) and brine (2 x 30mL), dried with $MgSO_4$ and evaporated in vacuo. The crude oil was purified by column chromatography (DCM) and pure acrylate monomer was obtained as a colourlessoil (10.6g, 92%).[1] H-NMR (400 MHz, $CDCl_3$): δ = 6.74 (dd, *J* = 17.3, 0.8 Hz, 1H), 6.39 (dd, *J* = 17.3, 10.5 Hz, 1H), 6.20 (dd, *J* = 10.5, 0.8 Hz, 1H). The ^{1}H spectrum matches the literature.[30]

Synthesis of C0

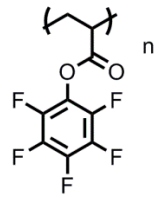

A Schlenk tube was charged with a stir bar, compound **5** (3.0 g, 12.60 mmol, 261 eq.), 4-cyano-4-((phenylcarbonothioyl)thio)pentanoic acid (13.5 mg, 0.048 mmol, 1.0 eq.), azobis-isobutyronitrile (AIBN, 1.19 mg, 7.24 μmol, 0.15 eq.), and dioxane (3.0 mL). The solution was degassed by doing three freeze-pump-thaw cycles. The Schlenk tube was placed into a preheated oil bath at 80 °C. The reaction was stopped after 2 hours and 45 minutes by placing the Schlenk tube in a liquid nitrogen bath. The monomer conversion was determined to be 37% by measuring ^{19}F NMR spectrum of the reaction mixture. **C0** was isolated by precipitation in methanol (three times) and dried in the vacuum oven to produce a pink powder. The degree of polymerization (DP) was calculated to be 97. THF-GPC: M_n = 16.0 kDa, $Đ$ = 1.16

General procedure for the synthesis of polymer Series C

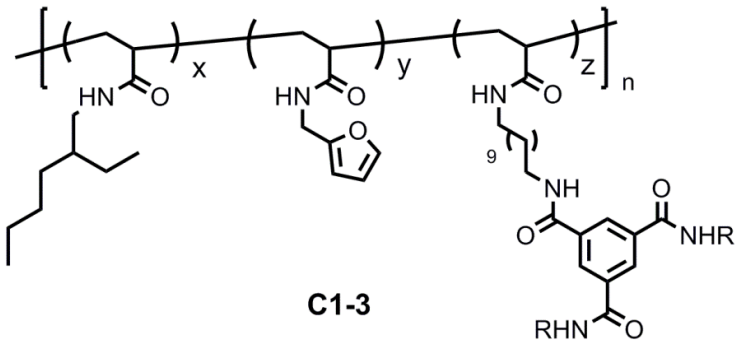

C1-3

Polymer **C0** (100 mg, 0.42 mmol) was dissolved in dry THF (4 mL) and left stirring under argon. BTA-NH_2 (see table below) and triethylamine (51 mg, 0.50 mmol) were dissolved in dry THF (2 mL) and added dropwise to the polymer solution. The mixture was heated at 50 ºC for 2 hours. After this time, 2-ethylhexyl amine (11 mg, 0.08 mmol) was dissolved in dry THF (1 mL) and added dropwise to the polymer solution. The mixture was heated for another 2 hours. To finish the functionalization, furfurylamine (49 mg, 0.50mmol) was dissolved in dry THF (1mL) and added dropwise to the solution, which was heated overnight. The crude solution was precipitated in cold ether, centrifuged and decanted. This process was repeated twice. The final solid was dissolved in THF and dialyzed for 2 days in THF (changing the solvent two times in that period). The solution was evaporated and the solid was dried in the vacuum oven overnight at 60ºC to yield the final compound as a crumbly yellow solid (appearance dependent on BTA content).

Polymer	**Eq. of BTA[1]**	**m BTA (mg)**
C1	0	0
C2	0.05	13.8
C3	0.20	55.1

[1] Number of equivalents added to the reaction mixture with respect to the repeat monomeric unit of the polyacrylate precursor

Figures S7-S9: ^{1}H NMR (400 MHz, Chloroform-d, 298 K) of polymer Series C.

C1

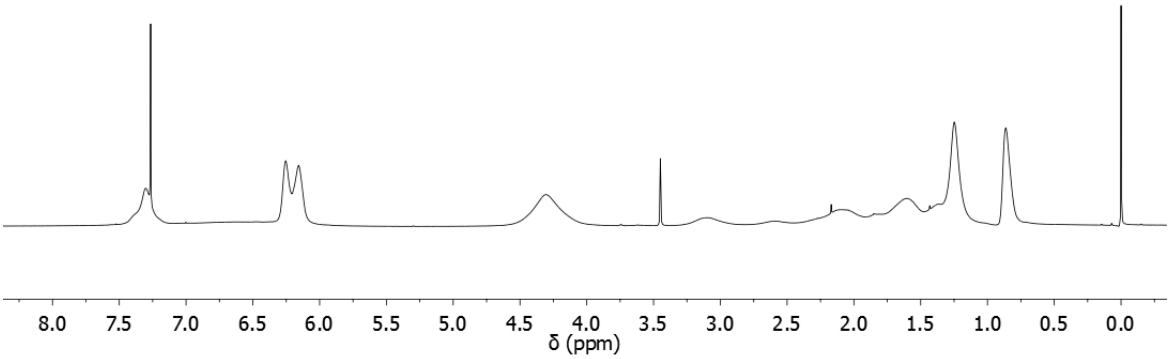
8.0
7.5
7.0
6.5
6.0
5.5
5.0
4.5
4.0
3.5
3.0
2.5
2.0
1.5
1.0
0.5
0.0
δ (ppm)

C2

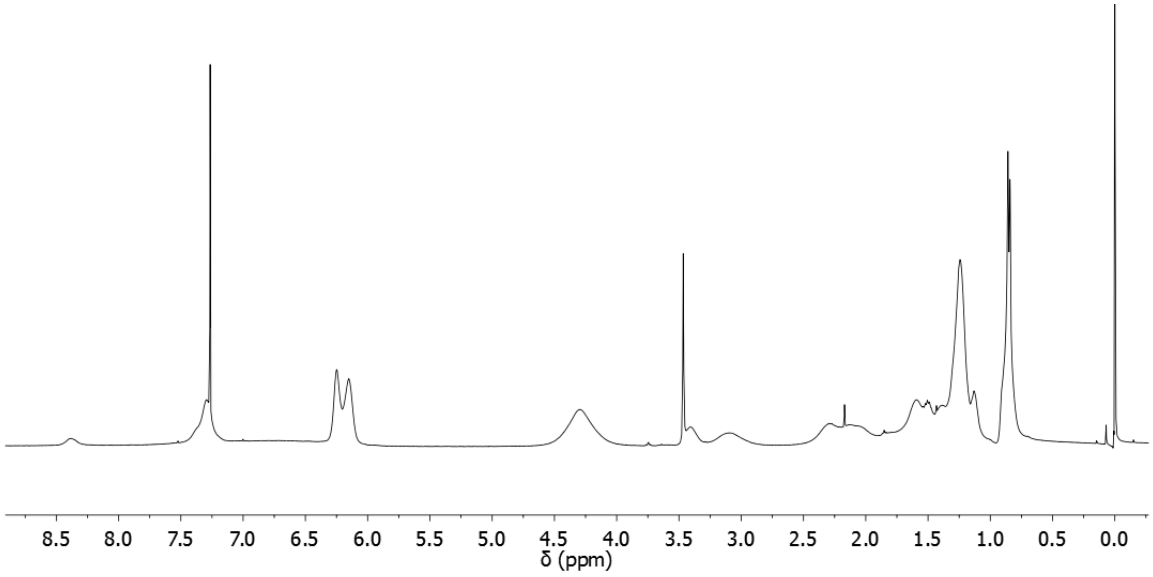
8.5
8.0
7.5
7.0
6.5
6.0
5.5
5.0
4.5
4.0
3.5
3.0
2.5
2.0
1.5
1.0
0.5
0.0
δ (ppm)

C3

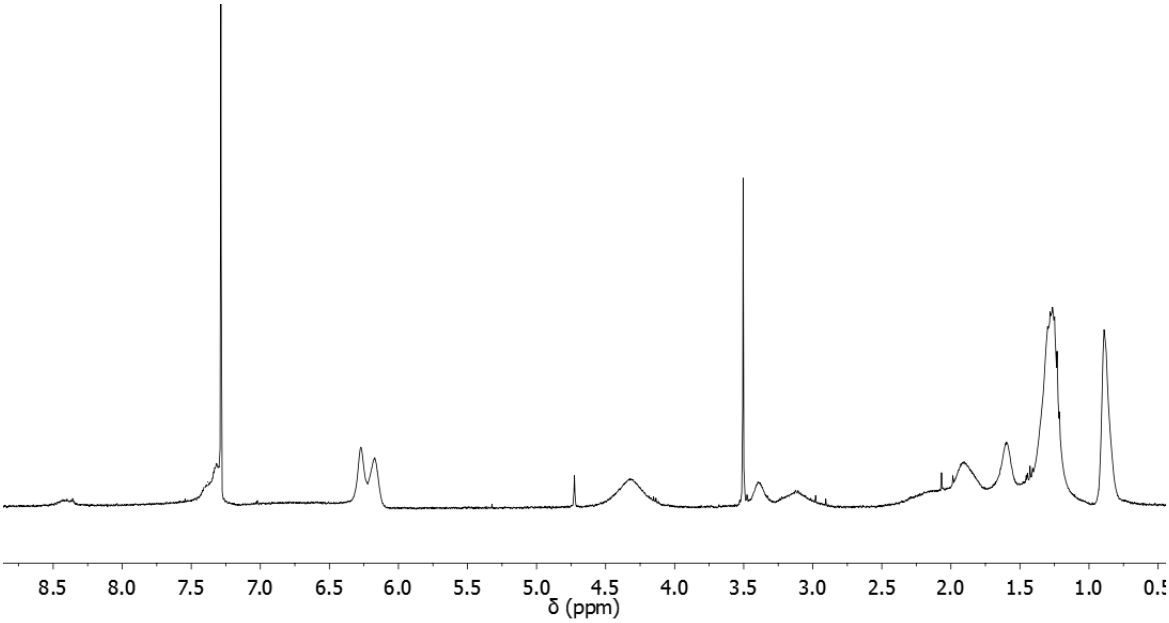

Reversible post-functionalization of C2 with 6.4

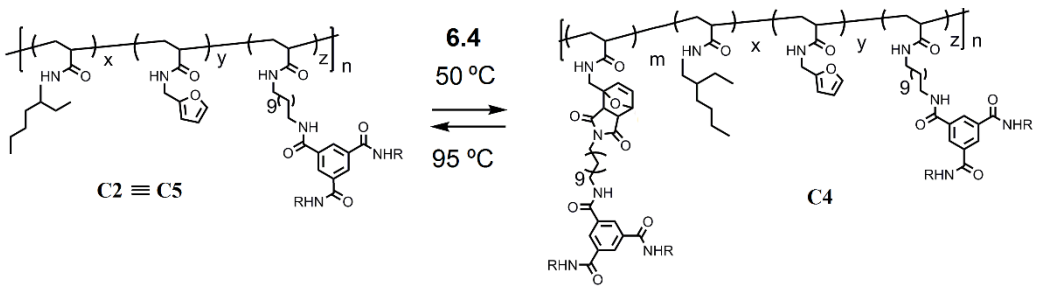

Polymer **C2** (5 mg, 0.027 mmol), and compound **6.4** (1.7 mg, 0.003 mmol) were dissolved in the $CHCl_3$ and heated at 50 ºC overnight. After this solvent the solvent was evaporated under vacuum and the crude redissolved in DCM before precipitating the polymer in cold ether. The product was centrifuged and precipitated once more. The final compound was dried in the vacuum oven at 50ºC overnight.

To reverse this reaction, the polymer was dissolved in DMF and heated at 95 ºC overnight. After this time, the solvent was evaporated in vacuo and the crude precipitated from DCM in cold ether before drying it in a vacuum oven at 50 ºC overnight.

Figure S10: ^{1}H NMR (400 MHz, Chloroform-*d*, 298 K) of (a) **C2**; (b) **C4**; (c) **C5**.

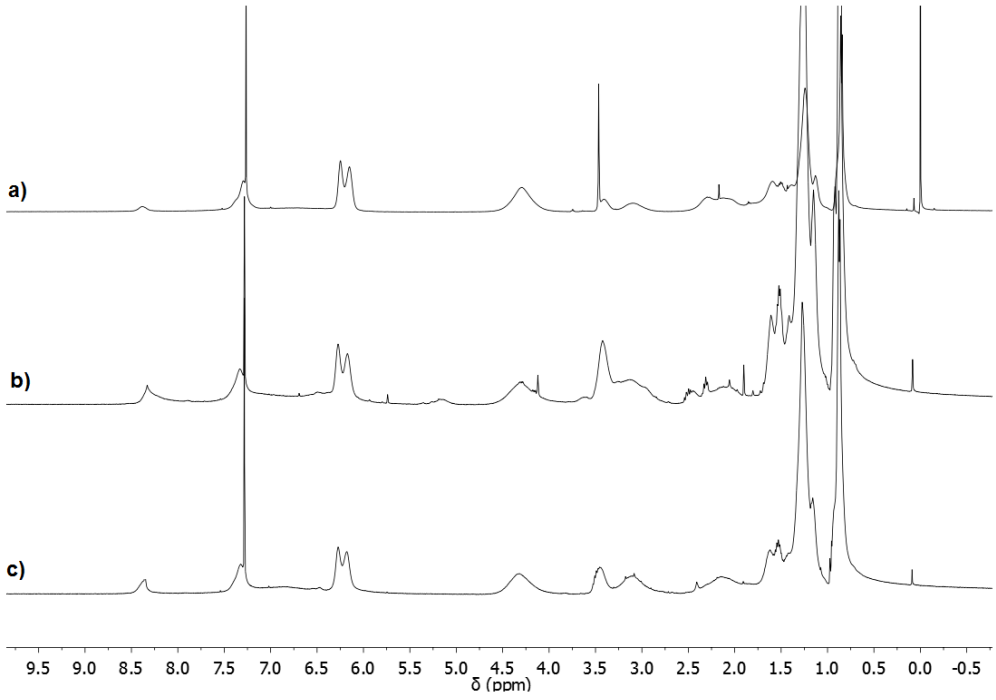

Adaptation experiments

Polymer **C2** (5 mg, 0.027 mmol), and compound **6.4** (1.7 mg, 0.003 mmol) were dissolved in MCH/DCE mixtures (2 mL) and heated at different temperatures for 4-8 days (see table below). When the reaction reached completion, the solvent was evaporated and the sample was dried in a vacuum oven at 50ºC overnight.

	Reaction solvent (MCH/DCE)	**T(°C)**
Constant solvent polarity	80/20	30
	80/20	35
	80/20	40
	80/20	50
Constant temperature	90/10	35
	80/20	35
	70/30	35
	60/40	35
	50/50	35
	0/100	35

Figure S11: ^{1}H NMR (400 MHz, Chloroform-*d*, 298 K) of adaptation experiments performed at constant solvent polarity (a) 30 °C; (b) 35 °C; (c) 40 °C; (d) 50 °C

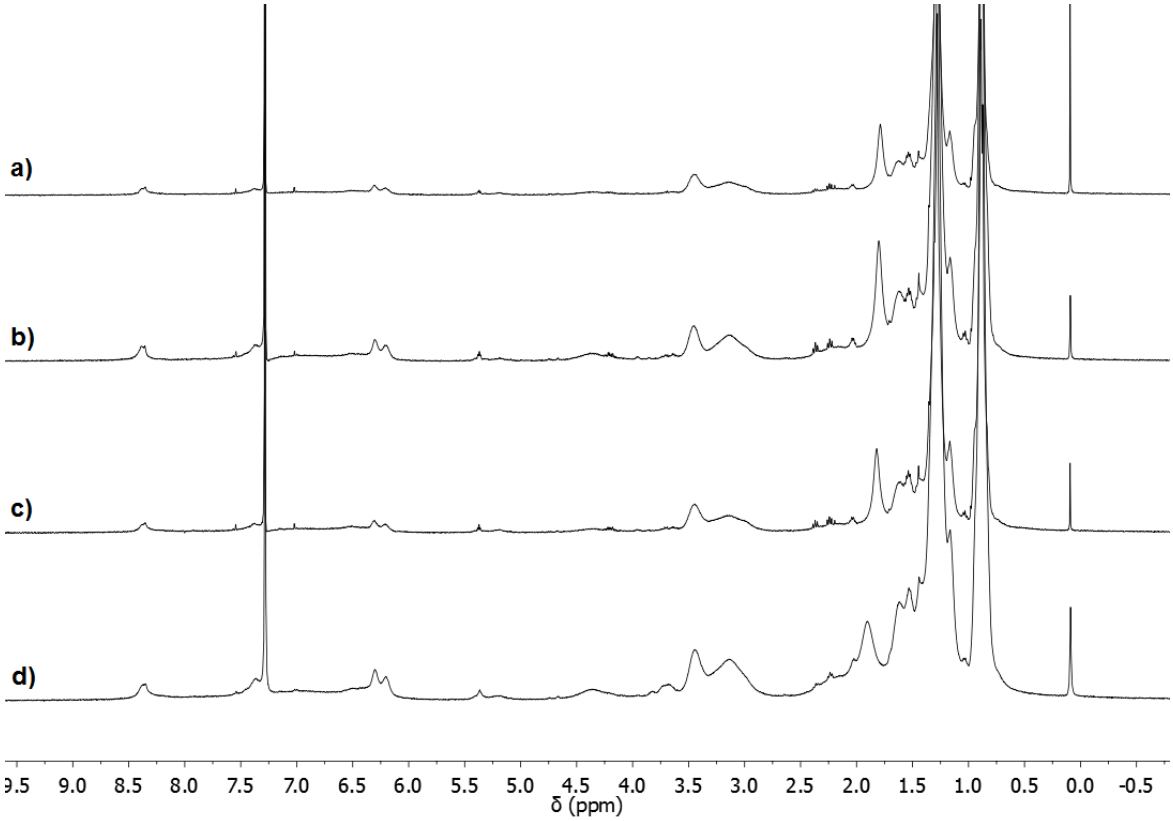
a)
b)
c)
d)
9.5 9.0 8.5 8.0 7.5 7.0 6.5 6.0 5.5 5.0 4.5 4.0 3.5 3.0 2.5 2.0 1.5 1.0 0.5 0.0 -0.5
δ (ppm)

6

6.7 Bibliography

[1] M. F. Perutz, *Molec. Biol. Evol*. 1983, 1, 1–28.

[2] G. Guichard, and I. Huc, *Chemical Communications*, **2011**, 47, 5933-5941.

[3] D. E. Discher, and A. Eisenberg, *Science*, **2002,** 297, 967-973.

[4] E. Stross, G. Iadevaia, D. Núñez-Villanueva and C. A. Hunter, *J. Am. Chem. Soc*., **2017**, 139, 12655-12663.

[5] J. Xu, S. Shanmugam, C. Fu, K-F. Aguey-Zinsou, and C. Boyer, *J. Am. Chem. Soc.*, **2016**, 138, 3094–3106.

[6] R. B. Merrifield, *J. Am. Chem. Soc*., **1963**, 85,2149–2154 .

[7] A. Al Ouahabi, L. Charles and J.-F. Lutz, *Journal of the American Chemical Society*, 2015, 137, 5629–5635.

[8] S. Pfeifer, Z. Zarafshani, N. Badi and J.-F. Lutz, *Journal of the American Chemical Society*, 2009, 131, 9195–9197.

[9] R. K. Roy, A. Meszynska, C. Laure, L. Charles, C. Verchin and J.-F. Lutz, *Nature Communications*, 2015, 6, 7237.

[10] S. Mavila, O. Eivgi, I. Berkovich, and N. G. Lemcoff, *Chem. Rev*., **2016**, 116, 878−961.

[11] M. Ouchi, N. Badi, J.-F. Lutz and M. Sawamoto, *Nat. Chem*., **2011**, 3, 917–924.

[12] M. Artar, E. Huerta, E. W. Meijer, and A. R. A. Palmans, in *Sequence-Controlled Polymers: Synthesis, Self-Assembly, and Properties*, American Chemical Society , USA, **2014**, p. 313

[13] R. Nguyen, and I. Huc, *Angew. Chem. Int. Ed*., **2001**, 40, 1774-1776.

[14] M. Artar, E. R. J. Souren, T. Terashima, E. W. Meijer, and A. R. A. Palmans, *ACS Macro Lett*. 2015, 4, 1099−1103

[15] M. A. J. Gillissen, I. K. Voets, E. W. Meijer, and A. R. A. Palmans, *Polym. Chem*. 2012, 3, 3166−3174.

[16] A. B. Benito, M. K. Aiertza, M. Marradi, L. Gil-Iceta, T. Shekhter Zahavi, B. Szczupak, M. Jiménez-González, T. Reese, E. Scanziani, L. Passoni, M. Matteoli, M. De Maglie, A. Orenstein, M. Oron-Herman, G. Kostenich, L. Buzhansky, E. Gazit, H.-J. Grande, V. Gómez-Vallejo, J. Llop and I. Loinaz, *Biomacromolecules*, 2016, 17, 3213–3221.

[17] E. Harth, B. Van Horn, V. Y. Lee, D. S. Germack, C. P. Gonzales, R. D. Miller and C. J. Hawker, *J. Am. Chem. Soc*., **2002**, 124, 8653–8660.

[18] C. F. Hansell, A. Lu, J. P. Patterson, R. K. O'Reilly, *Nanoscale*, **2014**, 6, 4102−4107.

[19] B. S. Murray and D. A. Fulton, *Macromolecules*, **2011**, 44, 7242–7252.

[20] A. W. Jackson, and D. A. Fulton , *Polym. Chem*., **2013**, 4, 31-45.

[21] E. J. Foster, E. B. Berda, and E. W. Meijer, *J. Am. Chem. Soc*. 2009, 131, 6964−6966.

[22] S. Cantekin, T. F. A. de Greef , and A. R. A. Palmans, Chem. Soc. Rev., **2012**, **41**, 6125-6137.

[23] G. M. ter Huurne, L. N. J. de Windt, Y. Liu, E. W. Meijer, I. K. Voets, and A. R. A. Palmans, *Macromolecules*, **2017** 50 (21), 8562-8569.

[24] N. Hosono, A. R. A. Palmans, and E. W. Meijer, *Chem. Commun*., **2014**, 50, 7990-7993.

[25] C. B. Anfinsen, *Science*1973, 181, 223-230.

[26] S. J. Rowan, S. J. Cantrill, G. R. L Cousin, J. K. M. Sanders, and J. F. Stoddart, *Angew. Chem. Int. Ed*., 2002, 41, 898-952.

[27] M. A. Tasdelen, *Polym. Chem*., 2011, 2, 2133-2145.

[28] J. H. K. Ky Hirschberg, Luc Brunsveld, Aissa Ramzi, Jef A. J. M. Vekemans, Rint P. Sijbesma, and E. W. Meijer, *Nature*, **2000**, 407,167–170.

[29] A. Sanyal, *Macromol*. *Chem. Phys*., **2010**, 211, 1417–1425.

[30] M. Eberhardt, R. Mruk, R. Zentel, and P. Theato, *Eur. Polym. J*. **2005**, 41, 1569−1575.

6. Environmental molecular adaptation of supramolecular polymer nanoparticles

Future work

In Chapter 3 we described the optimization of the reaction conditions to synthesize the complementary strands of homo- and heterodimers. Applying the same methodology, in Chapter 4 we developed the chemistry to replicate dimer molecules in a single replication cycle. The work in both chapters constitute the stepping stones before applying the same principles in the replication of longer oligomers. Therefore, the immediate first step to continue with this line of research would be to synthesize a sequence-defined oligomer with more monomer units, for example, a tetramer. Studying the replication process in a tetramer will allow us to identify the potential appearance of copying errors due to folding when the backbone becomes too flexible. Attempting to optimize the replication process in longer oligomers will show whether this system could potentially be used in more complex experimental set-ups, such as repeated selection and amplification cycles. In them, a sequence-defined oligomer replicated by the covalent strategy presented in this thesis could be optimized for a given function conferred by its functional groups and three-dimensional structure.

In Chapter 5 we synthesized a set of polycarbonate-based polymer nanoparticles that folded due to BTA supramolecular interactions. The appeal of such a backbone is its ease of synthesis, and its biodegradability and biocompatibility. A continuation of this project could involve preparing sets of water-soluble polycarbonate nanoparticles, with groups appended to the backbone that gave additional functionality to the system, such as molecular recognition, or the capacity to encapsulate and transport drug-like molecules. Studying such systems in aqueous environments would be the first step towards being able to design polycarbonate nanoparticle systems that could potentially be studied *in vivo*.

Finally, in Chapter 6 we attempted to study the molecular adaptation of nanoparticle systems that were synthesized under different conditions of temperature and polarity. Due to solubility problems, the results of the chapter were inconclusive. Therefore, the immediate work we would try to do would be to solve those issues, by either increasing the percentage of solubilizing units appended to the backbone or modifying them synthetically to increase the carbon count of each single unit, hence making the system more soluble. Once this was done, we once more would attempt to characterize the molecular adaptation of the new system by different spectroscopic techniques.